

**Analysis of the role of sphingosine kinases and the
host protein viperin in dengue virus replication
and pathogenesis**

By

Wisam Hamzah AL-Shujairi

B.Sc., M.Sc.

**A thesis submitted in fulfilment of the requirements for the degree of Doctor of
Philosophy**

Department of Microbiology and Infectious Diseases

College of Medicine and Public Health

Flinders University/Adelaide, South Australia

April 2018

TABLE OF CONTENTS

TABLE OF CONTENTS	II
ABSTRACT.....	IX
DECLARATION.....	XII
ACKNOWLEDGMENT	XIII
LIST OF FIGURES	XV
LIST OF ABBREVIATIONS	XVII
PUBLICATION AND PRESENTATION	XX
CHAPTER 1. INTRODUCTION	1
1.1 DENGUE VIRUS OVERVIEW	1
1.2 DENV HISTORY AND EPIDEMIOLOGY	1
1.3 DENV TRANSMISSION.....	5
1.4 DENV IN AUSTRALIA	5
1.5 DENV VIROLOGY	6
<i>1.5.1 Classification</i>	<i>6</i>
<i>1.5.2 DENV structure.....</i>	<i>6</i>
<i>1.5.3 DENV proteins.....</i>	<i>7</i>
1.5.3.1 DENV structural proteins.....	7
1.5.3.2 DENV non-structural proteins	9
1.6 DENV LIFE CYCLE	12
<i>1.6.1 DENV attachment</i>	<i>12</i>
<i>1.6.2 DENV entry and uncoating.....</i>	<i>13</i>
<i>1.6.3 DENV genome translation.....</i>	<i>15</i>

1.6.4	<i>DENV RNA replication</i>	15
1.6.5	<i>DENV release and assembly</i>	16
1.7	DENV TARGET CELLS	16
1.8	DENV CLINICAL MANIFESTATIONS	17
1.9	DENV DIAGNOSIS	20
1.10	RISK FACTORS FOR SEVERE DENV	20
1.10.1	<i>Host factors</i>	20
1.10.2	<i>DENV factors</i>	21
1.11	PATHOGENESIS OF SEVERE DENV	23
1.12	DENV IMMUNE RESPONSES	25
1.12.1	<i>Innate immune response and DENV innate immune evasion</i>	25
1.12.2	<i>Viperin, an interferon-stimulated gene</i>	27
1.12.3	<i>Adaptive immune response</i>	29
1.13	DENV PREVENTION AND CONTROL.....	30
1.14	DENV ANIMAL MODELS	31
1.14.1	<i>Non-human primate (NHP) models</i>	31
1.14.2	<i>Mouse models</i>	32
1.15	SPHINGOLIPIDS AND SPHINGOSINE-1-PHOSPHATE.....	33
1.16	SPHINGOSINE KINASES (SKs)	36
1.16.1	<i>SK1 and SK2 isoforms</i>	36
1.16.2	<i>SKs activation and subcellular localisation</i>	39
1.16.3	<i>SKs in viral infection</i>	39
1.17	HYPOTHESIS AND AIMS.....	43
1.18	OUTCOMES.....	43
CHAPTER 2.	MATERIALS AND METHODS	45
2.1	MATERIALS	45

2.1.1 Agarose gel electrophoresis.....	45
2.1.2 Antibodies.....	45
2.1.2.1 Primary antibodies	45
2.1.2.2 Secondary antibodies	45
2.1.3 Cells	45
2.1.4 Cell culture buffers and reagents.....	47
2.1.5 Cell culture media.....	47
2.1.5.1 Media for maintaining and culturing cells	47
2.1.5.2 Media for plaque assay	47
2.1.5.3 Reagents for plaque assay	47
2.1.6 Chemicals.....	48
2.1.7 General use buffers and solutions.....	48
2.1.8 Flow cytometry staining buffers and fixatives	49
2.1.9 Histological buffers and reagents.....	49
2.1.9.1 Tissue processing	49
2.1.9.2 Haematoxylin and eosin staining	49
2.1.9.3 Immunofluorescence staining	50
2.1.10 Molecular biology reagents and buffers	50
2.1.10.1 RNA extraction	50
2.1.10.2 DNase I treatment	51
2.1.10.3 Reverse transcription.....	51
2.1.10.4 Real time PCR.....	51
2.1.11 Primers.....	51
2.2 METHODS.....	54
2.2.1 Cell maintenance.....	54
2.2.2 Cell viability assay.....	54

2.2.3 <i>DENV stock and infection</i>	55
2.2.3.1 DENV production	55
2.2.3.2 DENV challenge	55
2.2.4 <i>DENV quantitation by plaque assay</i>	56
2.2.5 <i>Drug treatment of DENV infected cells</i>	57
2.2.5.1 Treatment with SK1 selective inhibitors.....	57
2.2.5.2 Treatment with SK2 selective inhibitors.....	57
2.2.6 <i>DENV infection in MEFs</i>	58
2.2.6.1 DENV infection in SK2 ^{-/-} iMEFs.....	58
2.2.6.2 IFN-β enzyme linked immunosorbent assay (ELISA).....	58
2.2.6.3 DENV infection in Vip ^{-/-} MEFs.....	59
2.2.7 <i>Agarose gel electrophoresis</i>	59
2.2.8 <i>DENV quantitation by reverse transcription polymerase chain reaction</i>	60
2.2.8.1 RNA extraction	60
2.2.8.2 DNase I treatment	60
2.2.8.3 RNA reverse transcription	60
2.2.8.4 Real-time quantitative polymerase chain reaction (qRT-PCR)	61
2.2.9 <i>Quantitation of DENV replication by flow cytometry</i>	62
2.2.10 <i>Protein assay</i>	63
2.2.11 <i>Sphingosine kinase activity and SIP analysis</i>	64
2.2.11.1 Sphingosine kinase 1 and 2 activity assay	64
2.2.11.2 SIP quantitation	65
2.2.12 <i>Mice</i>	65
2.2.13 <i>Ethics statement</i>	66
2.2.14 <i>Mouse intracranial DENV challenge and follow up</i>	66
2.2.15 <i>Histological analysis</i>	68

2.2.15.1 Tissue processing	68
2.2.15.2 Haematoxylin and Eosin Staining.....	68
2.2.15.3 Immunostaining	69
2.2.16 Statistics	69
CHAPTER 3. THE ROLE OF SK1 DURING DENV INFECTION <i>IN VITRO</i>	71
3.1 INTRODUCTION.....	71
3.2 RESULTS.....	72
3.2.1 <i>Inhibition of SK1 with SKi reduces DENV infection in different cell lines.....</i>	<i>72</i>
3.2.2 <i>SKi inhibits DENV infection in a concentration-dependent manner</i>	<i>74</i>
3.2.3 <i>SKi inhibits DENV infection at a post-binding step of viral replication</i>	<i>76</i>
3.2.4 <i>SKi has no effect on DENV RNA replication in a sub-genomic GFP reporter replicon system.....</i>	<i>78</i>
3.2.5 <i>Inhibition of SK1 with SK1-I impairs DENV infection in vitro</i>	<i>80</i>
3.2.6 <i>Inhibition of SK1 with SK1-I impairs DENV-induced innate responses</i>	<i>82</i>
3.3 DISCUSSION.....	84
CHAPTER 4. THE ROLE OF SK1 DURING DENV INFECTION <i>IN VIVO</i>	89
4.1 INTRODUCTION.....	89
4.2 DISCUSSION.....	112
CHAPTER 5. THE ROLE OF SK2 DURING DENV INFECTION	113
5.1 INTRODUCTION.....	113
5.2 RESULTS.....	114
5.2.1 <i>DENV infection is reduced in SK2^{-/-} iMEFs but not affected by inhibition of SK2 in vitro</i>	<i>114</i>
5.2.1.1 <i>DENV infection is restricted in the absence of SK2 in iMEF cells.....</i>	<i>114</i>
5.2.1.2 <i>DENV infection induces lower levels of IFN-β and ISGs in SK2 deficient compared</i>	

to WT iMEFs	116
5.2.1.3 DENV infection is not affected by chemical inhibition of SK2 activity in vitro.....	120
5.2.1.4 Inhibition of SK2 has no effect on DENV RNA replication in a replicon system ..	125
<i>5.2.2 The role of SK2 in vivo during DENV infection.....</i>	<i>127</i>
5.2.2.1 Establishment of DENV infection in SK2 ^{-/-} mice	127
5.2.2.2 SK2 deficiency has no effect on DENV neurovirulence and survival of mice.....	127
5.2.2.3 The absence of SK2 has no effect on DENV RNA levels in the brain of mice following ic injection	132
5.2.2.4 The absence of SK2 alters the SK1/S1P axis in the brain but this is not further altered following DENV infection.....	134
5.2.2.5 The absence of SK2 has no effect on T cell infiltration in the brain of mice following ic DENV infection	137
5.3 DISCUSSION.....	139

CHAPTER 6. THE ROLE OF VIPERIN DURING DENV INFECTION IN THE BRAIN..145

6.1 INTRODUCTION.....	145
6.2 RESULTS.....	146
<i>6.2.1 Viperin restricts DENV infection in vitro</i>	<i>146</i>
6.2.1.1 A deficiency of viperin in primary mouse cells promotes DENV infection.....	146
6.2.1.2 The increased DENV-replication in viperin deficient mouse cells is associated with higher innate immune responses in vitro	149
<i>6.2.2 Viperin has a minimal role during DENV infection in mice.....</i>	<i>151</i>
6.2.2.1 A deficiency of viperin has no significant effect on DENV neurovirulence and survival of mice following ic DENV infection.....	151
6.2.2.2 A deficiency of viperin has no significant effect on DENV RNA levels in the brain of mice following ic infection.....	155
6.2.2.3 A deficiency of viperin does not affect IFN-β and ISGs levels in mouse brain	

following DENV infection.....	157
6.2.2.4 A deficiency of viperin has no effect on T cell infiltration at end stage infection...	160
6.2.2.5 A deficiency of viperin significantly increases IL-6 but does not affect TNF- α mRNA levels following DENV infection.....	162
6.2.2.6 DENV infection in the brain induces comparable morphological changes in both WT and Vip ^{-/-} mice.....	164
6.2.2.7 Immunofluorescence staining of brain tissue from WT and Vip ^{-/-} mice following ic DENV infection	166
6.3 DISCUSSION.....	169
CHAPTER 7. GENERAL DISCUSSION.....	176
7.1 THE ROLE OF SK1 DURING DENV INFECTION.....	176
7.2 THE ROLE OF SK2 DURING DENV INFECTION.....	177
7.3 THE ROLE OF VIPERIN AGAINST DENV INFECTION.....	178
7.4 FUTURE DIRECTIONS	181
7.5 CONCLUSION.....	184
APPENDICES	185
REFERENCES.....	193

ABSTRACT

Dengue virus (DENV) infection is one of the most important arboviral infections in humans. Severe DENV infection is suggested to be an immunopathogenesis where induction of antiviral immune responses may worsen DENV disease. DENV infects around 100 million people annually in tropical and subtropical regions of the world, however DENV treatment is still only supportive without any specific therapies. Despite prolonged efforts to control or reduce DENV transmission, DENV infection continues to increase with a substantial economic burden in DENV endemic countries.

The sphingosine kinase (SK)/sphingosine 1 phosphate (S1P) axis regulates a wide range of cellular signalling processes including survival and proliferation. Further, the SK/S1P pathway is implicated in many diseases such as cancer, inflammatory disorders, and microbial infections. New roles for the function of SKs isoforms, SK1 and SK2 in different viral infections are emerging. The role of SKs enzymes during DENV infection are not fully defined. In this project, we aimed to investigate the effect of SK1 and SK2 on DENV infection and on DENV-induced immune responses in both *in vitro* and *in vivo* infection models. Induction of type I interferon (IFN) and interferon stimulated genes (ISGs) are important first-line host defences against viral infections, and thus we also here have assessed the role of one important ISG, viperin, against DENV infection.

A chemical reduction in SK1 activity using the inhibitors SKi and SK1-I, prior to DENV challenge reduced DENV infection *in vitro*. DENV infection *in vitro* upregulated the mRNA levels of IFN- β , ISGs viperin, IFIT1, IRF7, CXCL10, and tumour necrosis factor- α (TNF- α) and this response was reduced in cells treated with SK inhibitors. Although the reduced induction of these mRNA's may be due to the reduced DENV replication in the presence of SK inhibitors, these data suggest potential roles for SK1 in regulating DENV infection and DENV-induced innate responses *in vitro*.

Since DENV cannot replicate or cause an infection in mice, we employed a reliable model of

DENV-2 infection in the brain of wild type (WT) mice to investigate DENV replication in the context of the complex *in vivo* host cell responses and specifically to assess the effect of the lack of SKs enzymes on DENV infection *in vivo*. Intracranial (ic) DENV infection induced body weight loss and neurovirulence symptoms that reflects DENV replication in the mouse brain. DENV infection in the mouse brain resulted in an induction of IFN- β and viperin, Ifi2712a, IRF7, and CXCL10 at early stage and later during DENV infection. Further, DENV infection in the mouse brain caused an infiltration of CD8⁺ but not CD4⁺ T-cells. DENV ic infection, however does not alter the SK/S1P axis in the mouse brain and the lack of SK1 had no major effect on DENV infection or DENV-induced innate responses and T-cell infiltration. Taken together, these results indicate that SK1 reduced DENV infection in cultured cells but did not influence DENV replication in the mouse brain.

We also investigated the role of SK2 in DENV-infection. Our results showed that while the genetic lack of SK2 in immortalised mouse cells inhibited DENV infection and dysregulated IFN- β and ISGs responses, chemical inhibition of SK2 activity *in vitro* had no impact on DENV infection. Similarly, the genetic lack of SK2 had no effect on DENV infection and DENV-induced immune responses in the mouse brain following ic infection, as above. The lack of SK2, however did alter the SK/S1P axis independently of DENV infection, with a significant reduction in S1P levels in mouse brain, demonstrating a role for SK2 in regulating S1P levels in this tissue. This reduction in S1P in the brain, however still did not affect the infiltrating CD8⁺ T-cell level following DENV infection suggesting no role for the SK/S1P axis in T-cell infiltration in the DENV-infected mouse brain.

Our results and prior published studies showed an induction of viperin following DENV infection *in vitro* and *in vivo*. The genetic lack of viperin in primary mouse cells increased DENV infection that was associated with enhanced IFN- β expression *in vitro*. Viperin deficiency however had no major effect on DENV replication following ic infection of mouse brain and no effect on the induction of IFN- β and ISGs or TNF- α . The exceptions to this were mRNA levels for Ifi2712a and

IL-6 that were both upregulated in response to DENV infection and the lack of viperin further increased mRNA levels for both these factors following ic DENV infection. Histological analysis of DENV-infected mouse brains demonstrated that the hippocampus was the region most affected by ic DENV infection. The absence of viperin did not exacerbate these DENV-induced neuropathies and morphological changes in the hippocampus or CD8+ T-cell infiltration in the mouse brain. In this study, immunofluorescence staining of mouse brain section was undertaken to assess the main DENV target cells in the brain and the cell types expressing viperin. Results were not conclusive but were promising and suggestive of positive staining for DENV and viperin in some sections of the DENV-infected WT mouse brain.

Overall, this study has defined potential roles of SK1 *in vitro* in promoting DENV infection and ISG induction but this is not reflected by responses in the brain. Similarly, a lack of SK2 reduces DENV infection and ISG induction *in vitro* but not in the brain. In both cases, DENV-infection of the brain induces CD8+ T-cell infiltration but does not dysregulate the SK/S1P axis. The important ISG, viperin is anti-viral *in vitro* against DENV but lack of viperin does not affect DENV replication or ISG induction in the brain, with the exception of Ifi2712a and IL-6. This in particular, may warrant further future examination. The DENV-brain mouse model of infection used in this project can be used to further investigate certain aspects of DENV replication *in vivo*, such as studies to investigate the anti-viral potential of chemical SK inhibitors or S1P analogues on DENV replication in the brain. Additionally, our preliminary staining for DENV and viperin expression in mouse brain establishes a foundation for future work to define the principal DENV targeted cells and anti-viral responsive cells to further define the biological responses to DENV-infection in the brain.

DECLARATION

I certify that this thesis does not incorporate without acknowledgment any material previously submitted for a degree or diploma in any university; and that to the best of my knowledge and belief it does not contain any material previously published or written by another person except where due reference is made in the text.

Wisam H Al-Shujairi

ACKNOWLEDGMENT

I would first like to acknowledge the Iraqi Government and Iraqi Ministry of Higher Education and Scientific Research for providing me an opportunity to complete my doctoral degree in Australia. I am highly indebted to the staff of the Iraqi cultural attaché in Australia and New Zealand for their continuous support during my PhD study. I would like to dedicate this work to spirits of my father and my old brother who support me consistently during my life. I would like to thank my mother, brothers, and sisters who provide me through moral and emotional support during my life in general. I would like to express my special thanks to my wife for her encouragement, patience, and support throughout this long journey.

I would like to express my sincere gratitude to my supervisor A/Prof Jill Carr for giving me this opportunity to work on this project. I am so grateful to her for endless support and assistance during my PhD candidature. I truly appreciate her expert guidance in all the time of research and writing of this thesis.

I am grateful to Ms Julie Calvert for her laboratory assistance. I would also like to thank my fellow PhD students Mr Alex Abraham and Ms Sheila Cabezas for their advice, scientific discussion, and all the fun we have had over the years. I am so grateful to Dr Jen Clarke for her helpful comments and support during the early stages of my PhD candidature, and Dr Amanda Aloia for her assistance and advice.

I would like to acknowledge the head of the department of Microbiology and Infectious Diseases, Prof David Gordon for his academic support, Dr Penny Adamson and Ms Marlene Prigent for their assistance during my work in the department. I would like to include a special note of thanks to Prof Stuart Pitson for his academic comments and advice, Dr Briony Gliddon for provision the mice and Ms Lorena Davies for her laboratory assistance. I would also like to thank Prof Michael Beard and Dr Kylie Van der Hoek for their assistance and for provision the mice. I owe my thanks to Dr

Mohammed Alsharifi for his advice and academic comments.

My acknowledgment will be not complete without thank Ms Yvette DeGraaf and Ms Pat Vilimas for their expert support and advice. Finally, I would like to acknowledge Flinders University for providing me with all facilities that I have needed during my PhD candidature.

Finally, I would like to thank all my friends and to people who have helped me during this long adventure.

LIST OF FIGURES

Chapter 1

Figure 1. 1 Distribution of DENV around the world including areas at risk for the <i>Aedes</i> mosquito.	4
Figure 1. 2 DENV particle and RNA genome	8
Figure 1. 3 Schematic diagram of DENV life cycle	14
Figure 1. 4 Clinical course of DENV disease	18
Figure 1. 5 New DENV case classification by WHO in 2009	19
Figure 1. 6 DENV phylogenetic tree depicting the relationship within and among DENV serotypes and genotypes.....	22
Figure 1. 7 Schematic representation of dsRNA sensing, IFN production, and ISGs induction.....	26
Figure 1. 8 Sphingolipid metabolic pathway	35
Figure 1. 9 Human SK1 and SK2	38

Chapter 2

Figure 2. 1 Schematic representation of the intracranial injection technique.....	67
---	----

Chapter 3

Figure 3. 1 SKi inhibition restricts DENV infection in different cell lines	73
Figure 3. 2 Dose-dependent of DENV infection and SK1 activity by SKi	75
Figure 3. 3 Effect of SKi on DENV infection.....	77
Figure 3. 4 Effect of SKi on DENV RNA replication	79
Figure 3. 5 SK1-I treatment reduces DENV infection.....	81
Figure 3. 6 SK1-I treatment reduces DENV-induced innate responses.....	83

Chapter 5

Figure 5. 1 DENV infection is restricted in cells that lack SK2	115
Figure 5. 2 IFN- β is induced but at significantly lower levels in DENV-infected SK2 ^{-/-} iMEFs....	117

Figure 5. 3 Induction of ISGs is reduced in SK2 deficient iMEFs	119
Figure 5. 4 ABC treatment of HEK293 c18 cells does not affect DENV infection	122
Figure 5. 5 ABC treatment of HepG2 does not impair DENV infection.....	123
Figure 5. 6 K145 treatment does not impair DENV infection	124
Figure 5. 7 Effect of SK2 selective inhibitors on DENV RNA replication	126
Figure 5. 8 Body weight and survival curve of WT and SK2 ^{-/-} mice	130
Figure 5. 9 Lack of SK2 has no effect on DENV RNA levels in the brain following ic infection..	133
Figure 5. 10 Definition of the SK/S1P axis in WT and SK2 ^{-/-} mice following ic DENV infection	136
Figure 5. 11 T cell infiltration in the brain of WT and SK2 ^{-/-} mice following ic DENV infection .	138

Chapter 6

Figure 6. 1 Viperin deficiency enhanced DENV infection in MEFs	148
Figure 6. 2 Viperin deficiency modulates IFN-β and ISGs in 1°MEFs.....	150
Figure 6. 3 Body weight gain and survival curve of WT and Vip ^{-/-} mice.....	153
Figure 6. 4 DENV RNA levels in Vip ^{-/-} mice	156
Figure 6. 5 Induction of IFN-β and ISGs in the brain of WT and Vip ^{-/-} mice following ic DENV-2 injection.....	159
Figure 6. 6 CD4 and CD8 levels in WT and Vip ^{-/-} mice in the brain following ic DENV infection	161
Figure 6. 7 TNF-α and IL-6 responses in WT and Vip ^{-/-} mice in the brain following ic DENV infection	163
Figure 6. 8 Histopathological changes of the brain hippocampus in WT and Vip ^{-/-} mice following ic DENV infection	165
Figure 6. 9 Immunostaining of WT and Vip ^{-/-} mice brain tissues following DENV infection.....	168

Chapter 7

Figure 7. 1 Summary of the effect of SK1, SK2, and viperin during DENV infection.....	180
---	-----

LIST OF ABBREVIATIONS

μL	Microlitre
μM	Micromolar
1°MEF	Primary mouse-embryonic fibroblast
ABC	ABC294640
ADE	Antibody-dependent enhancement
ATCC	American type culture collection
ATP	Adenosine triphosphate
BMDCs	Bone marrow-derived dendritic cells
BMDMs	Bone marrow-derived macrophages
bp	Base-pair
BSA	Bovine serum albumin
CCL4	CC-chemokine ligand 4
cDNA	Complementary DNA
CHIKV	Chikungunya virus
CIB1	Calcium and integrin binding protein-1
CNS	Central nervous system
CPE	Cytopathic effect
CRL	C-type lectin receptor
CT	Cycle threshold
DCs	Dendritic cells
DENV	Dengue virus
DF	Dengue fever
DFH	Dengue haemorrhagic fever
DGK	Diacylglycerol kinase
DMEM	Dulbecco's Modified eagle's medium
DMSO	Dimethyl sulfoxide
dNTPs	Deoxynucleotide triphosphates
dpi	Days post-infection
ds	Double stranded
DSS	Dengue shock syndrome
DTT	Dithiothreitol
EBNA1	Epstein-Barr nuclear antigen 1
EBV	Epstein-Barr virus
ECs	Endothelial cells
EDTA	Ethylene diamine-tetra-acetic acid
EIAV	Equine infectious anaemia virus
ELISA	Enzyme-linked immunosorbent assay
ER	Endoplasmic reticulum
ERK	Extracellular signal-regulated kinase
FBS	Foetal bovine serum
GAPDH	Glyceraldehyde-3-phosphatedehydrogenase
GFP	Green fluorescent protein
h	Hour
HBSS	Hank's balanced salt solution
HCMV	Human cytomegalovirus
HCV	Hepatitis C virus
HIV-1	Human immunodeficiency virus 1

HLA	Human leukocyte antigen
HPLC	High-performance liquid chromatography
Hsp70	Heat shock protein 70
Hsp90	Heat shock protein 90
IAV	Influenza A-virus
ic	Intracranial
IE1	Immediate early protein
IF	Immunofluorescence
IFN	Interferon
IFN- α	Interferon-alpha
IFN- β	Interferon-beta
IFN- γ	Interferon gamma
IL	Interleukin
iMEF	Immortalised mouse-embryonic fibroblast
ip	Intraperitoneal
IRFs	Interferon regulatory factors
ISGs	Interferon-stimulated genes
ISRE	Interferon stimulated response element
iv	Intravenous
JAK	Janus kinase
JEV	Japanese encephalitis virus
kDa	Kilodaltons
KSHV	Kaposi's sarcoma-associated herpesvirus
LCMV	Lymphocytic choriomeningitis virus
LPS	Lipopolysaccharide
MDA5	Melanoma differentiation-associated gene 5
MDMs	Monocyte-derived macrophages
MEFs	Mouse-embryonic fibroblasts
MHC	Major histocompatibility complex
min	Minute
ml	Millilitre
mM	Millimolar
MOI	Multiplicity of infection
MR	Mannose receptor
mRNA	Messenger ribonucleic acid
MTase	Methyltransferase
MyD88	Myloid differentiation primary-response sting 88
NC	Nucleocapsid
NF- κ B	Nuclear factor-kappa B
NGC	New Guinea C
NGS	Normal goat serum
NHPs	Non-human primates
NITD	Adenosine analogue NITD008
NS	Non-structural
NTPase	Nucleotide triphosphatase
O/N	Overnight
ORF	Open reading frame
PAMPs	Pathogen-associated molecular patterns
PBS	Phosphate-buffered saline
pDCs	Plasmacytoid dendritic cells
PFU	Plaque forming unit
pi	Post-infection

Poly (I:C)	Polyinosinic-polycytidylic acid
PP2A	protein phosphatase 2A
PRRs	Pattern recognition receptors
RCs	Replication complexes
RdRp	RNA-dependent RNA polymerase
RIG-I	Retinoic acid-inducible gene-I
RSV	Respiratory syncytial virus
RT	Room temperature
RT-PCR	Reverse transcription polymerase chain reaction
RVPs	Reporter virus particles
S/N	Supernatant
S1P	Sphingosine-1-phosphate
S1PR1	Sphingosine-1-phosphate receptor 1
SAM	S-adenosyl methionine
SCID	Severe combined immunodeficiency
SD	Standard deviation
SDS	Sodium dodecyl sulphate
sec	Second
SEM	Standard error mean
shRNA	Small hairpin RNA
SIN	Sindbis virus
siRNA	Small interfering RNA
SK	Sphingosine kinase
SK1	Sphingosine kinase 1
SK2	Sphingosine kinase 2
ss	Single stranded
STAT	Signal transducer and activation of transcription
SV	Sendai virus
TBEV	Tick-borne encephalitis virus
TLC	Thin layer chromatography
TLR	Toll-like receptor
TNF- α	Tumour necrosis factor-alpha
TRAF2	TNF- α receptor associated factor 2
UTRs	Untranslated regions
v/v	Volume/volume
VPs	Vesicle packets
VRC	Viral replication complex
VSV	Vesicular stomatitis virus
w/v	Weight/volume
WHO	World Health Organisation
WNV	West Nile virus
WT	Wild type
WWII	World war II
YFV	Yellow fever virus
ZIKV	Zika virus

PUBLICATION AND PRESENTATION

Journal publications

A part of this thesis is published in the following journals:

Clarke JN, Davies LK, Calvert JK, Gliddon BL, **Al Shujari WH**, Aloia AL, et al. Reduction in sphingosine kinase 1 influences the susceptibility to dengue virus infection by altering antiviral responses. *J Gen Virol.* 2016;97(1):95-109. Epub 2015/11/07. doi: 10.1099/jgv.0.000334. PubMed PMID: 26541871.

Al-Shujairi WH, Clarke JN, Davies LT, Alsharifi M, Pitson SM, Carr JM. Intracranial Injection of Dengue Virus Induces Interferon Stimulated Genes and CD8+ T Cell Infiltration by Sphingosine Kinase 1 Independent Pathways. *PLoS One.* 2017;12(1):e0169814. Epub 2017/01/18. doi: 10.1371/journal.pone.0169814. PubMed PMID: 28095439.

Presentations

Al-Shujairi WH, Clarke JN, Carr JM. Dengue virus (DENV) infection induces interferon-stimulated genes and CD8+ T-cell infiltration in mice brain. Oral presentation at the Australian Society of Microbiology, Annual Meeting, Perth, Western Australia, 2016.

Al-Shujairi WH, Clarke JN, Carr JM. Sphingosine kinase 1 (SK1) has no major influence on dengue virus (DENV) infection in mice. Poster presentation. School of Medicine, PhD student's forum, Flinders University, Adelaide, November 2015.

CHAPTER 1. INTRODUCTION

1.1 Dengue virus overview

Dengue virus (DENV) causes one of the most important global arthropod-borne viral infections in humans. DENV belongs to the *flavivirus* genus within the family *Flaviviridae* [1]. Four DENV serotypes have been characterised, termed DENV-1, DENV-2, DENV-3, and DENV-4, which are related genetically but distinct antigenically. All are transmitted to humans following a bite by an infected *Aedes* mosquito, primarily *Aedes aegypti* [2]. DENV infection occurs particularly in tropical and subtropical regions of the world due to the distribution of the mosquito vector [3]. Infection with one of DENV serotypes confers long-term protective immunity to that serotype but not cross-protective immunity specific to other DENV serotypes [4]. DENV infection results in illness ranging from asymptomatic or mild febrile disease, dengue fever (DF), to more life-threatening severe forms known as dengue haemorrhagic fever (DHF) and dengue shock syndrome (DSS) [5], reclassified recently as dengue with or without warning signs, and severe dengue [6]. No effective antiviral treatment has been approved against DENV infection, however trials are ongoing [7]. Further, several approaches have been employed to control DENV transmission such as development of a protective vaccine against DENV and mosquito vector control measures. This introduction will briefly discuss these aspects of DENV and discuss in detail the host cell factors: sphingosine kinase and the interferon-stimulated gene, viperin, which are the focus of this thesis.

1.2 DENV history and epidemiology

The exact date for the origin of DENV is unclear with potential DENV infections reported in humans for centuries. The earliest record of a disease clinically compatible with DF was described in a Chinese Medical Encyclopaedia dated 992 A.D. The disease was named as a “water poison” due to the thought that it was connected with a flying insect associated with water [8]. The first

large outbreaks of disease that resembled DF were reported in West India in 1635 and Panama in 1699 [8]. By the late 18th century, a similar illness to the classic DF had caused intermittent epidemics in Asia, Africa and North America, and become widespread in tropical and subtropical areas of the world during the late 19th and early 20th centuries [9,10].

During World War II (WWII), the changing ecology and tremendous human movement facilitated the spread of the virus and its mosquito vector in Southeast Asia and the Pacific [11]. In India and during WWII, DENV-2 was first isolated from the sera of American soldiers in 1944 [12]. After WWII, unplanned urbanisation and increased globalisation provided a suitable environment for spreading of mosquito vectors that resulted in an emergence of DHF [11]. The first well-documented DHF outbreak occurred in Philippines in 1953-1954, which was followed by another major epidemic in Thailand in 1958 [13]. DHF afterwards has expanded to almost all Southeast Asian countries and become a major cause of viral infection among hospitalised children in these areas. DENV transmission on the American continent after WWII was restricted due to intensive campaigns to eradicate the *A. aegypti* vector initiated by the Pan American Health Organisation (PAHO) to control yellow fever disease transmission [14,15]. These vector eradication campaigns were ceased in America in the 1970s that may have resulted in the re-emergence of DHF, such as the DHF Cuba epidemic reported in 1981 [16].

Currently, DENV is the leading cause of the most significant mosquito-borne viral disease in the globe particularly in the tropical and subtropical regions [17] (Figure 1.1). DENV circulates in more than 100 countries, and regions including Asia-Pacific, Americas, Africa, and Middle East, and this distribution is expected to increase [9]. The estimate of the WHO suggests that 50 to 100 million people are infected by DENV each year, and 50% of world's population reside in the DENV at-risk areas [18]. A recent report, however modelled that over 390 million DENV infections occurred per annum, with 96 million of these cases requiring hospitalisation in 2010 [19]. Of these DENV infections, around 500,000 DENV patients experience severe DHF and more than 20,000 deaths

were recorded [15]. Further, about 75% of the DENV disease burden is reported in Southeast Asia and Western Pacific countries [6,20] causing a significant economic burden for these regions [17].

Several factors contribute to the expanding DENV distribution such as global warming and temperature rises that enhance the survival and migration of vectors outside the tropics [21].

Additionally, increased travel to DENV endemic regions may enhance virus introduction and local DENV transmission [21]. Despite the efforts to minimise DENV transmission and eliminate the vector host, DENV epidemics continue to occur and new regions of the world are becoming involved.

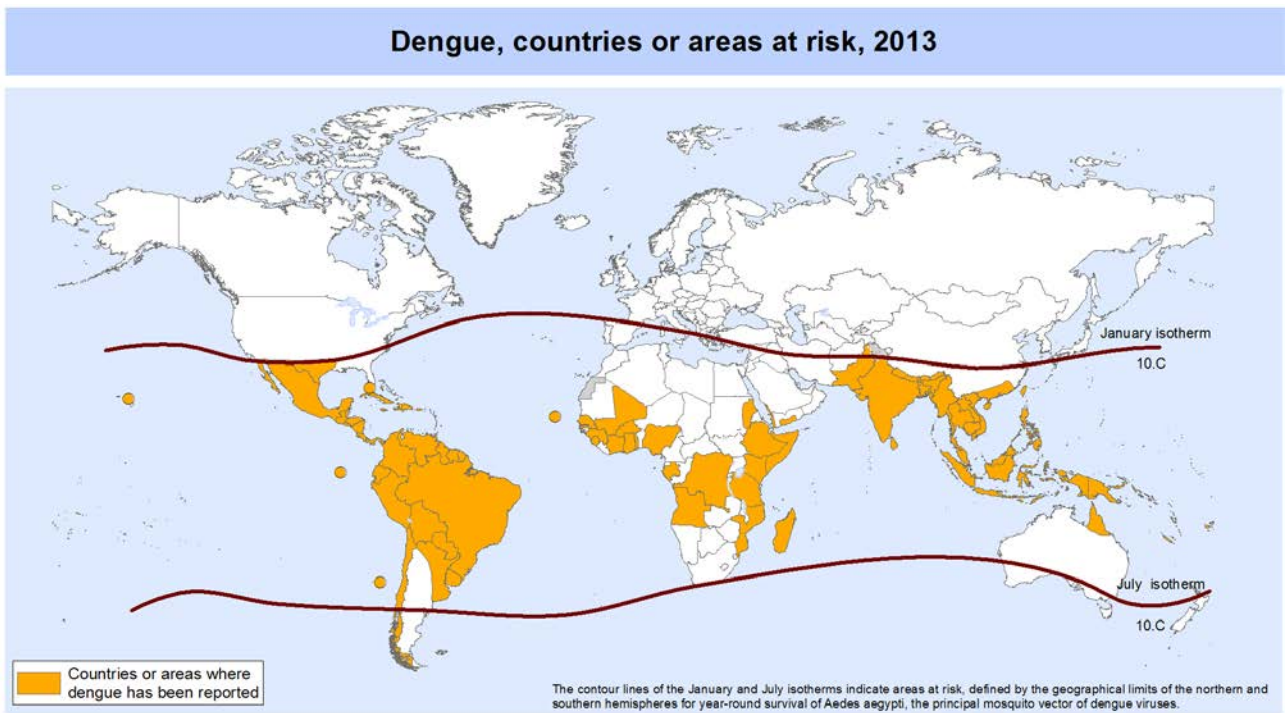


Figure 1. 1 Distribution of DENV around the world including areas at risk for the *Aedes* mosquito [22]

DENV is common in tropical and subtropical regions of the world with nearly 4 billion people living in areas of risk.

1.3 DENV transmission

DENV is a well-described arbovirus, where the infection is transmitted to humans primarily by the bite of an infected mosquito vector. The genus *Aedes*, in particular *A. aegypti*, is the main mosquito vector responsible for spreading DENV, although other species such as *A. albopictus* and *Culex* spp have also been reported to transmit DENV [6]. *A. aegypti* is prevalent in tropics and subtropics between latitudes 35°N and 35°S [23]. This mosquito preferentially feeds during the daylight hours and resides in close proximity to humans [9,21]. The females *A. aegypti* prefer to lay eggs in human-made water reservoirs such as disposed water containers, cans and tyres. The mosquito thrives during the wet seasons of the year and DENV infection subsequently become more frequent during this period of time [24].

Two different transmission cycles for DENV circulation in nature have been described: urban and sylvatic. During the urban DENV cycle, humans are the reservoir and amplification hosts while in the sylvatic cycle, non-human primates (NHPs) such as monkeys are the main DENV reservoir [25]. DENV gains access to the mosquito vector after the mosquito takes blood from an infected human during the period of viremia. The virus then reaches the mosquito midgut, where it infects and replicates and can shed to other tissues including the mosquito salivary gland. The infected mosquito can then introduce the virus through the salivary glands to the new uninfected host during subsequent blood meals [26]. Thus, one infected mosquito is able to transmit DENV to several new human hosts.

1.4 DENV in Australia

DENV outbreaks in Australia occur regularly [27]. Notifications of DENV infections represent the third most prevalent arboviral infection in Australia after Barmah Forest virus and Ross River virus infections [28]. DENV transmission in Australia is confined locally in the northern areas of Queensland where the *Ae. Aegypti* mosquito is present, although local transmission of DENV can

occur from a viraemic traveller or resident arriving from DENV-infected regions who introduce the virus to the mosquito [29]. The largest outbreak of DENV infection (over 1000 infections) that acquired locally were recorded in north Queensland during 2008-2009 [30]. Additionally, in the last few years, the number of DENV infections that were acquired by Australian travellers overseas has increased in most Australian states [28].

1.5 DENV virology

1.5.1 Classification

DENV is classified in the *flavivirus* genus of the family Flaviviridae that has two additional genera, *pestivirus* such as Bovine viral diarrhoea virus (BVDV), and *hepacivirus* such as Hepatitis C virus (HCV). The *flavivirus* name originated from Latin word *flavus* meaning yellow, due to the jaundice induced by yellow fever virus (YFV), one of the original viruses of the *flavivirus* family [31]. The genus *flavivirus* contains more than 70 viral species that are transmitted by an arthropod bite such as mosquitoes and ticks [32]. Many flaviviruses are pathogenic for humans with the most clinically important members including DENV, YFV, West Nile virus (WNV), tick-borne encephalitis virus (TBEV), Japanese encephalitis virus (JEV), and Zika virus (ZIKV) [33]. The members of the *flavivirus* family can be further sub-divided into mosquito-borne viruses and tick-borne viruses [34], although other flaviviruses have unknown vectors. A wide range of diseases can result from infection with flaviviruses including mild fever, severe haemorrhagic fever, and encephalitis [31].

1.5.2 DENV structure

The DENV genome consists of a single-stranded, positive-sense RNA molecule of ~ 11 kb in length [25,35] (Figure 1.2). The genome contains one open reading frame (ORF) flanked by two untranslated regions (UTRs), 5' (~ 100 nucleotides) and 3' (~ 400 nucleotides) that are important for viral replication and translation. The 5' end has a 7-methyl guanosine cap and unlike cellular mRNA, the 3' end does not have a poly (A) tail [36]. The RNA genome is translated into a large

single polyprotein, which is subsequently cleaved by host and viral-derived proteases to produce three structural proteins: capsid, pre-membrane, and envelope (C-prM-E) that constitute the viral particle, and seven non-structural proteins (NS1-NS2A-NS2B-NS3-NS4A-NS4B-NS5) that are responsible for viral replication as well as other unknown functions [25,37]. The prM protein is cleaved by the action of furin during virion maturation to produce membrane (M) protein.

The DENV mature particle is spherical in shape of ~ 50 nm in diameter with icosahedral symmetry and includes the RNA genome surrounded by the capsid and a lipid bilayer that is derived from the host cell endoplasmic reticulum (ER) [38]. An external protein shell covers the lipid envelope containing ~ 180 copies of each of the E and prM proteins [36,39]. The external shell has 60 trimeric spikes arranged icosahedrally, each spike consists of three prM-E heterodimers [39]. The mature DENV virion is highly affected by the temperature. Cryo-electron microscopy images showed that the mature virion has normal smooth surface at room temperature, while at 37°C DENV change his shape to a bumpy structure that is highly infective to mammalian cells [40,41].

1.5.3 DENV proteins

1.5.3.1 DENV structural proteins

Three structural DENV proteins, which constitute the viral particle, are generated from cleaving the single polyprotein co and post-translationally by the action of host and viral proteases. The C protein is a basic protein of ~ 12 kDa that is associated with the viral RNA genome [42]. The DENV C protein forms homodimer structures in solution, with each monomer subunit containing four alpha helices ($\alpha 1-\alpha 4$) [43]. Nuclear magnetic resonance analysis of the dimer C protein demonstrated an asymmetric distribution of basic charged residues over the protein surface. Half of these basic residues are located on one side of the dimer that mediate the interaction with RNA, while the hydrophobic region lies along the opposite side of the dimer mediates the C binding with the membranes [42]. The C protein plays an important role in viral assembly to ensure specific encapsidation of the genome.

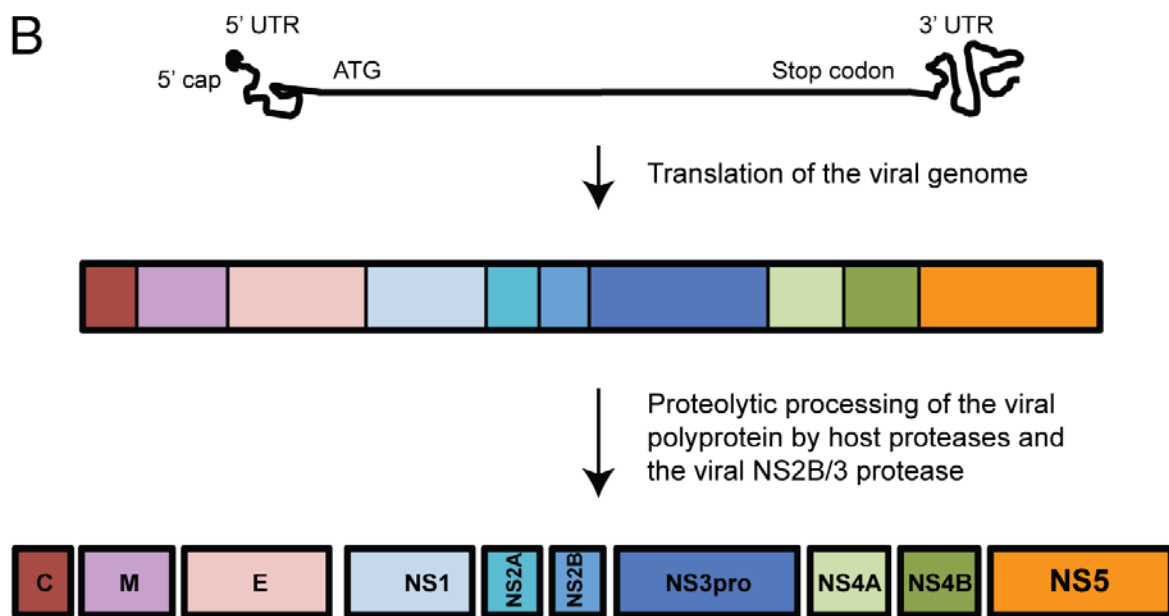
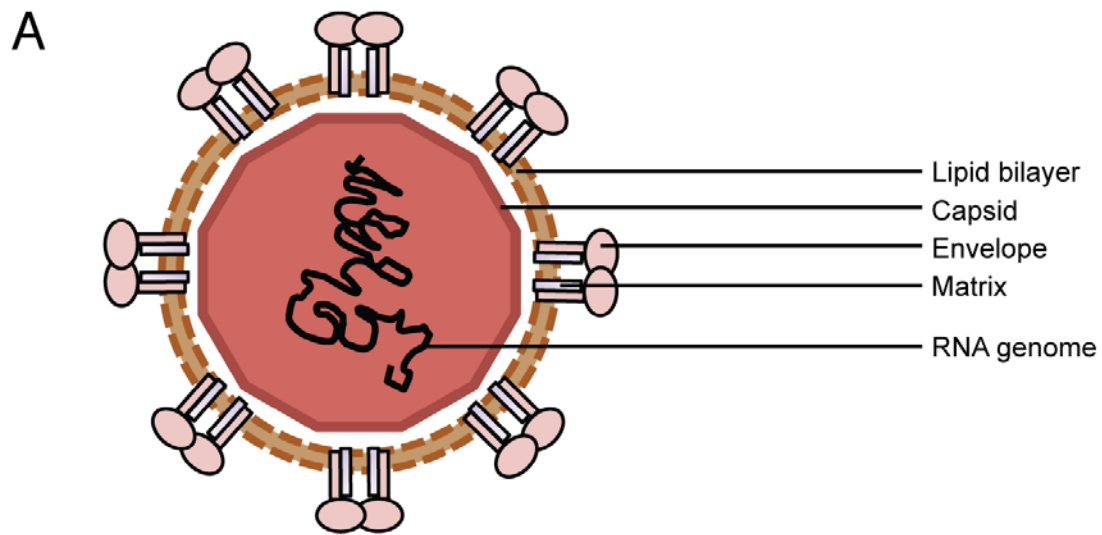


Figure 1. 2 DENV particle and RNA genome [44]

A. Mature DENV virion composed of an RNA genome and the capsid surrounded by a lipid bilayer in which E and M proteins are inserted. **B.** DENV genome is single stranded, positive polarity RNA with two UTRs at the 5' and 3' ends. The genome is translated into single polyprotein, which is further processed into three structural and seven non-structural proteins.

The DENV prM protein comprises 166 amino acids where the cleavage of prM to produce M and pr takes place at position 91. The generated M protein has an N-terminal region (the first 20 residues), an alpha-helical domain, and two transmembrane domains (MT1 and MT2) [45]. The prM is localised to the ER by the hydrophobic domain of C protein [32]. During synthesis, prM protein interacts with E protein to produce a heterodimer that acts as a chaperone for proper folding of E protein. During virus maturation, cleavage of prM into the mature M protein and pr peptide occurs in the trans-Golgi by the Golgi-resident protease furin, which also leads to formation of E homodimers from dissociation of the prM-E interaction. The M protein plays an essential role for DENV assembly and entry steps during the DENV replication [36,46].

The DENV E protein is the major glycoprotein on the DENV surface of ~ 56 kDa, which mediates viral attachment and membrane fusion [47]. The N-terminal ectodomain of the E protein contains three functionally distinct domains (DI, DII, and DIII) that are enriched in β -strands. Domain I is a β -barrel centrally located structure, which lies parallel to the viral envelope; domain II, is a finger like structure that carries a dimerisation region and a conserved fusion loop that mediates the fusion of the virus envelope with the acidic intracellular endosomal membrane; domain III has immunoglobulin-like folds and mediates E binding with cellular receptors [25,32]. The C-terminal part of E protein comprises a stem-anchor region containing two α -helices that lie parallel to the viral lipid layer [48]. The mature virion E protein has a homodimer arrangement. At low pH, the protein homodimers dissociate and trimerise irreversibly to display the fusion peptide and mediate endosomal fusion [37]. The E protein represents the main target for antibody-mediated neutralisation [49].

1.5.3.2 DENV non-structural proteins

Seven non-structural proteins are encoded from the single DENV polyprotein, NS1, NS2A and NS2B, NS3, NS4A and NS4B, and NS5 that mediates a variety of functions including DENV replication and modulation of the host immune response.

DENV NS1 is ~ 46 kDa glycoprotein synthesised as soluble monomers within mammalian cells, which then assemble in the lumen of the ER to form hydrophobic dimers [32,50]. The NS1 is relocated after dimerization within the cells to be associated with the cell membrane (mNS1) as a stable homodimer, to the site of viral replication within the cells, or to be secreted extracellularly (sNS1) as a hexameric barrel-shape lipoprotein form [51,52]. The intracellular NS1 has an essential role in the viral replication process since it is co-localised with dsRNA and with other components of the viral replication complex (VRC), however this role is not yet fully understood [53]. The clear function of the extracellular sNS1 is also not yet determined but sNS1 has been implicated in DENV pathogenesis and immune evasion [32,50]. The sNS1 is found at high levels in the circulation of DENV-infected patients [54] and is used as a diagnostic marker [55]. Recently, the DENV sNS1 has been shown to activate toll-like receptor 4 (TLR4) that induces the release of pro-inflammatory cytokines and vascular leak [56,57].

The DENV NS2A is a small (~ 22 kDa) hydrophobic protein containing five transmembrane segments. The N-terminal region of the NS2A is processed in the lumen of the ER by an unknown host protease, while the C-terminus is generated in the cell cytoplasm by viral protease cleavage. Three functional roles of NS2A have been demonstrated including viral replication, virion assembly, and inhibition of type I interferon (IFN- α/β) responses [58,59]. NS2B is a small integral membrane protein of ~ 14 kDa. The NS2B binds with NS3 to produce the viral protease and functions as a cofactor for optimal NS3 serine protease activity [60].

NS3 protein is a large (~ 70 kDa) multifunctional hydrophobic protein, which performs several activities important for polyprotein processing and for viral RNA replication. The N-terminus (~ 180 residues) of the NS3 carries the viral serine protease activity (NS3pro) that, as described above, requires an association with the cofactor domain of NS2B (~ 40 residues) [61,62]. The NS3/NS2B protease (in combination with a cellular protease) cleaves the viral polypeptide post-translationally to form the viral structural and non-structural proteins. The NS3pro activity represents an important target for developing anti-DENV drugs [63]. The C-terminal segment of NS3 confers RNA

helicase, nucleotide triphosphatase (NTPase), and 5' RNA triphosphatase (RTPase) activities [32,64]. The NS3 protein is required to generate the cap of the 5' UTR by virtue of the NS3 RTPase activity that is enhanced by an association with NS5. The NS3 helicase in combination with NS5 assists in viral replication through unwinding of the RNA strand [65]. In fact, the NTPase, RTPase, and helicase activities of NS3 are involved in RNA replication, and mutations that affect the activity of these enzymes reduce viral production [66].

The NS4A and NS4B are small integral membrane proteins of ~ 16 kDa and 27 kDa respectively. These proteins serve as a scaffold for the formation of the DENV replication complex at the ER. The structure of NS4A is proposed to have an N-terminal region, three transmembrane domains, and a C-terminal region [67]. The last 23 amino acid residues in the C-terminal of the NS4A acts as a signal to translocate NS4A into the lumen of the ER, which is then removed by the action of the host signalase enzyme [67]. The N-terminus 48 amino acids of the NS4A are localised to the cytoplasm and constitute an amphipathic helix, which mediates the NS4A oligomerisation [68], while the remaining transmembrane regions as well as the C-terminus are localised to the ER lumen. The NS4A has been suggested to induce intracellular alterations in host cytoplasmic membranes to form virus-induced vesicle packets that harbour the VRC [67]. Similarly, the NS4B N-terminal region is localised to the lumen of the ER while the C-terminal part is located in the cytoplasm. NS4B is associated with NS3 and with the viral dsRNA in ER-derived cytoplasmic foci assumed to act as sites for viral RNA replication [69]. NS4A and NS4B together with NS2A also confer antagonism of the IFN- α/β response [70,71]. NS4A is also shown to induce autophagy in epithelial cells (ECs) protecting them from death and enhancing viral replication [72].

NS5 is the largest DENV protein of ~ 105 kDa. The N-terminal part of NS5 comprises a methyltransferase (MTase) activity, which is responsible for the internal RNA methylation [73] and viral RNA cap formation [74]. In contrast, the C-terminal region of NS5 contains RNA-dependent RNA polymerase (RdRp) activity required for viral RNA replication [75]. The NS5 associates with NS3 to form a replication complex, which enhances the NTPase and RTPase activities of NS3.

Additionally, the DENV NS5 blocks the IFN response through suppression of the JAK/STAT signalling pathway [76]. NS5 has also been shown to localise to the nucleus and induce the production of IL-8 [77], and this localisation is essential for DENV replication [78]. These multiple essential functions of NS5 in viral RNA replication and modulation in immune response also make it an attractive target for developing anti-DENV drugs.

1.6 DENV life cycle

Various steps in the DENV life cycle involve virus binding to cell surface receptors, endocytosis, fusion with endocytic cellular membranes, genome translation and replication, polyprotein processing, assembly and release (Figure 1.3).

1.6.1 DENV attachment

The initial step in the DENV life cycle is attachment to susceptible cells through cell-surface receptors. DENV is able to infect a wide range of cells *in vitro*, but *in vivo* is largely restricted to cells of the monocyte lineage including monocytes, macrophage, dendritic, and Langerhans cells, suggesting that DENV could bind to various cellular receptors that could be proteins, carbohydrate, lectins, or lipid in nature [79]. Several cell surface receptors have been identified as factors that mediate the entry of the virus through an interaction with viral E glycoprotein. The glycosaminoglycan, heparin sulphate, which is present on the surface on many cell types, has been utilised by DENV for binding to target cells [80,81]. A variety of C-type lectin receptors (CLR) have been reported to interact with DENV E protein. Dendritic cell-specific intracellular adhesion molecule-3 grabbing non-integrin (DC-SIGN) expressed on immature DCs and mannose receptors (MR) expressed on macrophages mediate the binding of DENV to these cells [82,83]. C-type lectin domain family 5, member A (CLEC5A), another CLR, confers DENV interaction with monocytes and macrophages [84]. Additionally, other cell surface molecules such as heat shock protein 70 (Hsp70) and heat shock protein 90 (Hsp90) have been demonstrated to interact with the DENV E

protein [85]. DENV can also exploit Fc γ receptors (Fc γ R) on the surface of some immune cells such as monocyte and macrophages as a route for viral entry [86]. In addition, the LPS receptor, CD14 is another candidate receptor mediating DENV attachment to monocytes and macrophages [86]. In mosquito cells, several molecules have been identified as receptors for DENV entry. For example, prohibitin protein on the surface of C6/36 cells has been characterised to interact with DENV during infection [87]. Another two proteins of 80 and 67 kDa termed R80 and R67 in the mosquito midgut also mediate DENV binding to mosquito cells [88]. DENV interaction with this wide variety of cell-surface receptors can contribute to DENV internalisation and simultaneously trigger an inflammatory response.

1.6.2 DENV entry and uncoating

Following binding to the cellular receptors, DENV has to transfer its genome into the cell cytoplasm. DENV enters the cell by the receptor-mediated endocytosis [89]. After DENV internalisation, the next step is to release the nucleocapsid into the cytosol, which requires fusion of DENV E protein with the host cell membrane. The fusion between viral particle and endosomal membranes is pH dependent. The low pH environment within endosome triggers conformational changes in the E protein structure where the E homodimers dissociate into monomers that irreversibly assembled to form E trimers. In this arrangement, the fusion loop, that was previously buried between domains I and III, exposes at the top of E trimer and finally penetrates the endosomal membrane [47]. A fusion pore is formed and gradually enlarged and then eventually the viral RNA genome is released into the cell cytosol [79].

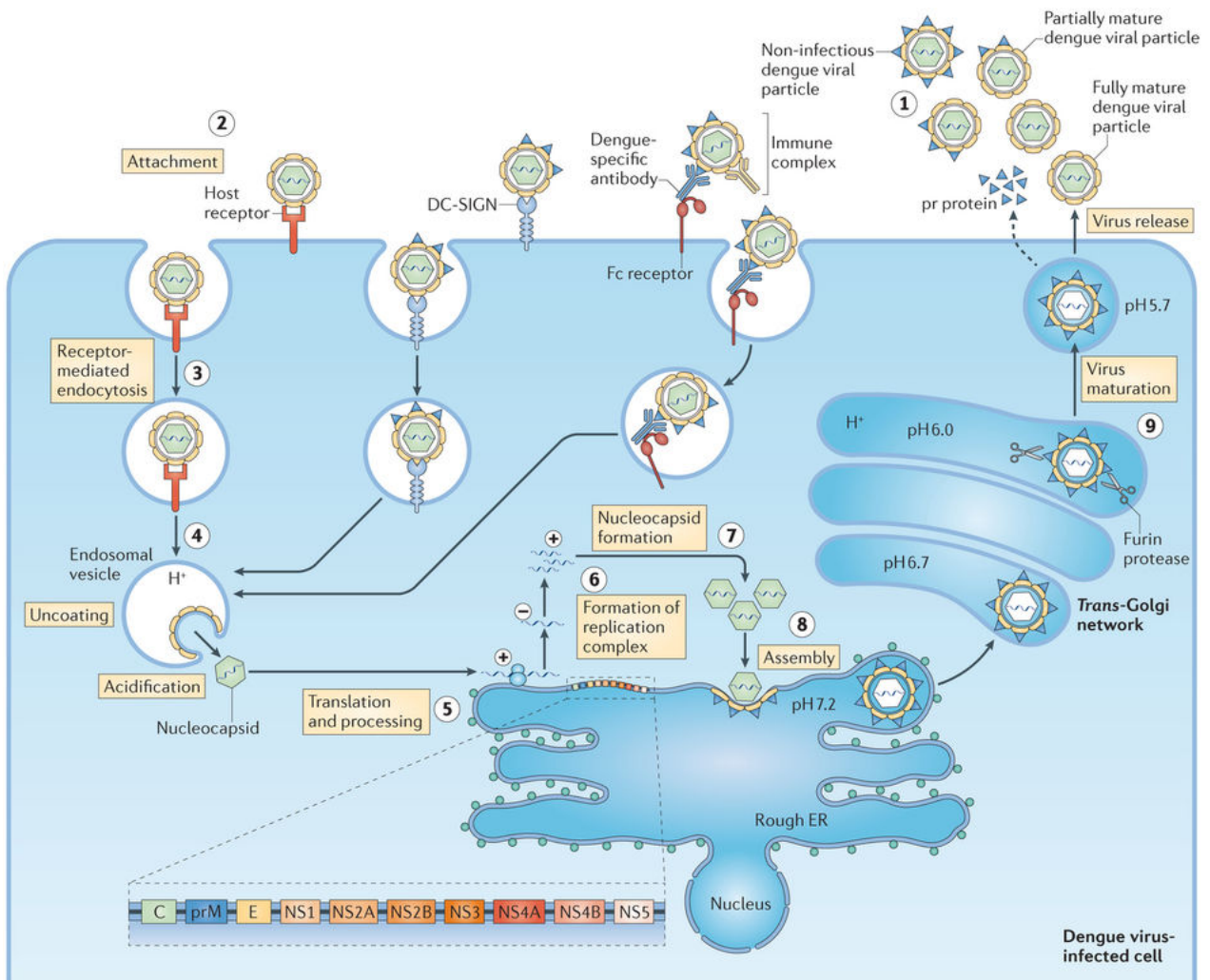


Figure 1. 3 Schematic diagram of DENV life cycle [90, reproduced with permission]

DENV infection is initiated when mature or partially mature DENV virions (1) attached to receptors on target cells (2), which is followed by viral entry via endocytosis within endosomal vesicles (3). Low pH within endosomes triggers DENV fusion with the membrane and releases the nucleocapsid into cytoplasm (4). DENV RNA translocates to the ER surface and then is translated into a single polyprotein (5). The viral replication complex assembles, followed by RNA synthesis via transcription of a negative sense RNA and then amplification of viral RNA (6). The newly formed RNA gains the capsid protein to be packaged as nucleocapsid (7). DENV assembly takes place on ER surface and acquires an envelope through budding into the lumen of ER (8). The immature virion transported into Trans-Golgi network where a host furin cleaves the prM into pr and M proteins (9). The pr remains associated until the mature virion is released by exocytosis.

1.6.3 DENV genome translation

Once the DENV genome is released into the cytoplasm, the capsid protein and RNA molecule disassemble. The RNA genome is recognised by the cell as a messenger RNA and can be directly translated by the host cell machinery since it is a plus-sense molecule [91]. The translation of the RNA genome occurs in close association with ER-derived membranes, which yields a single polyprotein molecule of 3391 amino acids long. The DENV polyprotein precursor is processed co- and post-translationally by the activities of cellular and NS2B-NS3 viral proteases into ten DENV proteins. Processing the one third at the 5' end of the RNA genome produces the structural viral proteins while the remainder is processed to NS proteins (as described in the section 1.5) [67]. During this process, the signal and stop-transfer sequences of the polyprotein direct the NS1, E and prM ectodomains to the ER lumen whereas C, NS3, and NS5 proteins are in the cytoplasm. The NS2A/B and NS4A/B are transmembrane proteins anchored in the lumen of ER [92].

1.6.4 DENV RNA replication

DENV induces several invaginations in the membrane of ER resulted in formation of vesicle packets (VPs). The VPs represent the site for RNA replication and contain all the RNA amplification machinery, or viral replication complex (VRC). The VRC comprises RNA replication components including viral NS proteins, RNA molecule, and some host factors [53,93]. The viral RC has a key role in RNA replication by producing a negative-strand RNA complementary to the positive-strand RNA, which in turn serves as a template to synthesise multiple copies of new plus-strand RNA that acts as both a template for synthesis of further viral proteins and genomic RNA to produce new virions [37]. This method of viral replication is termed 'semi-conservative' RNA replication [32].

1.6.5 DENV release and assembly

Following RNA synthesis, the assembly of DENV particles is initiated by the interaction of multiple copies of a dimeric C protein with the newly formed RNA genome to generate the nucleocapsids (NCs). The NCs bud into the lumen of ER to acquire a lipid envelope derived from ER membranes that carries with it prM and E proteins [32,36]. Immature virions migrate within vesicles from the ER to the Trans-Golgi Network where viral maturation takes place. An additional glycoprotein shell that comprises 180 copies each of prM/M and E proteins covers the lipid DENV envelope. The prM glycoprotein is cleaved by the cellular-derived furin to form pr peptide and M protein producing infectious and mature virions. DENV mature particles are transported to the cell surface and released from the cell via exocytosis [36,92].

1.7 DENV target cells

Monocytes and macrophages represents the primary targets for DENV *in vivo* [37], however they are not the main cells that initially encounter DENV. Following the bite from an infected mosquito vector, DENV is released into the host skin during a blood meal. Previous studies have demonstrated that the resident DCs (Langerhans cells, interstitial DCs) in the skin are the initial targets cells for DENV infection [94,95]. Immature (DCs) particularly showed a high permissiveness to DENV infection in comparison to mature DCs that are relatively resistant [94,95]. Further, DENV infection in DCs is more efficient than infection in macrophages when both cells are derived from the same donors [94,95] demonstrating a high selectivity for this first target cell type. DENV infection in immature DCs induced the production of TNF- α and IFN- γ , which in turn enhances the activation and maturation of DENV-infected DCs [96]. The activated DCs can disseminate the infection through the lymphatics and circulation to other tissues such as liver and spleen [97]. Other cells including hepatocytes, endothelial cells (ECs), and fibroblasts are potential targets for DENV infection [98].

1.8 DENV clinical manifestations

Following an incubation period of 4 to 8 days, infection with any DENV serotype can cause a wide range of symptoms. The vast majority of symptomatic infection is characterised by a classic febrile illness of DF, while a minority of infected people will develop severe illness of DHF or life-threatening DSS [2]. The illness that results from DENV infection has three clinical phases: febrile, critical, and recovery (Figure 1.4). The febrile phase is characterised by an abrupt onset of high fever, which is accompanied by severe headache and pain behind eyes, myalgia, arthralgia, and rash. Mild haemorrhagic signs may be observed during this phase such as petechiae and bleeding from the nose or gums. The febrile phase lasts from 2-7 days. The critical phase lasts for 2-3 days and occurs around the time of defervescence. In the critical phase, patients can experience severe DENV signs such as plasma leakage with or without haemorrhage and hypovolaemic shock. An increase in the haematocrit during this phase reflects haemoconcentration and the possibility of plasma leakage and is often accompanied by a decline in platelet counts (thrombocytopenia). In the recovery phase, which lasts 2-5 days, signs of the disease are resolved [6,99]. DHF and severe dengue illness is more often associated with secondary DENV infection, and although severe dengue is more common in children younger than 15 years, adults can also be affected [100]. In 2009, the WHO updated the dengue disease classification of DF, DHF and DSS with a new case classification. The new revised classification divided the DENV clinical manifestations into dengue without warning signs including mild fever, dengue with warning signs such as abdominal pain and vomiting, and severe dengue including signs of severe DHF and DSS (Figure 1.5) [6].

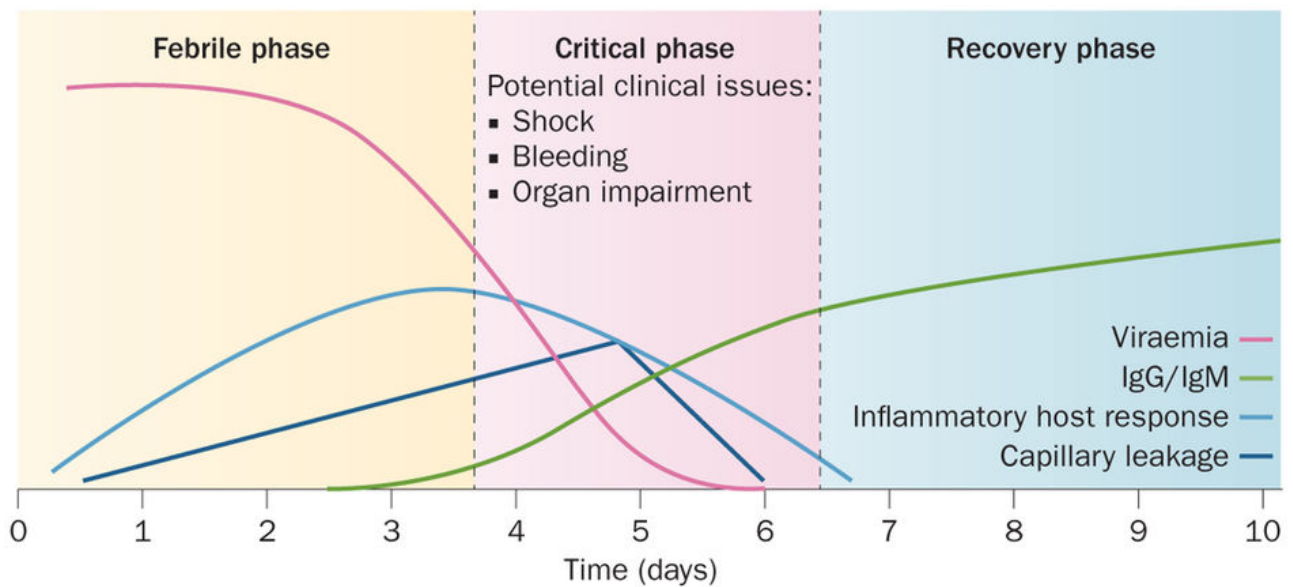


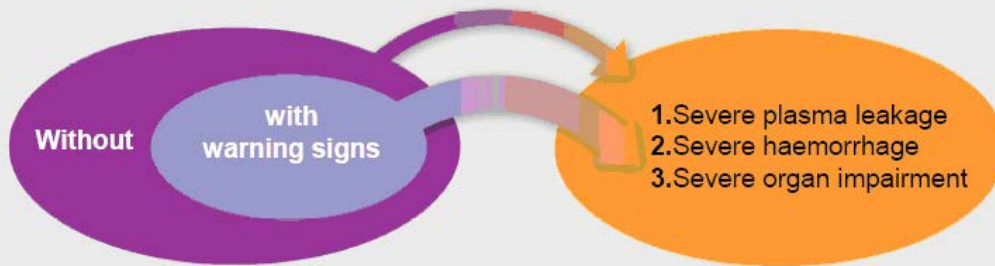
Figure 1. 4 Clinical course of DENV disease [99, reproduced with permission]

The course of DENV illness has three distinct phases. The febrile phase, when a DENV patients experience high grade fever that usually accompanied by headache, myalgia, and vomiting. This phase lasts from 2-7 days. The critical phase is the time around the period of defervescence between 3-7 days of illness, when some DF patients develop severe symptoms of the disease. The recovery phase is the time when the symptoms are resolved and the disease parameters normalise.

Dengue case classification by severity

Dengue ± warning signs

Severe dengue



Criteria for dengue ± warning signs

Probable dengue

Live in/travel to dengue endemic area. Fever and 2 of the following criteria:

- Nausea, vomiting
- Rash
- Aches and pains
- Tourniquet test positive
- Leucopenia
- Any warning sign

Laboratory confirmed dengue

(important when no sign of plasma leakage)

Warning signs*

- Abdominal pain or tenderness
- Persistent vomiting
- Clinical fluid accumulation
- Mucosal bleed
- Lethargy; restlessness
- Liver enlargement >2cm
- *Laboratory:* Increase in HCT concurrent with rapid decrease in platelet count

* Requiring strict observation and medical intervention

Criteria for severe dengue

1. Severe plasma leakage

- leading to:
- Shock (DSS)
 - Fluid accumulation with respiratory distress

2. Severe bleeding

as evaluated by clinician

3. Severe organ involvement

- Liver: AST or ALT ≥ 1000
- CNS: Impaired consciousness
- Heart and other organs

Figure 1. 5 New DENV case classification by WHO in 2009 [6, reproduced with permission]

A new case classification of dengue diseases launched by WHO in 2009 according to the levels of severity into dengue without or with warning signs and severe dengue.

1.9 DENV diagnosis

Laboratory diagnosis of DENV infection can be achieved by detection of viral nucleic acids in blood or by serological tests. During the febrile phase, DENV RNA can be detected directly from a patient's blood by reverse transcription polymerase chain reaction (RT-PCR). Detection of DENV NS1 antigen by enzyme-linked immunosorbent assay (ELISA) or lateral flow-rapid test is also used for confirmation of DENV diagnosis. Serological analysis of immunoglobulin by ELISA is commonly used for DENV diagnosis in patient sera. Anti-DENV IgM antibodies can be detected for a couple of weeks after primary infection with subsequent seroconversion to IgG. The existence of IgG antibodies in high levels, during the acute phase of the infection, however indicates a secondary DENV infection [4,35]. One commonly used method for serological confirmation of DENV is by a rapid test for NS1 antigen in conjunction with anti-DENV IgM and IgG, for example the rapid immunochromatographic test [55,101].

1.10 Risk factors for severe DENV

To better understand DENV pathogenesis, multiple risk factors should be considered that contribute to severe DENV infection. Both host factors (age and genetic background) and viral factors (serotypes and genotype) have been linked to severe DENV disease [35,37,102].

1.10.1 Host factors

Several human factors have been associated with DENV disease severity. Severe DENV disease is more often observed in young children under 15 years of age than in adults [103]. This association is thought to be related to the difference in microvascular permeability between children and adults [104]. Certain human leukocyte antigen (HLA) class I alleles have been associated with susceptibility to DHF [105]. Another study showed a correlation between HLA and some DENV serotypes such as DENV-1 and HLA *0207 and DENV-2 and HLA *B52 [106]. Previous studies demonstrated that African or people of African ancestry are more resistant to severe DENV

illnesses [107]. Further, DENV infection may be life-threatening if it occurs in individuals with pre-existing medical conditions such as asthma, diabetes mellitus, and sickle cell anaemia [2]. others host factors have been also implicated including female sex [35], ABO blood group [108], and a single nucleotide polymorphism in tumour necrosis factor- α (TNF- α) gene [109]. Additionally, gene expression profiling of blood samples obtained from DHF-infected patients shows a clear induction of a host immune response-associated genes including cell surface markers, T- and B-cells lymphocyte markers, and innate response components (cytokines and interferons) [110]. Thus, many host cell factors are involved in regulating DENV infection and associated with pathogenesis. Our laboratory has investigated the role of host cell enzyme, sphingosine kinase 1 and 2 in DENV infection, and this will be our focus during this project and is described in section 1.16.

1.10.2 DENV factors

All DENV serotypes can be responsible for dengue diseases. The four DENV serotypes are also phylogenetically further sub-divided into genotypes (Figure 1.6), which have distinct geographical distributions [111]. The antigenic differences among DENV serotypes has been proposed to be a determinant of the severity of disease outcome [112]. For example, DENV-2 serotype was initially thought to be associated with severe diseases. DENV-2, for instance, is additionally classified into many genotypes such as American and Asian-type viruses. Generally, the Asian-type genotypes have been suggested to be more virulent and associated with severe disease compared to the American-type genotypes [37]. Additionally, Asian DENV-2 isolates (Thai strain) have been demonstrated to replicate to higher titres in monocyte derived-macrophages (MDMs) and DCs than American isolates, suggesting a high replication ability of Asian DENV-2 strain in human cells [113,114]. The amino acid at the position 390 of E protein and particular sequences in the 5' and 3' UTRs have been suggested as determinants of DHF [115].

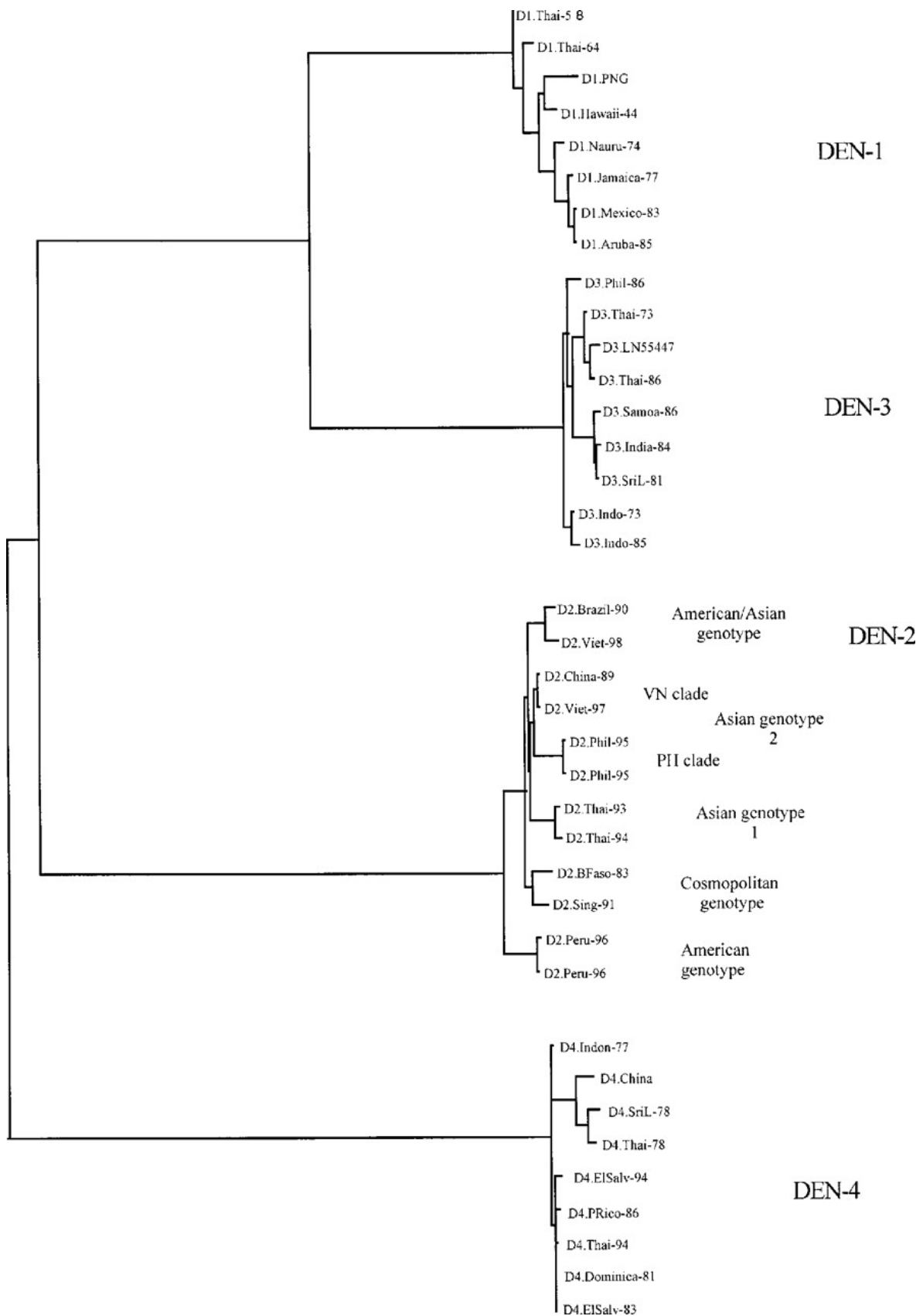


Figure 1. 6 DENV phylogenetic tree depicting the relationship within and among DENV serotypes and genotypes [116]

1.11 Pathogenesis of severe DENV

Strong evidence from multiple observations suggest that there is a higher risk for developing severe DENV disease during a secondary infection with a serotype different from that of primary infection [5,117]. One explanation for increased incidence of DHF/DSS is the presence of non-neutralising, cross-reactive antibodies formed during primary infection that bind to the virus and enhance its binding to Fc γ -receptor bearing cells, such as monocyte and macrophages, resulting in increased DENV replication and functional alterations within these important target cells. This phenomenon is known as antibody-dependent enhancement (ADE) of disease [5]. Mononuclear phagocytes are considered the main targets for DENV infection under ADE conditions [118]. The model of ADE also proposes an explanation for increased DF/DHF in infants born from dengue-immune mothers [119]. The ADE could promote DENV infection to a large number of permissive cells and subsequently increase the viral load and trigger the effector immune response including increased cytokine production that may result in increased capillary permeability [5]. Thus, ADE is proposed to occur in secondary DENV infection to exacerbate the disease and increase the risk for developing of DHF.

Induction of T-cells in response to DENV infection has an important role in viral clearance but can also contribute to severe DENV. A model of “original antigenic sin” has been proposed as a role of cross-reactive memory T-cells during secondary infection. The cross-reactive memory T-cells are reactivated during secondary infection specific for previous DENV serotype not the current different serotype [120]. This activation of the memory T-cells may further promote the production of inflammatory cytokines that can act on the endothelium leading to vascular leakage, and/or a delay in viral clearance since the cross-reactive memory T-cells show a low affinity for the present DENV serotype with high affinity for the prior serotype [121].

One of the main effectors of severe DENV disease are inflammatory or vasoactive cytokines and chemokines that are proposed to play an indirect role in the immunopathogenesis of DENV due to

their effects on vascular endothelial cells. Such cytokines can influence the integrity of the vascular endothelium causing loss of fluids and proteins into the extravascular space. Several studies have demonstrated that the levels of several key vasoactive cytokines are elevated in the circulation of patients during severe DENV infection such as IFN- γ , TNF- α and IL-2, IL-6, IL-8 and IL-1 β [122]. In particular, high concentrations of pro-inflammatory (IFN- γ , TNF- α) and anti-inflammatory (IL-10) cytokines have been detected in the blood of DHF patients from Vietnam [123], India [124], and Cuba [125]. Elevated levels of TNF- α has been detected in the sera from DENV-2 infected mice that has been associated with vascular leakage and a higher mortality rate. Treatment with anti-TNF- α antibodies significantly reduced the mice mortality rate [126], suggesting an important role of this cytokine in the pathogenic mechanisms of DENV-induced vascular leakage in mice. *In vitro*, TNF- α is released at high levels in DENV-infected cells [127], while blocking of TNF- α in a supernatant from DENV-infected cells blocks the ability to induce EC permeability [128].

Secreted NS1 and anti-NS1 antibodies have been shown to be involved in DENV pathogenesis by cross-reacting with surface molecules on endothelial cells and platelets, suggesting a phenomenon known as antigenic mimicry [129,130]. The cross-reactivity of anti-NS1 antibodies to platelets and endothelial surface proteins is proposed to lead to platelets dysfunction and endothelial cell damage and subsequently thrombocytopenia and plasma leakage [129]. The ability of NS1 to cross-react with platelets and the endothelium correlates with C-terminus of NS1 [130], where removal of this region abolished the effect of NS1-mediated platelet dysfunction [131]. Additionally, recently DENV NS1 has been demonstrated to directly induce vascular leak via interaction with TLR4 and this leak is inhibited by treatment with TLR4 agonist and TLR4 blocking antibodies [56,57].

Soluble DENV NS1 can also mediate the activation of complement where binding of non-neutralising anti-NS1 antibodies to NS1 on infected cells triggers the complement components attack. Further, NS1 diminished the activation of complement pathways through interaction with C4 protein [132]. High-level secretion of complement proteins at the endothelial surface give rise to production of pro-inflammatory cytokines that are associated with vascular permeability during

DHF [133]. Thus, in addition to the role of the complement system in protecting against DENV infection, complement may also contribute to severe DENV disease.

1.12 DENV immune responses

1.12.1 Innate immune response and DENV innate immune evasion

The innate arm of the immune system represents the first line of the host defences against DENV infection. Innate immune responses to an invading pathogen are initiated following recognition of foreign components, known as pathogen-associated molecular patterns (PAMPs) by host sensor molecules, known as pattern recognition receptors (PRRs) [134]. The Toll-like receptor (TLR) family are PRRs that can recognise viral PAMPs including TLR3 (dsRNA) [135], and TLR7 and TLR8 (ssRNA) [136]. In the context of DENV infection, TLR3 within endosomes, and the cytosolic retinoic-acid inducible gene I (RIG-I), and melanoma differentiation-associated gene 5 (MDA5) cellular sensors are involved in the recognition of DENV RNA [137,138]. Further, TLR7 can detect DENV RNA within the endosome of plasmacytoid DCs (pDCs) [139]. Recognition of DENV RNA by PRRs triggers downstream signalling pathways including phosphorylation of interferon (IFN) regulatory factor 3 and factor 7 (IRF3 and IRF7) and activation of nuclear factor-kappa B (NF- κ B) through adapter molecules (such as MyD88, and STING), which then translocate to the cell nucleus to induce production of IFNs and cytokines [140,141]. Type I (IFN- α/β) IFNs are then secreted outside the cells and initiate amplification of the antiviral signal through binding to specific IFN receptors (IFNAR) that exist on the surface of the most cell types. Binding of IFNs to their receptors induces the activation of the JAK/STAT signalling pathway, and the association of STAT molecules with IRF9 induces translocation to the nucleus to stimulate the transcription of diverse antiviral factors known as interferon-stimulated genes (ISGs) [142,143] (Figure 1.7). Production of IFNs and subsequent induction of ISGs creates an antiviral state that restricts the virus spreading within the host.

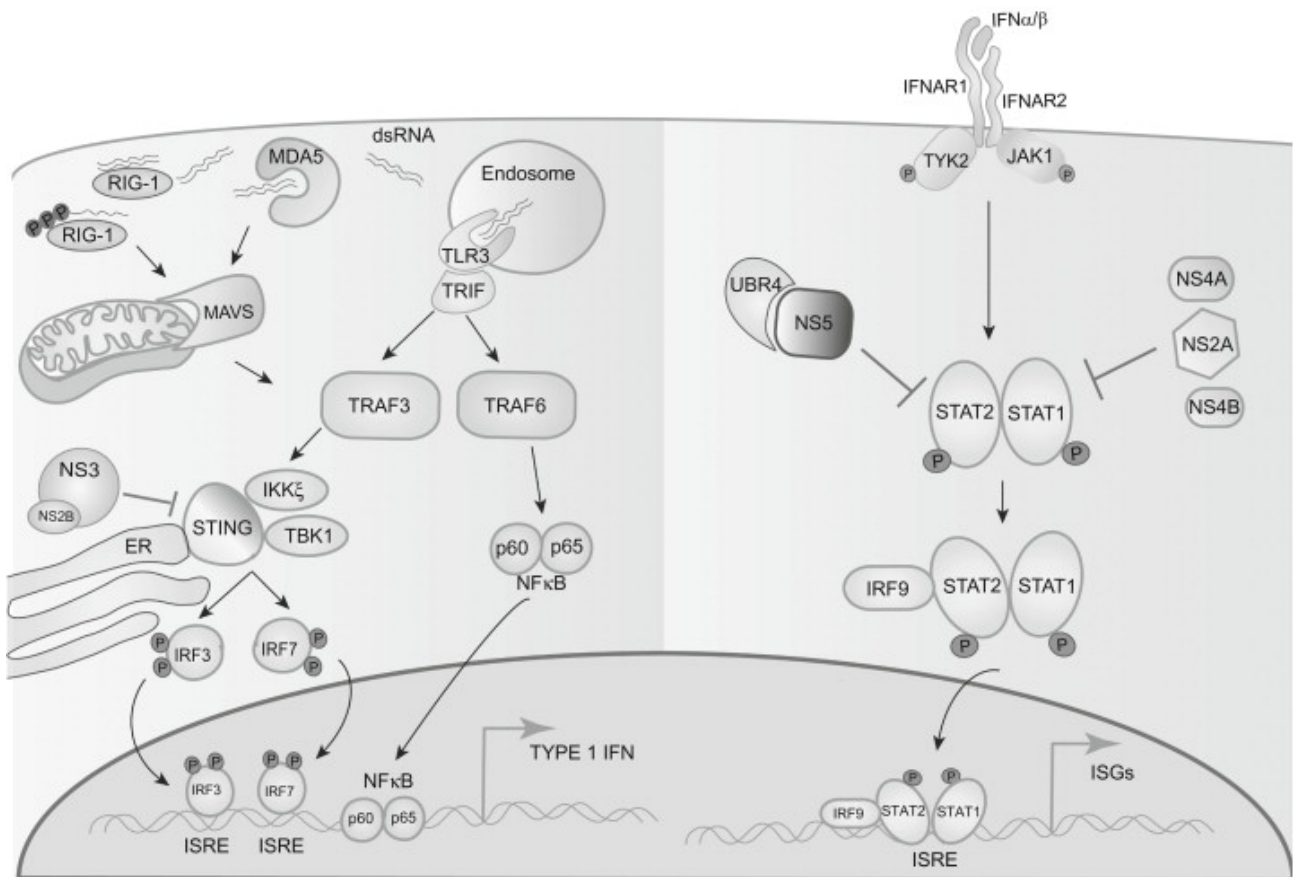


Figure 1. 7 Schematic representation of dsRNA sensing, IFN production, and ISGs induction [36, reproduced with permission]

Left panel: DENV dsRNA is recognised by TLR3, MDA5, and RIG-1 that results in activation of the STING molecule, phosphorylation of IRF3 and IRF7 and production of type I IFN. The DENV NS2B-3 protease blocks STING and antagonise the production of type I IFN. **Right panel:** Type I IFN bind to IFNAR leads to stimulate the activation of JAK/STAT1 and 2 pathways, interaction of IRF9 with STAT1 and 2 which altogether translocate into the nucleus to induce ISGs expression. The DENV NS2A, and NS4A and NS4B blocks STAT1, while NS5 inhibits STAT2 resulting in inhibition of type I IFN signalling.

IFNs, particularly type I IFN (α/β) are a potent antiviral factors and DENV needs to overcome IFN (α/β) immune responses to establish an infection. DENV has developed multiple mechanisms to antagonise both the induction of IFN and IFN signalling. The DENV NS2B/NS3 protease targets the human STING adapter molecule and inhibits the induction of type I IFN production [144]. In contrast, however, NS2B/NS3 cannot bind to mouse STING [144], suggesting a critical role of the interaction of NS2B/NS3 with STING in immune evasion and providing a rationale for the species specificity and lack of DENV infection in immunocompetent mice, as described in section 1.14.2. Another DENV strategy to inhibit type I IFN signalling is mediated by the NS5 protein that degrades human STAT2 to reduce IFN signalling [145]. Similar to the case above for STING, DENV NS5 cannot bind to mouse STAT2, again making this mechanism of immune evasion ineffective in mice and supporting this as an additional reason for the lack of DENV infection in mice [145]. Additionally, the *flavivirus* NS5 protein has also been shown to inhibit type I IFNs signalling by suppression of maturation and surface expression of IFNAR [146].

1.12.2 Viperin, an interferon-stimulated gene

The production of type I IFN-driven ISGs represents an early rapid immune response to viral infection. Of these ISGs, viperin (virus inhibitory protein, ER-associated, IFN-inducible) has shown direct antiviral activity against a wide group of viruses [147,148]. Viperin, also known as cig 5 and RSAD2, is a protein of ~ 42 kDa that is highly conserved between species. Viperin was first identified as a protein induced by human cytomegalovirus (HCMV) infection in human primary fibroblasts [149,150]. Several factors have been shown to induce viperin expression including IFN- α , - β , and - γ , lipopolysaccharide (LPS), poly (I:C), and a multitude of viruses [147,148]. Viperin is either induced dependent on the production of type I and II IFNs or directly independent on IFNs through other mechanisms including IRF1 and IRF3 driven pathways [151,152].

Human viperin is composed of three distinct domains, a variable N-terminal domain that contains an amphipathic α helix with a leucine zipper region, a centrally located radical S-

adenosylmethionine (SAM) domain, and a highly conserved C-terminal domain. The amphipathic α helix mediates the association of viperin onto the cytoplasmic face of the ER and lipid droplets [153,154], while the role of C-terminal domain remains unknown. The C-terminal domain, however is required for antiviral activity of viperin against hepatitis C virus (HCV) and DENV [155,156]. The central viperin domain contains 4 motifs that characterise the radical SAM family enzymes with one motif that carries the CxxxCxxC sequence responsible for binding iron-sulfur clusters [157,158].

Transcription of viperin is very low in unstimulated cells but is induced in response to a wide variety of viruses and other agents. For example, viperin is induced by HCMV infection in human fibroblasts, which in turn inhibits viral replication by decreasing the expression of the late viral structural proteins gB, pp28, and pp65 [150]. Induction of viperin expression is observed following Influenza A virus (IAV) and HIV-1 infections that inhibits viral infection through blocking viral release from the plasma membrane through effects on cellular lipid rafts [159,160]. Further, viperin has been reported to limit HCV replication by interaction with host human vesicle-associated membrane protein-associated protein of 33 kDa (hVAP-33) that impedes hVAP-33 association with the HCV NS5A protein [161], and/or the association of HCV NS5 with the host factor VAP-A at HCV VRCs [155]. Infection with the *flavivirus* WNV has also been shown to stimulate viperin induction, which restricts viral replication through suppression of viral RNA and/or protein synthesis steps [162]. In terms of DENV, another virus of the genus *flavivirus*, viperin expression is induced following DENV infection in multiple settings including human [163], macaques [164], mouse [165], and cultured cells [156,162,166,167]. A previous study from our laboratory has shown that viperin inhibits DENV replication *in vitro* by reducing viral RNA replication where the C-terminal part of viperin is required for its anti-DENV activity [156]. Further, viperin is co-localised in association with the DENV C protein, viral RNA, and NS3 on the surface of ER-derived lipid droplets, in which the interaction with NS3 proteins enhanced antiviral function of viperin against DENV infection [156]. Since viperin is rapidly induced following viral infection to

play an important antiviral role in controlling infections, other roles in modulating the innate immune signalling have been investigated and viperin has been shown to act independent of IFN to regulate TLR7 and TLR9 recognition of the viral nucleic acids in pDCs to promote production of the type I IFNs [168]. Notably, viperin has been shown to be antiviral against WNV infection in the mouse brain, and this is the premise of the study in chapter 6 and will be discussed in more detail in that chapter.

1.12.3 Adaptive immune response

Primary infection with one DENV serotype confers long-term protective immunity specific to that serotype. This protection is mediated by DENV-specific antibodies, DENV-specific memory T-cells, or both [169]. The antibody (humoral) response plays an important role in controlling DENV infection, dissemination and clearance from the body [24]. The DENV-specific antibody response is also vital in providing memory and protection from reinfection with a homologous DENV serotype. The antibody response to DENV infection, however, may also play a critical role in pathogenesis, as discussed in section 1.9, through the production of cross-reactive but non-neutralising antibodies that are recalled during a secondary heterotypic DENV infection. The E, prM, and NS1 glycoproteins are the main targets for the specific antibody response during DENV infection in humans with a weak response to DENV NS3 and NS5 proteins [121]. The main function of humoral immunity is to neutralise DENV infection. Neutralising DENV antibodies are primarily directed against the viral E protein, interfering with viral attachment to specific cell-surface receptors, and inhibition of post-binding fusion and internalisation [24,121].

Like the antibody response, the T-cell immune response plays a vital role in defence against DENV infection and viral pathogenesis. Immune T-cells respond to DENV infection by the recognition of T-cell epitopes that are expressed on almost all DENV proteins [170]. These epitopes are presented on the surface of DENV-infected cells in association with class II and I MHC specific for CD4+ and CD8+ T-cells respectively. Most of the T-cells epitopes, for both CD4+ and CD8+ T-cells, are

found in the DENV NS3 protein [121]. Specific T-cells exhibit anti-DENV functions by direct lysis of DENV-infected cells and production of cytokines. The cytokines secreted by DENV specific T-cells including IFN- γ , TNF- α , IL-2, and CC-chemokine ligand 4 (CCL4, also known as MIP-1 β), which also have been shown to contribute in DENV pathogenesis [171-173]. In addition to the protective role of the T-cells against DENV during primary infection, these cells also contribute to viral pathogenesis following infection with heterologous DENV serotypes. Cross-reactive memory T-cells, which are produced during the first exposure to DENV infection, can recognise either the conserved or the altered peptide ligand epitopes upon secondary DENV infection and become activated [2,24] as described in section 1.11. The activated memory T-cells are proposed to exacerbate DENV disease in a secondary infection caused by a heterologous DENV serotype through elevated production of inflammatory or vasoactive cytokines that resulted in vascular leakage and/or impaired clearance of viral infection [120,121], again as outlined in section 1.11.

1.13 DENV prevention and control

DF is a self-limiting disease and in most people will resolve spontaneously. Currently, there is no specific antiviral drugs available for treating DENV although inhibitors of DENV NS3 and NS5 proteins are promising avenues [7]. Generally, treatment is supportive including fluid replacement or platelet transfusion in severe cases [4]. The difficulty in determining who will develop severe DENV puts a burden on health systems, particularly in low socioeconomic regions and areas endemic for DENV that must manage high numbers of DENV cases.

The development of a safe and effective DENV vaccine that induces a balanced immune response has been a challenge. A number of DENV vaccine candidates are under development including chimeric, live-attenuated, recombinant, and inactivated vaccines [174]. The main goal of a vaccine is to elicit neutralising antibodies against DENV E protein. A tetravalent chimeric DENV vaccine (Dengvaxia) developed by Sanofi Pasteur (Lyon, France) is the first-licensed vaccine that has been approved for use in some countries including Mexico and Philippines [175,176]. Dengvaxia is only

licensed for use in children > 9 years old and has reported low efficacy in protection against DENV-2 infections in particular. Thus, the likely success of introduction of this vaccine has been questioned [177]. The impact, however of Dengvaxia on the incidence of DENV in countries where vaccination has been introduced remains to be seen.

Some new approaches have been developed towards controlling DENV via control of the numbers and transmission competence of the mosquito vector. The introduction of the *Wolbachia* bacterium into *A aegypti* has been demonstrated to reduce the ability of the mosquito to transmit DENV by both reducing the insect's lifespan, inhibiting DENV replication within the mosquito and reducing the viable offspring produced from the mosquito [178]. The *Wolbachia* infection in the mosquito has been released in parts of Northern Australia in DENV-endemic regions, which has successfully stabilised the *Wolbachia* containing *A aegypti* in the mosquito population over several years [179]. Similarly, *Wolbachia*-mediated vector control strategies have been implemented in countries such as Thailand [180], Brazil and Indonesia [181], and the impact on the incidence of DENV infection remains to be described.

1.14 DENV animal models

No comprehensive animal model that reflects infection, host responses and mimics human disease is available to study DENV pathogenesis. The development of an appropriate animal model for DENV infection has been a challenge due to the low replication levels of DENV clinical isolates in wild type mice (WT) and the absence of clinical illness in non-human primates (NHPs) [182]. Many studies have been undertaken to develop animal models that provide reliable information regarding DENV pathogenesis that are relevant to natural DENV infection in human, as summarised below.

1.14.1 Non-human primate (NHP) models

NHPs such as Monkeys have been thought to be a best model for investigating DENV pathogenesis since they have immune responses similar to that of humans. However, DENV strains isolated from

these animals are genetically different from those isolated from humans [183]. Additionally, NHPs replicate DENV to high titres in the circulation but do not show signs of severe infection, only mild symptoms at best [24]. Thus, NHPs are not reliable models used to study the mechanisms of DENV pathogenesis, but they are widely accepted as useful models to test the safety and efficacy of DENV vaccine candidates [184].

1.14.2 Mouse models

Initially the use of mice as models to study DENV infection was difficult because most DENV human isolates were unable to replicate well in this species [185]. Several murine models have been established to study DENV pathogenesis such as immunocompetent WT, interferon-receptor deficient, and humanised mouse models [184,186].

IFN- α/β and γ receptor deficient (AG129) mice have been utilised to investigate DENV pathogenesis where the IFN response is disrupted to enhance the susceptibility of mice to DENV infection [187]. DENV-2 strain (D2S10) inoculation via the iv route in AG129 mice induced plasma leakage and increased TNF- α serum levels [188]. Further, infection of the AG129 mouse with a high dose of DENV-2 D2Y98P strain through intraperitoneal route (ip) results in acute infection model characterised by viremia, production of pro-inflammatory cytokines and vascular leakage, damage to the mouse spleen and liver dysfunction [189]. The AG129 mouse model has its caveats in that there is no innate IFN response to infection, but it is a widely used model of DENV infection to study some aspects of pathogenesis *in vivo*. The AG129 mouse however is not optimal to study immune responses, particularly innate responses against DENV infection since these mice lack IFN responses - the most important first-line defence against viral infections such as DENV and our focus of interest here.

Humanised mice are beneficial to define human cell responses to DENV infection and overcome the species specificity of immune evasion strategies, discussed in 1.12.1. Severe combined immunodeficiency (SCID) mice, which are deficient in T- and B-cells, are permissive to DENV

infection after these mice are engrafted with human cells [190]. Prior to DENV infection, human tumour cells are engrafted into SCID mice followed by DENV challenge. DENV replicates within the SCID-tumour engrafted cells and will disseminate to infect other tissues giving rise to disease symptoms [182]. For instance, SCID mice have been transplanted with HepG2 cells followed by intraperitoneal (ip) DENV challenge, which results in DENV detection in the liver, serum, brain, lung, and small intestine within the SCID-HepG2 mice and signs of disease such as paralysis, elevated serum levels of TNF- α , and thrombocytopenia [191]. The humanised mouse model, however is not ideal to study DENV immune response since these mice have a defect in B-cells immune responses [192].

Immunocompetent WT mice are relatively resistant to DENV infection due to their intact immune system and lack of effective DENV immune evasion strategies for innate and IFN-responses, as described in 1.12.1, although they have been used to define some aspects of DENV pathogenesis. Direct intracranial (ic) injection of DENV-3 genotype I and DENV-2 New Guinea C strain can induce lethal encephalitis in C57BL/6 and BALB/c WT mice respectively [193,194]. Further, infection of C57BL/6 mice with DENV-2 16681 strain caused systemic haemorrhage after intradermal (id) injection [195], and caused liver dysfunction after intravenous (iv) infection [196]. Here, in our study, we aimed to utilise an immunocompetent C57BL/6 WT mouse model infected by the ic route, to test the role of the host factors, sphingosine kinases and viperin in DENV-2 infection.

1.15 Sphingolipids and sphingosine-1-phosphate

Sphingolipids are important for providing structural elements to the membranes of cells but also possess important signalling ability that regulates a wide range of cellular functions such as cell death, survival, and proliferation [197]. Sphingolipid metabolism occurs at the cytosolic surface of the ER resulting in the synthesis of bioactive metabolites including ceramide, sphingosine, and sphingosine-1-phosphate (S1P) (Figure 1.8) [198]. Ceramide, the central molecule in sphingolipid

metabolism, enhances growth arrest and apoptosis in response to various cell stress inducers, and thus is known as a pro-apoptotic molecule [199]. Similarly, the lipid sphingosine has been also associated with cell death [200]. Unlike ceramide and sphingosine, the bioactive S1P molecule promotes cell growth and proliferation [201]. The S1P lipid regulates a wide variety of important cellular events including cell survival, differentiation, angiogenesis, inflammation, and lymphocyte trafficking [202]. Further, S1P has dual signalling roles either intracellularly as a second messenger or is transported outside the cells and acts as a ligand for a family of five G protein-coupled S1P receptors (S1P₁₋₅) [203]. The cellular levels of S1P are regulated by two distinct enzymes: sphingosine kinase (SK) that catalyses the phosphorylation of sphingosine to produce S1P, and S1P lyase that mediates S1P degradation [204]. Control of the levels of ceramide and sphingosine, the pro-apoptotic lipids, versus the levels of pro-survival S1P is critical in determining cell fate, and maintaining the so-called “sphingolipid rheostat” [205]. SK plays a pivotal role in determining this balance of ceramide, sphingosine and S1P in the cell, and has been the central focus of our laboratory studies in the context of a DENV infection.

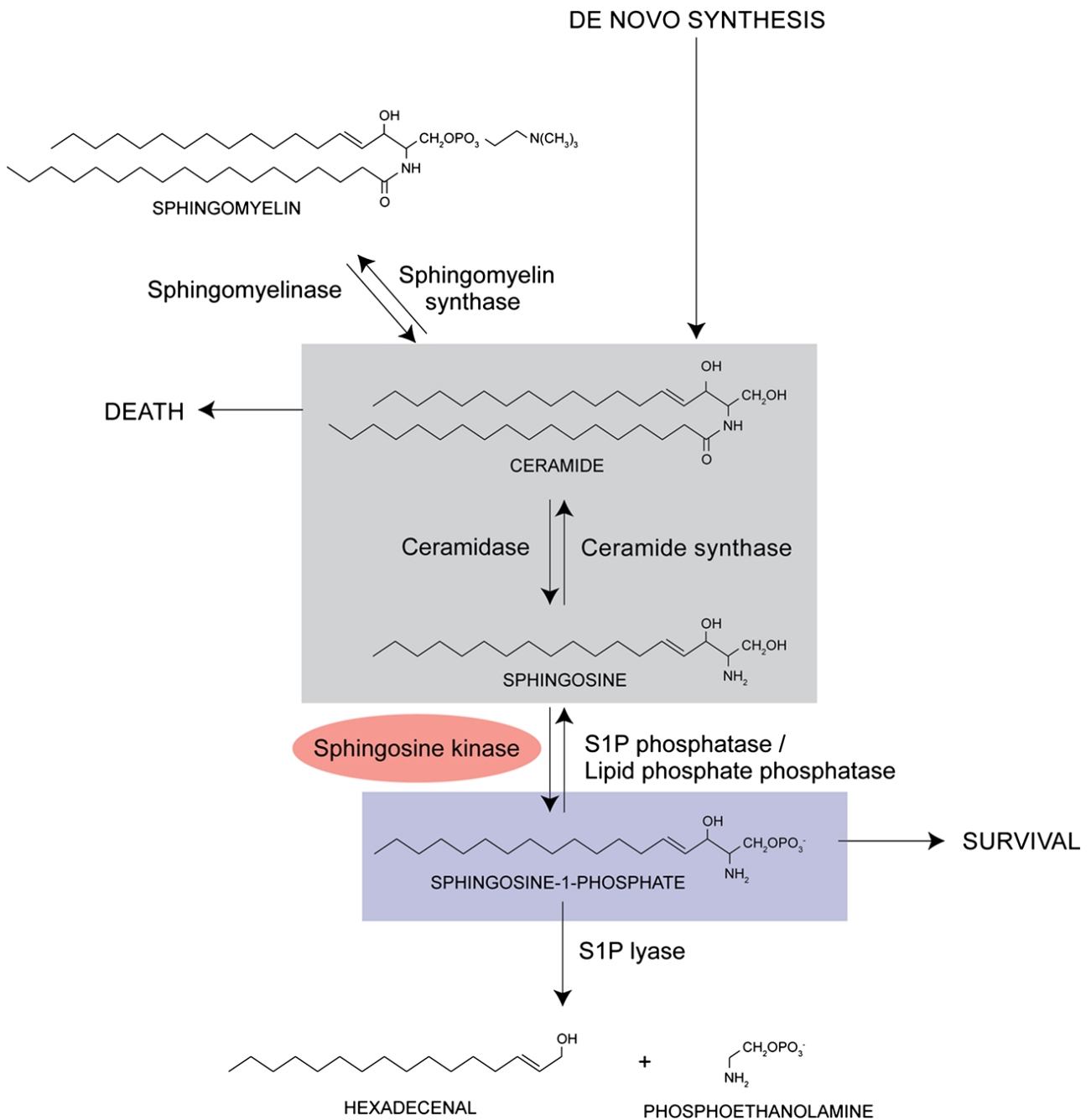


Figure 1. 8 Sphingolipid metabolic pathway [206, reproduced with permission]

The sphingolipid ceramide is generated de novo and then be either converted reversibly to form sphingomyelin or sphingosine. Both ceramide and sphingosine enhance cell death. Sphingosine kinases 1 and 2 phosphorylate the lipid sphingosine to produce sphingosine 1 phosphate (S1P) that enhances cell survival. The S1P is degraded in a non-reversible reaction by the action of S1P lyase.

1.16 Sphingosine kinases (SKs)

SKs are evolutionally conserved kinase enzymes that together with diacylglycerol (DGK) and ceramide kinases constitute a novel family of structurally related proteins [203]. As described in Figure 1.8, SK is the key enzyme in the sphingolipid metabolic pathway since it represents an important regulator for the levels of the main three bioactive products ceramide, sphingosine, and S1P in this system. Five highly conserved domains (C1-C5) have been identified in the polypeptide sequence of SKs [207]. The C1-C3 region contains the catalytic domain of SKs while C2 has the ATP-binding site at SGDGX₁₇₋₂₁K [208]. The C4 domain is present and conserved only in SKs and contains the recognition site for sphingosine [209] while the C5 domain is conserved in DGK and ceramide kinases [210]. The SK enzymes exhibit biological roles such as promoting cell survival and proliferation and thus have been the focus of interest in relation to cancer. Two human SK isoforms have been characterised, designated SK1 and SK2, which are encoded from two different genes, *SPHK1* and *SPHK2* (Figure 1.9) [205]. The SK isoforms share a high degree of sequence similarity [205], however they differ in size, tissue distribution, subcellular localisation, and catalytic properties [211], suggesting they have divergent physiological but complementing roles [212].

1.16.1 SK1 and SK2 isoforms

SK1 is a protein of 49 kDa and was the first mammalian SK isozyme to be cloned [213] followed by the cloning of the second SK isoform, SK2 of 65 kDa [214]. Unlike SK1, SK2 contains two extra regions located in the N-terminal and central part of the protein [214]. The SK1 enzyme is localised to the cell cytosol while SK2 resides in the ER and nucleus [205]. Both SK1 and SK2 catalyse the phosphorylation of the sphingosine substrate to yield S1P, as illustrated in Figure 1.8. The expression level of SK isoforms is variable among different tissues. SK1 is highly expressed in lung and spleen while SK2 is prominent in liver, heart, kidney and brain [213,214]. The physiological function of the SKs is quite different; in particular, the role of SK2 seems to be

complicated. Single knockout mice either SK1^{-/-} or SK2^{-/-} are viable and fertile suggesting they have a partially redundant role, while the double knockout and absence of both SK isoforms is lethal at the embryonic stage due to severe defects in neurogenesis and angiogenesis [215]. Initial studies however demonstrated that the SK1 isoform enhances cell survival and proliferation whereas SK2 has opposing function in promoting cell death [216]. This has, however, been questioned with studies also suggesting that SK2 is a growth promotor [217]. Both SK1 and SK2 isozymes are highly expressed in a number of solid tumours and targeting their activity or reduction in their levels using selective anti-SK1 and anti-SK2 compounds reduced the progression of cancers [218].

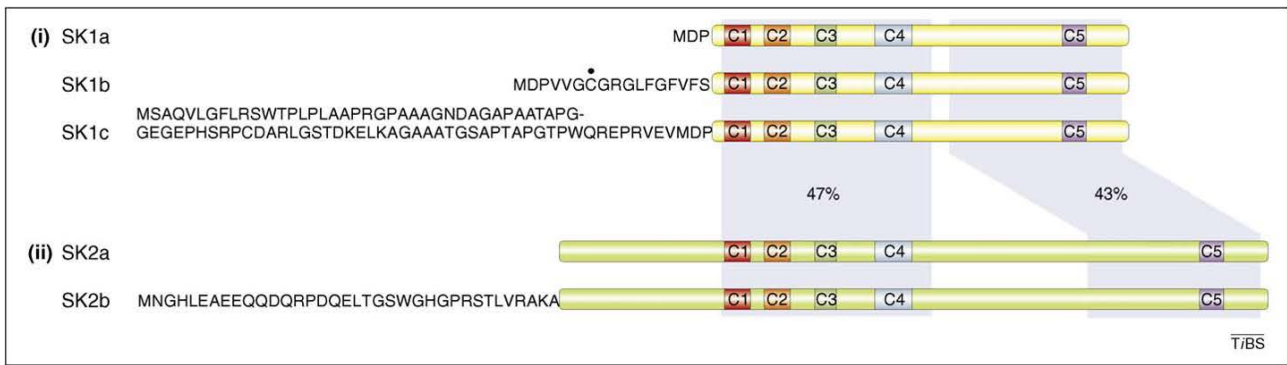


Figure 1. 9 Human SK1 and SK2 [205, reproduced with permission]

SK1 and SK2 contain five highly conserved regions designated C1-C5. SK1 and SK2 share sequence identity with 47% at N-terminal and 43% at C-terminal amino acids sequence identity. Three SK1 isotypes has been identified SK1a, b, and c that differ in their N-terminus end, while SK2 has two isoforms SK2a and b. Two extra regions exist in the N-terminal and central regions of SK2.

1.16.2 SKs activation and subcellular localisation

The SK1 enzyme has intrinsic catalytic activity independent of post-translational modification [219]. Under normal physiological conditions, the basal activity of SK1 maintains the ceramide and S1P balance within the cells. Upon exposure to a various stimuli including growth factors and cytokines, the catalytic activity of SK1 is enhanced and subsequently induces SK1 signalling function. An increase in SK1 activity following cytokine stimulation is due to the phosphorylation of SK1 at Ser225 that is mediated by extracellular signal-regulated kinases 1/2 (ERK1/2) while the SK1 affinity for sphingosine and ATP is not altered [220]. Of note, the SK1 phosphorylation at Ser225 also promotes translocation of SK1 from the cytosol to the plasma membrane, where SK1 has increased access to the substrate, sphingosine [220]. Calcium and integrin binding protein-1 (CIB1) is required for translocation of SK1 to the plasma membrane [221]. Factors that are known to stimulate SK1 include TNF- α , while hypoxic condition and elongation factor 1A have been described as stimuli of SK2 activity [211]. The activation of SK1 in most cases is transient due to dephosphorylation of SK1 at Ser225 by the action of protein phosphatase 2A (PP2A) enzyme [222]. Like SK1, SK2 activity is increased in response to external stimuli that induce SK2 phosphorylation at Ser351 and Thr578 by ERK1/2 [223]. The SK2 enzyme exists in nucleus and cytoplasm under normal condition but the SK2 distribution can be altered in some circumstances. SK2 is abundant in the ER during serum starvation, and decreased following protein kinase C activation [216,224].

1.16.3 SKs in viral infection

Newly described roles for SKs in viral infections have been emerging with studies implicating the SK1 enzyme in virus replication and pathogenesis [206]. A study by Machesky *et al.*, demonstrated that infection with human cytomegalovirus virus (HCMV) resulted in an increase the activity of SK1. This study also reported that SK1 overexpression enhances the accumulation of HCMV immediate early protein (IE1), reflecting viral replication, whereas inhibition of SK1 expression reduces virus production. Together, these results suggested that SK1 is important for HCMV

infection. Further, the increase in SK1 activity reportedly prolongs the survival of HCMV-infected cells [225]. Similarly, infection of lung epithelial cells with respiratory syncytial virus (RSV) increases the activity of SK1, which in turn activates ERK and Akt pathways, and increases the levels of S1P, which creates an environment that has been suggested to enhance RSV RNA replication [226]. In addition, overexpression of SK1 increases the susceptibility of cells to influenza A virus (IAV) infection and viral-induced cytopathic effect (CPE). These effects were associated with suppression of STAT1 activation suggesting a beneficial role for SK1 in promoting IAV replication via inhibition of STAT1 activation and thus also IFN stimulated pathways [227,228]. In contrast to the effect of overexpression of SK1, S1P lyase overexpression reduced IAV replication and enhanced STAT1 activation. These data suggesting an opposing role for S1P metabolising enzymes in modulating IAV infection [227]. Further, IAV infection is reported to increase SK1 expression and activation, which was thought to be important for efficient viral replication. Chemical inhibition of SK1 during IAV infection, however suppressed the activation of the NF- κ B pathway and subsequently reduced viral RNA and protein synthesis [229]. SK1 overexpression has been shown to increase measles virus replication and its CPE, while chemical inhibition of SK1 reduced viral replication. Further, the inhibition of SK1 affects measles virus-induced NF- κ B activation and suppressed viral protein synthesis [230]. Infection with bovine viral diarrhoea virus (BVDV), a *pestivirus* of the Flaviviridae family and thus related to DENV, inhibits SK1 catalytic activity through interaction with the viral NS3 protein to promote viral replication and pathogenesis. In support of this, chemical inhibition or siRNA-mediated knockdown of SK1 enhanced BVDV replication [231]. These various interactions of SK1 with viral infection are summarised in Table 1.1.

Table 1.1 Contrasting effect of SK1 on viral infection

Virus	Effect of infection on SK1	Effect of targeting SK1 activity	Infection outcome	Reference
RSV	increases SK1 activity and mRNA	Inhibits ERK and Akt pathways	Delays RSV-induced cell death	[226]
HCMV	increases SK1 activity and mRNA	Reduce HCMV IE1 protein expression	increases HCMV replication	[225]
BVDV	Reduces SK1 activity	Unknown	Increases BVDV replication and cell death	[231]
IAV	increases SK1 activity	Suppresses IAV-induced NF- κ B activation and reduces nuclear export of viral nucleoprotein complex	Increases IAV replication and protein synthesis	[227,229]
Measles	increases SK1 activity	Suppresses measles-induced NF- κ B activation	Increases measles replication and protein expression	[230]
DENV	Reduces SK1 activity	Enhances DENV cytopathic effect	Increases TNF- α induced cell death	[232,233]

In the context of DENV infection, data from our laboratory has shown that infection in HEK293 cells and a number of other cell types with DENV-2 causes a reduction in SK1 activity, late in the course of infection *in vitro* (48-72 hpi). This late reduction in SK1 during DENV infection was correlated with enhanced TNF- α -induced cell death and reduced TNF- α -induced NF- κ B activation [232]. Further, alterations in SK1 activity by either overexpression or chemical inhibition after DENV infection of HEK293 cells did not affect viral infection but enhanced viral induced-cell death [233]. In contrast in primary human ECs, our laboratory has shown that the activity of SK1 is increased early in infection (24 hpi) with DENV [166]. Further, targeting SK1 activity by selective SK1 inhibitors prior to DENV challenge in HEK293 restricts viral infection while overexpression of SK1 does not alter DENV infection [167]. Additionally, DENV infection in mouse-embryonic fibroblasts (MEFs) that lack the SK1 gene resulted in a reduction in viral infection in immortalised MEFs (iMEFs) but enhancement in primary MEFs (1^oMEFs) [167], a finding that was demonstrated to correlate with enhanced basal level of ISGs in the iMEF system.

In contrast to SK1, very few studies have investigated the role of SK2 during viral infection. The SK2 enzyme has been demonstrated to maintain the latency of Kaposi's sarcoma-associated herpesvirus (KSHV) where selective targeting of SK2 to inhibit SK2 activity induces the survival of KSHV-infected ECs [234]. Another study has shown that lipid peroxidation regulated in part through changes in SK2 activity reduced HCV replication *in vitro* and in a HCV-strain dependent manner [235]. Recently, a study conducted by Reid *et al.*, 2015, has described a role for SK2 in promoting infection with chikungunya virus (CHIKV) in HepG2 liver cells [236]. Chemical inhibition of SK2 and siRNA-mediated knockdown of SK2 dramatically reduced CHIKV infection. Further, SK2 was co-localised with CHIKV RNA and its VRC during viral replication supporting a role for this enzyme in assisting the viral replication process [236]. Since we have observed changes in SK1 during DENV infection, a similar role of SK2 as seen in CHIKV infection will be interesting to also investigate during DENV infection and is the focus of chapter 5.

1.17 Hypothesis and aims

Our overall laboratory goal is to define the host cell factors that influence DENV replication and may be useful targets for future antiviral or modulatory therapies. From the accumulating literature suggesting a role for SK1 and SK2 in viral infections, in combination with our novel *in vitro* data for SK1, we **hypothesise** that SK1 also plays a role in promoting DENV infection that is associated with changes in innate immune responses such as viperin gene induction. Additionally, a similar role in promoting DENV infection may also be performed by SK2. Further, since our previous laboratory data demonstrated a role for the ISGs viperin in restricting DENV infection *in vitro*, we also **hypothesise** that this antiviral factor can reduce DENV infection *in vivo*. Specifically, this study aimed to:

1. Further define the role of SK1 during DENV infection *in vitro* and *in vivo*
2. Provide the first investigation of the role of SK2 during DENV infection *in vitro* and *in vivo*
3. Define the role of the ISGs viperin during DENV infection *in vivo*

To achieve these objectives, we will inhibit the activity of SK1 and SK2 in various cells using selective or non-selective SK1 and SK2 inhibitors prior to DENV infection and perform infections in cell lines genetically lacking SK1 or SK2. We will also utilise immunocompetent laboratory animals (mice) genetically deficient in SK1 and SK2 genes and a DENV-infection model in the brain. Similarly, to extend our understanding of the anti-viral effect of viperin on DENV infection, we will use cell lines and mice with a genetic deficiency in viperin for *in vitro* and *in vivo* infection studies, with a particular focus on the brain.

1.18 Outcomes

In this study, we have showed that chemical inhibition of SK1 reduced DENV replication *in vitro*, and thus using anti-SK1 activity drugs may be promising therapeutics in treatment of DENV infection where no effective anti-DENV therapies are yet available. Even though we have not

shown a major effect of SK1 on DENV infection and DENV induced immune responses *in vivo*, this does not exclude the potential implication of this enzyme in modulating host immune responses against DENV infection. Our data showed that the lack of SK2 in iMEFs reduced DENV infection while inhibition of SK2 activity and the lack of SK2 in mouse brain has no effect on DENV replication. This indicates that while SK2 has a role in promoting DENV infection, use of the chemical SK2 inhibitors that are currently in progress as anti-cancer drugs are unlikely to be beneficial for DENV infection. Additionally, our results novel results with a rapid and high induction of a new investigated ISG, Ifi2712a, in response to DENV infection. This factor may have an essential role in controlling DENV infection that could be defined further in the future. Our data in this study supported prior evidence that viperin has antiviral activity against DENV infection, shown here for the first time in primary mouse cells, however viperin has little impact on DENV infection in mouse brain that could be explained by a compensatory role of other ISGs against DENV infection in that tissue. In this study, we have successfully used a mouse model for DENV infection through ic route that results in DENV replication. This model can be used for future studies to investigate further aspects of the role of a host immune response against DENV infection *in vivo*.

CHAPTER 2. MATERIALS AND METHODS

2.1 Materials

2.1.1 Agarose gel electrophoresis

2% (w/v) DNA grade agarose (Progen, cat # 200-001)

0.5X Tris Borate EDTA buffer

20 mM Tris base, 20 mM boric acid, and 0.5 mM EDTA (pH 8.3)

6X EZ-Vision® Three Dye, DNA Dye as Loading Buffer (Amresco, cat # N313)

pUC19 (HpaII) DNA marker (500 ng/μl) (GeneWorks, cat # SM0223)

2.1.2 Antibodies

2.1.2.1 Primary antibodies

Mouse anti-envelope glycoprotein 4G2 anti-DENV 2 (D1-4G2-4-15) prepared from hybridoma cells purchased from ATCC (1/10) (ATCC, cat # HB-112™). Kindly provided by Dr Nicholas Eyre, University of Adelaide.

Rabbit anti-viperin antibody (ab73864) (1/1000) (Abcam)

2.1.2.2 Secondary antibodies

Donkey anti-mouse Cy™3 (1/100) (Jackson ImmunoResearch Laboratories)

Donkey anti-rabbit Cy™5 (1/50) (Jackson ImmunoResearch Laboratories)

2.1.3 Cells

Cell lines employed in this study are as presented in Table 2.1

Table 2.1 Cell lines used in this study

Cells	Origin	Cell types	Use	Source
HEK293	Human embryo	Kidney fibroblast	DENV infection	ATCC
HEK293 c18	Human embryo	Kidney cells transformed with adenovirus 5 DNA and transfected with EBV EBNA1	DENV infection	ATCC
HEK293 c18 pREP	Human embryo	Kidney cells transformed with adenovirus 5 DNA and also transfected to contain GFP DENV reporter replicon (see section 2.2.9)	Flow cytometry	Generated by A/Prof Jill Carr, Flinders University
HEK293T	Human embryo	Kidney cells transformed with SV40 Large T antigen	DENV infection	Gift from Prof S. Pitson, Uni SA
HeLa	Human cervical carcinoma	Cervix epithelial	DENV infection	ATCC
Huh7	Human hepatocellular carcinoma	Liver hepatocyte	DENV infection	Gift from Prof Michael Beard, University of Adelaide
HepG2	Human hepatocellular carcinoma	Liver hepatocyte	DENV infection	Gift from Dr Dong Gui Hu, Flinders University
Vero	African Green monkey	Kidney epithelial	Plaque assay	ATCC
pMEF	Murine embryo cells	Primary fibroblast	DENV infection	Generated by Dr Briony Gliddon, UniSA
iMEF	Murine embryo cells	Immortalised fibroblast with SV40 Large T antigen	DENV infection	Generated by Dr Briony Gliddon, UniSA

2.1.4 Cell culture buffers and reagents

HyClone™ 1X Dulbecco's phosphate buffered saline solution (PBS) with calcium and magnesium (Thermo Scientific, cat # SH30028.02)

HyClone™ Hank's 1X balanced salt solution (HBSS) with calcium and magnesium (Thermo Scientific, cat # SH30268.02)

0.4% (w/v) Trypan Blue in PBS (BDH, CI 23850)

0.25% (v/v) HyClone™ Trypsin Protease (Life Sciences, cat # SH3004201)

Zeocin™ Selection Reagent (Gibco, cat # R25001)

2.1.5 Cell culture media

2.1.5.1 Media for maintaining and culturing cells

Dulbecco's Modified Eagle's Medium (DMEM) (HyClone, Thermo Scientific) supplemented with 10% (v/v) foetal bovine serum (FBS) (Gibco, Life Technologies), 100 U/ml penicillin and 0.1 mg/ml streptomycin (Sigma Aldrich), 2 mM L-glutamine (HyClone, Thermo Scientific). For culturing HEK293 c18 pREP cells (as described in section 2.2.9) zeocin (Gibco) was added at a concentration of 200 µg/ml.

2.1.5.2 Media for plaque assay

2X DMEM (Millipore) supplemented with 10% (w/v) sodium bicarbonate, 100 U/ml penicillin and 0.1 mg/ml streptomycin, 2 mM L-glutamine, and 10 mM HEPES (Sigma Aldrich).

2.1.5.3 Reagents for plaque assay

0.7% (w/v) SeaKem agarose

2.8 g of SeaKem agarose (Lonza, cat # 50014) in 400 ml cell culture grade water (HyClone, cat # SH 30529.02). Autoclaved prior to use.

0.33% (w/v) Neutral Red

3.3 g Neutral red (ICN Biomedicals, cat # 102438) in 1 L PBS. Filter sterilised and stored at room temperature (RT) in the dark.

2.1.6 Chemicals

SKi: 2-(*p*-hydroxyanilino)-4-(*p*-chlorophenyl) thiazole (Sigma-Aldrich)

SKi diluted in DMSO as 30 mM stock solution and stored in -20°C freezer

SK1-I: 1, 2, 4-Trideoxy-4-(methylamino)-1-(4-pentylphenyl)-*D*-erythro-pent-1-enitol hydrochloride) (Tocris Bioscience)

SK1-I diluted in DMSO as 100 mM stock solution and stored in -20°C freezer

ABC294640 (ABC): 3-(4-chlorophenyl)-adamantane-1-carboxylic acid (pyridin-4-ylmethyl) amide (a gift from Prof Stuart Pitson, University of South Australia)

ABC diluted in DMSO as 100 mM stock solution and stored in -20°C freezer

K145: 3-(2-amino-ethyl)-5-[3-(4-butoxyl-phenyl)-propylidene]-thiazolidine-2,4-dione (a gift from Prof Stuart Pitson, University of South Australia)

K145 diluted in DMSO as 50 mM stock solution and stored in -20°C freezer

NITD008: (BEI Resources, NR-36199)

NITD008 diluted in DMSO as 10 mM stock solution and stored in -20°C freezer

2.1.7 General use buffers and solutions

Ethanol Denatured 100% (Chem-Supply, UN 1170)

Chloroform (Chem-Supply, CA-038)

Dimethyl sulfoxide (DMSO) (BDH, 51402)

Methanol (RCI Labscan, AR 1115)

Nuclease-free water (Promega, cat # P1193)

2.1.8 Flow cytometry staining buffers and fixatives

4% (w/v) paraformaldehyde

4 g paraformaldehyde (Sigma-Aldrich, P6148) in 100 ml PBS

LIVE/DEAD[®] Fixable Red Dead Stain Kit (Molecular Probes/Life Technologies, cat # 1760576)

1% (w/v) Bovine Serum Albumin (BSA) (Sigma, A4503) in PBS

2.1.9 Histological buffers and reagents

2.1.9.1 Tissue processing

10% (v/v) Phosphate Buffered Formalin

100 ml of 37% formalin (Millipore), 900 ml RO water, 25.6 mM sodium dihydrogen orthophosphate dihydrate (Ajax Finechem, 0809446), 45.7 mM di-sodium hydrogen orthophosphate anhydrous (Chem-Supply, SA 026) (pH 6.8-7.4)

Surgipath Paraplast (paraffin wax) (Leica, ref # 39601006)

2.1.9.2 Haematoxylin and eosin staining

Xylene (Vetec Fine Chemicals, V024010)

Haematoxylin (Modified Harris)

13.23 mM Haematoxylin (Chroma, cat # 5B 535), 105.4 mM Potassium alum (Chem-Supply, AL-039), 5 mM Sodium iodate (BDH, cat # 30171), 300 ml Glycerol (Ajax Chemicals, cat # 242), 20 ml Glacial acetic acid (Ajax Chemicals, UN 2789), 700 ml Distilled water. Filtered prior to use.

0.5% (v/v) Acid alcohol

10 ml concentrated HCl (BDH, UN 1789) in 2 L of 70% (v/v) Absolute ethanol

0.05% (w/v) Lithium Carbonate

0.5 g lithium carbonate (Ajax Chemicals, UN 1289) in 1 L tap water

Eosin

For 400 ml eosin: 360 ml Absolute ethanol, 20 ml Distilled water, 20 ml of 5% aqueous eosin (Chroma, Y-CI 45380), 2 ml Glacial acetic acid (Ajax Chemicals UN 2789), 20 ml of 1% (v/v) Phloxine (Phloxinrot) (Chroma, CI 45410)

DPX mountant (BDH, 360294H)

2.1.9.3 Immunofluorescence staining

10 mM Sodium Citrate Buffer

10 mM Tri-sodium citrate dihydrate (Chem-Supply, SA034), 0.5 ml Tween 20 (0.05% v/v), 1 L Distilled water (pH 6.0)

0.05% (v/v) IGEPAL (Sigma Aldrich, CA-630) in water

Buffered Glycerol

1:2 of 0.5 M Sodium carbonate buffer (0.5 M Sodium carbonate, BDH 35786; 0.5 M sodium hydrogen carbonate, BDH 10247) and Glycerol (Ajax Chemicals, cat # 242) (pH 8.6)

2.1.10 Molecular biology reagents and buffers

2.1.10.1 RNA extraction

TRIzol[®] Reagent (Ambion[™] Life Technologies, cat # 15596018)

Isopropyl Alcohol 100% (Ajax Finechem, cat # 0705078)

2.1.10.2 DNase I treatment

10X DNase I Reaction Buffer (New England BioLabs, cat # B0303S)

DNase I (RNase-free) 2000 U/ml (New England BioLabs, cat # M0303S)

0.5 M EDTA (New England BioLabs, cat # 7011)

2.1.10.3 Reverse transcription

60 µM Random Primer Mix (New England BioLabs, cat # S1330S)

10X Moloney Murine Leukaemia Virus (M-MuLV) Reverse Transcriptase Reaction Buffer (New England BioLabs, cat # B0253S)

M-MuLV Reverse Transcriptase 200,000 U/ml (New England BioLabs, cat # M0253S)

RNase Inhibitor, Human Placenta 40,000 U/ml (New England BioLabs, cat # M0307S)

10 mM Deoxyribonucleotide triphosphates Mix (dNTPs) (Qiagen, cat # 201900)

2.1.10.4 Real time PCR

2X iTaq™ Universal SYBR® Green Supermix (Bio-Rad, cat # 1725124)

1X Sterile water for irrigation (Baxter)

2.1.11 Primers

All oligonucleotide primers were purchased from GeneWorks (Thebarton, South Australia).

Oligonucleotide dried pellets were resuspended in sterile water (Baxter) to obtain a final stock

solution of 100 µM and stored at -20°C. The primer stock solution was further diluted to a working

solution of 20 µM. Human and mouse primer sequences utilised in this study are presented in Table

2.2 and 2.3 respectively. Primer sequences for DENV-2 (GeneBank accession number is

AF038403.1) were targeted to the region 86-187 of C protein: *forward*

GCAGATCTCTGATGAATAACCAAC; *reverse* TTGTCAGCTGTTGTACAGTCG, with 102 bp

amplicon length.

Table 2.2 Human oligonucleotide primers used for amplification of mRNA

Name	Primers sequence	Accession no.	Amplicon size (bp)
Cyclophilin	<i>Forward</i> GGCAAATGCTGGACCCAACACAAA <i>Reverse</i> CTAGGCATGGGAGGGAACAAGGAA	NM_021130.4	355
GAPDH	<i>Forward</i> GGTGGTCTCCTCTGACTTCAACA <i>Reverse</i> GTTGCTGTAGCCAAATTCGTTGT	NM_001256799 .2	127
IFN- β	<i>Forward</i> TGTCAACATGASCAACAAGTGTCT <i>Reverse</i> GCAAGTTGTAGCTCATGGAAAGAG	NM_002176.2	86
Viperin	<i>Forward</i> GTGAGCAATGGAAGCCTGATC <i>Reverse</i> GCTGTCACAGGAGATAGCGAGAA	NM_080657.4	84
IRF7	<i>Forward</i> GAGCCCTTACCTCCCCTGTTAT <i>Reverse</i> CCACTGCAGCCCCTCATAG	NM_004029.2	158
CXCL10	<i>Forward</i> TCCACGTGTTGAGATCATTGC <i>Reverse</i> TCTTGATGGCCTTCGATTCTG	NM_001565.3	80
TNF- α	<i>Forward</i> CCCCAGGGACCTCTCTTAATC <i>Reverse</i> GGTTTGCTACAACATGGGCTACA	NM_000594.3	98

Table 2.3 Mouse oligonucleotide primers used for amplification of mRNA

Name	Primers sequence	Accession No.	Amplicon size (bp)
GAPDH	<i>Forward</i> GACGGCCGCATCTTCTTGTGC <i>Reverse</i> TGCCACTGCAAATGGCAGCC	NM_008084.3	120
SK1	<i>Forward</i> TGTCACCCATGAACCTGCTGTCCCTGCACA <i>Reverse</i> GCCCTTCTGCACCAGTGTA	NM_00117247 5.1	254
SK2	<i>Forward</i> TCTGGAGACGGGCTGCTTTA <i>Reverse</i> GCACCCAGTGTGAATCGAGC	NM_00117256 1.1	353
IFN- β	<i>Forward</i> AGAAAGGACGAACATTCGGAAA <i>Reverse</i> CCGTCATCTCCATAGGGATCTT	NM_010510.1	104
Viperin	<i>Forward</i> ACTCTGTCATTAATCGCTTCAACGT <i>Reverse</i> TCAATTAGGAGGCACTGGAAAAC	NM_021384.4	100
Ifi2712a	<i>Forward</i> CTGTTTGGCTCTGCCATAGGAG <i>Reverse</i> CCTAGGATGGCATTGTGTTGATGTGG	NM_029803.3	227
IRF7	<i>Forward</i> CACCCCATCTTCGACTTCA <i>Reverse</i> CCAAACCCAGGTAGATGGTGTA	NM_00125260 1.1	102
CXCL10	<i>Forward</i> GCCGTCATTTTCTGCCTCAT <i>Reverse</i> GGCCCGTCATCGATATGG	NM_021274.2	101
OAS1	<i>Forward</i> GGAGGTTGGAGTGCCAATGAAGTATC <i>Reverse</i> CTTCCCAAAGATGAAATGAAACAAAGACC	NM_00108392 5.1	85
IFIT1	<i>Forward</i> TCGCGTAGACAAAGCTCTTCATC <i>Reverse</i> TAGCAGAGCCCTTTTGTGATAATGTAA	NM_008331.3	90
CD4	<i>Forward</i> CCCAGGTCTCGCTTCAGTTTG <i>Reverse</i> AGGTAGGTCCCATCACCTCACAG	NM_013488.2	144
CD8- β	<i>Forward</i> GCTGGTAGTCTGCATCCTGCTTC <i>Reverse</i> TTGCTAGCAGGCTATCAGTGTTGTG	NM_009858.2	142
TNF- α	<i>Forward</i> CATCTTCTCAAATTCGAGTGACA <i>Reverse</i> TGGGAGTAGACAAGGTACAACCC	NM_013693.3	175
IL-6	<i>Forward</i> GAGGATAACCACTCCCAACAGACC <i>Reverse</i> AAGTGCATCATCGTTGTTCATACA	NM_031168.2	141

2.2 Methods

2.2.1 Cell maintenance

Cell lines were maintained in tissue culture flasks (Falcon) of different size (25 cm², 75 cm², and 125 cm² flasks) at 37°C with 5% CO₂ (Heraeus, Function Line). Cells were passaged every Monday and Thursday. Existing media was removed and adherent cells were washed with 1X PBS (Hyclone) and 0.25% trypsin was added to flask for cell detachment and dissociation by incubation for 4 min at 37°C. Trypsin was deactivated by adding fresh complete DMEM medium containing FBS. Cell counts were performed in appropriate dilution with 0.4% (w/v) trypan blue. Standard trypan blue dilution included 1:2 ratio and 10 µl of the cell:trypan blue mix was loaded into a haemocytometer counting chamber (HAWKSLEY, cat # AC1000). Cells were visualised under light microscopy and live cells were counted in 1 grid of 16 squares and multiplied by the dilution factor and 10⁴ (volume of a single square of the counting chamber) to calculate cells/ml. The desired number of cells was then added into a new flask. For 25 cm² flasks, 1×10⁵ cells were cultured in 7 ml; for 75 cm² flasks, 1×10⁶ cells were cultured in 17 ml; and for 125 cm² flasks, 2×10⁶ cells were cultured in 25 ml of complete DMEM. All cell lines were routinely monitored for mycoplasma by RT-PCR and this was kindly performed by Ms Julie Calvert. Cell culture manipulations were performed in a class II biosafety cabinet (CASP Series 90 CII, Australia).

2.2.2 Cell viability assay

SK2^{-/-} and WT iMEF lines were seeded at either 1 × 10³ or 5 × 10³ cells per well in a 96 well flat bottom plate in 200 µl DMEM and incubated at 37°C in 5% CO₂. At 24, 48, and 72 h post-seeding, cultured media was removed and cells were stained and fixed with 50 µl of 0.2% (w/v) crystal violet (Sigma-Aldrich, C3886-5G) in 20% (v/v) methanol and incubated for 15 min at RT. After incubation, unbound stain was removed and fixed cells washed with tap water. Bound stain was solubilised by adding 100 µl of 1% (w/v) sodium dodecyl sulphate (SDS) (Sigma, L-4509) for 60

min. The suspension was transferred to a single 96-well plate and the absorbance was measured at 540 nm using microplate reader (Titerteck Twinreader).

2.2.3 DENV stock and infection

2.2.3.1 DENV production

Infection studies utilised a full-length cDNA clone of DENV type-2 New Guinea C (NGC) termed MON 601 [113,237]. Virus stock was made by *in vitro* transcription of MON601 RNA using mMessage mMachine[®] T7 Kit (Ambion, cat # AM1344) according to manufacturer's instructions. *In vitro* transcribed DENV RNA was transfected into Baby Hamster Kidney-21 (BHK-21) cells, and then BHK-derived DENV supernatants (S/Ns) were harvested, and amplified in C6/36 insect cells. Virus-containing supernatants from insect cells were harvested, clarified by centrifugation, filtered (0.22 µM, Satorius filter), aliquoted, and then stored in -80°C freezer. Virus stocks were titred in Vero cells by plaque assay and quantitated by plaque forming units (PFU) per ml. Virus stocks were prepared and kindly provided by A/Prof Jill Carr.

2.2.3.2 DENV challenge

To achieve DENV infection, desired cell lines were seeded in cell culture plates (Falcon) at the day of subculturing at a density specific for each experiment in DMEM media. Plates were incubated overnight (O/N) to allow cells to attach. On the following day, virus stock was diluted in serum-free DMEM to perform viral infection at the desired multiplicity of infection (MOI), typically 1 or 0.1. The existing cultured media was removed from the cells and cells were challenged with DENV in a volume of 300 µl. Uninfected control wells were treated as above with an equivalent volume of serum-free DMEM, in some instances with equivalent volume of C6/36 culture media, when this control was appropriate. All plates were incubated for 90 min with gentle rocking every 15 min to protect cells from drying out. After incubation, the inoculum was removed, cells washed once with PBS and fresh complete DMEM was replaced. At the indicated time post-infection (pi) respective for each experiment, entire media was harvested, clarified by centrifugation at 2,900 x g (Dynamica

velocity 13μ centrifuge) for 4 min, aliquoted into screw-capped tubes, sealed in plastic bag, and stored at -80°C for plaque assay. For RNA analysis, 500 μl TRIzol reagent was added per well directly onto the cells, cell lysates harvested and RNA extracted as described in section 2.2.8.1.

2.2.4 DENV quantitation by plaque assay

Plaque assay was performed to measure infectious virus in a supernatant sample. Vero cells were seeded at 3×10^5 per well in a 6-well per plate in 2 ml complete 1X DMEM medium (HyClone, Thermo Scientific). The assay was performed in duplicate, and the cells were allowed to adhere for one day before DENV infection. Tenfold serial dilution was performed of test culture S/N and a positive control of known titre in a serum-free DMEM (HyClone, Thermo Scientific) with mixing of tubes by vortexing between dilutions. The culture medium was removed and the cells were infected with DENV-2 in a volume of 300 μl per well. The plates were incubated for 90 min at 37°C in 5% CO₂ with gentle rocking every 15 min. During the infection period, 0.7% SeaKem (w/v) agarose (Lonza) was melted in a microwave and cooled in an oven to 56°C. Post infection, infectious S/Ns were removed from wells, and the wells were washed once with 1X PBS. The wells were overlaid with 3 ml of 1:1 mix of 0.7% (w/v) SeaKem agarose and 2X DMEM with 10% FBS. Plates were allowed to set at room temperature for about 1 hour, and then the plates were incubated at 37°C with 5% CO₂ for 5 days. On day 5, wells were overlaid with 2 ml of 1:1 mix of 0.7% (w/v) SeaKem agarose and 2X DMEM containing 10% FBS and 0.03% (w/v) neutral red. Overlaid plates were allowed to set at RT for approximately 1 h, then inverted and incubated at 37°C with 5% CO₂ for 5 days or until plaques became visible. The number of plaques were counted from wells at the dilution where the plaques were clearly visible and used to calculate plaque forming units per ml (PFU/ml) of virus from the original sample. An image of an example plaque assay is shown in Appendix 1. PFU/ml was calculated using the following formula:

$$\text{PFU/ml} = \frac{\text{Number of plaques} \times \text{dilution factor}}{\text{Volume added for infection (300 } \mu\text{l)}} \times 1000$$

Volume added for infection (300 μ l)

2.2.5 Drug treatment of DENV infected cells

2.2.5.1 Treatment with SK1 selective inhibitors

HEK293 c18, 293T, HeLa, and Huh 7 cells were seeded in 24 well plates (Falcon) at a density of 7×10^4 cells per well in 500 μ l complete DMEM. Cells were allowed to adhere and pre-treated O/N with 5 μ M SKi at 37°C in 5% CO₂. In a dose response experiment cells were pre-treated with 0, 1 or 5 μ M SKi. For SK1-I cells were pre-treated for 1 h only but followed the same general protocol as follows. Media-containing SKi or SK1-I was collected, and DENV infection was performed in a volume of 200 μ l per well at MOI of 1 as described in section 2.2.3.2. After infection, inoculum was removed and media-containing 5 μ M SKi or SK1-I was replaced and the plates incubated until 6 hpi. At 6 hpi, SKi containing S/N was removed and 400 μ l of fresh complete DMEM without inhibitor was added. Hence the cells were pre-treated with SKi or SK1-I and post-treated for the first 6 h of infection only. At the indicated time pi, S/Ns were collected for DENV quantitation by plaque assay as described in section 2.2.4.

In some experiments, cells were either lysed in TRIzol reagent and harvested for DENV RNA analysis by RT-PCR or lysed with EB buffer for SK activity as described in sections 2.2.8 and 2.2.11 respectively.

2.2.5.2 Treatment with SK2 selective inhibitors

HEK293, HEK293 c18 cells, and HepG2 were seeded at a density of 4×10^5 cell per well in 6 well plates in 2 ml complete DMEM and allowed to attach O/N at 37°C in 5% CO₂. HEK293 and HEK293 c18 cells were pre-treated with 50 μ M ABC either O/N or 45 min, and HepG2 cell were pre-treated with 20 μ M ABC for 2 h prior to DENV infection. Additionally, HEK293 c18 cells at a density of 1×10^5 cells per well in a 6 well plate were treated with 0, 4, and 8 μ M K145 for 60 min

prior to DENV infection. Cells were then infected with DENV at MOI of 1 as described in section 2.2.3.2. The media with drug was replaced after infection and maintained until 6 hpi and then was replaced with fresh complete DMEM for the rest of experiment. At indicated time pi, S/Ns were removed for DENV quantification by plaque assay as described in section 2.2.4, and cells were lysed in TRIzol reagent and harvested for DENV RNA analysis by RT-PCR as described in section 2.2.8.

2.2.6 DENV infection in MEFs

2.2.6.1 DENV infection in SK2^{-/-} iMEFs

SK2^{-/-} immortalised MEFs (iMEFs) were isolated from mouse embryos lacking SK2 genes and were immortalised by Simian virus 40 (SV40) large T-antigen expression. SK2^{-/-} and their counterpart WT iMEFs were kindly provided by Dr Briony Gliddon (Centre for Cancer Biology and SA pathology, University of South Australia, Adelaide) and were used in infection experiments within 2 weeks of thawing. SK2^{-/-} and WT iMEF lines were plated in 6 wells plates at a density of 4×10^5 cells per well in 2 ml complete DMEM media and allowed to attach O/N. On the following day, media was removed and DENV challenge was performed at MOI of 1 or 0.1 as described in section 2.2.3.2. At 24 and 48 hpi, S/Ns were taken for DENV quantitation by plaque assay and quantitation of IFN- β by ELISA as described in sections 2.2.4 and 2.2.6.2 respectively.

Additionally, cells were lysed in TRIzol for DENV RNA and other gene mRNA analysis by RT-PCR as described in section 2.2.8.

2.2.6.2 IFN- β enzyme linked immunosorbent assay (ELISA)

Cultured S/N from DENV-infected WT and SK2^{-/-} iMEFs were collected at 24 and 48 hpi and mouse IFN- β protein was measured by ELISA according to manufacturer's instructions (LEGEND MAXTM Mouse IFN- β ELISA Kit with Pre-coated Plates, BioLegend[®] cat # 439407). Assays were kindly performed by Dr Amanda Aloia.

2.2.6.3 DENV infection in *Vip*^{-/-} MEFs

Viperin null mice were generated using CRISPR Design Tool (crispr.mit.edu) and generated according to protocol described previously [238]. Briefly, in mice bred identifier '72' the CRISPR system was identified to have caused a 113 bp genetic deletion in exon 1 of the mouse viperin gene. This creates a premature stop codon in the viperin mRNA leading to premature termination of viperin protein synthesis and a truncated, non-functional viperin protein. This deletion in the viperin gene and subsequent loss of protein production was validated using RT-PCR and western blot analysis performed by Dr Kylie Van der Hoek [239]. Primary MEFs (1°MEFs) were isolated from either WT or viperin '72' null mice by Ms Cathy Scougall and were generously provided by Prof Michael Beard (Molecular and Cellular Biology, Research Centre for Infectious Diseases, University of Adelaide, Adelaide) and hereafter referred to as *Vip*^{-/-}. The generated WT and *Vip*^{-/-} 1°MEFs were utilised in experiments before passage five. 1°MEFs were plated in 6 well plates at a density of 3×10^5 cells per well in 2 ml complete DMEM medium. Plates were incubated O/N to allow the cells to adhere before DENV infection at MOI of 0.1 as described in section 2.2.3.2. At 24, 48, and 72 hpi, S/N was taken for analysis of DENV release by plaque assay and cell lysates were harvested in TRIzol for RNA analysis by RT-PCR as described in sections 2.2.4 and 2.2.8 respectively.

2.2.7 Agarose gel electrophoresis

Products from PCR reactions and DNA molecular markers were pre-mixed with EZ-vision buffer containing a DNA interchelating dye for ultraviolet visualisation and loaded onto a 2% (w/v) of DNA grade agarose gel in 0.5% TBE. The gel was electrophoresed at 100V and imaged under UV transillumination using Gene Genius Bio Imaging System (Syngene).

2.2.8 DENV quantitation by reverse transcription polymerase chain reaction

2.2.8.1 RNA extraction

Total RNA was extracted from cells and mice brains using TRIzol[®] reagent (Invitrogen). Cells were lysed in 300 μ l of TRIzol whereas mice brains were lysed in 500 μ l of TRIzol. To extract RNA from the brain of mice, brain tissues were homogenised in TRIzol with a 2 \times 30 seconds cycles of sonication (Heat Systems Ultrasonics Inc Sonicator Cell Disruptor Mod W375) on ice at power 375 Watts 50/60 Hz. RNA extraction was performed according to the manufacturer's instructions. Initially, 0.2 ml of chloroform was added per 1 ml TRIzol, incubated for 10 min at RT, followed by centrifugation at 12,000 \times g for 15 min at 4°C (Heraeus Fresco 17 Microcentrifuge, Thermo Scientific). The upper aqueous phase that contains RNA was removed. 0.5 ml of 100% isopropanol per 1 ml TRIzol was added to the aqueous phase to precipitate RNA followed by centrifugation at 12,000 \times g for 10 min at 4°C. The RNA pellet was washed with 1 ml of 70% ethanol per 1 ml of TRIzol with brief centrifugation for 5 min at 7,500 \times g. The pellet was air-dried and resuspended in 20 μ l nuclease free water for cells and 50 μ l for mouse brain RNA.

2.2.8.2 DNase I treatment

The isolated RNA was DNase I treated to remove any genomic DNA contamination that may yield false-positive results. Briefly, for 20 μ l isolated RNA, 1X DNase reaction buffer and 10 U DNase I (New England BioLabs) was added, followed by incubation for 15 min at 37°C. 6.25 mM EDTA was added to stop the reaction and incubated for 10 min at 75°C. The reaction was briefly centrifuged and the DNase I-treated RNA supernatant was collected. Total RNA was quantitated by NanoDrop Lite (Thermo Scientific) at 260 nm and was stored at -80°C.

2.2.8.3 RNA reverse transcription

The extracted RNA was reverse transcribed into cDNA in two steps using a thermocycler system (GeneAmp[®] PCR system 9700, Applied Biosystems). The first step to denature the RNA and anneal the primer was achieved by adding 6 μ M random primer hexamer (New England BioLabs)

to 0.5 µg of total RNA, and RNase free-water was added to make a volume of 10 µl. The mixture was incubated to 65°C for 5 min and subsequently rapidly cooled to 4°C. In the second reaction reverse transcription was performed by addition of 1X M-MuLV reaction buffer (New England BioLabs), 0.5 mM dNTPs (Qiagen), 10 U RNase inhibitor (New England BioLabs), and 10 U M-MuLV reverse transcriptase (RT) (New England BioLabs) to the first reaction with RNase free-water added to make a 20 µl final volume. The reaction was incubated at 37°C for 90 min, terminated by heat inactivation of the enzyme at 95°C for 5 min, and subsequently cooled to 4°C. The generated cDNA was stored in -20°C until used.

2.2.8.4 Real-time quantitative polymerase chain reaction (qRT-PCR)

A real time qRT-PCR was carried out using 2 µl of cDNA template in a 10 µl reaction using 1X iTaq SYBER green (Bio-Rad) with 1 µM of each forward and reverse primer. All PCR primers were synthesised by GeneWorks with sequences as listed in Table 2.2 and 2.3. Real-time qRT-PCR was performed using Rotor-Gene 3000 real-time PCR system (Corbett research, Australia) under the following conditions: one cycle of 95°C for 5 min; 45 cycles of 95°C for 15 sec, 59°C for 30 sec, and 72°C for 30 sec, acquiring florescence in this last cycling step; and one cycle of 72°C for 60 sec. Melt curve was generated between 72 to 95°C in 1°C increments. All reactions were performed in duplicate. For DENV RNA quantification, the absolute copy number was determined using a standard curve generated by 10-fold serial dilution of MON601 DNA of known copy number from 15 pg/µl to 0.015 pg/µl using the following equation:

Number of copies = Amount of DNA (nanogram) × Avogadro's constant

Length of RNA (basepair) × 10⁹ × 660 (Daltons)

Where,

Avogadro's constant is 6.022×10^{23} molecules

660 is the average weight of a DNA basepair (bp) in Daltons

For quantitation of other mRNA transcripts, relative RT-PCR quantitation was determined by the ΔC_t method [240] using the following formula:

$$2^{-\Delta C_t}$$

Where, ΔC_t represents the difference between the C_t of the gene of interest and the C_t of the reference gene. PCR reactions for mRNA transcripts included controls of pre-defined high and low copy number as internal standards. PCR results were analysed using Corbett Rotor-Gene 6000 series software 1.7. All PCR reactions were normalised against the reference housekeeping genes either cyclophilin (human) or glyceraldehyde-3-phosphate dehydrogenase (GAPDH, human and mouse).

2.2.9 Quantitation of DENV replication by flow cytometry

To assess the effect of SK1 and SK2 selective inhibitors on DENV RNA replication level, we utilised HEK293 c18 cells containing a subgenomic, self-replicating DENV replicon with a green fluorescent protein (GFP) reporter gene. To generate these cells, HEK293 cells were co-transfected with two vectors: (1) pREP - a DENV-subgenomic replicon containing a GFP-reporter gene in place of the DENV C-prM and E genes and a zeocin selection marker (Appendix 2A); (2) a vector expressing DENV C-prM and E genes of the DENV-2 strain 16681 with a blasticidin selection marker (Appendix 2B). Both of these vectors were obtained under material transfer agreement (MTA) from Prof T. Pierson and are as described [241]. Supernatant was harvested from transfected cells that will produce replication defective reporter virus particles (RVPs), clarified and filtered and used to infect fresh HEK293 c18 cells. Infected cells were selected with zeocin (Invitrogen) at a concentration of 200 $\mu\text{g/ml}$ and should contain the pREP vector with the subgenomic GFP self-replicating DENV RNA but lack the DENV-structural elements and ability to make infectious virus. This was confirmed, with cells demonstrated to be DENV CA negative, DENV 3'UTR +ve by RT-PCR and negative for infectious virus production (data not shown). These cells were generated by BMedSci placement student Ms Amy Holman, characterised by Mr Sam Brookes and provided for

use by A/Prof Jill Carr and are referred to hereafter as HEK293 c18 pREP. HEK293 c18 pREP or parental HEK293 c18 cells were seeded in 6 well plates at a density of 5×10^5 cells in 2 ml of DMEM media. After ~ 4 h post-seeding, cells were treated with either 5 μ M SK1-I, 20 μ M ABC or 8 μ M K154. Cells were treated with an equivalent concentration of vehicle (DMSO) as a control. Cells were also treated with 10 μ M of NITD008 (NITD), a drug known to inhibit DENV RNA replication *in vitro*, which is used as a positive control. Cells were then incubated O/N at 37°C in 5% CO₂ and on the following day, cells were subjected to flow cytometry analysis.

Cells were detached with trypsin, harvested in 1 ml DMEM medium, and pelleted by centrifugation at 2,900 x g for 4 min. S/N was removed and cell pellets were washed with 1X PBS, and then stained with 200 μ l of LIVE/DEAD fixable red dead stain kit (Life Technologies) and incubated for 30 min on ice in the dark. Cells were pelleted, washed with PBS and fixed with 4% paraformaldehyde (PFA) at RT for 15 min. Cells were washed with PBS and the pellet was resuspended in PBS containing 1% (w/v) BSA and transferred to tubes appropriate for flow cytometry. Data were acquired with a BD Accuri C6 Plus (BD Biosciences) and analysed by CFlow Plus software (BD Bioscience).

2.2.10 Protein assay

Protein concentration in whole mice brain tissue and cell lysates were determined by a commercial protein assay. Samples were diluted 1/100 in 1X PBS and 5 μ l of each sample added to a 96 well plate in duplicate. A standard curve was generated from BSA of known concentration prepared in 1X PBS ranging from 0.0071825 mg/ml to 1 mg/ml. The commercial Bio-Rad Protein Assay Dye Reagent Concentrate (Bio-Rad, cat # 500-0006) was diluted 1/5 in Milli Q water and 200 μ l of reagent added to the standards and samples. The reaction was incubated at room temperature for 15 min and the absorbance was read at 595 nm using an ELISA plate reader (Beckman Coulter DTX880 multimode detector). A representative BSA standard curve is shown in Appendix 3.

2.2.11 Sphingosine kinase activity and S1P analysis

2.2.11.1 Sphingosine kinase 1 and 2 activity assay

Cells were lysed in EB: 50 mM Ultrapure Tris/HCl (pH 7.4) (Thermo Fisher Scientific, cat # 15567027), 150 mM NaCl (Ajax Finechem, AJA465), 2 mM Na₃VO₄ (Sigma, 56508), 10 mM NaF (Sigma, S7920), 10% (w/v) glycerol (Chem-Supply, GA010), 10 mM β-glycerophosphate (Sigma, G6521), 1 mM EDTA (titriplex III) (Merck, 1.08418.1000), 1mM dithiothreitol (DTT) (Sigma, D0632) and protease inhibitors (Roche, Complete mini) prepared by Ms Lorena Davies. Frozen brain tissues were homogenised in the lysis buffer using a glass mortar and pestle and then sonicated for 2 × 30 seconds cycles of sonication on ice in a Heat Systems Ultra-Sonics Inc Sonicator W-375 Cell Disruptor. SK1 and SK2 activities were selectively measured by ³²P transfer from [γ³²P] ATP to *D-erythro*-sphingosine under conditions of Triton X-100 for SK1 activity and 1 M KCl for SK2 activity, as previously described [242]. The SK activities were normalised against total protein content, as determined by protein assay as described in section 2.2.10. SK1 and SK2 assays were performed by Ms Lorena Davies. 20 µl of lysates were incubated with 80 µl of a reaction mixture containing 100 µM sphingosine (prepared from a 2 mM sphingosine *D-erythro* (Enzo, cat # BML-EI155) solubilised in 5% (w/v) Triton X-100 for SK1 activity or solubilised in BSA with 1 M KCl for SK2 activity), 20 mM [γ³²P] ATP (10 µCi) (Pharmacia Biotech, cat # 27100601) containing 200 mM MgCl₂, and 50 mM 4-deoxypyridoxine (Sigma, cat # D0501) for 30 min at 37°C. The lipids was extracted by the addition of 270 µl of chloroform/methanol/concentrated HCl (100:200:1 v/v), 20 µl of 5 M KCL, and 70 µl chloroform. The mixture was vortexed and centrifuged to separate phases at 13,000 x g for 5 min. The upper aqueous phase was removed and 50 µl of the lower chloroform phase was spotted onto aluminium backed Silica gel thin-layer chromatography (TLC) plate (Sigma, Z193291, pore size 60 Å). The TLC plate was resolved using 1-butanol/ethanol/glacial acetic acid/water (8:2:1:2 v/v) and exposed to a storage phosphor screen O/N and read with Typhoon FLA 9000 (GE Healthcare, Life Sciences) to quantify radiolabelled S1P. SK activity is defined as the amount of enzyme to generate 1 pmol

S1P/mg protein.

2.2.11.2 S1P quantitation

S1P levels were measured as previously described [243] with some modifications. Briefly, 20 µl of brain homogenate was suspended in 200 µl methanol with 0.25% concentrated HCl. Alkaline extraction of the lipids was performed by addition of 400 µl chloroform, 30 µl of 10 M NaOH, 580 µl of 2 M KCl and 200 µl methanol with 200 pmol C17 (*D-erythro*-sphingosine C17) (Cayman, cat # 10007902) and centrifuged for 5 min at 16,000 x *g*. The upper aqueous/methanol phase was collected and acid extraction was performed with 40 µl concentrated HCl and 300 µl chloroform. The upper phase was aspirated and 200 µl of lower chloroform phase was collected and chloroform was evaporated using a rotary vacuum system. The dried lipids were resuspended in 275 µl methanol/70 mM K₂HPO₄ (9:1) with 1 mM EDTA by sonication in a bath sonicator for 30 sec. A derivatization mixture of 10 mg *o*-phthalaldehyde (Sigma, P0657), 200 µl ethanol, 10 µl β-mercaptoethanol and 10 ml of a 3% boric acid solution (adjusted to pH 10.5 with KOH) was prepared and 25 µl of this was added to the lipid samples and incubated for 15 min at room temperature followed by centrifugation. S1P levels were then determined by high-performance liquid chromatography (HPLC) analysis with an EVO C18 column (Phenomenex, Lane Cove, NSW, Australia) as previously described [243]. A standard curve of S1P concentrations (Cayman, cat # 62570) was used to calculate unknown S1P levels. The S1P quantitation was performed by Ms Lorena Davies.

2.2.12 Mice

Three to four weeks old male and female wild type (WT) C57BL/6 and homozygous knockout for the *Sphk1* and *Sphk2* genes encoding SK1 (SK1^{-/-}) and SK2 (SK2^{-/-}) [215,244] mice respectively were used. SK1^{-/-} and SK2^{-/-} mice were obtained from Dr Briony Gliddon in the laboratory of Prof Stuart Pitson (Centre for Cancer Biology and SA Pathology, University of South Australia, Adelaide). Three to four week old male and female homozygous viperin null mice (Vip^{-/-}) mice

were generated and genotyped as described in section 2.2.6.3, obtained from Dr Kyle Van der Hoek in the laboratory of Prof Michael Beard (Molecular and Cellular Biology, Research Centre for Infectious Diseases, University of Adelaide, Adelaide), were used. WT C57BL/6 mice were also obtained from School of Medicine Animal House Facility (SoMAF), Flinders University, Adelaide. All mice were kept in a pathogen-free environment on a 12 h cycle of light and darkness with *ad libitum* access to food and water.

2.2.13 Ethics statement

All animal procedures were performed in accordance with Flinders University Animal Welfare committee approval number 870/14 and Institutional Biosafety Committee approval NLRD 2011-10. All procedures were performed inside a class II hood in an OGTR certified PC2 facility.

2.2.14 Mouse intracranial DENV challenge and follow up

Mice were anaesthetised by inhalation of isoflurane and were injected by intracranial route (ic) with 800 pfu DENV-2 MON601 strain diluted in PBS in a volume of 10 µl using an insulin needle (Figure 2.1). Mock control mice were injected ic with an equivalent amount of PBS only. Post injection, mice were monitored visually for recovery. Throughout all the animal experiments in this study only one mouse was euthanised due to poor recovery following ic injection. All ic injections were performed in a class II hood in a OGTR certified PC2 facility by A/Prof Jill Carr with assistance by the candidate (Mr Al-Shujairi), with the exception of mock controls for the final *Vip*^{-/-} experiment, which were undertaken by the candidate. This was to ensure adherence to biosafety and injection competence requirements.

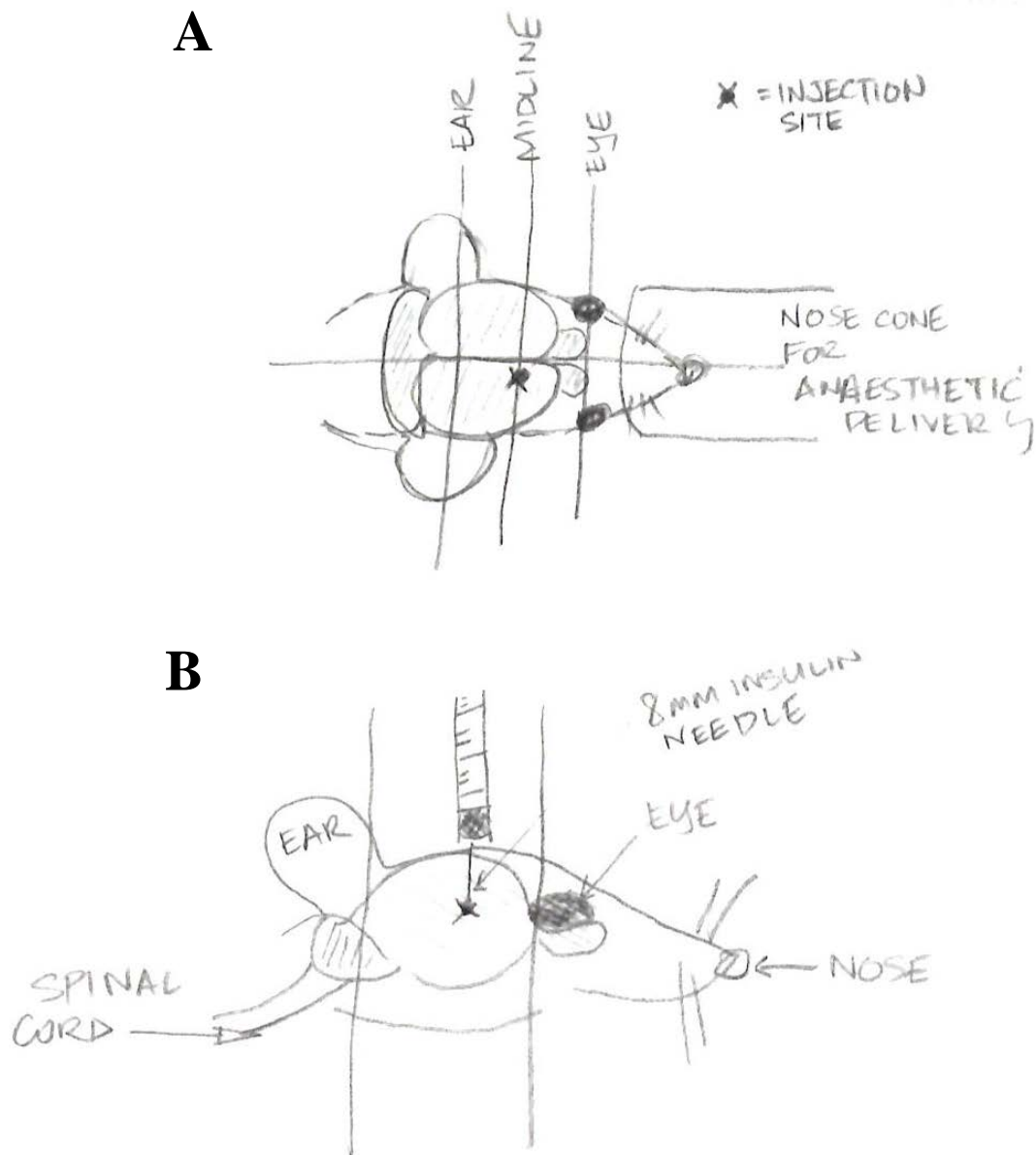


Figure 2. 1 Schematic representation of the intracranial injection technique

The injection site was identified by the intersection of the central line of the mouse skull and the midline between the eyes and ears. Virus was injected non-stereotactically at the point, as shown in (A). Injection was performed with an 8 mm length insulin needle and thus will penetrate into the brain, as shown in (B). Injection site methodology was validated by A/Prof Jill Carr through injection of Evans blue dye. Image created by A/Prof Jill Carr.

Post DENV or mock infection, animals were visually monitored twice daily for signs of DENV-induced neurological disease including slow movement, hunched posture, or reduction in hind limb function. In addition, animals were monitored daily for body weight. Any sign of neurological disease or loss of more than 10% of body weight represented a termination point and animals were euthanised immediately by isoflurane anaesthetic inhalation and humane decapitation. Brain tissues were harvested at termination and divided into two parts. The ipsilateral section was resuspended in 500 µl TRIzol reagent (Ambion) for RNA extraction and real-time quantitative PCR (qRT-PCR) analysis and the contralateral section was snap frozen in liquid nitrogen stored at -80°C for SK activity assay and S1P quantification or fixed for histological analysis.

2.2.15 Histological analysis

2.2.15.1 Tissue processing

The contralateral mouse brain sample was fixed in 10% phosphate buffered formalin (pH 6.8-7.4). The fixed tissue sample was dehydrated in deionised water for 30 min followed by emersion in a series of graded ethanol (70%, 80%, 90%, 100%, and 100%) for 1 h each, and cleared in chloroform O/N. The processed tissue was infiltrated with molten paraffin wax using a heated vacuum chamber at 62°C and embedded in fresh paraffin wax to make a permanent wax block. Tissue blocks were stored at room temperature. Tissue processing was performed in the Flinders School of Medicine imaging facility. For analysis embedded tissues were sectioned by Ms Pat Vilimas (Flinders Microscopy Facility, Flinders University). 5 µm sections were cut from mouse brain tissue embedded in paraffin, collected onto snowcoat slides and allowed to dry O/N, then stored at RT for later use.

2.2.15.2 Haematoxylin and Eosin Staining

Histopathological changes in the mouse brain in response to ic DENV infection were analysed using haematoxylin and eosin staining (H&E). Paraffin sections, generated as in section 2.2.15.1, were dewaxed in xylene for 4 min and rehydrated by passing them in decreasing concentration of

ethanol (100%, 100%, 90%, 70%) for 2 min each followed by rinse in deionised water. H&E staining method was performed using modified Harris type haematoxylin and eosin. Slides were stained in haematoxylin for 10 min, then washed in running tap water for 2 min. Slides were differentiated quickly in 1% (v/v) acid alcohol, washed in running tap water, and blued in 0.05% (w/v) lithium carbonate (alkaline solution) for 4 min. Slides were then counterstained in eosin for 30 sec, then washed with running tap water for 2 min. Slides were dehydrated in 100% ethanol for 10 sec, and cleared in xylene for 2 min. Slides were mounted with DPX and viewed under upright BX53 brightfield microscope (Olympus, Australia) equipped with a DP27 colour camera. Images were acquired using cellSens Entry v1.16 software.

2.2.15.3 Immunostaining

Sections were permeabilised by incubation in 0.05% IGEPAL for 20 min at RT washed with water then subjected to antigen retrieval by boiling in 10 mM sodium citrate buffer for 10 min at 96°C. Sections were blocked with 4% (v/v) normal goat serum (NGS), 5% (v/v) FBS, and 0.4% (w/v) BSA in HBSS for 30 min at RT. Slides were then incubated with mouse anti-DENV 4G2 and rabbit anti-viperin (ab73864) primary antibodies diluted in 2% NGS/HBSS O/N at 4°C in a humidified chamber. Slides were washed 3 times for 5 min each and incubated with Donkey anti-mouse CyTM3 (1/100) and with Donkey anti-rabbit CyTM3 (1/100) secondary antibodies diluted in 2% NGS/HBSS for 2 h at RT in the dark. After washing the slides 3 times for 5 min each, nuclei were stained with Hoechst 33342 (5 µg/ml) (Molecular Probes, cat # D9564) for 20 min at RT. Slides were washed with PBS, mounted with buffered glycerol and sealed with nail polish. Slides were viewed under upright AX50 fluorescence microscope (Olympus, Australia) equipped with a Hamamatsu Orca cooled CCD camera and MicroManager Imaging software.

2.2.16 Statistics

Data are expressed as means ± standard deviation (SD) or means ± standard error mean (SEM) and statistically analysed using GraphPad Prism software version 7.01 (GraphPad Software). A

statistically significant difference between samples was assessed using either Student's unpaired *t*-test or Student's unpaired *t*-test with Welch's correction, one-way analysis of variance (ANOVA) and two-way ANOVA with Bonferroni's multiple comparisons test. Kaplan-Meier survival curves were analysed by log rank test (Mantel Cox). Results having p values of < 0.05 were considered statistically significant. Values for n; the number of replicates in each experiment and the number of times each experiment was replicated, are indicated in figure legends for each experiment.

CHAPTER 3. THE ROLE OF SK1 DURING DENV INFECTION

IN VITRO

A part of this chapter (Figure 3.1A and Figure 3.5A) was published within the following publication:

Clarke JN, Davies LK, Calvert JK, Gliddon BL, **Shujari WH**, Aloia AL et al. Reduction in sphingosine kinase 1 influences the susceptibility to dengue virus infection by altering antiviral responses. *J Gen Virol* 2016; 97: 95–109.

3.1 Introduction

Sphingolipids mediate a wide range of cellular signalling functions. Of these lipids, S1P is a bioactive molecule that has been involved in various biological processes inside or outside the cells such as cell development, lymphocyte migration, and host immunity [245,246]. S1P is produced from a precursor lipid, sphingosine, by the action of SK1 and SK2, which in turn regulate cell death and survival decision [205,247]. Despite the fact that the SK1 and SK2 enzymes generate the same product (S1P), they diverge in many aspects that include different physiological roles [205,211].

During the last few years, the role of SK during viral infections, particularly SK1, has begun to be investigated [206]. Increased SK1 activity by overexpression of SK1 during infection with HCMV [225], IAV [229], and measles virus [230] enhanced viral production. Further, suppression of SK1 activity by BVDV infection is advantageous for promoting viral replication [231]. In the context of DENV infection, work from our laboratory has previously shown that endogenous cellular activity of SK1 is altered following DENV infection *in vitro* [166,233]. Thus, we aimed to further investigate the role of SK1 during DENV infection *in vitro*.

Specifically, in this chapter, we sought to define the effect of inhibition of SK1 prior to DENV infection *in vitro* using the known chemical SK1 inhibitors, SKi and SK1-I. We initially assessed

the dose of SKi that would inhibit DENV infection without producing any sign of cell toxicity. We next assessed whether SKi treatment could affect DENV entry or RNA replication and further investigated the effect of inhibition of SK1 on the induction of IFN- β and ISGs, which have shown antiviral activity against DENV infection *in vitro* including viperin, IFIT1, IRF7, and CXCL10, in response to DENV infection. These outcomes supported other complementing work in our laboratory and some of these findings were published in 2016 [167].

3.2 Results

3.2.1 Inhibition of SK1 with SKi reduces DENV infection in different cell lines

Previous studies, and including preliminary data from our laboratory, reported that inhibition of SK1 using various selective SK1 (eg. SK1-I), or non-selective SK chemical inhibitors (eg. SKi) restricted viral infection *in vitro* [225,227,230]. Thus, we sought to define the boarder characteristics of the effect of SK inhibition on DENV infection in terms of cell specificity and dose-response using SKi [248], a dual SK1 and SK2 inhibitor. HEK293 c18, 293T, HeLa, and Huh7 cells were pre-treated with 5 μ M SKi and DENV infected at MOI of 1. At 24 and 48 hpi, culture S/N was taken for quantitation of DENV by plaque assay. Results showed that DENV levels in culture S/N was significantly reduced in SKi-treated cell lines at 24 and 48 hpi (Figure 3.1), with the exception of 293T cells where DENV was reduced at 24 but not 48 hpi (Figure 3.1A and B). These results indicate that chemical targeting of SK reduces DENV infection in a variety of different cell lines. Subsequent experiments utilised the HEK293 c18 cell line since these cells demonstrated higher DENV infectious release and a significant inhibition of SKi on DENV infection compared to other cells.

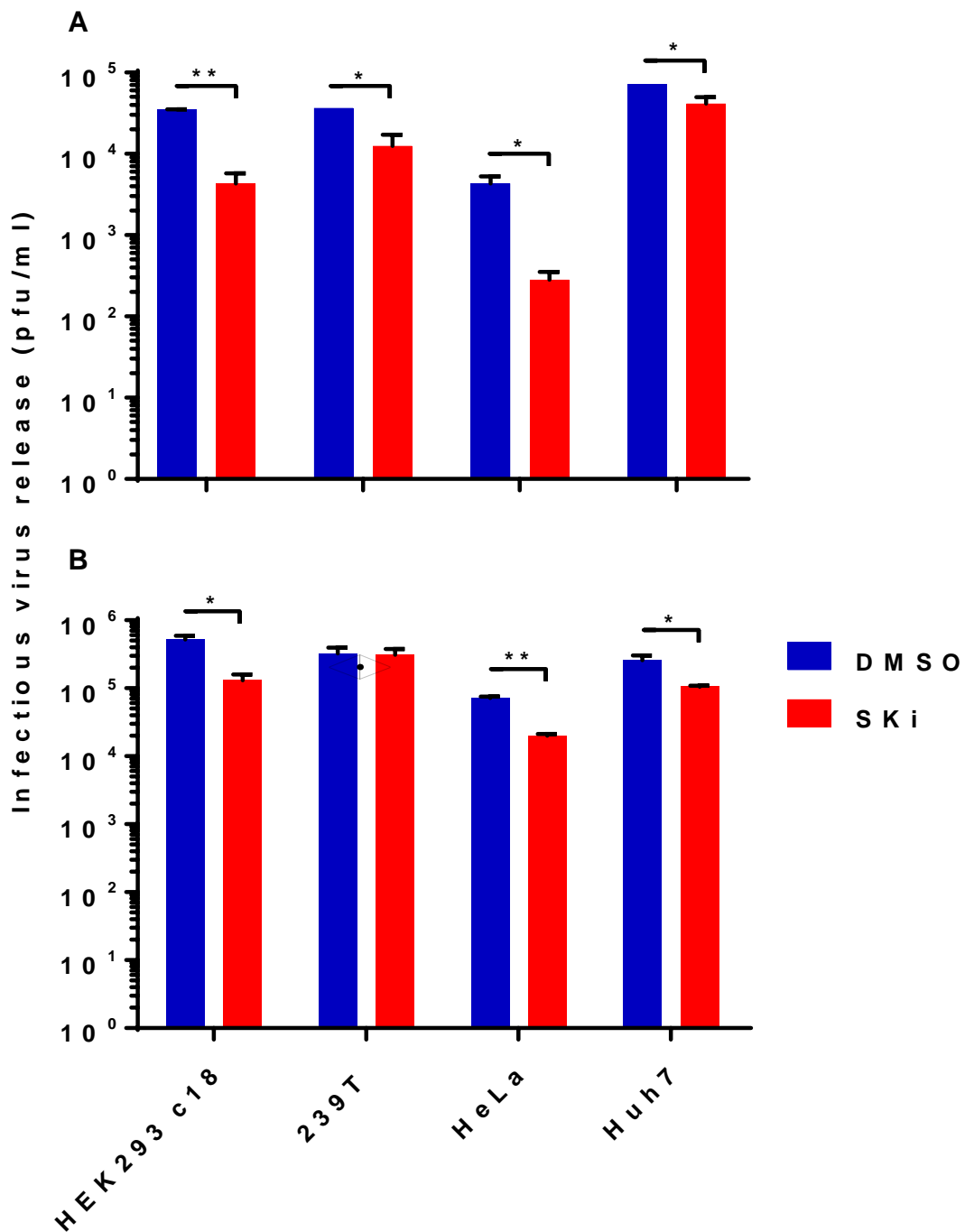


Figure 3.1 SKi inhibition restricts DENV infection in different cell lines

HEK293 c18, 293T, HeLa, and Huh7 cells were pre-treated O/N with 5 μ M SKi, and DENV challenged at MOI of 1. Cultured S/Ns were collected for quantitation of DENV by plaque assay at (A) 24 and (B) 48 hpi. Results represent mean \pm SD of n=2 assay replicates from two independent experiments. Statistical significance was determined using unpaired student's *t*-test to DMSO control. * $p < 0.05$, ** $p < 0.005$.

3.2.2 SKi inhibits DENV infection in a concentration-dependent manner

To assess the most effective concentration of SKi that inhibits SK1 and SK2 activity, and DENV infection but is not toxic to the cells, HEK293 c18 cells were treated with 0, 1, and 5 μM SKi O/N, and infected with DENV at MOI of 1. Of note, HEK293 c18 cells were checked for morphological signs of toxicity by microscopy. At 24 hpi, cell lysates and culture S/N were taken for quantitation of SK1 and SK2 activity by *in vitro* SK assay or DENV infectious virus by plaque assay. SKi treatment reduced the activity of SK1 in a dose-dependent manner that was significant at 5 μM SKi. SK2 activity, however was not affected by SKi treatment at the doses used here (Figure 3.2A). Concurrently, results showed that DENV infection was reduced by SKi treatment in a dose-dependent fashion with significant inhibition at 5 μM (Figure 3.2B). These data indicate that the reduction in DENV infectious virus release by 5 μM SKi was associated with a reduction in SK1 rather than SK2 activity.

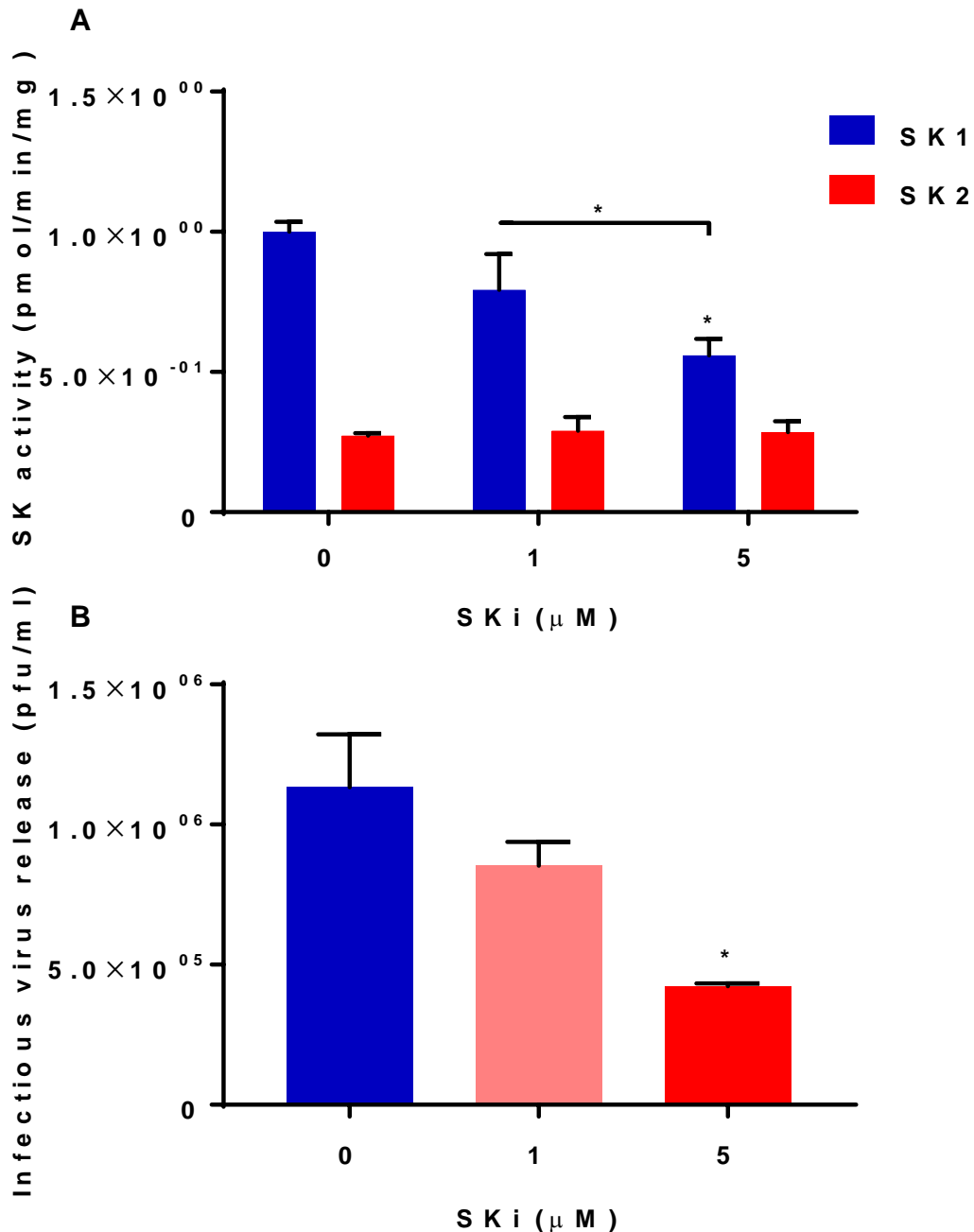


Figure 3. 2 Dose-dependent of DENV infection and SK1 activity by SKi

HEK293 c18 were treated O/N with 0, 1, and 5 μ M SKi and DENV infected at MOI of 1. At 24 hpi cell lysates and supernatant harvested to quantitate: **(A)** SK1 and SK2 activity by SK assay, **(B)** DENV production by plaque assay. Results represent mean \pm SD of n=2 assay replicates from two independent experiments. Statistical significance was determined for **(A)** using two-way ANOVA and **(B)** using one-way ANOVA to 0- μ M SKi control. * $p < 0.05$.

3.2.3 SKi inhibits DENV infection at a post-binding step of viral replication

We further investigate whether the SKi treatment affects DENV replication at the viral binding and entry or post-entry step. HEK293 c18 cells were pre-treated with 5 μ M SKi and DENV infected at MOI of 1. Following infection cells were rigorously washed to remove extracellular DENV inoculum. S/N was collected for DENV quantification by plaque assay and total RNA was extracted immediately following infection (2 hpi) and during established infection (24 hpi) for measuring DENV RNA by qRT-PCR. Results of both plaque assay and RT-PCR demonstrate a comparable level of virus and viral RNA at 2 hpi, which represents input virus that has bound to or entered the cell during the infection period (Figure 3.3). A significant approximately half log reduction in DENV infectious virus release was observed at 24 hpi following treatment with SKi compared to DMSO control cells (Figure 3.3A). This reduction was not accompanied by a decline in DENV RNA at 24 hpi with SKi treatment (Figure 3.3B). These findings suggest that SKi inhibition does not impair the amount of DENV that can bind and enter a cell, and the effect of SKi is likely to be a post-entry reduction in viral production process.

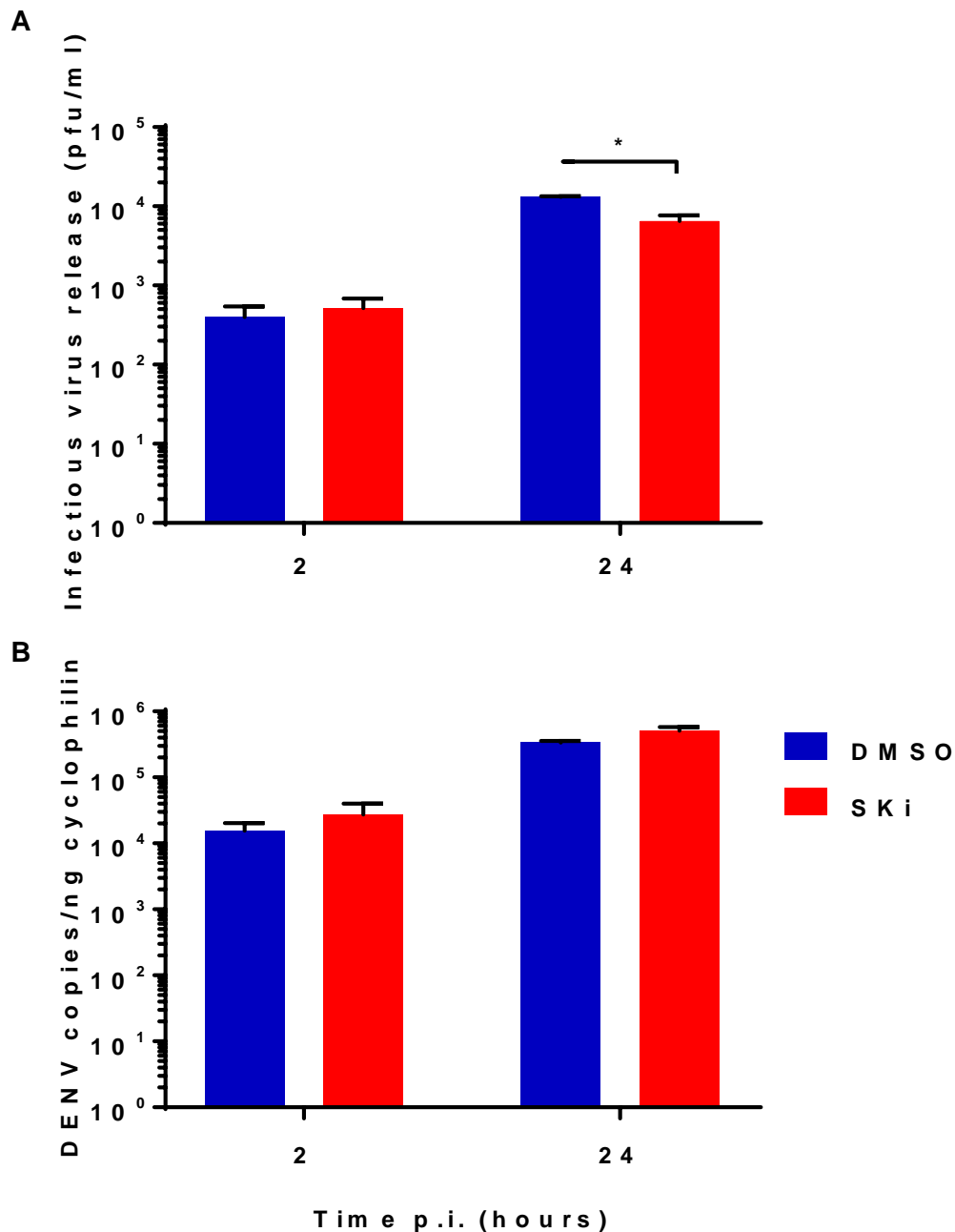


Figure 3.3 Effect of SKi on DENV infection

HEK293 c18 cells were pre-treated O/N with 5 μ M SKi, and DENV infected at MOI of 1. Cells were extensively washed to remove unbound DENV inoculum and samples taken at 2 and 24 hpi.

(A) S/N for plaque assay. (B) RNA was isolated and DENV quantitated by RT-PCR. Copy number was determined from a standard curve and normalised against cyclophilin. Results represent mean \pm SD of n=2 assay replicates from two independent experiments. Statistical significance was determined using two-way ANOVA to DMSO control. * p < 0.05.

3.2.4 SKi has no effect on DENV RNA replication in a sub-genomic GFP reporter replicon system

Since virus binding and accumulation of DENV RNA are comparable following SKi treatment, we next sought to assess the impact of SKi treatment directly on DENV RNA replication *in vitro*. To achieve this, we employed HEK293 c18 cells containing a self-replicating DENV-subgenomic replicon containing a GFP reporter gene. This cell line was generated in our laboratory, as described in chapter 2 section 2.2.9, from vectors provided by Prof Ted Pierson [241] and we have termed this cell HEK293-pREP. Quantitation of GFP expression by flow cytometry was validated (Appendix 4). HEK 293 pREP cells, where GFP reflects production of DENV RNA, were treated with 5 μ M SKi or 10 μ M NITD, a known inhibitor of DENV RNA replication and thus a positive control and allowed to replicate for 24 h prior to flow cytometry analysis. Results showed no difference in the histogram profile of GFP expressing cells following treatment with 5 μ M SKi compared to vehicle treated cells (Figure 3.4A) and this was confirmed by statistical comparison of the GFP mean fluorescent intensity (MFI) (Figure 3.4C). In contrast, treatment with 10 μ M NITD showed a clear reduction in GFP in SKi -treated compared to untreated cells, as viewed by histogram plots and a statistically significant reduction in GFP MFI (Figure 3.4B and C).

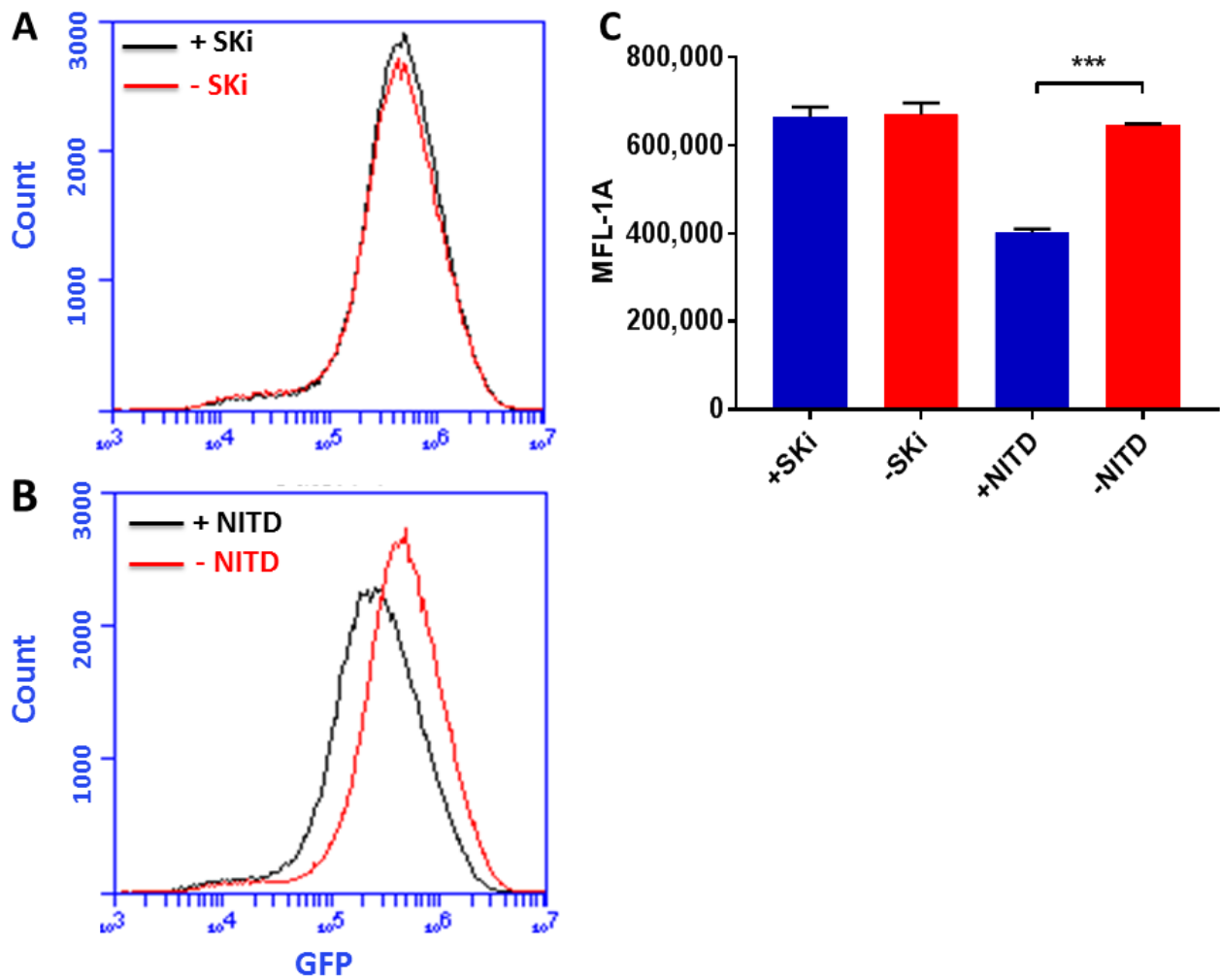


Figure 3. 4 Effect of SKi on DENV RNA replication

HEK293 c18 pREP cells (containing a subgenomic GFP-DENV replicon, see section 2.2.9) were treated with SKi for 24 h prior to fixation and flow cytometry. Histograms showing profile difference in GFP intensity following treatment with (A) 5 μ M SKi and (B) 10 μ M NITD positive control. (C) MFI of GFP in response to treatment, as in A and B. Results represent mean \pm SEM of n=3 assay replicates. Statistical significance was determined by unpaired student *t*-test. *** $p < 0.0005$.

3.2.5 Inhibition of SK1 with SK1-I impairs DENV infection *in vitro*

The data above suggested targeting of SK chemically using SKi reduced DENV infection. Although SKi is a non-selective SK1 and SK2 inhibitor, under our laboratory conditions the reduction in DENV infection was associated with SKi-mediated reduction in SK1 but not SK2 activity. Here, we further defined the effect of chemical inhibition of SK1, using SK1-I, a SK1 selective chemical inhibitor [249] on DENV infection. HEK293 c18 cells were pre-treated with 5 μ M SK1-I and infected with DENV at MOI of 1. At 2, 24, and 48 hpi, S/Ns were harvested and DENV infectious virus release was measured by plaque assay, and cell lysates were obtained and total RNA extracted for DENV RNA analysis by qRT-PCR. Input virus (2 hpi) was comparable between cells with and without SK1-I and DENV RNA and infectious virus release increased with time (Figure 3.5). At 24 and 48 hpi, DENV infectious virus was significantly reduced in SK1-I treated cells compared to DMSO-treated cells (Figure 3.5A). DENV RNA levels were also significantly decreased in the cells treated with SK1-I compared to DMSO control cells (Figure 3.5B). These results suggest that chemical inhibition of SK1 impairs DENV infection *in vitro*.

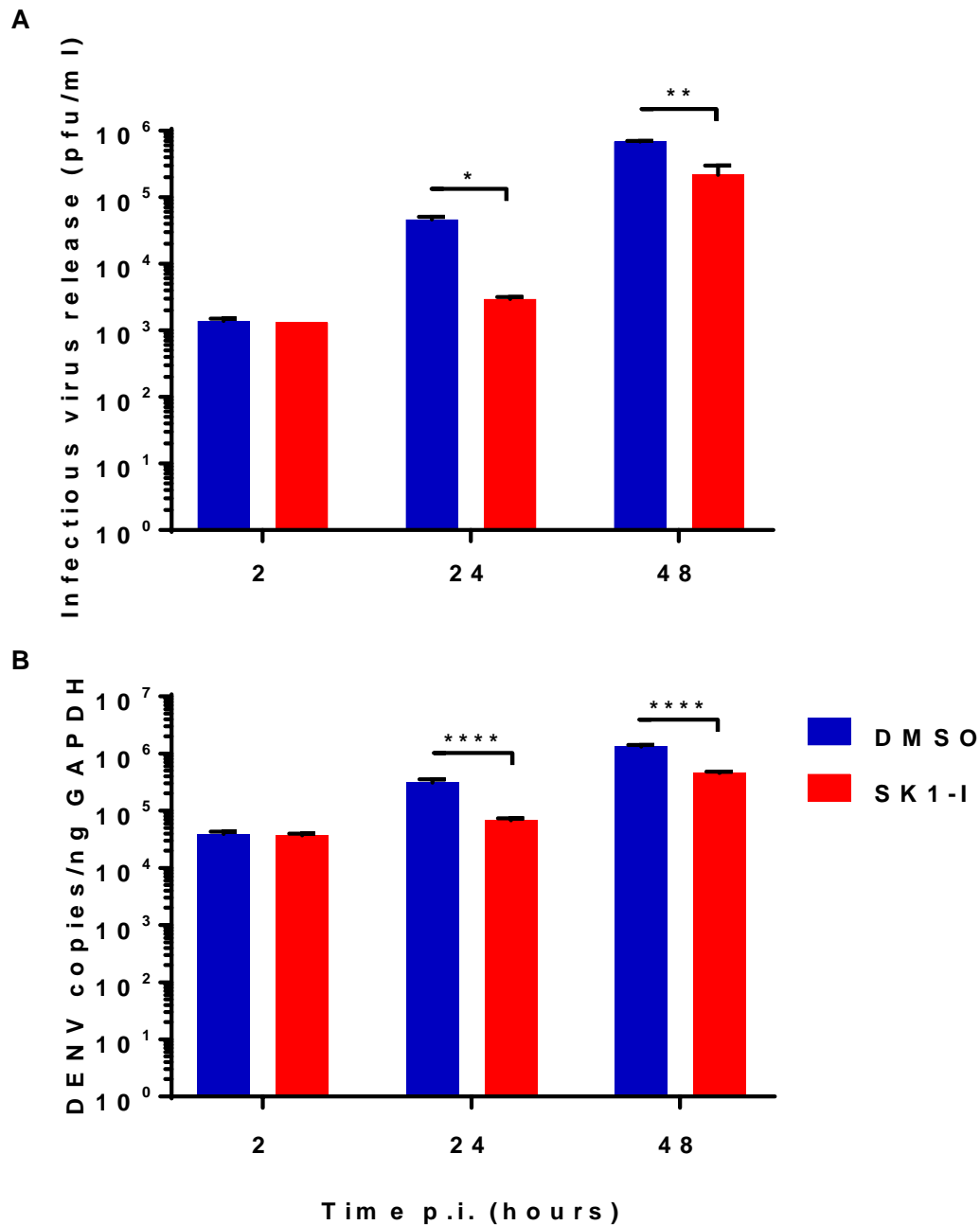


Figure 3.5 SK1-I treatment reduces DENV infection

HEK293 c18 cells were pre-treated for 1 h with 5 μ M SK1-I and infected with DENV at MOI of 1. At indicated time pi, (A) S/N was taken for plaque assay, and (B) RNA was isolated and DENV quantitated by RT-PCR. Copy number was determined from a standard curve and normalised against GAPDH. Results represent mean \pm SD of n=2 assay replicates from two independent experiments. Statistical significance was determined by two-way ANOVA. * $p < 0.05$, ** $p < 0.005$, **** $p < 0.00005$.

3.2.6 Inhibition of SK1 with SK1-I impairs DENV-induced innate responses

We further assessed the effect of SK1 inhibition on innate immune responses against DENV infection *in vitro*. HEK293 c18 cells were pre-treated with 5 μ M SK1-I and DENV challenged at MOI of 1. Cell lysates were harvested, and mRNA levels for IFN- β , ISGs and TNF- α were measured by qRT-PCR at 24 and 48 hpi. The qRT-PCR's used in our laboratory for these factors were previously established by other colleagues but reaction for IRF7 was additionally established and validated (Appendix 5). Results showed that IFN- β , ISGs viperin, IFIT1, IRF7, CXCL10, in addition to TNF- α were induced at 48 hpi in DENV-infected cells compared to uninfected cells (Figure 3.6). Further, the mRNA levels of IFN- β , ISGs viperin, IFIT1, IRF7, CXCL10, and TNF- α in DENV-infected SK1-I treated cells were significantly lower than DMSO control cells at 48 hpi (Figure 3.6).

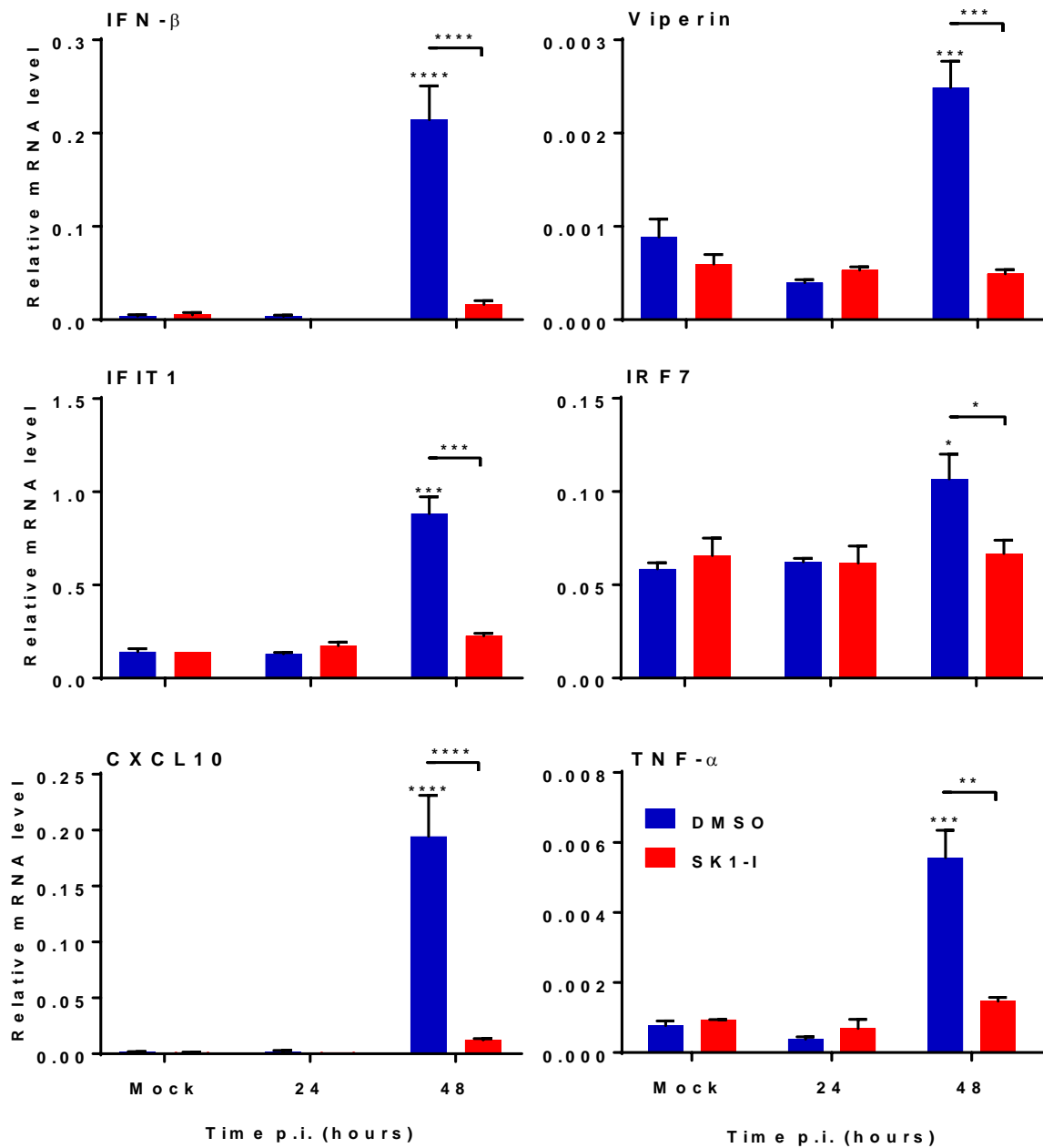


Figure 3. 6 SK1-I treatment reduces DENV-induced innate responses

HEK293 c18 cells were pre-treated for 1 h with 5 μ M SK1-I and infected with DENV at MOI of 1. At indicated time pi, RNA was isolated and mRNA levels for IFN- β , viperin, IFIT1, IRF7, CXCL10, and TNF- α were measured by qRT-PCR. Values were normalised to GAPDH and relative RNA level determined by Δ Ct method. Data represent mean \pm SD of n=2 assay replicates from two independent experiments. Statistical significance was determined using two-way ANOVA to mock-infected control. * p < 0.05, ** p < 0.005, *** p < 0.0005, **** p < 0.00005.

3.3 Discussion

SK1 plays a vital role in cell survival or death decision through balancing the intracellular levels of ceramide, a pro-apoptotic lipid, and S1P, the pro-proliferative lipid, and these regulatory actions are known as the ceramide/S1P rheostat [250]. There is substantial and growing evidence suggesting that targeting of SK1 may be employed in the therapy of a wide range of diseases including cancer [218] and autoimmune diseases [251]. Further, a growing literature demonstrates that chemical targeting of SK1 by specific inhibitors affects viral infection *in vitro* [206]. Thus, in this study here, we assessed the role of SK1 during DENV infection *in vitro* through inhibition of SK1 using chemical inhibitors.

Previous data from our laboratory has shown that HEK293 cells and monocyte-derived macrophages (MDMs) treated with SKi *after* an established DENV infection at a time where the cells are producing new viral RNA and particles had no significant effect on DENV infectious release [233]. Here we investigated if SK1 inhibition *prior* to and during the early stages (< 6 hpi) following DENV challenge could affect the subsequent DENV infection. Our results show that chemical SK inhibition using SKi prior to DENV infection significantly reduced DENV infection in a number of cell lines and in a dose-dependent manner in HEK293 c18 cells. Of note, 5 μ M SKi significantly decreased DENV infectious release and without any toxic effects on these cells when examined visually under light microscopy. Our results are inconsistent with the data that showed SKi treatment increased BVDV levels in a dose-dependent manner [231]. We observed here that SK1 activity was significantly reduced at 24 hpi following treatment with 5 μ M SKi, although in comparison SK2 activity that was not affected by SKi treatment. These data confirmed that SKi is a potent compound that inhibits SK1 activity but not SK2 under the conditions used herein, and as described previously [252]. Further supporting the idea that inhibition of SK1 is the factor mediating the reduced DENV infection following treatment with SKi, inhibition of SK1 activity via a selective SK1 inhibitor, SK1-I, also significantly impaired DENV infectious release and DENV

RNA levels in HEK293 c18 cells. These results indicate that targeting of endogenous SK1 activity prior to DENV challenge inhibits viral infection, suggesting a requirement for SK1 for robust DENV replication. Consistent with our observations, previous investigations demonstrated that a chemical inhibition of SK activity reduced HCMV, IAV, and measles infections *in vitro* [225,229,230]. In contrast, however, inhibition the activity of SK1 was beneficial and promoted efficient BVDV replication [231]. Additionally, our results here are consistent with our recent laboratory published data suggesting DENV infectious release and DENV RNA levels were significantly reduced in SK1^{-/-} iMEFs at 24 and 48 hpi, although this effect was not replicated in primary SK1^{-/-} MEFs for reasons related to changes in the IFN response such as a defect in ability to induce ISGs and p-STAT1 [167,253].

A chemical reduction of SK1 has been demonstrated to impair viral infections by a variety of biological mechanism. SK inhibition reduced IAV RNA production through suppression of NF-κB activation and impeded the nuclear export of viral ribonucleoprotein complex [229]. Additionally, treatment with SK inhibitors, such as SKI-II, decreased the production of measles virus proteins and reduce the activation of measles-induced NF-κB that resulted in impaired viral infectious release and replication [230]. Further, inhibition of SK1 activity accelerated the RSV and HCMV-induced cell death led to reduce viral production [225,226]. In contrast, reduction in SK1 activity promoted BVDV replication by unknown mechanism [231]. Here, inhibition of SK1 with a selective chemical agent, SK1-I, inhibited DENV production and decreased viral RNA levels.

Sphingolipids, such as ceramide and S1P, are constituents of the plasma membrane. Potentially, alternations in the composition of these lipids may affect virus entry into cells. For instance, ceramide has shown to inhibit the entry of HIV [254] and HCV [255] into target cells. Further, cholesterol-rich membrane microdomains was reported to be essential for uptake of flaviviruses such as DENV [85] and WNV [256]. Since SKs control the cellular levels of ceramide, sphingosine and S1P [205], inhibition of SK activity is likely to influence the balance of the sphingolipids in cellular membranes and may affect the process of DENV entry. Quantitation of infectious DENV

and DENV RNA present immediately following infection, representing bound and/or viral entry, was not affected by SKi treatment, suggesting a post-binding/entry effect of SKi on DENV. Further investigation, however, showed that SKi treatment has no effect on DENV RNA replication using a GFP-reporter subgenomic replicon system. Thus, targeting reduction in SK1 activity with SKi has no direct impact on DENV RNA replication. In contrast to this, inhibition in DENV RNA accumulation by SK1-I treatment was observed suggesting differences in the mechanisms of action of these different SK inhibitors, and the rationale for this remains to be investigated. Consistent with our data with SK1-I, targeting of SK with SKI-II inhibitor did not inhibit IAV entry step although other parts of the viral life cycles such as RNA synthesis were affected [229]. Further, inhibition of measles virus replication in response to SK inhibition with SKI-II has been demonstrated to occur via a post entry mechanism by SKI-II treatment [230]. Thus, although SK inhibitors have the potential to effect the plasma membrane composition, the existing literature and our data supports effects on viral replication at post-entry and viral replication levels.

As described above, concurrent and complementing work in our laboratory had defined DENV infection in SK1^{-/-} immortalised (i) MEF. Results concur with our SKi/SK1-I treatment, suggesting that reduced SK1 activity is associated with reduced DENV infection. Using this SK1^{-/-} iMEF system, microarray analysis that was further validated by qRT-PCR demonstrated that the reduced susceptibility of the SK1^{-/-} iMEF cells was associated with significant up-regulation of the basal levels of a number of innate factors such as IRF7, CXCL10, and OAS1 [167]. Thus, in this chapter, we investigated whether the reduced DENV-infection observed in SK1-I pre-treated cells was due to up-regulation of innate responses. We observed here that DENV infection induces the transcription of IFN- β and ISGs IFIT1, IRF7, CXCL10, and the inflammatory mediator TNF- α in both SK1-I-treated and DMSO-treated cells at 48 hpi. Further, the mRNA levels of the IFN- β and ISGs IFIT1, IRF7, and CXCL10 were significantly lower in SK1-I-treated cells in response to DENV infection and the important anti-DENV ISG, viperin, was not induced at all. In contrast to our data in SK1^{-/-} iMEF, no significant difference was observed in basal levels of IFN- β and ISGs in

SK1-I treated cells. Additional data from colleagues in the laboratory has defined that the up-regulation of ISGs in SK1^{-/-} MEF is specific to the immortalised MEF line and was not reproduced in 6 independent primary SK1^{-/-} MEF isolates [13]. Together, this suggests that the reduced DENV-infection seen in SKi/SK1-I pre-treated cells is not due to higher levels of innate factors, not reflected by DENV infection in SK1^{-/-} MEF and that a reduction of SK1 activity prior to DENV infection reduces the cells ability to induce the antiviral effectors following DENV infection. This however, is complicated by the reduced stimulation of innate responses as a consequence of the lower DENV replication, but we cannot exclude that this also involves a contribution of SK1 to the induction of these responses. In support of this, a prior report has demonstrated that a chemical inhibition of SK1 activity and the absence of SK1 in SK1^{-/-} mice decreased IL-1 stimulated and IRF1-mediated CXCL10 and CCL5 induction [257]. Recent data from colleagues in our laboratory has shown that type I IFN responses are altered in the context of SK1^{-/-} MEF (primary) that is associated with reduced cell surface IFNAR1 protein and IRF1 mRNA in uninfected cells and reduced ability to stimulate Y701 phosphorylation of STAT1 following DENV-infection or type I IFN stimulation [253]. These results demonstrate that reduced SK1 can affect innate cell signalling pathways. Similar responses, however, do not occur in SK1-I or SK1 shRNA expressing cells [253], thus demonstrating that there are inherent differences in the innate DENV-induced responses in mouse cells genetically lacking SK1 (eg SK1^{-/-} 1°MEFs) and human cells treated with agents to transiently reduce SK1 activity (eg SK1-I). Thus, the effect of SK1 on innate responses following infection is still unclear and may be context dependent on the manner in which SK1 is manipulated.

In summary, in this study, we have established that DENV infection in cells in the presence of SK1 inhibitors reduces DENV infection in a number of different cell lines and in a dose-dependent manner. The effect of SK1 is likely post virus binding and likely via an early step in viral replication although this requires further investigation to define the specific steps in the viral life cycle targeted. Reduced DENV infection following SK1 inhibition was not associated with an increase in cellular innate responses to infection, as we have observed in an SK1^{-/-} iMEF line [167],

but was associated with reduced induction of IFN- β , ISGs and TNF- α following infection. It remains to be determined however, if this reflects a role of SK1 in induction of these innate response, or is simply a secondary consequence of the lower DENV replication in SK1-I treated cells. Given the growing pharmaceutical interest in SK1 (and SK2 – see chapter 5) inhibitors, the potential for use of SK1 inhibitors to reduce DENV infection, without exacerbating the damaging inflammatory response associated with severe DENV disease is a promising avenue and suggests future analysis of the effects of SK1 inhibitors *in vitro*.

Alongside the studies in this chapter, we investigated the need for SK1 for DENV infection in an *in vivo* model, using intracranial DENV challenge in immunocompetent WT and SK1 null mice (chapter 4).

CHAPTER 4. THE ROLE OF SK1 DURING DENV INFECTION

IN VIVO

This chapter contains the following publication:

Al-Shujairi WH, Clarke JN, Davies LT, Alsharifi M, Pitson SM, Carr JM. Intracranial Injection of Dengue Virus Induces Interferon Stimulated Genes and CD8+ T Cell Infiltration by Sphingosine Kinase 1 Independent Pathways. PLoS One. 2017;12(1):e0169814. Epub 2017/01/18. doi: 10.1371/journal.pone.0169814. PubMed PMID: 28095439.

4.1 Introduction

No effective therapies are available to alleviate the large number of DENV infections and DENV-associated disease each year. A better understanding of the DENV-induced immune responses are crucial to develop reliable anti-DENV strategies such as an effective vaccine or drug candidate against all DENV serotypes. To assist studies in this area, numerous attempts have been undertaken to develop a suitable DENV infection animal model that could mimic DENV disease in humans in the context of a competent immune system [184,186]. The inability of DENV to replicate or cause an infection in C57BL/6 immunocompetent mice with a working immune response is important obstacle in this field [185] and different animal models for DENV are discussed in chapter 1 section 1.14. Routes of DENV infection such as ic direct injection in an immunocompetent mouse model does result in DENV replication and DENV-induced neuropathies and death [237,258].

Recent *in vitro* data from our laboratory has shown DENV infection is significantly reduced in the absence of SK1 in iMEF cells, and the induction of IFN- β and ISGs such as viperin and CXCL10 are dysregulated following DENV infection in SK1^{-/-} iMEFs [167]. Additionally, in chapter 3 of this thesis, we demonstrated that chemical inhibition of SK1 enzyme activity restricts DENV infection in cultured cells (*in vitro*) and a reduction in SK1 activity reduces the ability of DENV to

induce the host innate immune response. Here, we utilised a neurovirulence model of DENV infection to assess the role of SK1 during DENV infection *in vivo* in the context of a competent immune system. We utilised WT and SK1 null mice in which the SK1 gene is deleted as described in section 2.2.7, and a direct DENV injection (ic) into the brain on the background of C57BL/6 of immunocompetent mice.

In this chapter, we investigated the DENV-induced disease in the brain of WT and SK1^{-/-} mice following ic infection through measurement of body weight loss and appearance of neurovirulence symptoms. We assessed DENV replication and the induction of IFN- β and ISGs by RT-PCR and T-lymphocyte infiltration by RT-PCR for CD4 and CD8, as well as H&E staining. In addition, we defined changes in the SK1/S1P axis by measurement of SK mRNA by RT-PCR, SK enzyme activity using an *in vitro* assay and S1P level by HPLC during DENV infection in the mouse brain. This data has been published, as following.

RESEARCH ARTICLE

Intracranial Injection of Dengue Virus Induces Interferon Stimulated Genes and CD8⁺ T Cell Infiltration by Sphingosine Kinase 1 Independent Pathways

Wisam H. Al-Shujairi^{1*}, Jennifer N. Clarke¹, Lorena T. Davies², Mohammed Alsharifi³, Stuart M. Pitson², Jillian M. Carr¹

1 Microbiology and Infectious Diseases, School of Medicine, Flinders University, Adelaide, South Australia, Australia, **2** Centre for Cancer Biology, University of South Australia and SA Pathology, Adelaide, South Australia, Australia, **3** Vaccine Research Laboratory, Research Centre for Infectious Diseases, and Department of Molecular and Cellular Biology, School of Biological Sciences, University of Adelaide, Adelaide, South Australia, Australia

* alsh0246@flinders.edu.au



OPEN ACCESS

Citation: Al-Shujairi WH, Clarke JN, Davies LT, Alsharifi M, Pitson SM, Carr JM (2017) Intracranial Injection of Dengue Virus Induces Interferon Stimulated Genes and CD8⁺ T Cell Infiltration by Sphingosine Kinase 1 Independent Pathways. PLoS ONE 12(1): e0169814. doi:10.1371/journal.pone.0169814

Editor: Xia Jin, Institut Pasteur of Shanghai Chinese Academy of Sciences, CHINA

Received: September 1, 2016

Accepted: December 21, 2016

Published: January 17, 2017

Copyright: © 2017 Al-Shujairi et al. This is an open access article distributed under the terms of the [Creative Commons Attribution License](https://creativecommons.org/licenses/by/4.0/), which permits unrestricted use, distribution, and reproduction in any medium, provided the original author and source are credited.

Data Availability Statement: All relevant data are within the manuscript.

Funding: This work was supported by the National Health and Medical Research Council (NHMRC) Project Grant GNT1044212, the Fay Fuller Foundation, and a NHMRC Senior Research Fellowship (GNT1042589).

Competing Interests: The authors have declared that no competing interests exist.

Abstract

We have previously reported that the absence of sphingosine kinase 1 (SK1) affects both dengue virus (DENV) infection and innate immune responses *in vitro*. Here we aimed to define SK1-dependency of DENV-induced disease and the associated innate responses *in vivo*. The lack of a reliable mouse model with a fully competent interferon response for DENV infection is a challenge, and here we use an experimental model of DENV infection in the brain of immunocompetent mice. Intracranial injection of DENV-2 into C57BL/6 mice induced body weight loss and neurological symptoms which was associated with a high level of DENV RNA in the brain. Body weight loss and DENV RNA level tended to be greater in SK1^{-/-} compared with wildtype (WT) mice. Brain infection with DENV-2 is associated with the induction of interferon-β (IFN-β) and IFN-stimulated gene (ISG) expression including viperin, Ifi2712a, IRF7, and CXCL10 without any significant differences between WT and SK1^{-/-} mice. The SK2 and sphingosine-1-phosphate (S1P) levels in the brain were unchanged by DENV infection or the lack of SK1. Histological analysis demonstrated the presence of a cellular infiltrate in DENV-infected brain with a significant increase in mRNA for CD8 but not CD4 suggesting this infiltrate is likely CD8⁺ but not CD4⁺ T-lymphocytes. This increase in T-cell infiltration was not affected by the lack of SK1. Overall, DENV-infection in the brain induces IFN and T-cell responses but does not influence the SK/S1P axis. In contrast to our observations *in vitro*, SK1 has no major influence on these responses following DENV-infection in the mouse brain.

Introduction

Sphingolipids, which are an integral part of membranes in all eukaryotic cells, have been involved in a variety of cell signalling functions [1]. One of these signalling sphingolipids is sphingosine-1-phosphate (S1P) which has well-known critical roles in cell growth and development [2] and T-lymphocyte recruitment [3]. This latter property has drawn considerable recent attention and has led to the clinical use of S1P analogues in the treatment of diseases such as multiple sclerosis [4]. S1P is a normal metabolite produced following the phosphorylation of sphingosine by the sphingosine kinases (SKs) which can play an important role in cell signalling and inflammation [5]. For example, a recent study by Harikumar *et al.*, showed that SK1 was required for interferon regulatory factor (IRF)-1-mediated induction of CXCL10 and CCL5 chemokines following interleukin 1 (IL-1) stimulation [6]. There are two forms of SK, designated SK1 and SK2 [7]. Both isozymes show a high degree of sequence similarity although they vary in size, catalytic properties, tissue distribution, and subcellular localisation [8], and have been proposed to have complementing but also distinct physiological roles [1, 9].

A role for SK1 during viral infections is emerging, as we have recently reviewed [10]. Several viruses have been shown to modulate the activity or level of SK1 for efficient viral infection. For instance, bovine viral diarrhoea virus (BVDV) reduced the catalytic activity of SK1 to promote viral replication [11]. In contrast, an increase of SK1 expression and activity during human cytomegalovirus (HCMV) [12], influenza A virus [13], and measles virus (MV) [14] infections enhanced viral replication. Moreover, SK1 can promote viral infections through different biological mechanisms. SK1 has been shown to prolong survival of virus-infected cells [12], and viral protein synthesis [14]. We have previously shown that SK1 activity is altered during dengue virus (DENV) infection [15, 16], and that a reduction in SK1 affects the ability of DENV to induce interferon-stimulated genes (ISGs) *in vitro* [17]. Here, we investigated the effect of SK1 on DENV replication and the induction of ISGs using an *in vivo* model comprising intracranial (ic) injection of DENV.

DENV is a globally important human pathogen that can cause a wide spectrum of clinical presentations from a febrile illness to a life-threatening infection with bleeding complications [18]. The disease severity and pathogenicity is thought to be immune-mediated in which immune responses to DENV exacerbate damage to the host [19–21]. Unlike DENV-infection in humans, DENV does not replicate well or cause symptoms reflective of human disease in immunocompetent wild type (WT) mice [22], but can cause a similar pathology in mice deficient in the interferon (IFN) response, such as in the AG129 IFN receptor knockout mouse model [23]. Analysis of neurovirulence—the induction of symptoms of brain infection including reduction in hind limb function has been a widely used historical method to indicate the presence of virus following ic inoculation. Ic injection of DENV into WT mice, although not reflective of a natural mode of DENV-infection, is associated with DENV replication and neurological symptoms [24, 25] but additionally, may reflect some aspects of DENV-associated neurological disease in humans [26]. Although DENV does not antagonise IFN responses in mice as it does in humans [27], in our study we utilised the DENV ic mouse infection model as a means to assess the role of SK1 in DENV infection and induction of ISGs *in vivo* in an immunocompetent animal. We compared virus replication and immune responses following ic injection of DENV into WT and SK1^{-/-} mice. Our data define novel ISG and T-cell responses, and a lack of change in the SK/S1P axis in the brain following DENV infection and demonstrate that SK1 is not a key regulator of these processes in the brain.

Materials and Methods

Ethics statement

All animal procedures were performed in accordance with Flinders University Animal Welfare committee approval number 870/14 and Institutional Biosafety Committee approval NLRD 2011–10.

Mice

Three to four weeks of age WT C57BL/6 ($n = 24$) and homozygous knockout for the *Sphk1* gene encoding SK1 ($SK1^{-/-}$) ($n = 17$) [28] mice were used in this study. All mice were kept in a pathogen-free environment on a 12 hours cycle of light and darkness with *ad libitum* access to food and water.

Virus production

Mice were infected using MON601, a full-length cDNA clone of DENV-2 New Guinea C strain [29]. The virus stock was produced from *in vitro* transcribed RNA that was transfected into baby hamster kidney clone 21 (BHK-21) cells and amplified in *Aedes albopictus* C6/36 cells. Cell culture supernatants containing virus was harvested, clarified, filtered, and stored at -80°C . The titre of infectious virus was determined by plaque assay using African green monkey kidney (Vero) cells and quantitated as plaque forming unit per ml (pfu/ml).

DENV-2 challenge and follow-up

WT and $SK1^{-/-}$ mice were anaesthetised by isoflurane inhalation, and infected by ic injection with 800 pfu of DENV-2 MON601 diluted in phosphate-buffered saline (PBS) in a volume of 10 μl . Mock control mice were injected ic with PBS. Animals were visually monitored twice daily for signs of DENV-induced neurological disease including slow movement, hunched posture, or reduction in hind limb function. In addition, animals were monitored for body weight. Any sign of neurological disease or loss of more than 10% of body weight represented a termination point and animals were sacrificed immediately by isoflurane anaesthetic inhalation and humane decapitation. Brain tissues were harvested at sacrifice and divided into two parts. The ipsilateral section was resuspended in TRIzol reagent (Ambion Life Technologies) for RNA extraction and real-time quantitative PCR (qRT-PCR) analysis and the contralateral section was snap frozen in liquid nitrogen for SK activity assay and S1P quantification or fixed for histological analysis.

Real-time quantitative RT-PCR

Total RNA was extracted from brain tissues using TRIzol (Ambion Life Technologies), according to the manufacturer's instructions. The extracted RNA was DNase I treated (Zymo Research) and quantitated by spectrophotometry (NanoDrop elite, Thermo Scientific). Total RNA (0.5 μg) was reverse transcribed using M-MuLV reverse transcriptase (NEB) and random hexamers (NEB) in a 20 μl final volume, and subjected to a real-time qRT-PCR. qRT-PCR was carried out using 2 μl of cDNA template in a 10 μl reaction using iTaq SYBER green (BioRad) with 20 μM of each forward and reverse primer. All PCR primers were synthesised by GeneWorks with sequences as listed in Table 1. Real-time qRT-PCR was performed using Rotor-Gene 3000 real-time PCR system (Corbett research, Australia) under the following conditions: one cycle of 95°C for 5 minutes; 45 cycles of 95°C for 15 seconds, 59°C for 30 seconds, and 72°C for 30 seconds; and one cycle of 72°C for 60 seconds followed by melt curve analysis. Quantitative DENV copy number was calculated from a standard curve generated from

Table 1. Primer sequences used in this study for qRT-PCR.

Name	Primers Sequence		Accession No.
DENV-2 capsid region	Forward	GCAGATCTCTGATGAATAACCAAC	D00346.1
	Reverse	TTGTCAGCTGTGTACAGTCG	
GAPDH	Forward	GACGGCCGCATCTTCTTGTGC	NM_008084.3
	Reverse	TGCCACTGCAAATGGCAGCC	
SK1	Forward	TGTCACCCATGAACCTGCTGTCCCTGCACA	NM_001172475.1
	Reverse	GCCCTTCTGCACCAGTGTA	
SK2	Forward	TCTGGAGACGGGCTGCTTTA	NM_001172561.1
	Reverse	GCACCCAGTGTGAATCGAGC	
IFN-β	Forward	AGAAAGGACGAACATTCGGAAA	NM_010510.1
	Reverse	CCGTCATCTCCATAGGGATCTT	
Viperin	Forward	ACTCTGTTCATTAATCGCTTCAACGT	NM_021384.4
	Reverse	TCAATTAGGAGGCACTGGAAAAC	
Irf2712a	Forward	CTGTTTGGCTCTGCCATAGGAG	NM_029803.3
	Reverse	CCTAGGATGGCATTGTTGATGTGG	
IRF7	Forward	CACCCCATCTTCGACTTCA	NM_001252601.1
	Reverse	CCAAAACCCAGGTAGATGGTCTA	
CXCL10	Forward	GCCGTCATTTCTGCCTCAT	NM_021274.2
	Reverse	GGCCCGTCATCGATATGG	
CD4	Forward	CCCAGGTCCTCGCTCAGTTTG	NM_013488.2
	Reverse	AGGTAGGTCCCATCACCTCACAG	
CD8-β	Forward	GCTGGTAGTCTGCATCCTGCTTC	NM_009858.2
	Reverse	TTGCTAGCAGGCTATCAGTGTGTG	

doi:10.1371/journal.pone.0169814.t001

known concentration of MON601 DNA quantitated by spectrophotometry. DNA copy numbers from 15 pg/μl to 0.015 pg/μl were analysed in concurrent real-time PCR to generate a standard curve from which unknown DENV RNA copy numbers were calculated. Relative RT-PCR quantitation was determined by the ΔCt method [30] for all other genes. All PCR reactions were normalised against the reference housekeeping gene glyceraldehyde-3-phosphate dehydrogenase (GAPDH).

Measurement of sphingosine kinase activity

Frozen brain tissues were homogenised and sonicated in a buffer consisting of 50 mM Tris/HCl (pH 7.4) containing 150 mM NaCl, 2 mM Na₃VO₄, 10 mM NaF, 10% (w/v) glycerol, 10 mM β-glycerophosphate, 0.05% (w/v) Triton X-100, 1 mM EDTA and protease inhibitors (Roche, Complete mini). SK1 and SK2 activities were selectively measured by ³²P transfer from [³²P] ATP to D-erythro-sphingosine under conditions of Triton X-100 for SK1 activity and 1 M KCl for SK2 activity, as previously described [31]. The SK activities were normalised against total protein content, as determined by Bio-Rad protein assay.

S1P quantitation

S1P levels were measured as previously described [32] with some modifications. Briefly, 20 μl of brain homogenate was suspended in 200 μl methanol with 0.25% conc. HCl. Alkaline extraction of the lipids was performed by addition of 400 μl chloroform, 30 μl of 10 M NaOH, 580 μl of 2 M KCl and 200 μl methanol with 200 pmol C17-S1P and centrifuged (5 min, 16000xg). The upper aqueous/methanol phase was collected and acid extraction was performed with 40 μl conc. HCl and 300 μl chloroform. The upper phase was aspirated and 200 μl

of lower chloroform phase was collected and chloroform was evaporated using a speed vacuum system. The dried lipids were resuspended in 275 μ l methanol/70 mM K_2HPO_4 (9:1) with 1 mM EDTA by sonication in a bath sonicator for 30 sec. A derivatization mixture of 10 mg *o*-phthalaldehyde, 200 μ l ethanol, 10 μ l β -mercaptoethanol and 10 ml of a 3% boric acid solution (adjusted to pH 10.5 with KOH) was prepared and 25 μ l of this was added to the lipid samples and incubated for 15 min at room temperature followed by centrifugation. SIP levels were then determined by HPLC analysis with an EVO C18 column (Phenomenex, Lane Cove, NSW, Australia) as previously described [32].

Histological analysis

Mouse brains were harvested and fixed in 10% (v/v) buffered formalin. Brain tissues were embedded and block mounted in paraffin. Sections were cut into 5 μ m thickness, stained with haematoxylin and eosin (H&E) and examined under brightfield microscopy (BX50, Olympus).

Statistical analysis

Statistical analyses were carried out using GraphPad Prism software version 6.07. A statistically significant difference between samples was assessed using Students unpaired *t*-test with Welch's correction. Kaplan-Meier survival curves were analysed by log rank test (Mantel-Cox). To examine the body weight loss and appearance of clinical signs of disease Fisher's exact test was used.

Results

DENV-2 infection induces neurological symptoms and weight loss in WT and SK1^{-/-} mice. To define the susceptibility of WT and SK1^{-/-} mice to DENV-2 ic infection, we compared the growth rates and survival of mock and DENV-infected WT and SK1^{-/-} mice. Animals were challenged by ic injection with 800 pfu/mouse DENV-2, and body weight and neurological symptoms (slow movement, hunched posture, and reduction in hind limb movement) recorded daily. Mock-infected mice did not demonstrate any loss in body weight or neurological symptoms (Fig 1A–1D). Although there was a tendency towards a greater and earlier body weight loss in DENV-infected SK1^{-/-} mice compared with DENV-infected WT mice, there was no significant difference in terms of the overall number of mice that lost body weight, the time of onset of body weight loss, nor the percentage of mice that lost more than 7% of body weight (Table 2). When average body weight gain as a percentage of the initial body weight was analysed, results showed that both DENV-infected WT mice and SK1^{-/-} mice started to lose body weight at 6 days post infection (dpi) in comparison to mock-infected mice (Fig 1A and 1C). As expected, analysis of survival demonstrated a significantly higher mortality in DENV-infected compared to mock-infected mice (Fig 1B and 1D). Comparison of body weight loss and survival of DENV-infected WT and SK1^{-/-} mice support the trends in Table 2 and demonstrate that DENV-infected SK1^{-/-} mice show a significantly greater weight loss at 7 dpi than WT mice (Fig 1E). At this time point, 7 out of 17 WT mice (~41%) and 7 out of 13 SK1^{-/-} mice (~54%) were sacrificed due to either excessive body weight loss and/or appearance of signs of DENV-induced neurovirulence. This is reflected by an apparent higher survival rate of WT compared to SK1^{-/-} mice at 7 and 8 dpi, although this was not statistically significant (Fig 1F). These results suggest that C57BL/6 mice deficient in SK1 tend to be more susceptible to body weight loss following DENV-2 infection than their counterpart WT mice but the overall disease profile is comparable.

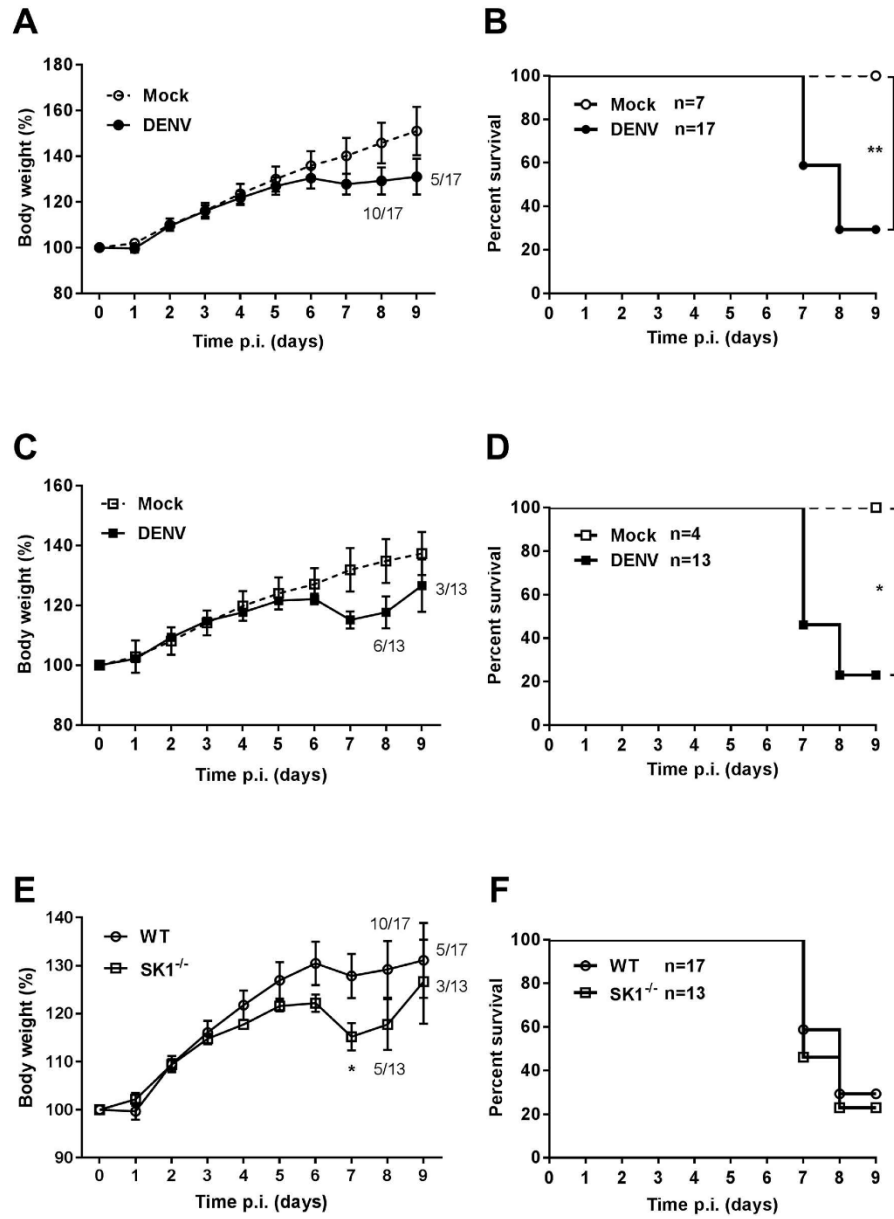


Fig 1. Susceptibility of WT and SK1^{-/-} mice to DENV-2 infection. 3–4 week old C57BL/6 WT (n = 17) and SK1^{-/-} (n = 13) mice were ic injected with 800 pfu DENV-2 MON601. Mock WT (n = 7) and SK1^{-/-} (n = 4) control mice were ic injected with vehicle only. Body weight and neurological symptoms were recorded. Body weight is expressed as a percentage of initial body weight. Survival reflects mice that do not show neurological symptoms or >10% of body weight loss. **A and B.** Comparison of body weight and survival curves of mock with DENV-infected WT mice; **C and D.** Comparison of body

weight and survival curve of mock with DENV-infected SK1^{-/-} mice; **E and F.** Comparison of body weight percentage and survival curves of DENV-infected WT and SK1^{-/-} mice. Data are expressed as mean ± SEM. Statistical analysis of survival curves were determined by long-rank test. * = p < 0.05, ** = p < 0.005.

doi:10.1371/journal.pone.0169814.g001

DENV-2 RNA levels are not significantly different between WT and SK1^{-/-} mice but correlate with DENV-induced disease. DENV replication in the brain following ic injection was validated by analysis of the time course of DENV RNA changes in WT mice. qRT-PCR analysis demonstrated increasing DENV RNA level with time with 3 dpi representing an early time point where DENV RNA levels were increasing (Fig 2A). Eight WT or SK1^{-/-} mice were injected ic with DENV-2 and brain tissues harvested at 3 dpi. DENV RNA levels at 3 dpi tended to be higher in SK1^{-/-} compared with WT mice (p = 0.083), but were not significantly different (Fig 2B). RNA levels were also quantitated in WT and SK1^{-/-} mice at the termination of experiments. DENV RNA level was significantly higher at day 7–8, than at 9–14 dpi in both WT and SK1^{-/-} mice (Fig 2C). The sacrifice of mice at 7–8 dpi was due to symptomatic presentation and ethical termination, but those sacrificed at 9–14 dpi showed body weight loss but lacked neurological symptoms and represented an elective time for termination of the experiment. Based on the disease presentation and comparable level of DENV RNA at 7 and 8 dpi, we have considered this combined time point as ‘end-stage disease’. We have indicated the 9–14 dpi animals in Figs 4–7 as half-filled symbols but excluded these animals from our statistical analysis since they did not show DENV-induced disease. It should be noted, however that the inclusion of the 9–14 dpi mice in the data set did not influence the statistical outcomes. At end-stage disease (7–8 dpi), DENV RNA levels again tended to be higher in SK1^{-/-} mice brains in comparison to WT mice (Fig 2C) but were not significantly different (p = 0.116). These data suggest that DENV-2 can replicate and cause body weight loss and neurological symptoms when introduced directly into the mouse brain, with a moderate but not statistically significant increase in DENV RNA in SK1^{-/-} compared to WT mice.

DENV-2 infection induces IFN-β and interferon-stimulated genes (ISGs) but this is not different in WT and SK1^{-/-} mice. Type 1 interferon, such as IFN-β, is an important part of the early immune response to DENV infection and to define this response following DENV-2 infection in the brain we analysed mRNA levels for IFN-β and the ISG’s viperin, Ii2712a, IRF7

Table 2. Summary of body weight loss and signs of DENV-induced neurovirulence in WT and SK1^{-/-} mice and analysed by Fisher’s exact test.

Criteria	Mice strains				P
	WT		SK1 ^{-/-}		
	Number	%	Number	%	
Body weight loss					
Weight loss	15	88.24	12	92.31	0.999
No weight loss	2	11.76	1	7.69	
% Body weight loss					
< 7%	8	53.33	2	16.67	0.107
> 7%	7	46.67	10	83.33	
Days pi onset loss					
< 7 dpi	3	20.00	5	41.67	0.398
> 7 dpi	12	80.00	7	58.33	
Appearance of neurovirulence					
Neurovirulence	10	58.82	9	69.23	0.708
No neurovirulence	7	41.18	4	30.77	

doi:10.1371/journal.pone.0169814.t002

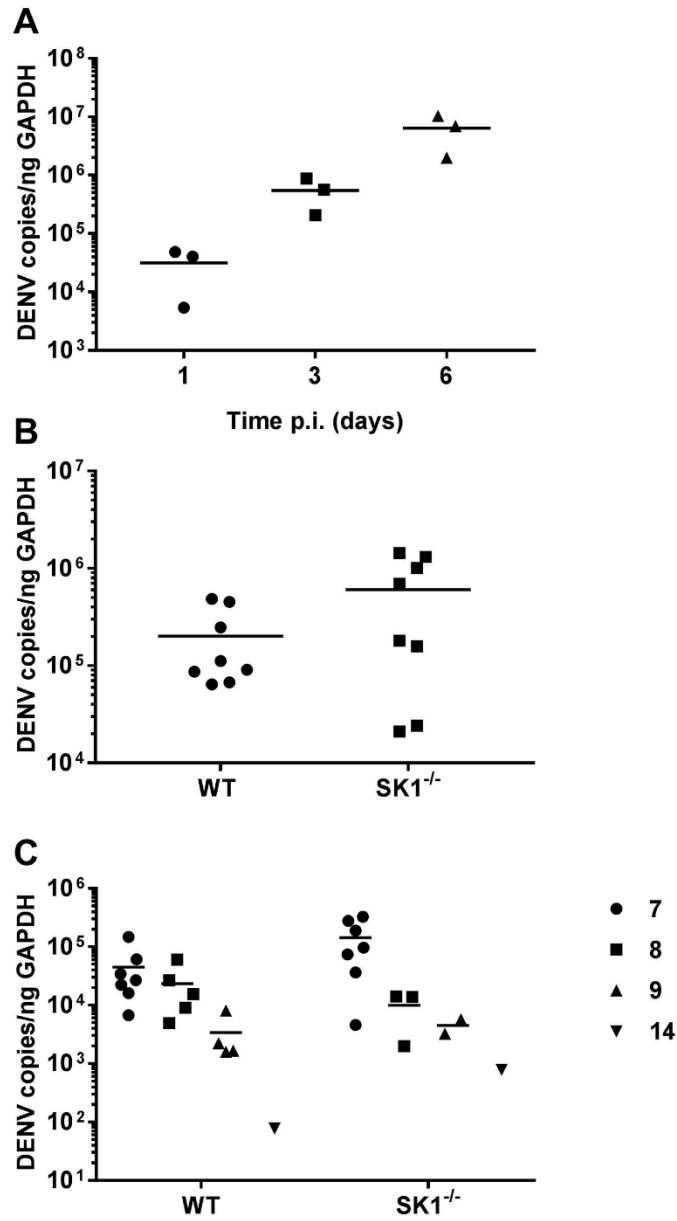


Fig 2. DENV-2 RNA levels increase WT and SK1^{-/-} mice following ic DENV infection. WT and SK1^{-/-} mice were ic infected with DENV, as in Fig 1. RNA was isolated from infected mice brain tissues and analysed by real time qRT-PCR for DENV. A. Total DENV-2 RNA increases with time in WT mice, n = 3 at each time point; B. RNA was isolated from infected WT and SK1^{-/-} mice brain tissues at 3 dpi, n = 8 for each strain; C. RNA was isolated from infected mice brain tissues at the time of humane sacrifice, representing 7 (n = 7), 8

(n = 5), 9 (n = 4) or 14 (n = 1) dpi for WT and 7 (n = 7), 8 (n = 3), 9 (n = 2) or 14 (n = 1) dpi for SK1^{-/-} mice. Each symbol represents an individual mouse sample. Data represent average PCR values from individual mice. Statistical significance was assessed by unpaired Student *t*-test.

doi:10.1371/journal.pone.0169814.g002

and CXCL10 in WT mice by qRT-PCR. Results show increased IFN- β mRNA, late in the course of infection at 6 dpi (Fig 3A). In comparison to this late induction of IFN- β , all the ISGs analysed were rapidly and significantly induced, as early as 1 dpi, for viperin and IRF7 or 3 dpi, for Ifi2712a and CXCL10 (Fig 3B).

Comparison of responses in WT and SK1^{-/-} mice at 3 dpi, showed that IFN- β and ISGs (viperin, Ifi2712a, IRF7 and CXCL10) mRNA levels were induced following DENV-infection but did not differ between WT and SK1^{-/-} mice (Fig 4A). At end stage disease, IFN- β mRNA levels tended to be increased ($p = 0.224$ WT; 0.086 SK1^{-/-}), while the ISGs viperin, Ifi2712a, IRF7 and CXCL10 were all significantly and highly induced by DENV-infection (Fig 4B). As seen at 3 dpi (Fig 4A), IFN- β and ISG mRNA levels were not significantly different between DENV-infected WT and SK1^{-/-} mice at end stage disease (Fig 4B). These data suggest that ISGs are induced early during DENV infection in the mouse brain, prior to the detectable induction of IFN- β , with the induction of ISGs persisting until end stage disease. The lack of SK1 however, has no effect on this response.

DENV-2 infection in the brain does not alter the SK/S1P axis. To validate the lack of SK1 in SK1^{-/-} mice and assess the impact of this and DENV-infection on the SK/S1P axis in the brain, we quantitated SK1 and SK2 mRNA, performed isoform-specific SK activity assays and determined S1P levels in the brain at end stage disease. qRT-PCR for SK1 mRNA and *in vitro* assays for SK1 activity in the brain verified the lack of SK1 in the mice (Fig 5A). Additionally, neither SK1 mRNA nor activity were altered in DENV-infected WT mice (Fig 5A). The lack of SK1 could be compensated for by an increase in SK2 levels. Results, however demonstrated no change in SK2 mRNA nor SK2 activity in SK1^{-/-} mice brains (Fig 5B). Again, neither SK2 mRNA or SK2 activity was altered in DENV-infected WT or SK1^{-/-} mice (Fig 5B). Further, S1P levels were quantitated in brain lysates. Notably, S1P levels were not different between WT and SK1^{-/-} mice, nor did they change following DENV-infection of either mouse strain (Fig 5C).

DENV-2 infection induces CD8⁺ but not CD4⁺ T-cell infiltration in the brain. CXCL10 which we have demonstrated to be induced (Figs 3 and 4), and S1P which is unchanged following DENV-infection, can both influence T-cell migration. Thus, we examined cell infiltration by histological H&E staining and the presence of mRNA for the T-lymphocyte markers, CD4 and CD8 by qRT-PCR in WT mouse brain tissue throughout the course of DENV ic infection. H&E staining of fixed brain tissue demonstrated the presence of a cellular infiltrate at 6 dpi in DENV compared to mock-infected mouse brain (Fig 6A). Results show no change in the level of CD4, but a marked and significant increase in CD8 by day 6 pi (Fig 6B), suggesting CD8⁺ T-cell infiltration following DENV-infection in the WT mouse brain.

The levels of CD4 and CD8 mRNA were compared by qRT-PCR in WT and SK1^{-/-} mice at 3 dpi and end stage disease (Fig 7). Results again demonstrate a lack of increase in CD4 mRNA levels following DENV-infection of WT or SK1^{-/-} mice at either time point pi and no significant difference between DENV-infected WT and SK1^{-/-} mice (Fig 7A). The levels of CD8 mRNA, however were significantly higher in DENV-infected WT and SK1^{-/-} mice compared to their mock-infected controls at end stage disease (Fig 7B), but once again there was no significant difference in CD8 mRNA between DENV-infected WT and SK1^{-/-} mice. These data suggest that CD8⁺ but not CD4⁺ T-lymphocytes infiltrate the brain of DENV-infected mice

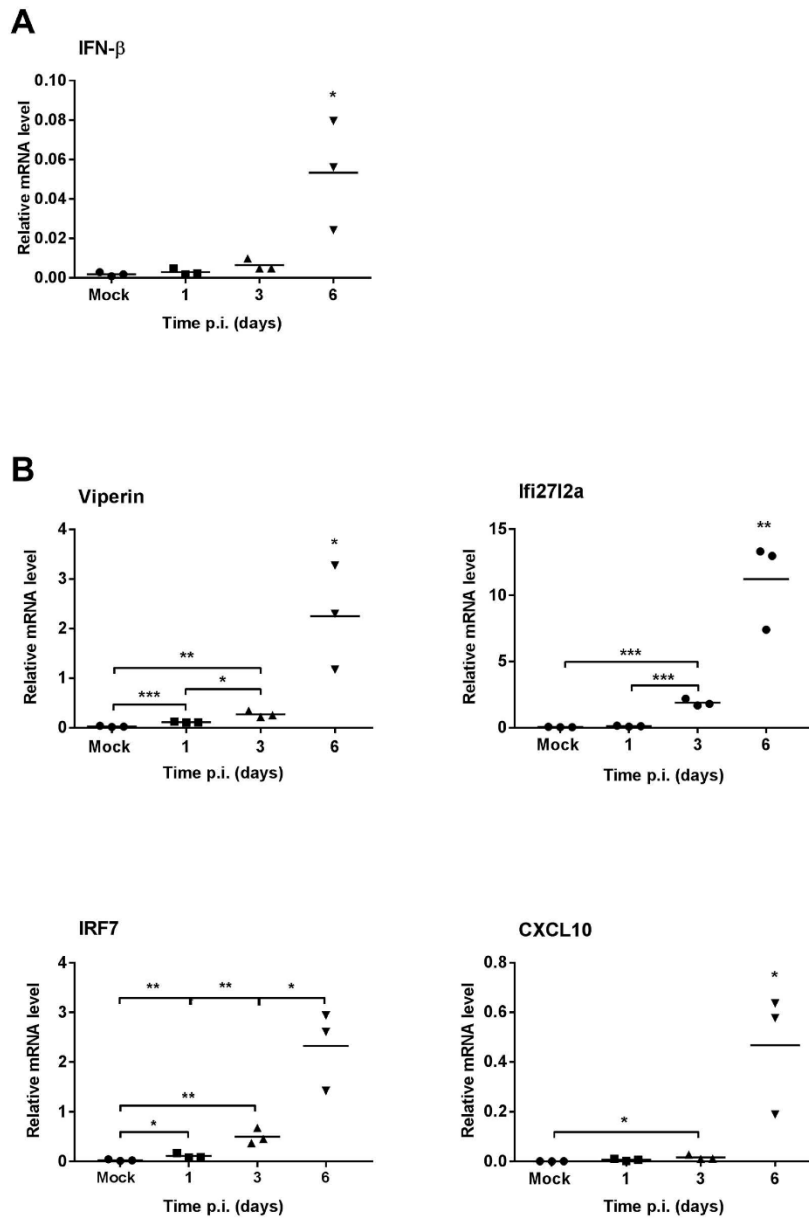


Fig 3. The time course of induction of IFN- β and ISGs in WT mice following ic infection with DENV-2. WT mice ($n = 3$ at each time point) were ic infected with DENV, as in Fig 1. At the time point indicated RNA was isolated from infected mice brain tissues and analysed by real time qRT-PCR for **A**. IFN- β ; **B**. ISGs viperin, Ifi2712a, IRF7 and CXCL10. Data represent average PCR values from individual mice and normalized against GAPDH by $\Delta\Delta C_t$ method. Statistical significance was assessed by unpaired student *t*-test * = $p < 0.05$, ** = $p < 0.005$, *** = $p < 0.0005$.

doi:10.1371/journal.pone.0169814.g003

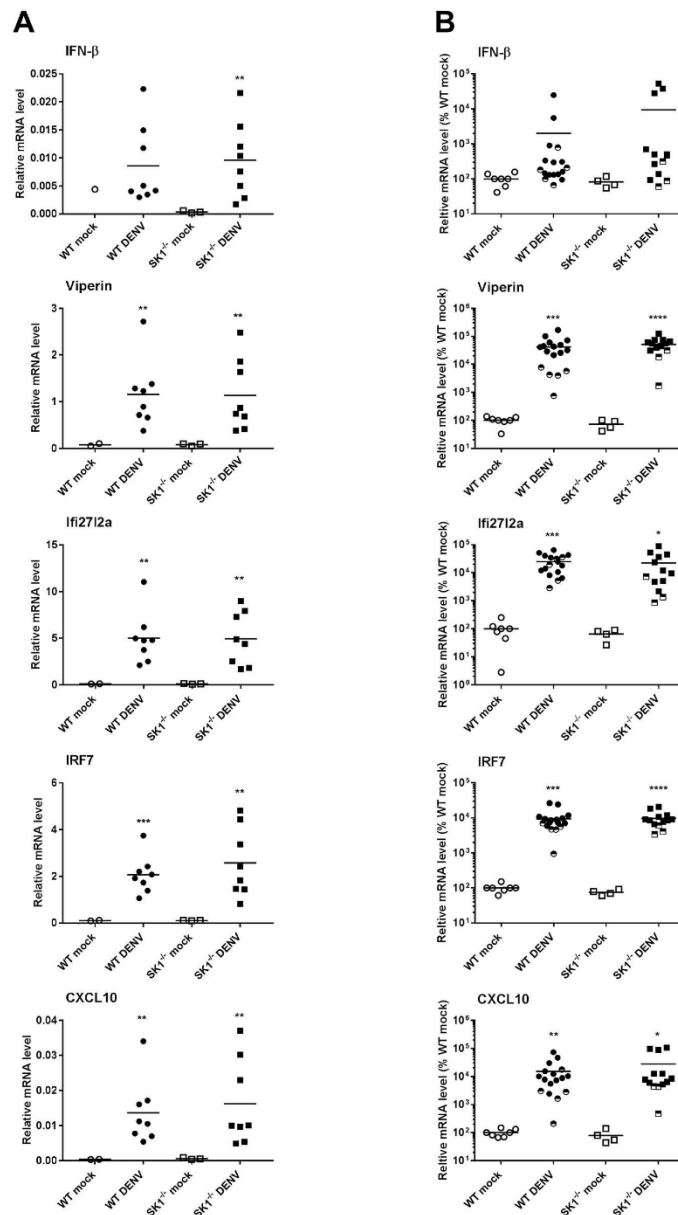


Fig 4. Induction of IFN-β and ISGs in WT and SK1^{-/-} mice following ic infection with DENV-2. WT and SK1^{-/-} mice were ic infected with DENV, as in Fig 1. RNA was isolated from infected mice brain tissues and analysed by real time qRT-PCR **A**, at 3 dpi for IFN-β, viperin, Irf2712a, and CXCL10. n = 8 WT and SK1^{-/-} DENV-infected, n = 2 WT mock and n = 3 SK1^{-/-} mock-infected mice; **B**, at end stage disease for IFN-β, viperin, Irf2712a, and CXCL10. n = 12 WT and n = 10 SK1^{-/-} DENV-infected, n = 7 WT mock and n = 4 SK1^{-/-}

mock-infected mice. Data points representing non-symptomatic animals (9–14 dpi) are indicated by the half-filled symbols. Statistical analysis has been performed on symptomatic DENV-infected mice only (7–8 dpi), excluding $n = 5$ WT and $n = 3$ SK1^{-/-} at 9/14 dpi. Data represent average PCR values from individual mice and normalized against GAPDH by $\Delta\Delta C_t$ method. Statistical significance was assessed by unpaired student *t*-test. * = $p < 0.05$, ** = $p < 0.005$, *** = $p < 0.0005$, **** = $p < 0.00005$.

doi:10.1371/journal.pone.0169814.g004

but there is no major role of SK1 in driving CD8⁺ T-cell migration into the brain during DENV-infection.

Discussion

A growing number of studies have reported SK1 as a factor that contributes to the modulation of several viral infections *in vitro* [10]. Our own studies have suggested changes in SK1 in response to DENV-2 infection [15, 33] and a role for SK1 early in infection in promoting DENV-induction of ISGs *in vitro* [17]. In the study here we have investigated the role of SK1 during DENV-2 infection *in vivo* using immunocompetent C57BL/6 mice and direct ic DENV infection.

Following DENV-2 infection, as expected, WT and SK1^{-/-} mice exhibited body weight loss and signs of neurovirulence compared to mock-infected mice. This reflects the pathogenicity and virulence of the DENV-2 MON 601 strain in mouse brain, as has been previously reported [29, 34]. Similar to other studies of DENV ic infection, not all mice develop neurological symptoms [29, 34]. We have further shown here that symptomatic DENV-infection with body weight loss and neurological signs is positively associated with the level of DENV RNA in the brain with a lower level of DENV RNA in the brains of asymptomatic mice at 9–14 dpi. The data from these mice has been represented graphically but we have excluded these from our statistical analysis. Interestingly, these asymptomatic mice strikingly group together with lower induction of viperin compared to symptomatic mice (Fig 4B) but are interspersed with the symptomatic mice in terms of responses such as CD8⁺ mRNA levels (Fig 7B). This suggests an association of viperin with symptomatic DENV-infection in the brain, and this remains to be investigated further.

Mice that are deficient in SK1 showed moderately greater and earlier body weight loss and tended to have higher levels of DENV RNA following DENV-2 infection than their counterpart WT mice. Since SK1 is a pro-survival factor [35], it is possible that without SK1 mice are more prone to weight loss and growth deficiencies. Additionally, the trend towards an increase in DENV RNA in SK1^{-/-} mice, although not statistically significant ($p = 0.116$), is consistent with our recent data showing enhancement of DENV-2 infection in SK1^{-/-} primary mouse embryonic fibroblast (MEF), that we demonstrated is associated with a reduced ability of DENV to induce ISGs in the absence of SK1 [17]. Thus, we assessed the SK1-dependency of the induction of ISGs in this DENV-brain infection model. We chose to analyse the mRNA level of selected important type I IFN driven ISGs: viperin [36], IRF7 [37], and CXCL10 [38] that have been described previously as antiviral factors against DENV and we have previously shown to be induced in a SK1-dependent manner in response to DENV infection *in vitro* [17]. Ifi2712a was also assessed as an ISG, previously reported to be induced in the brain in response to West Nile Virus (WNV) infection [39], and for which the response to DENV-infection has not been previously defined. At 6 dpi and end stage disease the level of IFN- β mRNA tended to be increased. In contrast there was a more rapid (1–3 dpi) and significant induction of ISGs viperin, Ifi2712a, IRF7 and CXCL10 that persisted until end stage disease. IFIT1 and OAS1, which are similarly anti-viral against DENV [40, 41] were also induced rapidly but were not analysed in our complete experimental set (data not shown). This is the first report of

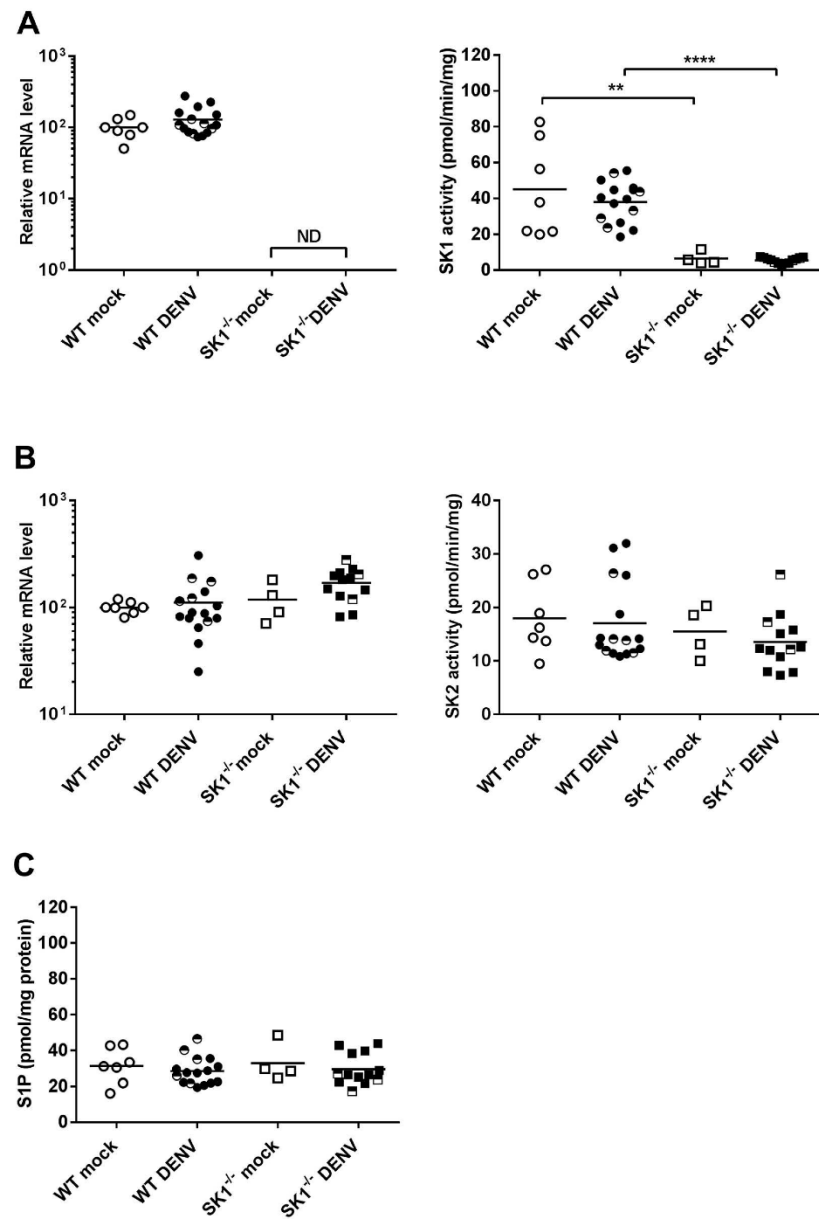


Fig 5. Definition of the SK/S1P axis in WT and SK1^{-/-} mice following ic infection with DENV-2. WT and SK1^{-/-} mice were ic infected with DENV, as in Fig 1 and at end stage disease, brain tissue was harvested and snap frozen or stored in TRIzol. RNA was extracted from TRIzol and lysates prepared in EB buffer from snap frozen tissue. **A.** SK1 mRNA was determined by qRT-PCR (left panel) and isoenzyme specific SK1 activity assay (right panel); **B.** SK2 mRNA was determined by qRT-PCR (left panel) and isoenzyme specific SK2 activity assay

(right panel); **C.** S1P was quantitated in brain lysates by HPLC. $n = 11$ WT and $n = 10$ SK1^{-/-} DENV-infected, $n = 7$ WT mock and $n = 4$ SK1^{-/-} mock-infected mice. PCR data represent average PCR values from individual mice and normalized against GAPDH by Δ Ct method. SK activity data and S1P quantitation are expressed relative to total protein quantitation. Statistical significance was assessed by unpaired student *t*-test. ** = $p < 0.05$, **** = $p < 0.00005$. ND, not detected. Data points representing non-symptomatic animals (9–14 dpi) are indicated by the half-filled symbols. Statistical analysis has been performed on symptomatic DENV-infected mice only, excluding $n = 5$ WT and $n = 3$ SK1^{-/-} at 9/14 dpi.

doi:10.1371/journal.pone.0169814.g005

induction of these ISGs in the brain following DENV-infection and the first report of DENV-induction of Ifi2712a. The discordance between the induction of IFN- β and these ISGs contrasts to studies that show IFN- β to be a major driver of neuronal ISGs response during WNV infection in the brain [42, 43] and ISGs following DENV-infection in some cells [16, 44]. This

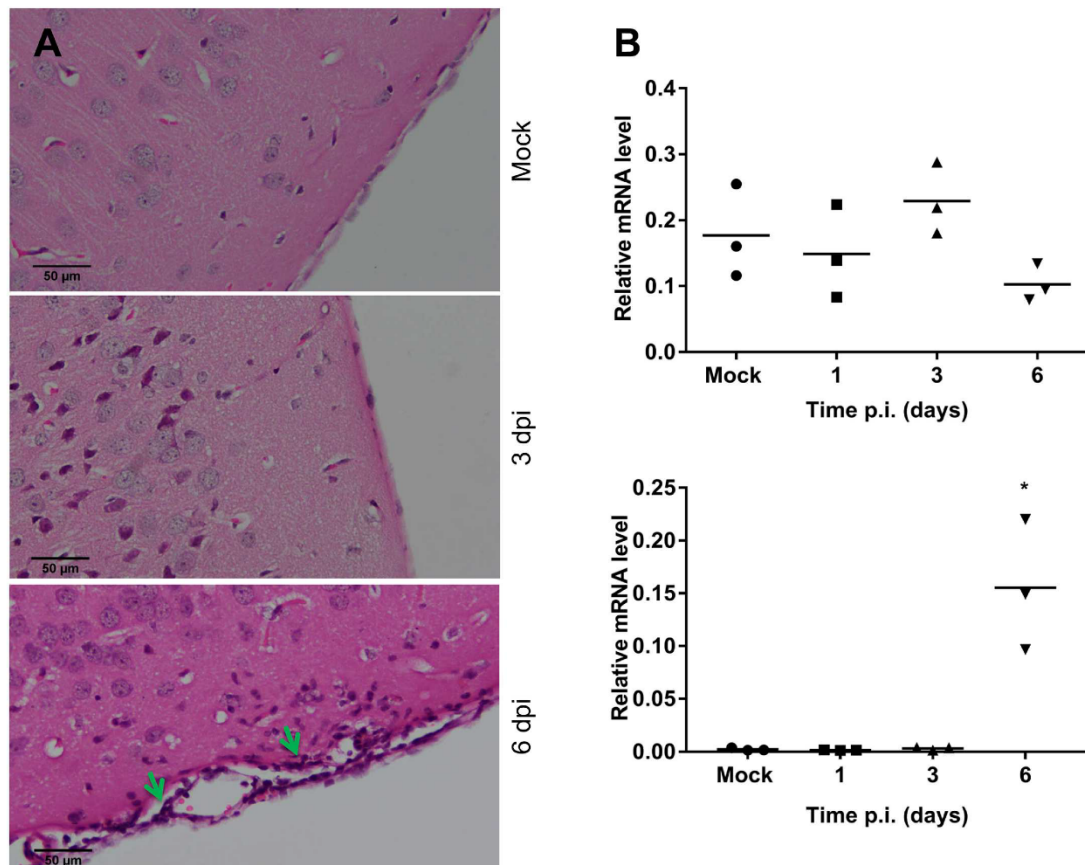


Fig 6. T-cell infiltration in the brain of WT mice following ic infection with DENV-2. WT mice were ic infected with DENV, as in Fig 1 and brain tissue was harvested. **A.** at 3 and 6 dpi, tissue was fixed and processed for H&E staining. Images are representative of $n = 3$ mice. Arrows indicate sites of cellular infiltrate; **B.** at the indicated time point RNA was extracted and CD4 and CD8 mRNA determined by qRT-PCR with $n = 3$ mice at each time point. Data represent average PCR values from individual mice and normalized against GAPDH by Δ Ct method. Statistical significance was assessed by unpaired student *t*-test. * = $p < 0.05$.

doi:10.1371/journal.pone.0169814.g006

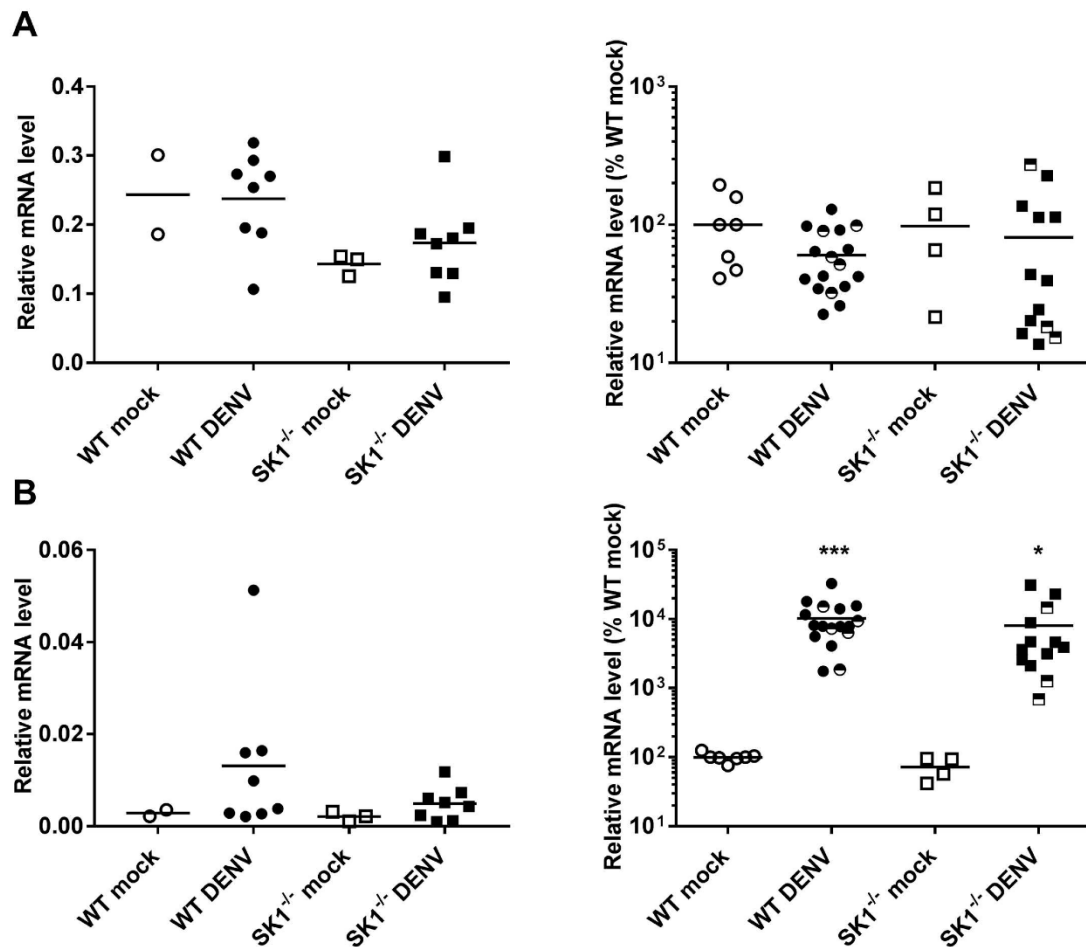


Fig 7. T-cell infiltration in the brain of WT and SK1^{-/-} mice following ic infection with DENV-2. WT and SK1^{-/-} mice were ic infected with DENV, as in Fig 1 and brain tissue harvested at 3 dpi and end stage disease. RNA was isolated from infected mice brain tissues and analysed by real time qRT-PCR for **A.** CD4 mRNA; **B.** CD8 mRNA. At 3 dpi n = 8 WT and SK1^{-/-} DENV-infected, n = 2 WT mock and n = 3 SK1^{-/-} mock-infected mice. At end stage disease (7–8 dpi) n = 12 WT and n = 10 SK1^{-/-} DENV-infected, n = 7 WT mock and n = 4 SK1^{-/-} mock-infected mice. Data points representing non-symptomatic animals (9–14 dpi) are indicated by the half-filled symbols. Statistical analysis has been performed on symptomatic DENV-infected mice only, excluding n = 5 WT and n = 3 SK1^{-/-} at 9/14 dpi. Data represent average PCR values from individual mice and normalized against GAPDH by $\Delta\Delta C_t$ method. Statistical significance was assessed by unpaired student t-test. * = $p < 0.05$, ** = $p < 0.005$, *** = $p < 0.0005$.

doi:10.1371/journal.pone.0169814.g007

suggests that IFN- β may not be the major driver of induction of these ISGs following DENV infection in the brain. Potentially, other factors such as IFN- γ or λ may be more important in this tissue [45–47]. Studies have shown the activation of microglial cells, an increase in neurological disease severity when these cells are depleted and a role for microglia in production of cytokines and chemokines such as RANTES, IFN- γ , IL-6, MCP-1 and MCP5 following

DENV-infection in the brain [48]. Similarly, in our model of DENV-ic infection, these resident microglial cells may be the source of the induction of ISGs we have observed here.

The induction of ISGs is evident prior to the presence of symptomatic infection but was not significantly different between WT and SK1^{-/-} mice. This contrasts to our prior data from *in vitro* studies where embryonic fibroblasts from SK1^{-/-} mice or cells treated with an SK1 inhibitor (SK1-I) show reduced DENV-induction of ISGs such as viperin, IFIT1 and CXCL10 [17]. Similarly, genetic deletion or chemical inhibition of SK1 reduced the IL-1 induced expression of CXCL10 [6]. This suggests that in contrast to MEF and peripheral responses, the deficiency of SK1 does not compromise the induction of ISGs in the model herein of DENV-infection of the brain. Further, that lack of a major effect of the lack of SK1 on DENV-disease suggests that similarly SK1-dependent inflammatory pathways are not involved in regulating DENV replication and pathogenicity in the brain. This contrasts to LPS [49] or ischemia-induced neuroinflammation [50] where SK1 has been shown to be present in microglia and to promote the induction of factors such as TNF- α , IL-1 and nitric oxide [49] but intriguingly a lack of SK1 exacerbates LPS induced neuroinflammation [51]. Our observed lack of influence of SK1 on DENV in the brain may be due to pathogen or stimulus specific roles for SK1 in brain inflammation or tissue specific roles for SK1, where in the brain SK2 is known to be the dominant SK isoform [52]. The brain is an immune privileged site and previous studies have also reported differences in the expression of ISGs between the brain and other tissues. For example, mRNA levels for genes such as OAS, MDA5, and STAT1 as well as ISGs IFIT1, IFIT2, and ISG15 are greater in the liver than the brain of mice [53, 54]. Studies also showed expression of ISGs vary between the different cell types within the brain itself. For example, the basal and inducible levels of OAS were lower in neurons than microglia in response to MHV infection [53] and higher levels of both basal and induced ISGs (e.g. IFIT1 and IRF7) are observed in microglia than oligodendrocytes [53, 55]. Additionally, mouse cortical neurons fail to express basal levels of ISG54 and ISG56 [56] while distinct neuronal subsets in the brain differentially express Irf27, IRF1 and viperin that make these cells more susceptible to WNV infection [43]. Thus, although we saw no overall effect of a lack of SK1 in a whole brain extract, and *in situ* analysis of SK1 and ISGs in different cells of the brain may be informative.

The SK/SIP axis is a finely regulated system [57]. Our findings demonstrated that the lack of SK1 in the mouse brain was not compensated for by changes in SK2 mRNA or activity, consistent with prior studies in the periphery [28, 58]. Further, SK1^{-/-} mice do not have altered levels of SIP in the brain. Additionally, DENV-infection did not affect SK1 or SK2 mRNA or activity in the brain. This contrasts to the early increase in SK1 activity that we have documented in DENV-infected EC [16] and inhibition late in infection in a number of cell types *in vitro* [15], which again may reflect tissue-specific responses of SK1 to infection. Further, SK2 mRNA or activity or SIP levels in the brain were not different following DENV-infection of WT and SK1^{-/-} mice.

Following viral infection, one would expect to see an immune cell infiltrate to the site of infection. We demonstrated a marked cell infiltrate in DENV-infected mouse brain by H&E staining and further characterised the nature of this cellular infiltrate as CD8⁺ but not CD4⁺ T-cells by RT-PCR analysis, although we did not analyse the presence of monocytes, a cell type also known to infiltrate the brain in WNV infection [59, 60]. A prior study has shown both CD4⁺ and CD8⁺ T cells infiltration into the brain following DENV-3 challenge in C57BL/6 mice [25], or DENV-2 challenge in BALB/c mice [34]. Further, Hsieh *et al.* showed predominant CD8⁺ compared to CD4⁺ T cell infiltration in DENV-infected mouse brain [38]. Similarly, the infiltration of T cells has been demonstrated in mouse brains during infection with other flaviviruses. Increased CD8⁺ but not CD4⁺ mRNA levels were detected in Japanese encephalitis virus (JEV)-infected mouse brains [61], and similarly CD8⁺ T-cells infiltrate

WNV-infected mouse brains [62] and following ic challenge with the Alphavirus, Semliki Forest virus (SFV) [63]. In contrast, both CD4+ and CD8+ T cells have been reported in mice challenged with a WNV [60, 64] and Yellow fever (YF)-17D virus [65]. Thus, there is an overall consensus from a number of *flavivirus* and other virus infections in the brain that CD8+ T-cells are a major infiltrating cell type, and our data is consistent with this suggestion.

CXCL10 has been implicated in T-cell migration into the brain in WNV and SFV infections [63, 66] and S1P is an important regulator of T-cell migration from lymph nodes in the periphery [67]. CXCL10 was induced following DENV-brain infection of WT mice in our study but S1P was unchanged, supporting a potential role of CXCL10 but not S1P in driving CD8+ T-cell infiltration during DENV-infection of the brain. The induction of CXCL10 mRNA at 3 dpi and prior to the onset of T-cell infiltration at 6 dpi further supports this association. Additionally, in our study a lack of SK1 did not affect DENV-induced responses of CXCL10 or S1P and consistent with this, a lack of SK1 did not affect T-cell infiltration in the brain during DENV infection.

In summary, in this study we have shown that SK1 has a moderate effect on body weight loss and DENV RNA levels following DENV-2 infection in the mouse brain but has no overall major impact on DENV-induced disease. While DENV-infection induced ISGs and CD8+T-cell infiltration, the SK/S1P axis is not affected by DENV-infection and none of these factors were significantly affected by the absence of SK1. This data has defined innate responses to DENV-infection in the brain and demonstrate that in contrast to our studies showing a role of SK1 in promoting ISG induction following DENV-infection *in vitro*, and other studies demonstrating a role for SK1 in non-infectious neuroinflammation, in the scenario of DENV-infection of the brain, SK1 does not play a role in these processes.

Acknowledgments

Thank-you to Ms Pat Vilimas and Yvette deGraaf at Flinders Microscopy for assistance with tissue processing and staining, the staff at the School of Medicine animal facility and Mrs Julie Calvert for laboratory assistance. Thank-you to Dr Briony Gliddon for breeding and provision of SK1^{-/-} mice. This work was supported by the National Health and Medical Research Council (NHMRC) Project Grant GNT1044212, the Fay Fuller Foundation, and a NHMRC Senior Research Fellowship (GNT1042589).

Author Contributions

Conceptualization: WHA SMP JMC.

Data curation: WHA JMC.

Formal analysis: WHA MA.

Funding acquisition: SMP JMC.

Investigation: WHA JNC LTD SMP JMC.

Methodology: WHA JNC LTD SMP JMC.

Project administration: SMP JMC.

Resources: LTD SMP.

Supervision: MA SMP JMC.

Validation: WHA SMP JMC.

Visualization: WHA.

Writing – original draft: WHA.

Writing – review & editing: WHA MA SMP JMC.

References

1. Pitson SM. Regulation of sphingosine kinase and sphingolipid signaling. *Trends Biochem Sci.* 2011; 36(2):97–107. Epub 2010/09/28. doi: [10.1016/j.tibs.2010.08.001](https://doi.org/10.1016/j.tibs.2010.08.001) PMID: [20870412](https://pubmed.ncbi.nlm.nih.gov/20870412/)
2. Alvarez SE, Milstien S, Spiegel S. Autocrine and paracrine roles of sphingosine-1-phosphate. *Trends Endocrinol Metab.* 2007; 18(8):300–7. Epub 2007/10/02. doi: [10.1016/j.tem.2007.07.005](https://doi.org/10.1016/j.tem.2007.07.005) PMID: [17904858](https://pubmed.ncbi.nlm.nih.gov/17904858/)
3. Baeyens A, Fang V, Chen C, Schwab SR. Exit Strategies: S1P Signaling and T Cell Migration. *Trends in immunology.* 2015; 36(12):778–87. Epub 2015/11/26. doi: [10.1016/j.it.2015.10.005](https://doi.org/10.1016/j.it.2015.10.005) PMID: [26596799](https://pubmed.ncbi.nlm.nih.gov/26596799/)
4. Gonzalez-Cabrera PJ, Brown S, Studer SM, Rosen H. S1P signaling: new therapies and opportunities. *F1000prime reports.* 2014; 6:109. Epub 2015/01/13. doi: [10.12703/P6-109](https://doi.org/10.12703/P6-109) PMID: [25580263](https://pubmed.ncbi.nlm.nih.gov/25580263/)
5. Alemany R, van Koppen CJ, Danneberg K, Ter Braak M, Meyer Zu Heringdorf D. Regulation and functional roles of sphingosine kinases. *Naunyn Schmiedebergs Arch Pharmacol.* 2007; 374(5–6):413–28. Epub 2007/01/24. doi: [10.1007/s00210-007-0132-3](https://doi.org/10.1007/s00210-007-0132-3) PMID: [17242884](https://pubmed.ncbi.nlm.nih.gov/17242884/)
6. Harikumar KB, Yester JW, Surace MJ, Oyeniran C, Price MM, Huang WC, et al. K63-linked polyubiquitination of transcription factor IRF1 is essential for IL-1-induced production of chemokines CXCL10 and CCL5. *Nature immunology.* 2014; 15(3):231–8. Epub 2014/01/28. doi: [10.1038/ni.2810](https://doi.org/10.1038/ni.2810) PMID: [24464131](https://pubmed.ncbi.nlm.nih.gov/24464131/)
7. Kohama T, Olivera A, Edsall L, Nagiec MM, Dickson R, Spiegel S. Molecular cloning and functional characterization of murine sphingosine kinase. *J Biol Chem.* 1998; 273(37):23722–8. Epub 1998/09/03. PMID: [9726979](https://pubmed.ncbi.nlm.nih.gov/9726979/)
8. Neubauer HA, Pitson SM. Roles, regulation and inhibitors of sphingosine kinase 2. *FEBS J.* 2013; 280(21):5317–36. Epub 2013/05/04. doi: [10.1111/febs.12314](https://doi.org/10.1111/febs.12314) PMID: [23638983](https://pubmed.ncbi.nlm.nih.gov/23638983/)
9. Siow DL, Anderson CD, Berdyshev EV, Skobeleva A, Natarajan V, Pitson SM, et al. Sphingosine kinase localization in the control of sphingolipid metabolism. *Advances in enzyme regulation.* 2011; 51(1):229–44. doi: [10.1016/j.advenzreg.2010.09.004](https://doi.org/10.1016/j.advenzreg.2010.09.004) PMID: [21075134](https://pubmed.ncbi.nlm.nih.gov/21075134/)
10. Carr JM, Mahalingam S, Bonder CS, Pitson SM. Sphingosine kinase 1 in viral infections. *Reviews in medical virology.* 2013; 23(2):73–84. Epub 2012/05/29. doi: [10.1002/rmv.1718](https://doi.org/10.1002/rmv.1718) PMID: [22639116](https://pubmed.ncbi.nlm.nih.gov/22639116/)
11. Yamane D, Zahoor MA, Mohamed YM, Azab W, Kato K, Tohya Y, et al. Inhibition of sphingosine kinase by bovine viral diarrhea virus NS3 is crucial for efficient viral replication and cytopathogenesis. *J Biol Chem.* 2009; 284(20):13648–59. Epub 2009/03/19. doi: [10.1074/jbc.M807498200](https://doi.org/10.1074/jbc.M807498200) PMID: [19293152](https://pubmed.ncbi.nlm.nih.gov/19293152/)
12. Machesky NJ, Zhang G, Raghavan B, Zimmerman P, Kelly SL, Merrill AH Jr., et al. Human cytomegalovirus regulates bioactive sphingolipids. *J Biol Chem.* 2008; 283(38):26148–60. Epub 2008/07/23. doi: [10.1074/jbc.M710181200](https://doi.org/10.1074/jbc.M710181200) PMID: [18644793](https://pubmed.ncbi.nlm.nih.gov/18644793/)
13. Seo YJ, Blake C, Alexander S, Hahm B. Sphingosine 1-phosphate-metabolizing enzymes control influenza virus propagation and viral cytopathogenicity. *J Virol.* 2010; 84(16):8124–31. doi: [10.1128/JVI.00510-10](https://doi.org/10.1128/JVI.00510-10) PMID: [20519401](https://pubmed.ncbi.nlm.nih.gov/20519401/)
14. Vijayan M, Seo YJ, Pritzl CJ, Squires SA, Alexander S, Hahm B. Sphingosine kinase 1 regulates measles virus replication. *Virology.* 2014; 450–451:55–63. Epub 2014/02/08. doi: [10.1016/j.virol.2013.11.039](https://doi.org/10.1016/j.virol.2013.11.039) PMID: [24503067](https://pubmed.ncbi.nlm.nih.gov/24503067/)
15. Carr JM, Kua T, Clarke JN, Calvert JK, Zebol JR, Beard MR, et al. Reduced sphingosine kinase 1 activity in dengue virus type-2 infected cells can be mediated by the 3' untranslated region of dengue virus type-2 RNA. *J Gen Virol.* 2013; 94(Pt 11):2437–48. Epub 2013/08/14. doi: [10.1099/vir.0.055616-0](https://doi.org/10.1099/vir.0.055616-0) PMID: [23939980](https://pubmed.ncbi.nlm.nih.gov/23939980/)
16. Calvert JK, Helbig KJ, Dimasi D, Cockshell M, Beard MR, Pitson SM, et al. Dengue Virus Infection of Primary Endothelial Cells Induces Innate Immune Responses, Changes in Endothelial Cells Function and Is Restricted by Interferon-Stimulated Responses. *Journal of Interferon & Cytokine Research: the official journal of the International Society for Interferon and Cytokine Research.* 2015. Epub 2015/04/23.
17. Clarke JN, Davies LK, Calvert JK, Gliddon BL, Al Shujari WH, Aloia AL, et al. Reduction in sphingosine kinase 1 influences the susceptibility to dengue virus infection by altering anti-viral responses. *J Gen Virol.* 2015. Epub 2015/11/07.

18. Simmons CP, Farrar JJ, Nguyen v V, Wills B. Dengue. *N Engl J Med*. 2012; 366(15):1423–32. Epub 2012/04/13. doi: [10.1056/NEJMra1110265](https://doi.org/10.1056/NEJMra1110265) PMID: [22494122](https://pubmed.ncbi.nlm.nih.gov/22494122/)
19. Halstead SB, Mahalingam S, Marovich MA, Ubol S, Mosser DM. Intrinsic antibody-dependent enhancement of microbial infection in macrophages: disease regulation by immune complexes. *The Lancet Infectious diseases*. 2010; 10(10):712–22. Epub 2010/10/05. doi: [10.1016/S1473-3099\(10\)70166-3](https://doi.org/10.1016/S1473-3099(10)70166-3) PMID: [20883967](https://pubmed.ncbi.nlm.nih.gov/20883967/)
20. Nascimento EJ, Hottz ED, Garcia-Bates TM, Bozza F, Marques ET Jr., Barratt-Boyes SM. Emerging concepts in dengue pathogenesis: interplay between plasmablasts, platelets, and complement in triggering vasculopathy. *Critical reviews in immunology*. 2014; 34(3):227–40. Epub 2014/06/19. PMID: [24941075](https://pubmed.ncbi.nlm.nih.gov/24941075/)
21. Simmons CP, Dong T, Chau NV, Dung NT, Chau TN, Thao le TT, et al. Early T-cell responses to dengue virus epitopes in Vietnamese adults with secondary dengue virus infections. *J Virol*. 2005; 79(9):5665–75. Epub 2005/04/14. doi: [10.1128/JVI.79.9.5665-5675.2005](https://doi.org/10.1128/JVI.79.9.5665-5675.2005) PMID: [15827181](https://pubmed.ncbi.nlm.nih.gov/15827181/)
22. Bente DA, Rico-Hesse R. Models of dengue virus infection. *Drug discovery today Disease models*. 2006; 3(1):97–103. Epub 2007/12/19. doi: [10.1016/j.ddmod.2006.03.014](https://doi.org/10.1016/j.ddmod.2006.03.014) PMID: [18087566](https://pubmed.ncbi.nlm.nih.gov/18087566/)
23. Johnson AJ, Roehrig JT. New mouse model for dengue virus vaccine testing. *J Virol*. 1999; 73(1):783–6. Epub 1998/12/16. PMID: [9847388](https://pubmed.ncbi.nlm.nih.gov/9847388/)
24. Velandia-Romero ML, Acosta-Losada O, Castellanos JE. In vivo infection by a neuroinvasive neurovirulent dengue virus. *Journal of NeuroVirology*. 2012; 18(5):374–87. doi: [10.1007/s13365-012-0117-y](https://doi.org/10.1007/s13365-012-0117-y) PMID: [22825914](https://pubmed.ncbi.nlm.nih.gov/22825914/)
25. Amaral DC, Rachid MA, Vilela MC, Campos RD, Ferreira GP, Rodrigues DH, et al. Intracerebral infection with dengue-3 virus induces meningoencephalitis and behavioral changes that precede lethality in mice. *Journal of neuroinflammation*. 2011; 8:23. Epub 2011/03/11. doi: [10.1186/1742-2094-8-23](https://doi.org/10.1186/1742-2094-8-23) PMID: [21388530](https://pubmed.ncbi.nlm.nih.gov/21388530/)
26. Carod-Artal FJ, Wichmann O, Farrar J, Gascon J. Neurological complications of dengue virus infection. *The Lancet Neurology*. 2013; 12(9):906–19. Epub 2013/08/21. doi: [10.1016/S1474-4422\(13\)70150-9](https://doi.org/10.1016/S1474-4422(13)70150-9) PMID: [23948177](https://pubmed.ncbi.nlm.nih.gov/23948177/)
27. Gack MU, Diamond MS. Innate immune escape by Dengue and West Nile viruses. *Current opinion in virology*. 2016; 20:119–28. Epub 2016/10/30. doi: [10.1016/j.coviro.2016.09.013](https://doi.org/10.1016/j.coviro.2016.09.013) PMID: [27792906](https://pubmed.ncbi.nlm.nih.gov/27792906/)
28. Allende ML, Sasaki T, Kawai H, Olivera A, Mi Y, van Echten-Deckert G, et al. Mice deficient in sphingosine kinase 1 are rendered lymphopenic by FTY720. *J Biol Chem*. 2004; 279(50):52487–92. Epub 2004/10/02. doi: [10.1074/jbc.M406512200](https://doi.org/10.1074/jbc.M406512200) PMID: [15459201](https://pubmed.ncbi.nlm.nih.gov/15459201/)
29. Gualano RC, Pryor MJ, Cauchi MR, Wright PJ, Davidson AD. Identification of a major determinant of mouse neurovirulence of dengue virus type 2 using stably cloned genomic-length cDNA. *J Gen Virol*. 1998; 79 (Pt 3):437–46. Epub 1998/03/31.
30. Schmittgen TD, Livak KJ. Analyzing real-time PCR data by the comparative C(T) method. *Nature protocols*. 2008; 3(6):1101–8. Epub 2008/06/13. PMID: [18546601](https://pubmed.ncbi.nlm.nih.gov/18546601/)
31. Pitman MR, Pham DH, Pitson SM. Isoform-selective assays for sphingosine kinase activity. *Methods in molecular biology (Clifton, N.J.)*. 2012; 874:21–31. Epub 2012/04/25.
32. Leclercq TM, Moretti PA, Vadas MA, Pitson SM. Eukaryotic elongation factor 1A interacts with sphingosine kinase and directly enhances its catalytic activity. *J Biol Chem*. 2008; 283(15):9606–14. Epub 2008/02/12. doi: [10.1074/jbc.M708782200](https://doi.org/10.1074/jbc.M708782200) PMID: [18263879](https://pubmed.ncbi.nlm.nih.gov/18263879/)
33. Wati S, Rawlinson SM, Ivanov RA, Dorstyn L, Beard MR, Jans DA, et al. Tumour necrosis factor alpha (TNF-alpha) stimulation of cells with established dengue virus type 2 infection induces cell death that is accompanied by a reduced ability of TNF-alpha to activate nuclear factor kappaB and reduced sphingosine kinase-1 activity. *J Gen Virol*. 2011; 92(Pt 4):807–18. Epub 2010/12/15. doi: [10.1099/vir.0.028159-0](https://doi.org/10.1099/vir.0.028159-0) PMID: [21148274](https://pubmed.ncbi.nlm.nih.gov/21148274/)
34. Oliveira ER, Amorim JF, Paes MV, Azevedo AS, Goncalves AJ, Costa SM, et al. Peripheral effects induced in BALB/c mice infected with DENV by the intracerebral route. *Virology*. 2015; 489:95–107. Epub 2016/01/10. doi: [10.1016/j.virol.2015.12.006](https://doi.org/10.1016/j.virol.2015.12.006) PMID: [26748331](https://pubmed.ncbi.nlm.nih.gov/26748331/)
35. Bryan L, Kordula T, Spiegel S, Milstien S. Regulation and functions of sphingosine kinases in the brain. *Biochim Biophys Acta*. 2008; 1781(9):459–66. Epub 2008/05/20. doi: [10.1016/j.bbalt.2008.04.008](https://doi.org/10.1016/j.bbalt.2008.04.008) PMID: [18485923](https://pubmed.ncbi.nlm.nih.gov/18485923/)
36. Helbig KJ, Carr JM, Calvert JK, Wati S, Clarke JN, Eyre NS, et al. Viperin is induced following dengue virus type-2 (DENV-2) infection and has anti-viral actions requiring the C-terminal end of viperin. *PLoS Negl Trop Dis*. 2013; 7(4):e2178. Epub 2013/05/03. doi: [10.1371/journal.pntd.0002178](https://doi.org/10.1371/journal.pntd.0002178) PMID: [23638199](https://pubmed.ncbi.nlm.nih.gov/23638199/)
37. Chen HW, King K, Tu J, Sanchez M, Luster AD, Shresta S. The roles of IRF-3 and IRF-7 in innate antiviral immunity against dengue virus. *J Immunol*. 2013; 191(8):4194–201. Epub 2013/09/18. doi: [10.4049/jimmunol.1300799](https://doi.org/10.4049/jimmunol.1300799) PMID: [24043884](https://pubmed.ncbi.nlm.nih.gov/24043884/)

38. Hsieh MF, Lai SL, Chen JP, Sung JM, Lin YL, Wu-Hsieh BA, et al. Both CXCR3 and CXCL10/IFN-inducible protein 10 are required for resistance to primary infection by dengue virus. *J Immunol*. 2006; 177(3):1855–63. Epub 2006/07/20. PMID: [16849497](#)
39. Lucas TM, Richner JM, Diamond MS. The Interferon-Stimulated Gene Iff2712a Restricts West Nile Virus Infection and Pathogenesis in a Cell-Type- and Region-Specific Manner. *J Virol*. 2016; 90(5):2600–15. Epub 2015/12/25.
40. Perelygin AA, Scherbik SV, Zhulin IB, Stockman BM, Li Y, Brinton MA. Positional cloning of the murine flavivirus resistance gene. *Proc Natl Acad Sci U S A*. 2002; 99(14):9322–7. Epub 2002/06/25. doi: [10.1073/pnas.142287799](#) PMID: [12080145](#)
41. Lin RJ, Yu HP, Chang BL, Tang WC, Liao CL, Lin YL. Distinct antiviral roles for human 2',5'-oligoadenylate synthetase family members against dengue virus infection. *J Immunol*. 2009; 183(12):8035–43. Epub 2009/11/20. doi: [10.4049/jimmunol.0902728](#) PMID: [19923450](#)
42. Samuel MA, Diamond MS. Alpha/beta interferon protects against lethal West Nile virus infection by restricting cellular tropism and enhancing neuronal survival. *J Virol*. 2005; 79(21):13350–61. Epub 2005/10/18. doi: [10.1128/JVI.79.21.13350-13361.2005](#) PMID: [16227257](#)
43. Cho H, Proll SC, Szretter KJ, Katze MG, Gale M Jr., Diamond MS. Differential innate immune response programs in neuronal subtypes determine susceptibility to infection in the brain by positive-stranded RNA viruses. *Nat Med*. 2013; 19(4):458–64. Epub 2013/03/05. doi: [10.1038/nm.3108](#) PMID: [23455712](#)
44. Dalrymple NA, Mackow ER. Endothelial cells elicit immune-enhancing responses to dengue virus infection. *J Virol*. 2012; 86(12):6408–15. Epub 2012/04/13. doi: [10.1128/JVI.00213-12](#) PMID: [22496214](#)
45. Chesler DA, Reiss CS. The role of IFN-gamma in immune responses to viral infections of the central nervous system. *Cytokine & growth factor reviews*. 2002; 13(6):441–54. Epub 2002/10/29.
46. Zhou L, Wang X, Wang YJ, Zhou Y, Hu S, Ye L, et al. Activation of toll-like receptor-3 induces interferon-lambda expression in human neuronal cells. *Neuroscience*. 2009; 159(2):629–37. Epub 2009/01/27. doi: [10.1016/j.neuroscience.2008.12.036](#) PMID: [19166911](#)
47. Lazear HM, Daniels BP, Pinto AK, Huang AC, Vick SC, Doyle SE, et al. Interferon-lambda restricts West Nile virus neuroinvasion by tightening the blood-brain barrier. *Science translational medicine*. 2015; 7(284):284ra59. Epub 2015/04/24. doi: [10.1126/scitranslmed.aaa4304](#) PMID: [25904743](#)
48. Tsai TT, Chen CL, Lin YS, Chang CP, Tsai CC, Cheng YL, et al. Microglia retard dengue virus-induced acute viral encephalitis. *Sci Rep*. 2016; 6:27670. Epub 2016/06/10. doi: [10.1038/srep27670](#) PMID: [27279150](#)
49. Nayak D, Huo Y, Kwang WX, Pushparaj PN, Kumar SD, Ling EA, et al. Sphingosine kinase 1 regulates the expression of proinflammatory cytokines and nitric oxide in activated microglia. *Neuroscience*. 2010; 166(1):132–44. Epub 2009/12/29. doi: [10.1016/j.neuroscience.2009.12.020](#) PMID: [20036321](#)
50. Zheng S, Wei S, Wang X, Xu Y, Xiao Y, Liu H, et al. Sphingosine kinase 1 mediates neuroinflammation following cerebral ischemia. *Experimental neurology*. 2015; 272:160–9. Epub 2015/03/24. doi: [10.1016/j.expneurol.2015.03.012](#) PMID: [25797575](#)
51. Grin'kina NM, Kamabi EE, Damania D, Wadgaonkar S, Muslimov IA, Wadgaonkar R. Sphingosine Kinase 1 deficiency exacerbates LPS-induced neuroinflammation. *PLoS One*. 2012; 7(5):e36475. Epub 2012/05/23. doi: [10.1371/journal.pone.0036475](#) PMID: [22615770](#)
52. Blondeau N, Lai Y, Tyndall S, Popolo M, Topalkara K, Pru JK, et al. Distribution of sphingosine kinase activity and mRNA in rodent brain. *Journal of neurochemistry*. 2007; 103(2):509–17. Epub 2007/07/12. doi: [10.1111/j.1471-4159.2007.04755.x](#) PMID: [17623044](#)
53. Zhao L, Birdwell LD, Wu A, Elliott R, Rose KM, Phillips JM, et al. Cell-type-specific activation of the oligoadenylate synthetase-RNase L pathway by a murine coronavirus. *J Virol*. 2013; 87(15):8408–18. Epub 2013/05/24. doi: [10.1128/JVI.00769-13](#) PMID: [23698313](#)
54. Zhao L, Rose KM, Elliott R, Van Rooijen N, Weiss SR. Cell-type-specific type I interferon antagonism influences organ tropism of murine coronavirus. *J Virol*. 2011; 85(19):10058–68. Epub 2011/07/15. doi: [10.1128/JVI.05075-11](#) PMID: [21752905](#)
55. Kapil P, Butchi NB, Stohman SA, Bergmann CC. Oligodendroglia are limited in type I interferon induction and responsiveness in vivo. *Glia*. 2012; 60(10):1555–66. Epub 2012/06/28. doi: [10.1002/glia.22375](#) PMID: [22736486](#)
56. Daffis S, Samuel MA, Keller BC, Gale M Jr., Diamond MS. Cell-specific IRF-3 responses protect against West Nile virus infection by interferon-dependent and -independent mechanisms. *PLoS Pathog*. 2007; 3(7):e106. Epub 2007/08/07. doi: [10.1371/journal.ppat.0030106](#) PMID: [17676997](#)
57. Hait NC, Oskeritzian CA, Paugh SW, Milstien S, Spiegel S. Sphingosine kinases, sphingosine 1-phosphate, apoptosis and diseases. *Biochim Biophys Acta*. 2006; 1758(12):2016–26. Epub 2006/09/26. doi: [10.1016/j.bbame.2006.08.007](#) PMID: [16996023](#)

58. Michaud J, Kohno M, Proia RL, Hla T. Normal acute and chronic inflammatory responses in sphingosine kinase 1 knockout mice. *FEBS letters*. 2006; 580(19):4607–12. Epub 2006/08/01. doi: [10.1016/j.febslet.2006.07.035](https://doi.org/10.1016/j.febslet.2006.07.035) PMID: [16876794](https://pubmed.ncbi.nlm.nih.gov/16876794/)
59. Getts DR, Terry RL, Getts MT, Muller M, Rana S, Shrestha B, et al. Ly6c+ "inflammatory monocytes" are microglial precursors recruited in a pathogenic manner in West Nile virus encephalitis. *J Exp Med*. 2008; 205(10):2319–37. Epub 2008/09/10. doi: [10.1084/jem.20080421](https://doi.org/10.1084/jem.20080421) PMID: [18779347](https://pubmed.ncbi.nlm.nih.gov/18779347/)
60. Winkelmann ER, Luo H, Wang T. West Nile Virus Infection in the Central Nervous System. *F1000Research*. 2016; 5. Epub 2016/02/27.
61. Fujii Y, Kitaura K, Nakamichi K, Takasaki T, Suzuki R, Kurane I. Accumulation of T-cells with selected T-cell receptors in the brains of Japanese encephalitis virus-infected mice. *Japanese journal of infectious diseases*. 2008; 61(1):40–8. Epub 2008/01/26. PMID: [18219133](https://pubmed.ncbi.nlm.nih.gov/18219133/)
62. Wang Y, Lobigs M, Lee E, Mullbacher A. CD8+ T cells mediate recovery and immunopathology in West Nile virus encephalitis. *J Virol*. 2003; 77(24):13323–34. Epub 2003/12/04. doi: [10.1128/JVI.77.24.13323-13334.2003](https://doi.org/10.1128/JVI.77.24.13323-13334.2003) PMID: [14645588](https://pubmed.ncbi.nlm.nih.gov/14645588/)
63. Michlmayr D, McKimmie CS, Pingen M, Haxton B, Mansfield K, Johnson N, et al. Defining the chemokine basis for leukocyte recruitment during viral encephalitis. *J Virol*. 2014; 88(17):9553–67. Epub 2014/06/06. doi: [10.1128/JVI.03421-13](https://doi.org/10.1128/JVI.03421-13) PMID: [24899190](https://pubmed.ncbi.nlm.nih.gov/24899190/)
64. Glass WG, Lim JK, Cholera R, Pletnev AG, Gao JL, Murphy PM. Chemokine receptor CCR5 promotes leukocyte trafficking to the brain and survival in West Nile virus infection. *J Exp Med*. 2005; 202(8):1087–98. Epub 2005/10/19. doi: [10.1084/jem.20042530](https://doi.org/10.1084/jem.20042530) PMID: [16230476](https://pubmed.ncbi.nlm.nih.gov/16230476/)
65. Bassi MR, Kongsgaard M, Steffensen MA, Fenger C, Rasmussen M, Skjodt K, et al. CD8+ T cells complement antibodies in protecting against yellow fever virus. *J Immunol*. 2015; 194(3):1141–53. Epub 2014/12/30. doi: [10.4049/jimmunol.1402605](https://doi.org/10.4049/jimmunol.1402605) PMID: [25539816](https://pubmed.ncbi.nlm.nih.gov/25539816/)
66. Klein RS, Lin E, Zhang B, Luster AD, Tollett J, Samuel MA, et al. Neuronal CXCL10 directs CD8+ T-cell recruitment and control of West Nile virus encephalitis. *J Virol*. 2005; 79(17):11457–66. Epub 2005/08/17. doi: [10.1128/JVI.79.17.11457-11466.2005](https://doi.org/10.1128/JVI.79.17.11457-11466.2005) PMID: [16103196](https://pubmed.ncbi.nlm.nih.gov/16103196/)
67. Schwab SR, Cyster JG. Finding a way out: lymphocyte egress from lymphoid organs. *Nature immunology*. 2007; 8(12):1295–301. Epub 2007/11/21. doi: [10.1038/ni1545](https://doi.org/10.1038/ni1545) PMID: [18026082](https://pubmed.ncbi.nlm.nih.gov/18026082/)

4.2 Discussion

In this study, we have used an appropriate WT mouse model to examine DENV infection, DENV-induced neurovirulence, and host innate responses to DENV infection in the immunocompetent mouse brain. Consistent with previous studies, direct ic DENV injection into the brain caused infection characterised by appearance of signs of neurovirulence and enhanced mortality rate. Additionally, DENV infection triggers antiviral immune responses including induction of IFN- β and stimulation of ISGs production. DENV infection in mice brain caused accumulation of CD8⁺ but not CD4⁺ T-cells. Of note, DENV infection does not change the SK1/S1P pathways. In conclusion, our ic DENV infection provides a useful model with broader implications for use to further investigate various aspects of DENV replication and host response, and to fulfil our laboratories need for a reliable *in vivo* model of DENV infection for future studies.

While the chemical inhibition of SK1 reduces DENV infection *in vitro* (chapter 3) and genetic absence of SK1 in iMEFs also restricts DENV infection [167], we have demonstrated here that genetic deletion of SK1 in the brain of immunocompetent mice has no important role during ic DENV infection. Unfortunately, our data in this chapter in general does not support our findings *in vitro* as described in chapter 3, and the previous data from our laboratory that has demonstrated a role for SK1 in DENV infection *in vitro*. Since SK2 is the primary SK isoform in the brain, we decided to assess the role of this second SK isoform, SK2, during DENV infection firstly *in vitro* using both chemical agents that target SK2 activity and a MEF line in which SK2 is absent, and secondly using an *in vivo* mouse model that lacks SK2 gene and infection in the brain, as described in this chapter.

CHAPTER 5. THE ROLE OF SK2 DURING DENV INFECTION

5.1 Introduction

The role of SK1 during viral infections including dengue virus has been studied [206], including data presented in chapters 3 and 4. Little is known however about the importance of SK2 for viral infections. A recent study showed that targeting of SK2 by selective chemical inhibitor (ABC) significantly restricts CHIKV infection *in vitro* [236]. Thus, the role of SK2 in viral infection is beginning to emerge. We have previously described in chapter 3 that targeting of SK1 by the chemical SK1 selective inhibitor, SK1-I, significantly reduces DENV infection *in vitro*.

Additionally, DENV infection in SK1 deficient iMEFs was significantly impaired [167]. Of note, the absence of SK1 in iMEF also reduced the innate type I IFN- β and ISGs responses following DENV infection [167]. In contrast, we have shown that the lack of SK1 in live animals has a minimal effect on DENV infection and on the induction of IFN- β and ISGs in response to DENV infection in the brain (chapter 4) [165]. Since SK2 is the more prominent form of SK in the brain, we were interested to assess the effect of SK2 on DENV infection *in vitro* and also in this tissue.

In the first part of this chapter, we examined the effect of the lack of SK2 on DENV infectious virus release and DENV RNA levels in SK2^{-/-} iMEF cells, and in cells treated to inhibit SK2 activity *in vitro*. Additionally, we assessed the effect of the lack of SK2 on the induction of antivirals IFN- β and ISGs in iMEFs. In the second part of this chapter, we have tested the impact of knockout of SK2 gene on DENV infection in the mouse brain.

5.2 Results

5.2.1 DENV infection is reduced in SK2^{-/-} iMEFs but not affected by inhibition of SK2 *in vitro*

5.2.1.1 DENV infection is restricted in the absence of SK2 in iMEF cells

We employed iMEFs that were generated from WT and SK2^{-/-} mouse embryos as models for viral infection in the absence of SK2. Comparison of growth rate was performed using crystal violet staining, which demonstrated no difference in growth rate between WT and SK2^{-/-} iMEFs (Appendix 6). WT and SK2^{-/-} iMEFs were DENV infected and at 24 and 48 hpi, S/Ns were harvested and infectious DENV quantitated by plaque assay. RNA was extracted using TRIzol and absolute DENV copy number was quantitated by a real time qRT-PCR. Results from three independent experiments showed that DENV release was significantly reduced at 24 and 48 hpi in DENV-infected SK2^{-/-} iMEFs compared to WT iMEFs (Figure 5.1A). Similarly, quantification of DENV copy numbers by qRT-PCR demonstrated that DENV RNA level was comparable at 2 hpi, representing input DENV RNA, but significantly reduced in DENV-infected SK2^{-/-} iMEFs compared to WT iMEFs at both 24 and 48 hpi (Figure 5.1B). This data is similar to our results with SK1^{-/-} iMEFs and suggests that SK2 might be important for promoting DENV infection.

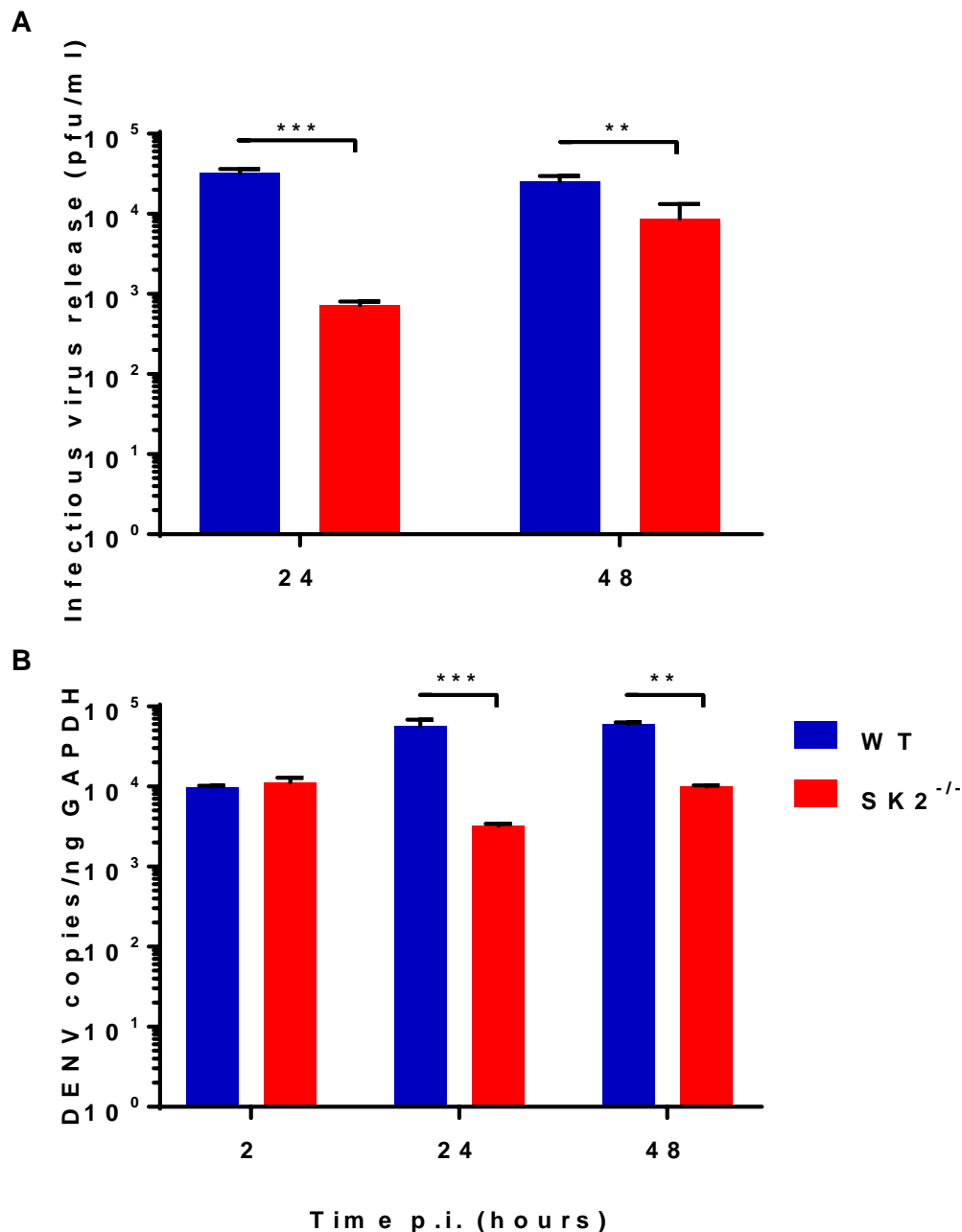


Figure 5. 1 DENV infection is restricted in cells that lack SK2

MEFs were obtained from WT and SK2^{-/-} mouse embryo and immortalised, as described in chapter 2, section 2.2.6.1. Cells were DENV infected at MOI of 1. **(A)** S/Ns were collected at 24 and 48 hpi for plaque assay. **(B)** RNA was isolated and DENV copy number was quantitated by RT-PCR and normalised against GAPDH. Results represent mean \pm SEM of n=3 assay replicates from three independent experiments. Statistical significance was determined by two-way ANOVA. ** p < 0.005, *** p < 0.0005.

5.2.1.2 DENV infection induces lower levels of IFN- β and ISGs in SK2 deficient compared to WT iMEFs

We sought to analyse the effect of the lack of SK2 on induction of IFN- β and ISGs in response to DENV infection. Using the same samples from experiments outlined in Figure 5.1 RNA was analysed by RT-PCR and the cell supernatant for IFN- β by ELISA. IFN- β mRNA was significantly induced in WT iMEFs at 24 and 48 hpi compared to 2 hpi. For SK2^{-/-} iMEFs, IFN- β was induced only at 48 hpi compared to 2 hpi SK2^{-/-}. Additionally, IFN- β was significantly lower at 48 hpi in SK2^{-/-} compared to WT iMEFs (Figure 5.2A). Similarly, significant induction of IFN- β protein was observed at 24 and 48 hpi in both DENV-infected iMEF cell lines when compared to 2 hpi but again at significantly lower levels in SK2^{-/-} compared to WT iMEFs (Figure 5.2B). These results demonstrate IFN- β can be induced without SK2 following viral infection in iMEFs but at levels that are lower than counterpart WT iMEFs.

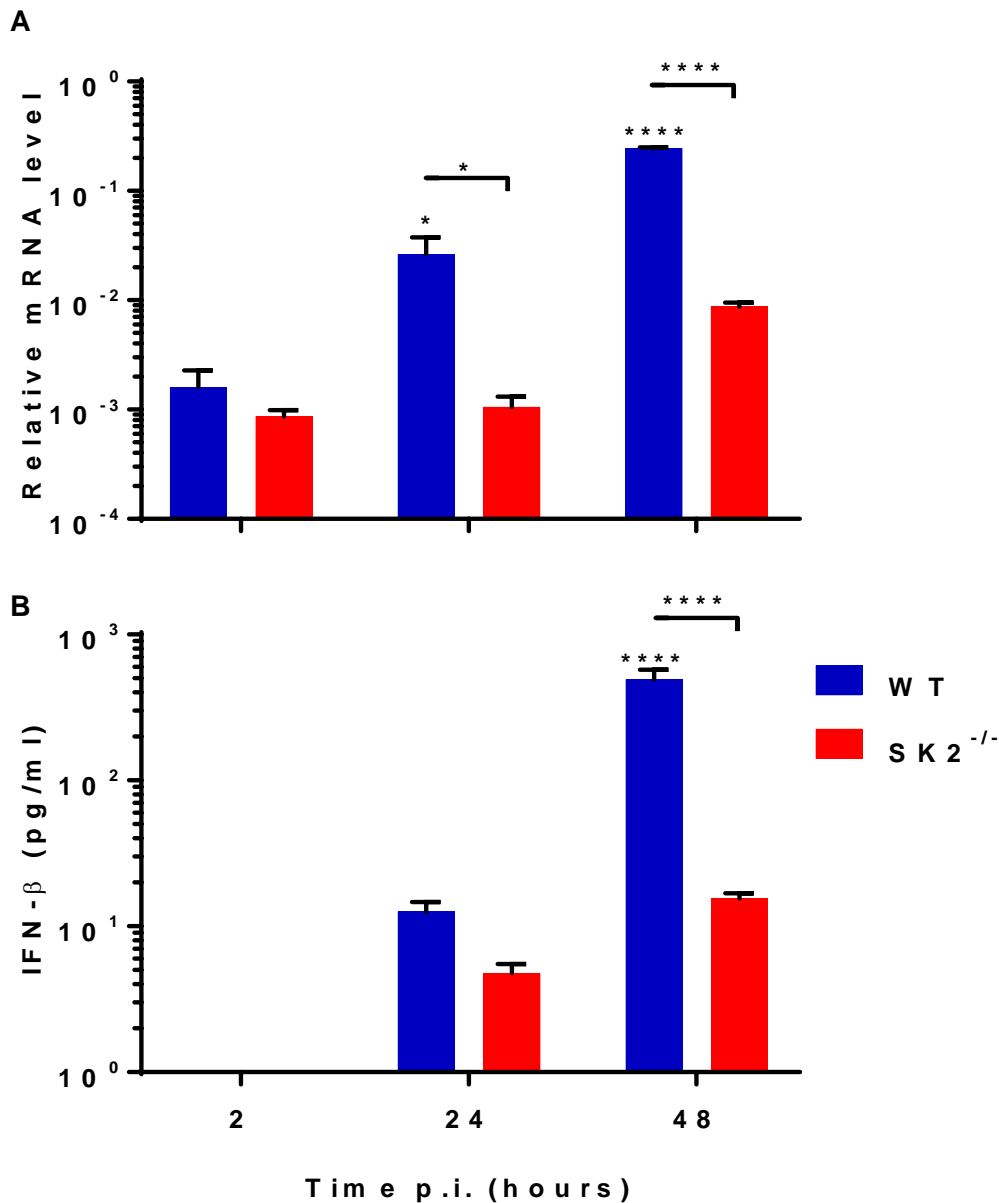


Figure 5. 2 IFN-β is induced but at significantly lower levels in DENV-infected SK2^{-/-} iMEFs

WT and SK2^{-/-} iMEFs were DENV infected at MOI of 1 as in figure 5.1. (A) RNA was extracted and mRNA level for IFN-β was determined by RT-PCR. Values were normalised to GAPDH and relative RNA level determined by Δ Ct method. (B) IFN-β protein was quantitated in cultured supernatant from DENV-infected cell by ELISA. Data represent mean \pm SEM of n=3 assay replicates from three independent experiments. Statistical significance was determined using two-way ANOVA to 2 hpi control from each cell line. * p < 0.05, **** p < 0.00005.

Normally, IFN exerts its antiviral activity by the induction of hundreds of effector ISGs. Thus, subsequent induction of ISGs was expected in iMEFs in response to DENV infection. We assessed the time-course of the mRNA induction of important ISGs: viperin, IFIT1, IRF7, and CXCL10 that we previously characterised by qRT-PCR in DENV-infected WT and SK1^{-/-} iMEFs in chapter 3. Notably, results showed significant upregulation of viperin, IFIT1, IRF7, and CXCL10 mRNAs in both DENV-infected WT and SK2^{-/-} iMEFs compared to mock-infected control (Figure 5.3). As for IFN- β results, induction of above ISGs in DENV-infected SK2^{-/-} iMEFs however, again was significantly lower than WT iMEFs at both 24 and 48 hpi (Figure 5.3). Additionally, we found that mRNA levels for viperin, IFIT1, IRF7, and CXCL10 at 2 hpi, which was considered as basal mRNA level immediately following the infection period, were elevated in DENV-infected SK2^{-/-} iMEFs compared to DENV-infected WT iMEFs (Figure 5.3). These data collectively demonstrated that DENV-infection induces IFN- β and subsequently of ISGs in iMEF but this induction was reduced in SK2^{-/-} iMEFs.

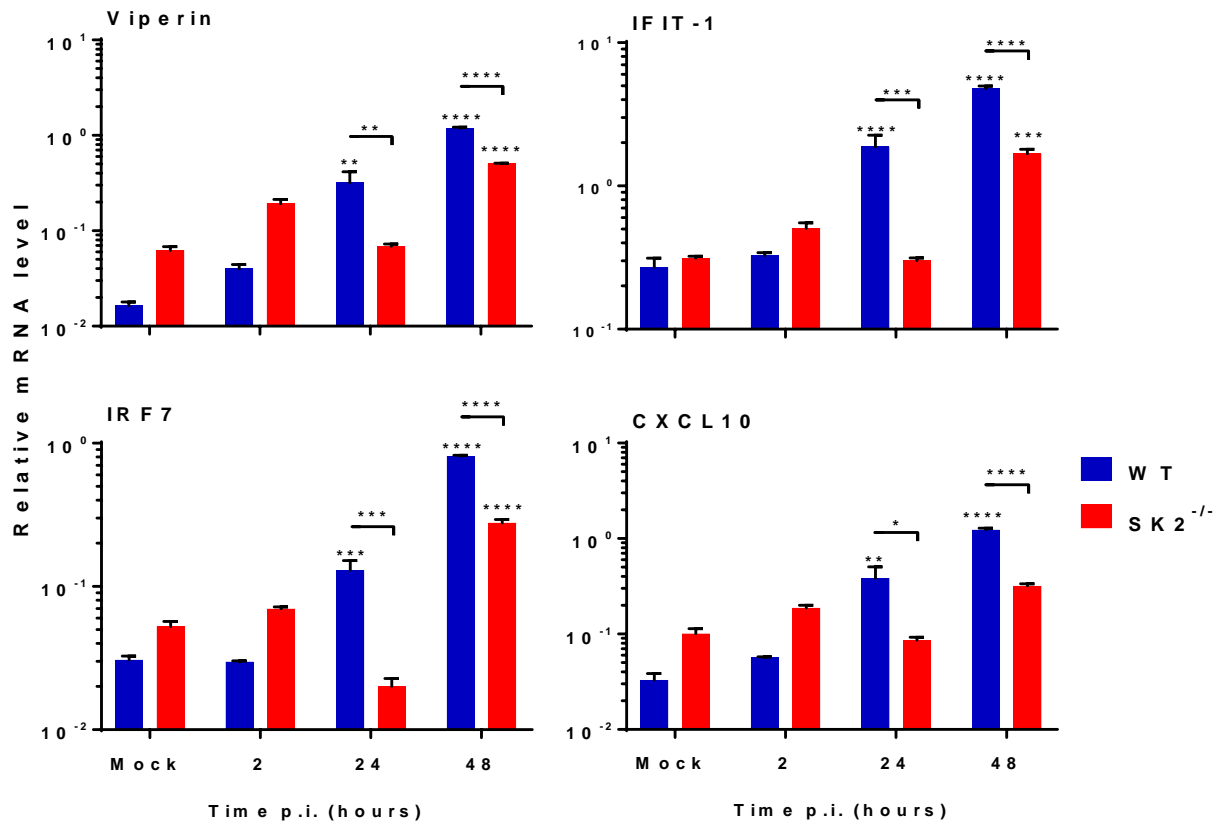


Figure 5. 3 Induction of ISGs is reduced in SK2 deficient iMEFs

WT and SK2^{-/-} iMEFs were DENV infected at MOI of 1 as in figure 5.1. RNA was isolated at indicated time pi and mRNA levels for viperin, IFIT1, IRF7, and CXCL10 were measured by qRT-PCR. Values were normalised to GAPDH and relative RNA level determined by ΔC_t method. Data represent mean \pm SEM of n=3 assay replicates from three independent experiments. Statistical significance was determined using two-way ANOVA to mock control from each cell line. * p < 0.05, ** p < 0.005, *** p < 0.0005, **** p < 0.00005.

5.2.1.3 DENV infection is not affected by chemical inhibition of SK2 activity in vitro

We next sought to assess the effect of chemical SK2 inhibition on DENV infection *in vitro*. Two potent compounds, ABC [259] and K145 [260] were employed as specific SK2 inhibitors. To assess the toxicity of ABC and K145 drugs on cell growth *in vitro*, HEK293 cells and HEK293 c18 cells were pre-treated with different concentrations of inhibitors prior to viral infection. In general, treatment of HEK293 cells O/N with either 100 μ M or 50 μ M ABC prior to DENV infection showed visual cytotoxic effects observed by light microscopy (Appendix 7). Further, 30 min pretreatment of HEK293 cells with either 4 μ M or 8 μ M K145 was also cytotoxic (data not shown). In contrast, treatment of HEK293 c18 cells, which express the Epstein Barr Virus (EBV) EBNA1 protein to reduce susceptibility to cell death, with ABC and K145 as above did not show visual signs of cell toxicity. Thus, HEK293 c18 cells were used to examine DENV infection following chemical SK2 inhibition.

HEK293 c18 cells were pre-treated with 50 μ M ABC either O/N or 45 min, and DENV challenged at MOI of 1. ABC treatment was maintained in the culture until 6 hpi, and then replaced with fresh drug-free medium for the remainder of the experiment. At the indicated time points, S/N was harvested, and infectious viral release was measured by plaque assay. Results showed that 50 μ M ABC treatment does not significantly alter DENV release in HEK293 c18 with O/N (Figure 5.4A) or 45 min (Figure 5.4B) treatment when compared to the respective vehicle control. Prior published work has demonstrated that 2h pre-treatment of HepG2 cells with 20 μ M ABC inhibits CHIKV infection [236]. We sought to use these same conditions for ABC treatment with HepG2 cells but with DENV infection instead. Notably, pre-treatment of HepG2 cells with 20 μ M ABC for 2 h does not show any cytotoxic effect (data not shown). Subsequent DENV infection was performed, S/N harvested for quantitation of DENV production in by plaque assay and total RNA isolated for analysis by qRT-PCR. Results demonstrate that ABC treatment of HepG2 cells does not affect release in infectious DENV or DENV RNA at 24 or 48 hpi compared to vehicle (DMSO) control (Figure 5.5A and B). To further examine whether the inhibition of SK2 would affect DENV

infection, we utilised another compound, K145. As for ABC, in general, pre-treatment of K145 at either 4 μ M and 8 μ M showed visual signs of cell cytotoxicity in HEK293 cells but not in HEK293 c18 cells. Thus, HEK293 c18 cells were pre-treated with K145 at different concentrations for 60 min prior to DENV infection at MOI of 1. At 24 hpi, S/Ns were harvested for plaque assay, and total RNA extracted for RT-PCR. Results demonstrated a potential reduction in infectious DENV release (Figure 5.6A) and DENV RNA levels (Figure 5.6B) in a concentration-dependent fashion although this change was not significant. Taken together, these data indicate that inhibition of SK2 by treatment with two potent SK2 selective inhibitors does not alter DENV infection suggesting SK2 has no major influence on viral infection *in vitro*.

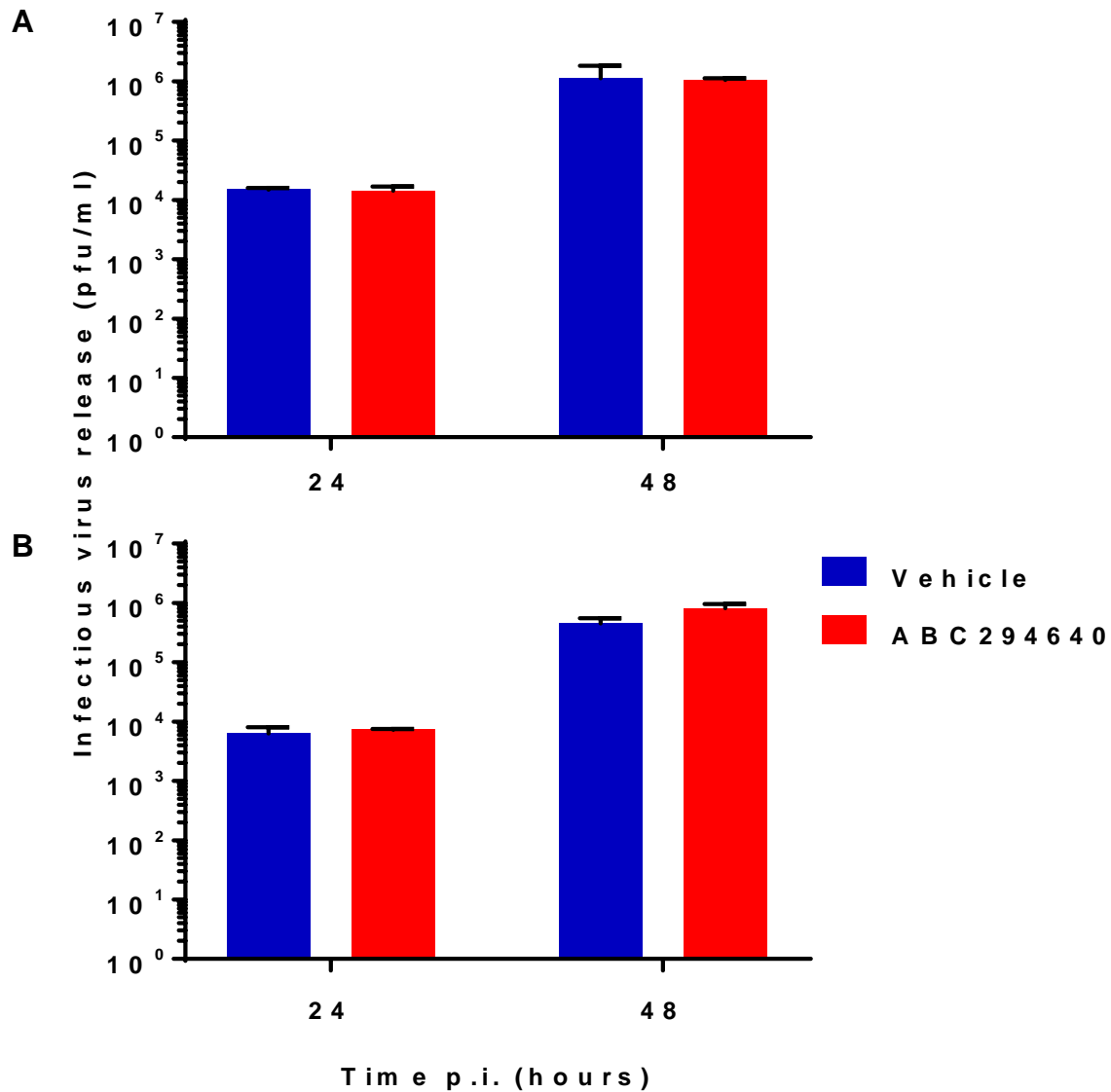


Figure 5. 4 ABC treatment of HEK293 c18 cells does not affect DENV infection

HEK293 c18 cells were pre-treated with 50 μ M ABC O/N (A) and 45 min (B) before infection and maintained until 6 hpi. Cells were DENV infected at MOI of 1 and S/N harvested. DENV release was determined by plaque assay. Results represent mean \pm SD of n=2 assay replicates from two independent experiments. Statistical significance was determined using two-way ANOVA.

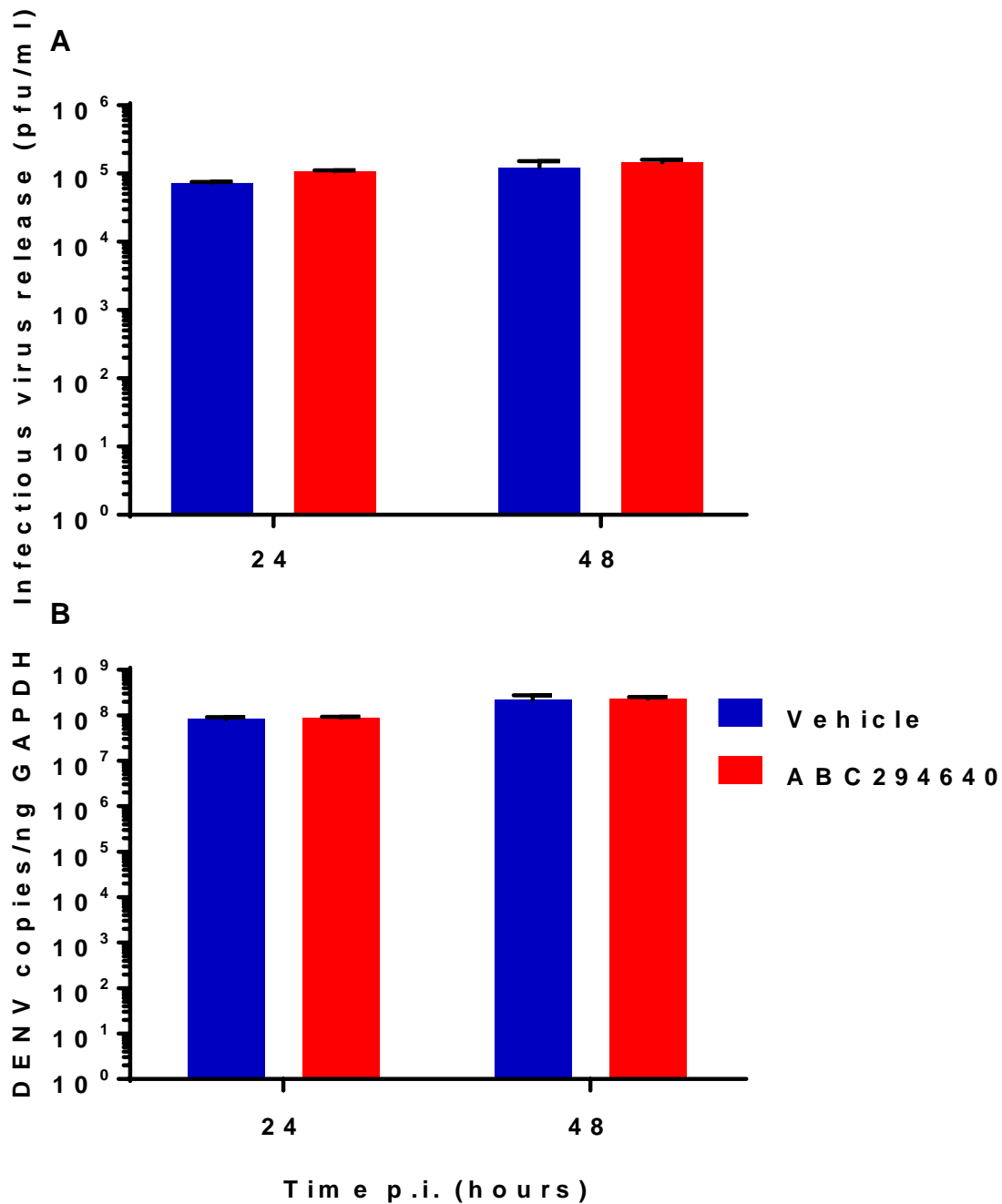


Figure 5. 5 ABC treatment of HepG2 does not impair DENV infection

HepG2 cells were pre-treated with 20 μ M ABC dose for 2 h before DENV infection was performed at MOI of 1 and drug left in culture until 6 hpi. (A) S/N harvested at 24 and 48 hpi for plaque assay. (B) RNA was isolated and DENV copy number was quantitated by RT-PCR and normalised against GAPDH. Results represent mean \pm SD of n=2 assay replicates from two independent experiments. Statistical significance was determined using two-way ANOVA.

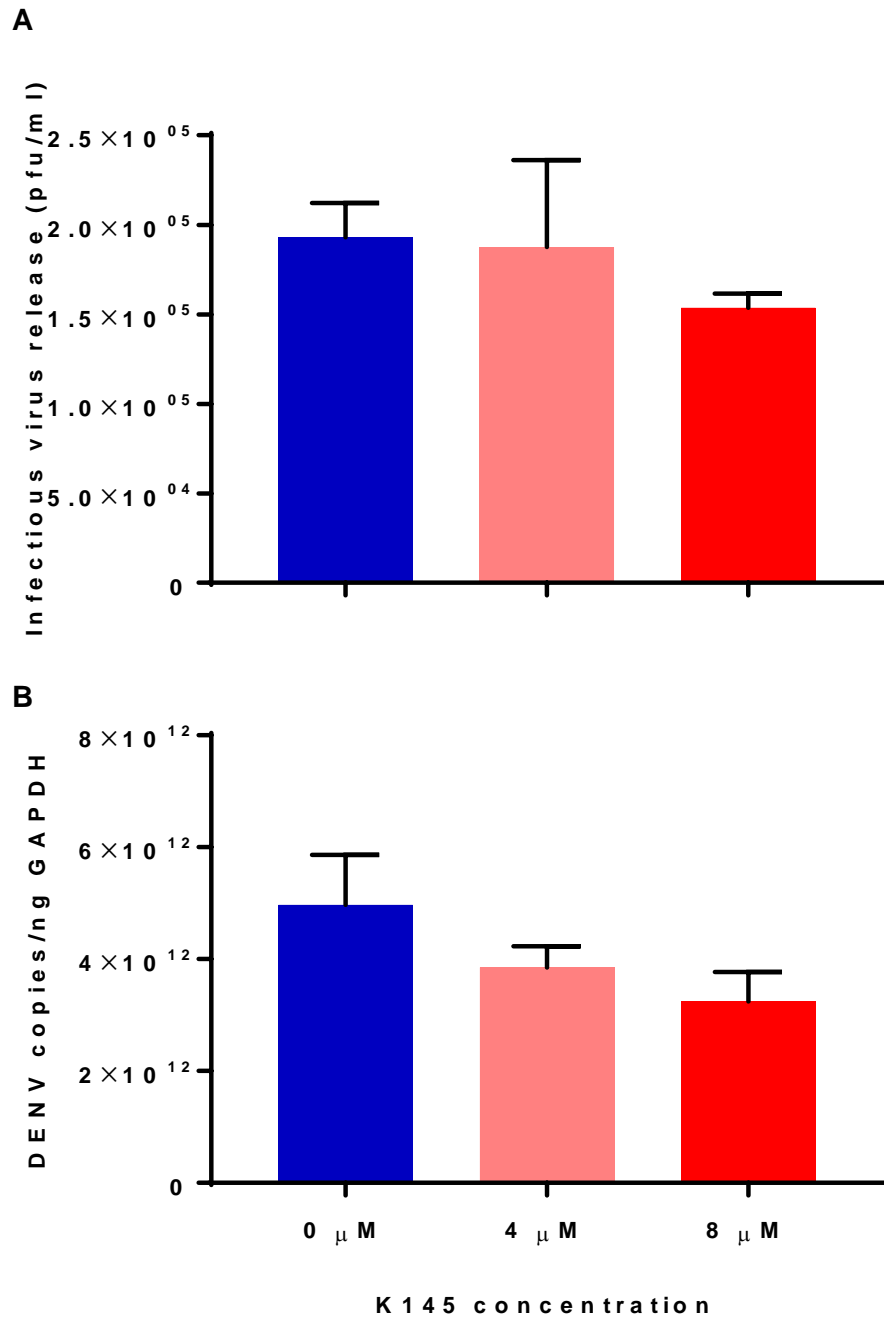


Figure 5.6 K145 treatment does not impair DENV infection

HEK293 c18 cells were pre-treated with K145 at different concentrations for 60 min prior to DENV infection and drug left in culture for 6 hpi. (A) Infectious virus release was quantitated by plaque assay at 24 hpi, and (B) viral RNA was assessed by qRT-PCR at 24 hpi and normalised to GAPDH. Results represent mean \pm SD of n=2 assay replicates from two independent experiments. Statistical significance was determined using two-way ANOVA.

5.2.1.4 Inhibition of SK2 has no effect on DENV RNA replication in a replicon system

We have shown in chapter 3 and above that chemical inhibition of SK1 or SK2 activity does not significantly impair DENV RNA replication. We employed HEK293 c18 cells containing a self-replicating DENV-subgenomic replicon containing a GFP reporter gene [241], that we have termed pREP cells to further test the effect of SK2 inhibitors on the level of DENV RNA replication by flow cytometry analysis. HEK 293 pREP cells, where GFP reflects production of DENV RNA, were treated with either 20 μ M ABC or 8 μ M K145 for 24 h prior to GFP analysis by flow cytometry. Results showed no differences in the histogram profile of GFP expressing cells following treatment with either ABC and K145 compared to their vehicle treated cells (Figure 5.7A and B) and this was confirmed by comparison of the GFP MFI (Figure 5.7D). In contrast, treatment with 10 μ M NITD, a known inhibitor of DENV RNA replication and thus a positive control, showed a clear reduction in GFP compared to untreated cells, as viewed by histogram plots or GFP MFI (Figure 5.7C and D). Thus, inhibition of SK2 does not influence DENV RNA production.

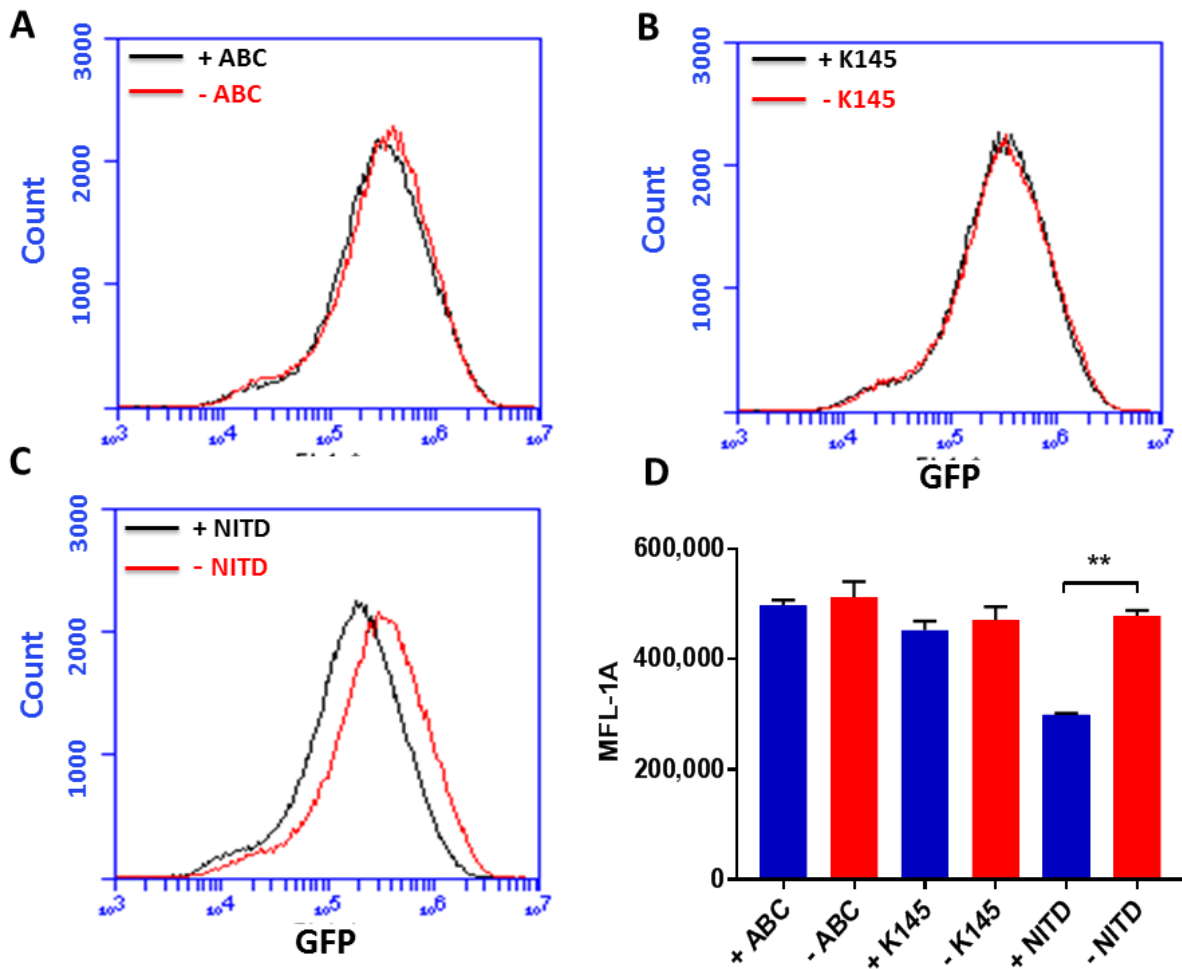


Figure 5.7 Effect of SK2 selective inhibitors on DENV RNA replication

HEK293 c18 pREP cells (containing a subgenomic GFP-DENV replicon) were treated with drug for 24 h prior to fixation and flow cytometry. Representative histograms following treatment with (A) 20 μ M ABC; (B) 8 μ M K145 or (C) 10 μ M NITD (positive control) (D) MFI of GFP in response to treatment, as in A-C. Results represent mean \pm SEM of n=3 assay replicates. Statistical significance was determined by un-paired student *t*-test. ** p < 0.005.

5.2.2 The role of SK2 *in vivo* during DENV infection

5.2.2.1 Establishment of DENV infection in SK2^{-/-} mice

We demonstrated in chapter 4 that the absence of SK1 has no major effect on DENV infection, ISG induction, and CD8⁺ T cell infiltration in a mouse model of DENV infection in the brain [165].

Following on from results of this chapter demonstrating reduced DENV replication in SK2^{-/-} iMEFs but a lack of effect of SK2 inhibitors on DENV replication, we aimed to assess the role of SK2 in a brain model of DENV infection. We employed C57BL/6 SK2^{-/-} mice that were genetically deficient in SK2 as previously described [215] and DENV-infected 12 WT and 12 SK2^{-/-} mice via the ic route with an additional 4 WT and 4 SK2^{-/-} mice ic injected with PBS, as mock (control) mice.

5.2.2.2 SK2 deficiency has no effect on DENV neurovirulence and survival of mice

We initially defined whether the absence of SK2 might have an effect on growth and survival rates of mice in response to DENV infection. As described above, WT and SK2^{-/-} mice were challenged with DENV while mock mice were injected with PBS only. Post-infection, body weight and neurological signs of disease (slow movement, hunched posture, and reduction in hind limb movement) were observed. The duration of animal study was nine days (end time point), however mice that showed either signs of disease symptoms or more than 10% body weight loss were euthanised prior to the end time point. Mock-infected WT and SK2^{-/-} mice did not demonstrate any loss in body weight or appearance of DENV neurovirulence signs (Figure 5.8A and C). The body weight change of WT and SK2 deficient mice was normalised by calculation as a percentage to the initial body weight and averaged. Results showed that both DENV-infected WT and SK2^{-/-} mice started to lose body weight at day 6 pi in comparison to mock-infected control mice (Figure 5.8A and C). As expected, mortality rate analysis demonstrated significantly higher mortality of DENV-infected WT and SK2^{-/-} mice compared to their respective mock-infected mice (Figure 5.8B and D). Comparison of body weight loss between DENV-infected WT and SK2^{-/-} mice showed a significantly greater weight loss in SK2^{-/-} mice at day 7 pi than infected WT mice. At this time

point, 9 out of 12 of WT or SK2^{-/-} DENV-infected mice were euthanised due to either excessive weight loss or the presence of neurological signs (Figure 5.8E). The remaining 3 SK2^{-/-} DENV-infected mice were euthanised at day 8 pi, while the remaining 3 WT mice did not meet ethical euthanasia end-points and were euthanised at day 9 pi, as the experimental termination point. This is reflected by a higher survival rate of viral infected WT mice at day 8 pi compared to SK2^{-/-} mice, however this was not statistically significant (Figure 5.8F). Although there was a tendency towards a greater and earlier body weight loss in DENV-infected SK2^{-/-} mice compared with DENV-infected WT mice, no significant difference was observed in terms of the overall number of mice that lost body weight, the time of onset of body weight loss, nor the percentage of mice that lost more than 10% of body weight (Table 5.1). These data indicate that C57BL/6 mice in which SK2 was genetically deleted tend to be more susceptible to ic DENV infection than WT mice although the overall disease profile is comparable.

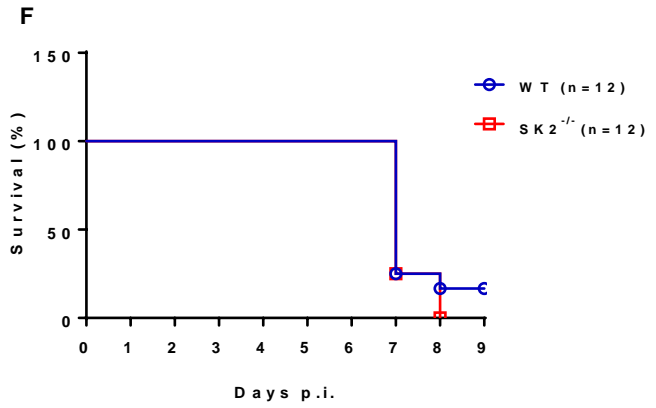
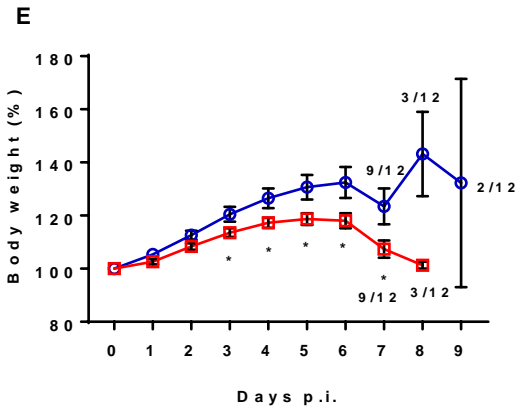
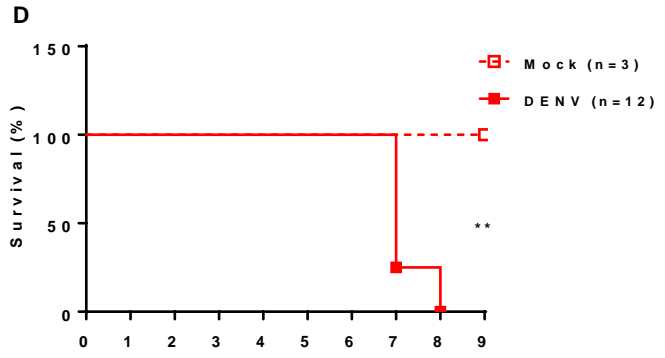
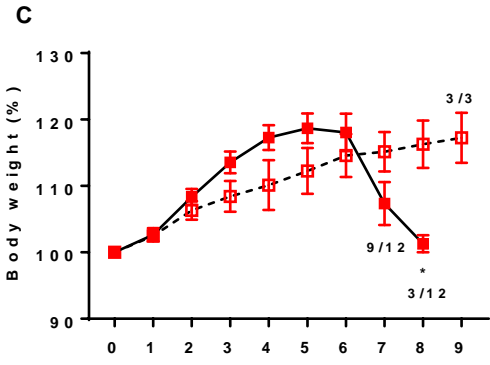
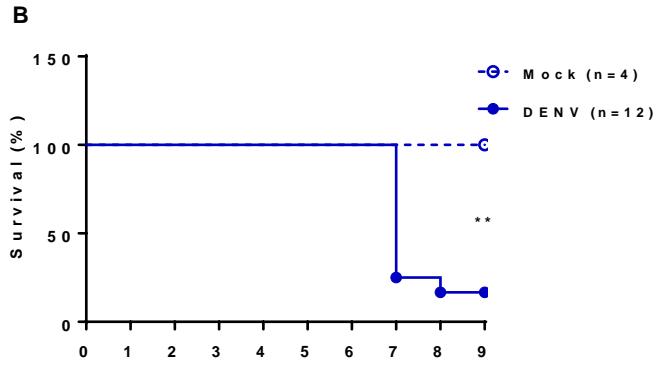
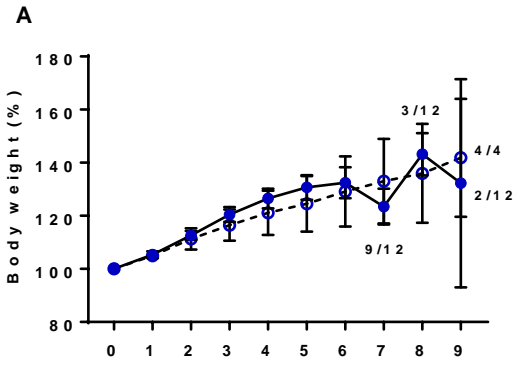


Figure 5. 8 Body weight and survival curve of WT and SK2^{-/-} mice

3-4 weeks old C57BL/6 Harlan WT (n=12) and SK2^{-/-} (n=12) mice were ic injected with 800 pfu/ml DENV. Mock WT (n=4) and SK2^{-/-} (n=3) control mice were ic injected with vehicle only. Body weight and neurological symptoms were recorded. Body weight is expressed as a percentage of initial body weight. Survival reflects mice that do not show neurological signs or > 10% of body weight loss. **A** and **B**. Comparison of body weight and survival curve of mock with DENV-infected WT mice; **C** and **D**. Comparison of body weight and survival curve of mock with DENV-infected SK2^{-/-} mice; **E** and **F**. Comparison of body weight and survival curve of DENV-infected WT and SK2^{-/-} mice. Data are expressed as mean ± SEM. Statistical significance for body weight was determined using unpaired student *t*-test. Statistical analysis of survival curves were determined by log rank test. * = p < 0.05, ** = p < 0.005.

Table 5. 1 Summary of body weight loss and signs of DENV-induced neurovirulence in WT and SK2^{-/-} mice and analysed by Fisher's exact test (n=12 each WT and SK2^{-/-} mice)

	Mouse strain				<i>p</i>
	WT		SK2 ^{-/-}		
	#	%	#	%	
Body weight loss					
Weight loss	11	91.67	12	100.00	0.999
No weight loss	1	08.33	0	00.00	
% Body weight loss					
> 10%	5	45.46	7	58.33	0.684
≤ 10%	6	54.54	5	41.67	
Days pi onset loss					
> 6 dpi	6	54.54	5	41.67	0.684
≤ 6 dpi	5	45.46	7	58.33	
Appearance of neurovirulence					
Signs	11	91.67	12	100.00	0.999
No signs	1	08.33	0	00.00	

5.2.2.3 The absence of SK2 has no effect on DENV RNA levels in the brain of mice following ic injection

During DENV infection in SK1^{-/-} mice, there is a trend toward a higher DENV RNA level in SK1^{-/-} compared to WT mice, although this was not significant [165]. Thus, we next defined DENV replication in mouse brain following ic infection when SK2 is genetically deleted. WT and SK2^{-/-} mice were ic infected, as above, brains were harvested, and total RNA extracted. DENV RNA levels were quantitated by qRT-PCR. Results showed that DENV RNA was undetectable in the brain of mock-infected mice. As in chapter 4, the presence of DENV neurovirulence symptoms was associated with higher DENV levels in the brain where the one WT mouse that was euthanised at day 9 pi and did not show any neurovirulence symptoms, also had the lowest DENV RNA level (Figure 5.9). DENV RNA levels in the brain of DENV-infected SK2^{-/-} mice were not significantly different to that of DENV-infected WT mice (Figure 5.9). This data demonstrates that DENV RNA levels in mice brains at the termination point of our experiments (end stage) was not impacted by the lack of SK2.

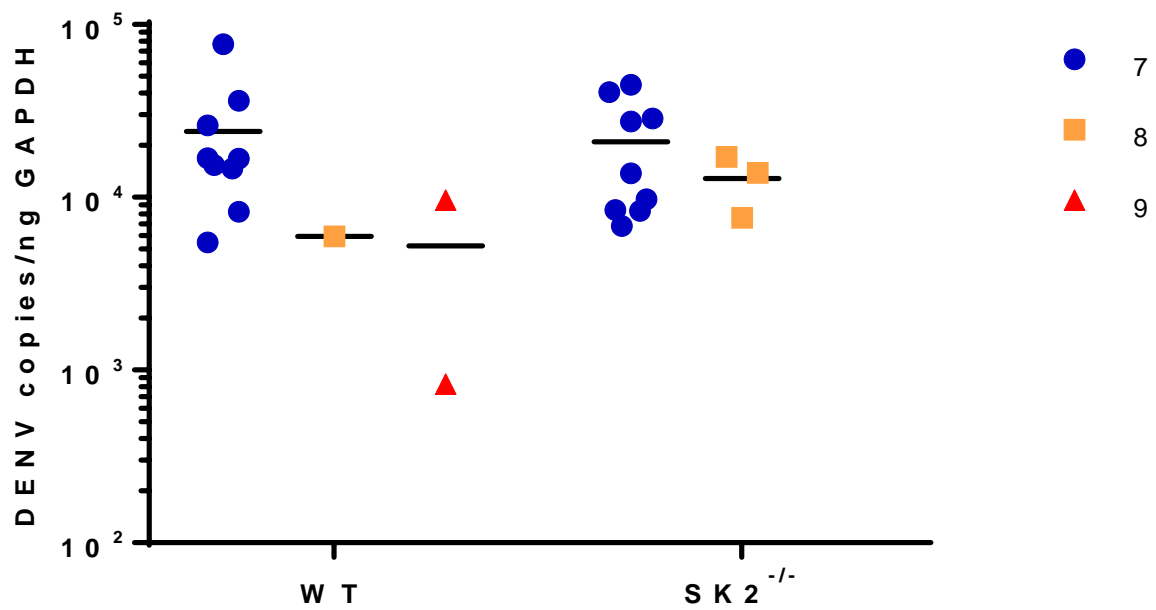


Figure 5. 9 Lack of SK2 has no effect on DENV RNA levels in the brain following ic infection

12 WT and 12 SK2^{-/-} were injected intracranially with 800 PFU/ml DENV. Mice were euthanised at end stage disease, and RNA extracted from brain tissue at the time of euthanasia representing 7 (n=9), 8 (n=1) or 9 (n=2) dpi for WT and 7 (n=9) or 8 (n=3) dpi for SK2^{-/-} mice. DENV RNA levels were analysed by qRT-PCR and copy number determined from a standard curve of a DENV DNA clone. Data represent average PCR values from individual mice, normalised against GAPDH. Statistical significance was assessed by two-way ANOVA.

5.2.2.4 The absence of SK2 alters the SK1/S1P axis in the brain but this is not further altered following DENV infection

We have reported that DENV infection in SK1^{-/-} mice does not change the SK/S1P axis in the mouse brain [165]. Thus, we next assessed whether the lack of SK2 alters the SK/S1P axis in mouse brain tissue and if this is further affected by DENV infection. To confirm the deletion of the SK2 gene in SK2^{-/-} mice, we quantitated the SK2 mRNA levels by qRT-PCR analysis. The lack of SK2 mRNA expression in both DENV and mock infected SK2^{-/-} mice confirmed that SK2 gene was deleted (Figure 5.10A). Additionally, comparison of SK2 mRNA levels in mock and DENV-infected WT mice, showed no significant change in SK2 mRNA level (Figure 5.10A). We next measured the mRNA levels of SK1 in mouse brain. SK1 mRNA levels tended to be lower in mock infected WT compared with SK2^{-/-} mice, although this was not significantly different (Figure 5.10B). Overall, however no significant difference was observed in SK1 mRNA levels in both DENV and mock-infected SK2^{-/-} compared to DENV and mock-infected WT mice (Figure 5.10B). Further, we quantitated S1P in DENV-infected brain lysates by HPLC. Notably, S1P levels were significantly reduced in both mock and DENV-infected SK2^{-/-} mice compared to their respective WT mice (Figure 5.10C). S1P levels tended to be higher in DENV infected SK2^{-/-} mice compared to mock infected controls, although this was not significantly different (Figure 5.10C). Thus, the lack of SK2 reduced the level of S1P in mouse brain, but did not affect SK1 mRNA level, or as above, DENV replication.

Figure 5. 10 Definition of the SK/S1P axis in WT and SK2^{-/-} mice following ic DENV infection

WT and SK2^{-/-} mice were ic infected with DENV, as in Figure 5.9 and at end stage disease, brain tissue was harvested and snap frozen or stored in TRIzol. RNA was extracted from TRIzol and cell lysates were prepared from snap frozen tissue. **A.** SK2 mRNA and **B.** SK1 mRNA were determined qRT-PCR. PCR data represent average PCR values from individual mice and were normalised against GAPDH by Δ Ct method. **C.** S1P was quantitated in brain lysates by HPLC. n=9 WT and n=9 SK2^{-/-} DENV-infected, n=3 WT mock and n=3 SK2^{-/-} mock-infected mice. S1P quantitation was expressed relative to total protein quantitation. Statistical significance was assessed by one-way ANOVA. **= p < 0.005, ****= p < 0.00005.

5.2.2.5 The absence of SK2 has no effect on T cell infiltration in the brain of mice following ic DENV infection

S1P plays a crucial role in T-cell trafficking and migration [261]. Since we have demonstrated that the absence of SK2 significantly reduce the levels of S1P in mouse brain, we sought to assess the effect of the lack of SK2 on T-cell infiltration following DENV infection. The T-cell infiltration was analysed by the presence of mRNA for the T lymphocyte markers, CD4 and CD8 by qRT-PCR. WT and SK2^{-/-} mice were ic infected as above, brains were harvested, total RNA extracted, and CD4 and CD8 mRNAs analysed by RT-PCR. Results showed no change in the CD4 mRNA levels following DENV infection in WT and SK2^{-/-} mice compared to mock control mice at end stage disease (Figure 5.11A). Additionally, no significant difference was observed between DENV-infected WT and SK2^{-/-} mice. In contrast, the mRNA levels of CD8 was significantly higher in DENV-infected mice brains compared to their respective mock-infected mice at end stage disease (Figure 5.11B), but again no significant difference was found in CD8 levels in DENV-infected SK2^{-/-} compared to DENV-infected WT mice. These results indicate that CD8⁺ T-cells infiltrate the DENV-infected mouse brain rather than CD4 but the lack of SK2 and lower levels of S1P does not affect this infiltration.

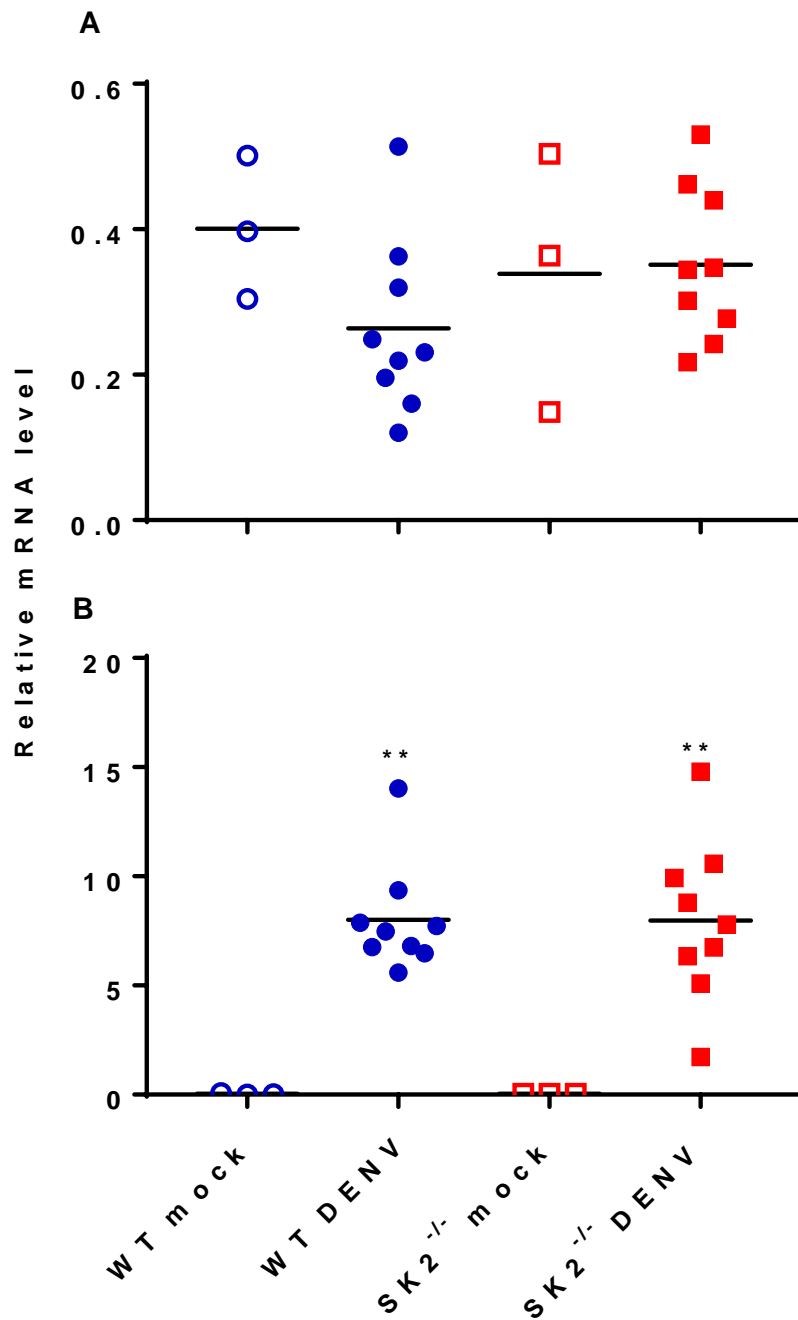


Figure 5.11 T cell infiltration in the brain of WT and SK2^{-/-} mice following ic DENV infection

WT and SK2^{-/-} mice were ic infected with DENV, as in Fig 9. RNA extracted from infected brain tissues at end stage disease and analysed by qRT-PCR for **A.** CD4 mRNA; **B.** CD8 mRNA. PCR data represent average PCR values from individual mice and normalised against GAPDH by ΔCt method. n=9 WT and n=9 SK2^{-/-} DENV-infected, n=3 WT mock and n=3 SK2^{-/-} mock-infected mice. Statistical significance was assessed one-way ANOVA. **= p < 0.005.

5.3 Discussion

In this chapter, we conducted a study to define the role of SK2 during DENV infection *in vitro* as well as *in vivo*. Prior published literature has suggested a role of SK1 during viral infections [206]. Additionally, work from our laboratory has focused on the SK1 functions and changes during DENV infection [167] that have been further described in chapter 3 and 4 of this thesis. In contrast to experiments on SK1, studies that have investigated the role of SK2 in viral replication and pathogenesis are very limited. Two studies in 2014 have demonstrated a critical role for SK2 in regulating HCV replication [235] and in enhancing the latency of KSHV-infected endothelial cells [234]. The only study to date that clearly reported the function of SK2 during infection with a mosquito-borne pathogen, CHIKV, was reported by Reid *et al.*, which showed that SK2 was associated with the VRC and inhibition of SK2 significantly reduced CHIKV infection *in vitro* [236]. Here, we utilised mouse cells that lacked SK2 and cells treated with two different SK2 inhibitors for DENV infection *in vitro*, in addition to employing SK2 null mice for DENV infection *in vivo*.

We have found that DENV infection was significantly restricted at 24 and 48 hpi in SK2^{-/-} compared to WT iMEF cells. These data suggested a potential important role of SK2 in promoting DENV replication and virus production. These findings are similar to our report of DENV infection in SK1^{-/-} iMEFs in which DENV infection was significantly reduced [167]. In this prior study, however, we found the reduced replication in SK1^{-/-} iMEFs was specific to the immortalised cell line and not reproduced in 1°MEFs [167]. The difference in DENV infection between primary and immortalised SK1 MEFs in our previous study was shown to correlate with gene expression profiles that likely affect their response to DENV infection such as elevated basal levels of ISGs such as IRF7 and viperin [167]. Elevated levels of basal ISGs has been reported in SV40 LTAg transformed and immortalised cells [262], and we previously proposed that although we have an immortalised WT control, for an unknown reason, these effects are significantly higher in cells

lacking SK1 [167]. Similarly, our results here demonstrate elevated levels of ISGs: viperin, IFIT, IRF7, and CXCL10 that have been reported previously to have antiviral activity against DENV infection *in vitro* [156,162,263,264], at 2 hpi in SK2^{-/-} iMEFs, which was associated with significantly reduced ability of DENV to replicate robustly in SK2^{-/-} iMEF line. Large-T antigen expression from SV40 of polyomavirus, as has been used for immortalisation of our MEF used herein, in MEFs has been reported to induce high expression of ISGs in MEFs [262]. Consistent with our findings in SK1^{-/-} iMEF [167], induction of IFN- β and ISGs viperin, IFIT1, IRF7 and CXCL10 was significantly reduced in SK2^{-/-} compared to WT iMEFs. These finding could suggest a potential role of SK2 in innate response to DENV infection, although it is also likely that the lower induction of these factors relates to the lower level of DENV RNA and replication that will stimulate these responses. Thus, we suggest that the higher basal levels of ISGs in SK2 null MEFs are crucial determinants for cells susceptibility to viral invasion and creating antiviral states that resulted in lower DENV infection, but that these results are potentially confounded by the immortalised MEF system used. Due to time restrictions and prioritisation of goals, we chose not to generate and test SK2^{-/-} 1^oMEF to further investigate this and chose an alternative means of inhibiting SK2, via selective chemicals.

Our results were in general not in agreement with our data and from others that showed viral infection was impaired by a chemical reduction of SK1 [167,225,227,230], as discussed in chapter 3. Thus, a reduction in DENV infection through inhibition of SK2 activity might also be expected since SK1 and SK2 isozymes are proposed to have complementing physiological roles [205]. Here, we have utilised two known potent SK2 selective compounds, ABC and K145 that inhibit SK2 activity *in vitro* [259,260], to examine the effect of SK2 reduction on DENV infection.

We observed that inhibition of SK2 via treatment with different ABC inhibitor concentrations did not impair DENV infection in two different cell lines, HEK293 c18 and HepG2. Additionally, inhibition of SK2 activity in HEK293 c18 cells via K145 treatment tended to reduce DENV infection in HEK293 c18 cells in a dose-dependent fashion but this was not significant. Further,

treatment of cells containing a GFP-expressing subgenomic DENV replicon with 20 μ M ABC and 8 μ M K145, did not affect DENV RNA replication. These results demonstrate that inhibiting SK2 activity has no effect on DENV infection *in vitro*. Unfortunately, we did not quantitate SK2 activity following treatment with the SK2 selective inhibitors (ABC and K145) to confirm the inhibition effect of these agents on SK2. Thus, our lack of effect of SK2 inhibition on DENV infection may be influenced by this. The specific inhibition activity of ABC and K145 however has been reported previously [259,260], and these particular drug preparations have been successfully validated in the laboratory of Prof Stuart Pitson. The lack of effect of SK2 inhibition on DENV replication however was inconsistent with other studies that have demonstrated a role for SK2 during viral infections. One study showed that the SK2 enzyme maintains the latency of KSHV-infected cells [234]. Another study revealed that lipid peroxidation regulated in part by SK2 reduced HCV replication, and chemical inhibition or depletion of SK2 promoted HCV replication [235]. Recently, a study by Reid *et al.*, 2015 [236] showed that SK2 had a positive role in promoting CHIKV infection where chemical inhibition of SK2 activity via treatment with different SKI-II and ABC concentrations or siRNA-mediated knockdown of SK2 led to restriction of CHIKV infection in HepG2 cells. Thus, our results using comparable levels of ABC, similarly in HepG2 cells are directly comparable to the study of CHIKV but here failed to affect DENV replication. This suggests potential viral specific functions for SK2.

We established a mouse model of DENV infection by ic route to study the role of SK1 *in vivo*, in a mouse that has fully competent IFN responses (see chapter 4). Following on from our *in vitro* analysis of the effect of SK2 on DENV infection, we investigated the role of SK2 during DENV infection *in vivo* using this model: immunocompetent C57BL/6 mice and direct ic DENV infection. Following DENV infection as expected, both WT and SK2^{-/-} mice exhibited body weight loss and signs of DENV neurovirulence compared to their respective mock control mice. This reflects the pathogenicity of DENV in mouse brain as showed in our prior model of DENV infection in mice [165]. All 12 DENV-infected SK2 null mice developed neurovirulence symptoms that was

associated with high mortality rate but this was not significantly different compared to WT mice. Using qRT-PCR analysis, DENV RNA levels in SK2^{-/-} mice was not significantly different in comparison to WT mice but as described in chapter 4, the levels of DENV RNA in the brain of WT and SK2^{-/-} mice strains again correlated with neurological disease. This report is consistent with data presented in chapter 3, where DENV infection in SK1 null mice compared to WT mice using this same ic infection model was not significantly different [165]. The lack of effect of loss of SK2 on DENV infection *in vivo* is also consistent with our lack of observed effect of SK2 inhibitors on DENV replication *in vitro*. This *in vivo* data, however contrasts with our *in vitro* data above where DENV infection is significantly reduced in SK2^{-/-} iMEFs. As we have rationalised above, we believe these findings in SK2^{-/-} iMEFs are flawed and an artefact of the iMEF system where basal levels of anti-viral ISGs are enhanced. Thus, without SK2, mice succumb to body weight loss at higher rate than WT mice but the susceptibility to DENV neurovirulence and RNA replication were comparable. Given the lack of effect of SK2 on DENV replication, and the time restrictions of this study, we chose not to pursue analysis of ISGs in the brain of SK2^{-/-} mice.

We demonstrated that the absence of SK2 in mouse brain was not associated with increased SK1 mRNA levels, which might be anticipated to occur to compensate for the SK2 deficiency. Similarly, the results of chapter 4 showed the lack of SK1 in mouse brain did not alter the SK2 mRNA levels [165]. Additionally, SK1 or SK2 mRNA levels were not different significantly in the brain of mice after DENV infection, in the context of WT, SK1 [165] or SK2 null mice. Consistent with these results, no compensatory role of SK1 was observed in the spinal cord of SK2 null mice [265].

Both SK isozymes, SK1 and SK2, can phosphorylate sphingosine substrate to produce S1P [247]. Genetic deletion of SK1 in mice has been shown to decrease the levels of S1P in circulation to less than 50% of WT [244]. S1P levels, however in tissues such as brain, liver, and kidney of SK1^{-/-} mice were not affected [244]. In contrast, S1P levels in circulation of SK2 null mice were reduced by only 25% suggesting that SK1 has the major role in determining circulating S1P levels [266]. In the lymphoid tissues of SK2^{-/-} mice such as spleen, thymus, and lymph nodes, S1P levels were not

significantly different compared to WT [267], but in the brain, where SK2 is known to be the major isoform of SK, the S1P levels have not been reported yet.

Importantly, our results here demonstrated that S1P levels were significantly reduced in the brain of SK2^{-/-} mice, consistent with the major role of the SK2 isoform in this tissue. Consistent with our results from chapter 4 and as we have published [165], DENV infection does not influence S1P levels in the brain in the context of WT, SK1^{-/-} and SK2^{-/-} mice. Our data suggested that the absence of SK2 affected the SK/S1P balance in the mouse brain but still failed to influence DENV infection. Thus, this data does not support a major contribution of the SK2/S1P axis in affecting DENV-infection in mice brain.

One of the important function of S1P is to regulate the migration of activated T cells from lymphoid organs [268]. Since S1P levels in the brain of SK2^{-/-} mice was significantly reduced compared to WT as described in 5.2.2.4, SK2, via changes in tissue S1P levels, might have a role in regulating T-cell infiltration into DENV-infected mouse brain. Our data demonstrated that CD8⁺ but not CD4⁺ T-cell infiltrated the brain of both WT and SK2 null mice following DENV infection. These results are consistent with our publication [165] and results of chapter 4 in DENV-infected WT and SK1 null mouse brain. Further, the CD8 levels in the brain of SK2 null mice was similar to WT following DENV infection. Thus, a dramatic reduction in SK2 and also S1P levels in the brain resulted in comparable levels of CD8⁺ T-cells in response to DENV-infection suggesting that SK2/S1P has no role in modulating T-cell infiltration into the brain following DENV infection.

Many prior studies demonstrated the role of SK2 during inflammation. For example, SK2 siRNA-mediated downregulation in a mouse model of collagen-induced arthritis increased the severity of the disease and release of pro-inflammatory cytokines [269]. Further, like SK1, SK2 is reported to enhance tumour growth, and genetic deletion or chemical inhibition of SK2 has anti-cancer effect [211]. In experimental models, targeting of SK2 by ABC selective inhibition has showed potential therapeutic properties against a wide range of diseases such as the progression of diabetic

retinopathy and osteoarthritis in rats [270,271]. Further, treatment with ABC exhibited anti-cancer activity in mouse tumour models [272] and human tumour cells [273]. Currently, ABC is in phase I clinical trials for treatment of advanced solid cancers [211,274]. In our case of DENV infection, however ABC is not a promising drug for regulating DENV replication, but ABC treatment could reduce DENV-induced inflammation (without affecting DENV replication) since it showed a modest anti-inflammatory activity in inflammatory diseases and fibrotic models [275], although this property needs more investigations.

In summary, our data suggest that the absence of SK2 in mouse cells *in vitro* results in a reduction in DENV infection, although we propose this result is likely an artefact of the immortalised MEF cell system. Treatment of human cells with SK2 inhibitors has no effect on DENV replication and consistent with the results of these inhibitors, DENV infection in the SK2^{-/-} mouse brain results in an enhanced susceptibility of mice to body weight loss but has no overall impact on DENV RNA level or DENV-induced disease. While S1P levels are reduced in the brain of SK2^{-/-} mice, the SK/S1P axis is not affected by DENV infection. Further, T-cell infiltration induced by DENV-infection was not affected by lack of SK2 and a reduction in S1P in the brain. SK2 selective inhibitors are advancing in clinical trials and theoretically could be applied to settings where SK2 is an important factor, such as the brain, and in important infectious scenarios in the brain, such as DENV or other flavivirus-mediated encephalitis. The results here, however suggest that SK2 inhibitors will be of little benefit in regulating DENV infection or T-cell mediated pathology in this setting.

CHAPTER 6. THE ROLE OF VIPERIN DURING DENV INFECTION IN THE BRAIN

6.1 Introduction

A host immune response to an invading virus is initiated following recognition of viral PAMPs by a host PRRs such as TLRs and RIG-I [276,277]. In the terms of DENV infection, TLR3 is the main molecule that recognises DENV antigens within endosomal compartments [137,278], however DENV can be also sensed by TLR9 and TLR7 intracellularly [139,278]. After DENV recognition, an antiviral immune response is initiated by activation of IRFs which subsequently induce the production of IFNs [279]. IFNs exhibit antiviral responses through induction of immune signalling cascades including JAK/STAT1 and STAT2 pathways that trigger the production of numerous ISGs, which perform multiple antiviral functions [280,281].

Viperin is one of these ISGs that was first described to be induced due to HCMV infection in primary human fibroblasts through induction of type I IFN- α and - β , which in turn inhibits HCMV infection in these cells [150]. Since then, many studies have reported the role of viperin against viral infections either directly by blocking viral replication or indirectly by regulating the host immune response to viral infection [148,282].

Previous studies including data from our laboratory has shown that viperin has anti-viral activity against DENV [156,162,163]. Specifically, our laboratory has shown that DENV-2 infection induces viperin. Additionally, when viperin is overexpressed in a cell DENV RNA level is reduced, potentially by an interaction with the DENV NS3 protein and VRC [156]. Our laboratory has further defined the regulation of induction of viperin during DENV-2 infection. In DENV-infected EC, blocking of IFN- β during DENV infection reduced the induction of ISGs, including viperin suggesting of IFN- β dependent induction of viperin by DENV [166]. We recently reported, as

shown in chapters 4 and 5, that viperin is highly induced in mouse brain following ic DENV-2 challenge both early in infection and prior to the onset of disease (day 3 pi) and at termination of experiments at end stage of disease [165]. Thus, in this chapter, we were interested to investigate this further and define the role of viperin during DENV-2 infection in the brain.

Here, we initially validated the previously described anti-viral role of viperin in mouse cells using primary MEF from viperin null mice and further defined the effect of the lack of viperin on the induction of IFN- β and other ISGs such as IFIT1 and IRF7 *in vitro*. We further examined the antiviral potential of viperin in the brain by ic DENV challenge in viperin null mice and examination of disease, DENV RNA level and induction of ISGs. Results demonstrate that while viperin is anti-viral against DENV *in vitro*, in the complexity of the responses in the brain a lack of viperin has no effect on DENV-induced disease, DENV replication or induction of other ISG responses.

6.2 Results

6.2.1 Viperin restricts DENV infection *in vitro*

Prior data including those from our laboratory have demonstrated that viperin is important effector against DENV infection *in vitro* [156,162]. Here, we sought to investigate effects of viperin *in vivo* using a CRISPR-Cas generated viperin null mouse line and first aimed to validate the effect of a lack of viperin using cells from these mice on DENV infection *in vitro*.

6.2.1.1 A deficiency of viperin in primary mouse cells promotes DENV infection

To assess the effect of the lack of viperin on DENV infection in the mouse system, we utilised primary embryonic fibroblast cells generated from mice of WT and Vip^{-/-} backgrounds as models for analysis. The WT and Vip^{-/-} 1^oMEFs looked morphologically similar and grew at similar rates *in vitro* (data not shown). Low passage WT and Vip^{-/-} 1^oMEFs were seeded, DENV infected, and the time-course of viral infection analysed. Cultured S/N was harvested to quantitate DENV infectious

virus production by plaque assay. RNA was extracted and absolute DENV copy number was determined by a real time qRT-PCR. Combined results from three independent experiments showed that infectious virus release was significantly increased by approximately 0.5 log in DENV-infected $Vip^{-/-}$ 1°MEFs compared to WT cells at 24, 48, and with nearly a 1 log increase by 72 hpi (Figure 6.1A). Similarly, quantitation of DENV RNA levels demonstrated a significant increase in $Vip^{-/-}$ 1°MEFs in comparison to WT 1°MEFs across all time pi (Figure 6.1B). Additionally, we attempted to derived macrophages from bone marrow cells harvested from WT and $Vip^{-/-}$ mice for DENV challenge but inconsistency in cell death between WT and $Vip^{-/-}$ bone marrow-derived macrophages (BMDMs) made this comparison unreliable.

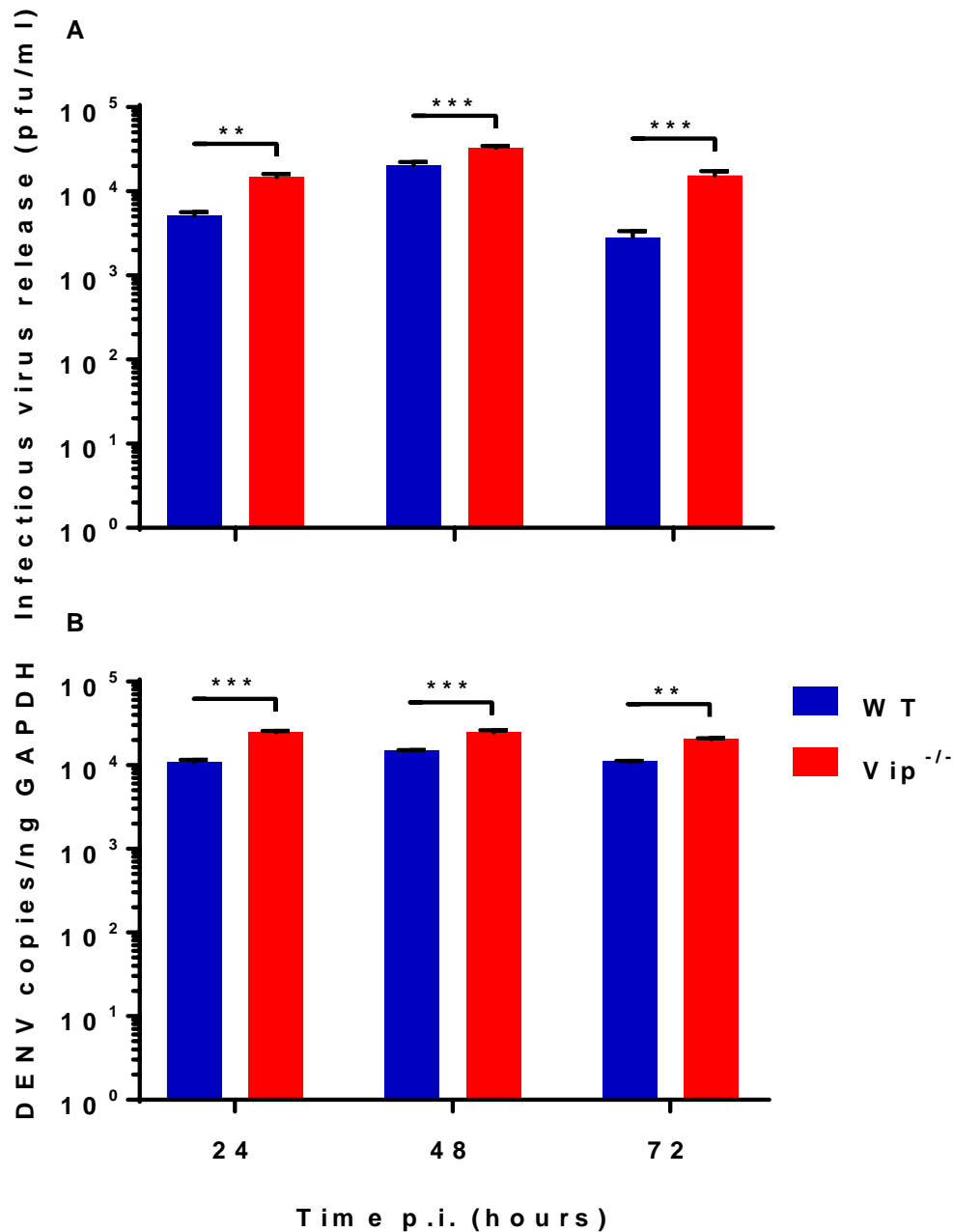


Figure 6.1 Viperin deficiency enhanced DENV infection in MEFs

MEFs were obtained from WT and Vip^{-/-} mice and utilised as primary cells (1°MEFs). MEF lines were plated and DENV infected at MOI of 0.1. (A) S/Ns were taken at 24, 48, and 72 hpi for plaque assay. (B) RNA was isolated and DENV copy number was quantitated by RT-PCR and normalised against GAPDH. Results represent mean ± SEM of n=3 assay replicates from three independent experiments. Statistical significance was determined by two-way ANOVA. ** p < 0.005, *** p < 0.0005.

6.2.1.2 The increased DENV-replication in viperin deficient mouse cells is associated with higher innate immune responses in vitro

Viperin has reported to regulate the production of type I IFN via TLR7 and TLR9 in pDCs in response to viral infection [168]. To assess the role of viperin in modulating IFN- β and ISG responses following DENV infection, primary cells were infected, as above, RNA extracted and mRNA levels of IFN- β and ISGs IFIT1, Ifi2712a, IRF7, and CXCL10 analysed by RT-PCR. Levels of mRNA for IFN- β and ISGs IFIT1, Ifi2712a, IRF7, and CXCL10 were significantly elevated in both DENV-infected WT and Vip^{-/-} 1°MEFs compared to the respective mock-infected 1°MEFs. At 48 hpi, IFN- β mRNA levels were significantly higher in DENV-infected Vip^{-/-} in comparison to WT 1°MEFs (Figure 6.2). Of note, higher DENV RNA levels were associated with the elevated IFN- β levels in Vip^{-/-} 1°MEFs as shown in Figure 6.1B. At 72 hpi, the mRNAs for the ISGs IFIT1, Ifi2712a, and CXCL10 were significantly upregulated in DENV-infected Vip^{-/-} compared to WT 1°MEFs (Figure 6.2). In contrast, at 48 hpi this was only significantly different for CXCL10 (Figure 6.2). This suggests that DENV RNA may be the major driver of the difference in IFN- β seen in WT and Vip^{-/-} cells. The higher level of DENV RNA and IFN- β seen in Vip^{-/-} cells however, does not appear to drive consistent and significant higher induction of IFIT1, Ifi2712a and IRF7 in the absence of viperin. In contrast, the induction of CXCL10, an ISG but also driven by NF- κ B-mediated signals, is still reflective of the higher DENV RNA and IFN- β levels seen in the absence of viperin, suggesting that viperin may contribute to DENV-induced ISGs such as IFIT1, Ifi2712a and IRF7 but not CXCL10.

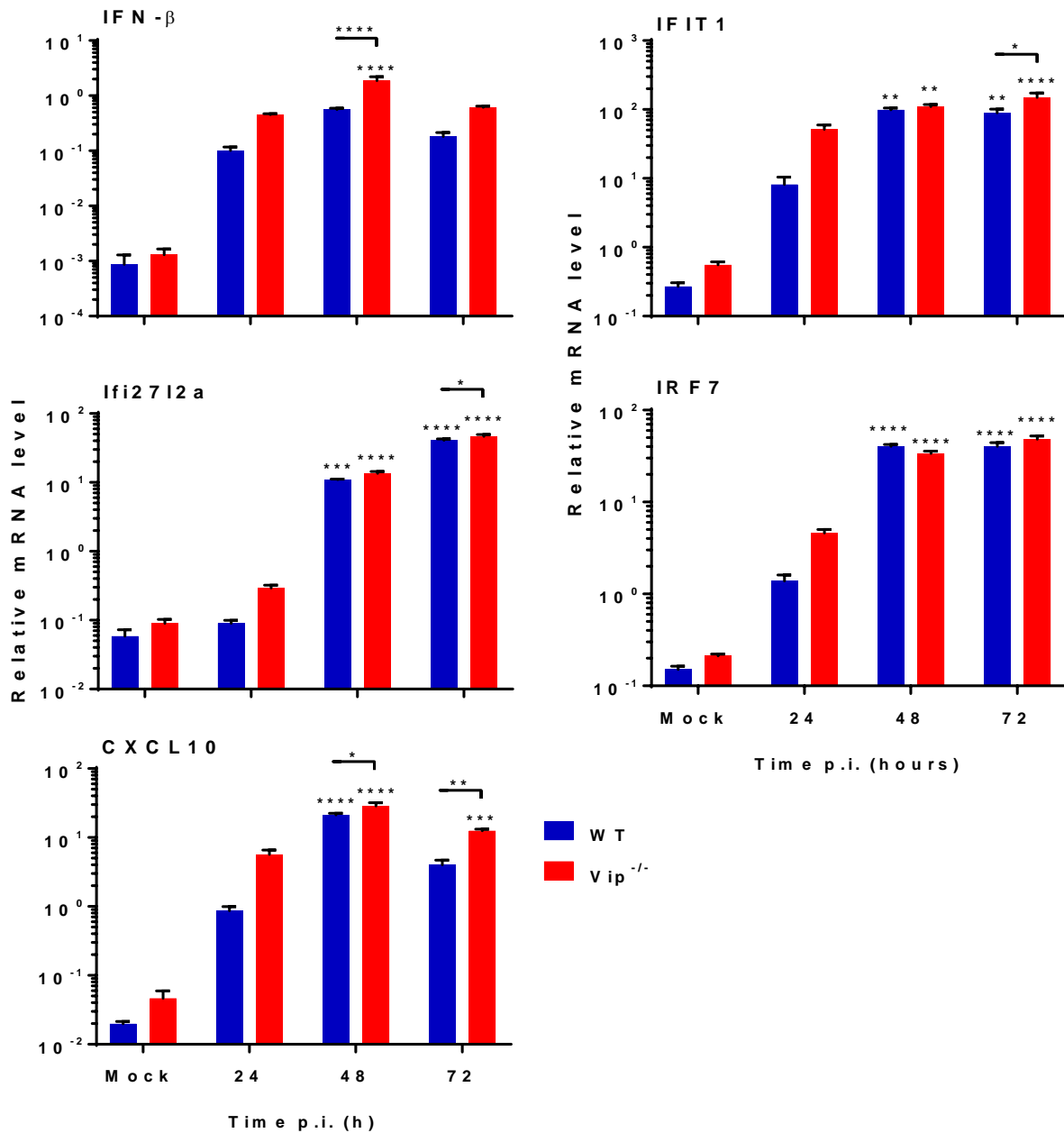


Figure 6. 2 Viperin deficiency modulates IFN- β and ISGs in 1°MEFs

WT and *Vip*^{-/-} 1°MEFs were DENV infected at MOI of 0.1 as in Figure 6.1. RNA was isolated at indicated time pi and mRNA levels for IFN- β , IFIT1, Ifi2712a, IRF7, and CXCL10 were measured by qRT-PCR using Δ Ct method and normalised against GAPDH. Results represent mean \pm SEM of n=3 assay replicates from three independent experiments. Statistical significance was determined by two-way ANOVA compared to mock-infected control. * p < 0.05, ** p < 0.005, *** p < 0.0005, **** p < 0.00005.

6.2.2 Viperin has a minimal role during DENV infection in mice

Our studies above, demonstrate that in cells taken from our CRISPR-Cas viperin null mice, the lack of viperin increases DENV replication, suggesting that consistent with the literature, viperin is anti-viral against DENV *in vitro*. No prior study has investigated the role of viperin against DENV infection *in vivo*. Although we would anticipate enhanced DENV replication in the absence of viperin, a complicating factor here is the lack of a good immunocompetent mouse model for DENV replication [185] for use as a WT control. Hence, we used the ic DENV mouse challenge model established in chapter 4, where infection can be readily achieved in WT mice. Additionally, a role for viperin specifically in astrocytes of the brain has previously been described in restricting brain infection in WNV-infected mice [283] and thus the brain is a relevant tissue to study in relation to viperin function.

6.2.2.1 A deficiency of viperin has no significant effect on DENV neurovirulence and survival of mice following ic DENV infection

We demonstrated previously that WT C57BL/6 mice develop weight loss and signs of neurovirulence such as loss of hind limb function following DENV infection by ic injection route. To define whether the absence of viperin affects the susceptibility of mice to this model of DENV infection, WT (n=8) and *Vip*^{-/-} (n=8) mice were ic infected with 800 pfu/ml of DENV-2 MON601 strain and mock mice from each group (n=4) were ic injected with PBS. Post-challenge, body weight and neurological signs of disease (slow movement, hunched posture, and reduction in hind limb movement) were observed. As described in chapter 4, the maximum duration of the study was eight days (end time point), or mice that showed either signs of disease or loss of more than 10% of body weight were euthanised prior to day 8. Since the mice in this study are 3 weeks of age and actively growing, the average body weight of WT and *Vip*^{-/-} mice was calculated as a percentage of the initial body weight. Mock-infected WT and *Vip*^{-/-} mice did not demonstrate any loss in body weight or appearance of DENV neurovirulence symptoms (Figure 6.3A and C). WT mice showed a

significant reduction in body weight gain by 4 dpi (Figure 6.3A) and 50% of mice began to lose weight by day 6 pi (Table 6.1). In contrast, *Vip*^{-/-} mice did not show a significant reduction in body weight gain until 7 dpi (Figure 6.3C), although all mice began to lose weight by day 5-6 pi (Table 6.1). As expected, the mortality rate of DENV infected WT and *Vip*^{-/-} mice were significantly higher compared to their respective mock-infected mice (Figure 6.3B and D). Comparison of body weight between DENV-infected WT and *Vip*^{-/-} mice showed no significant difference except at day 5 pi where WT mice demonstrated significantly lower body weight gain than *Vip*^{-/-} mice (Figure 6.3E). At day 7 pi, all of *Vip*^{-/-} and 6 out of 8 WT DENV-infected mice were euthanised due to either excessive weight loss or presence of neurological symptoms (Figure 6.3E). This is reflected by significantly higher mortality rate of DENV-infected *Vip*^{-/-} mice at day 7 pi compared to WT mice (Figure 6.3F).

Although the time of body weight loss approached significance ($p=0.076$) with an earlier onset in *Vip*^{-/-} mice, there was however no significant difference in the overall number of mice that lost body weight, the time of onset of body weight loss, nor the percentage of mice that lost more than 10% of body weight (Table 6.1).

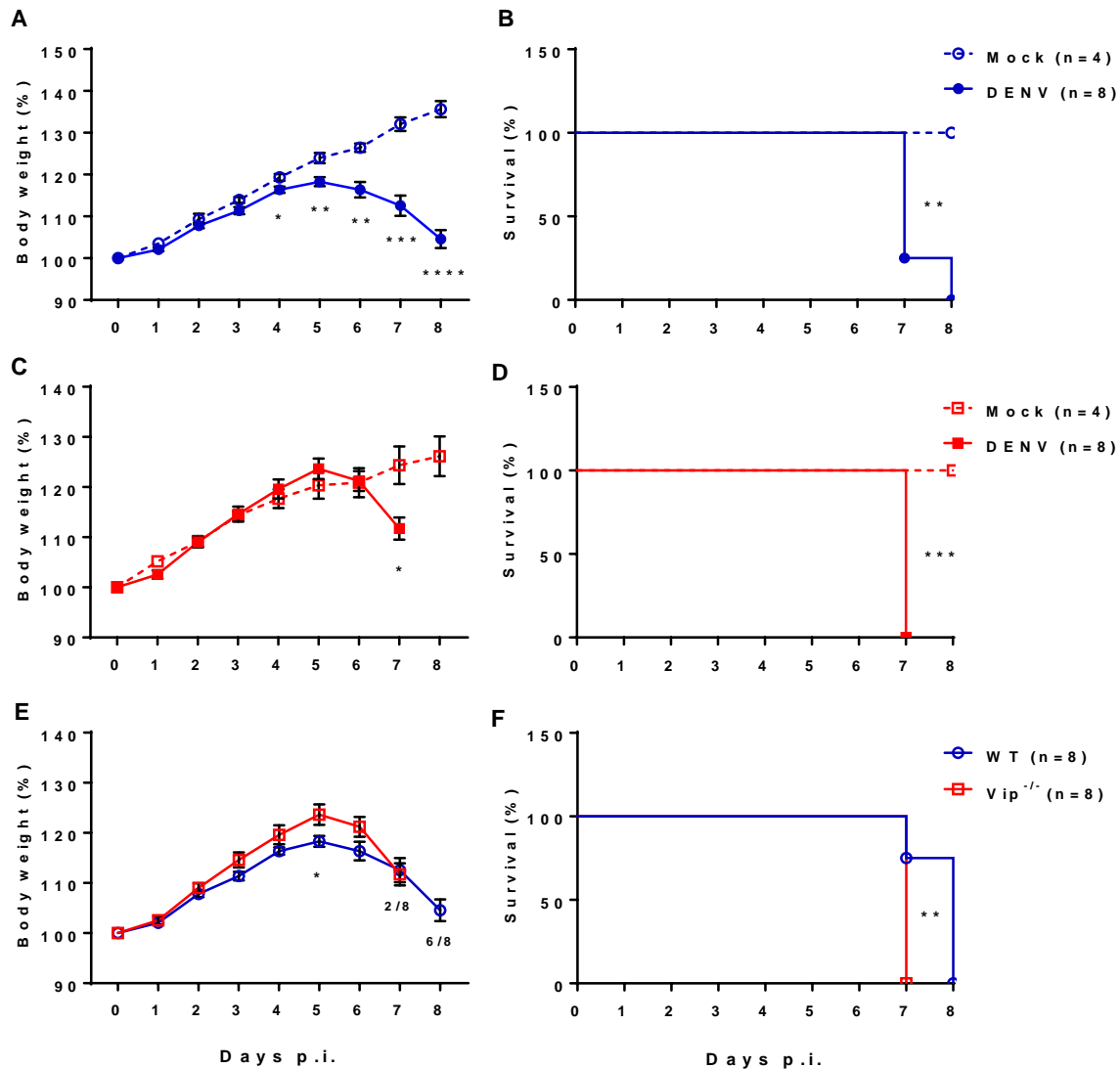


Figure 6.3 Body weight gain and survival curve of WT and Vip^{-/-} mice

3-4 weeks old C57BL/6 WT (n=8) and Vip^{-/-} (n=8) mice were ic injected with 800 pfu/ml DENV-2 MON601 strain. Mock WT (n=4) and Vip^{-/-} (n=4) control mice were ic injected with vehicle only. Body weight and neurological symptoms were recorded. Body weight is expressed as a percentage of initial body weight. Survival reflects mice that do not show neurological symptoms or >10% of body weight loss. Comparison of body weight and survival curves of (A and B) mock with DENV-infected WT mice; (C and D) mock with DENV-infected Vip^{-/-} mice; (E and F) DENV-infected WT and Vip^{-/-} mice. Data are expressed as mean \pm SEM. Statistical significance for body weight was determined using unpaired student *t*-test. Statistical analysis of survival curves were determined by log rank test. * = $p < 0.05$, ** = $p < 0.005$, *** = $p < 0.0005$, **** = $p < 0.00005$.

Table 6. 1 Summary of body weight loss and signs of DENV-induced neurovirulence in WT (n=8) and Vip^{-/-} (n=8) mice and analysed by Fisher's exact test

	Mouse strain				<i>p</i>
	WT		Vip ^{-/-}		
	#	%	#	%	
Body weight loss					
Weight loss	8	100.00	8	100.00	0.999
No weight loss	0	00.00	0	00.00	
% Body weight loss					
≥ 10%	6	75.00	6	75.00	0.999
< 10%	2	25.00	2	25.00	
Days pi onset loss					
≤ 6 dpi	4	50.00	8	100.00	0.076
> 6 dpi	4	50.00	0	00.00	
Appearance of neurovirulence					
Severe signs	3	37.50	4	50.00	0.999
Mild signs	5	62.50	4	50.00	

6.2.2.2 A deficiency of viperin has no significant effect on DENV RNA levels in the brain of mice following ic infection

We next sought to define DENV replication in the brain of mice that lack of viperin, following ic DENV infection. WT and *Vip*^{-/-} mice were infected, brains were harvested at day 3 pi or at 7-8 dpi (end stage disease), as described above. Total RNA was extracted, and DENV RNA was quantitated by qRT-PCR. DENV RNA was undetectable in the brain of mock-infected mice. No significant difference was observed in DENV RNA levels at day 3 pi between DENV-infected WT and *Vip*^{-/-} mice (Figure 6.4A). At day 7-8 pi (end-stage disease), DENV RNA levels in the brain of DENV-infected *Vip*^{-/-} mice was not significantly different compared to WT mice (Figure 6.4B). Collectively, these results demonstrate that DENV RNA levels in mouse brain at either day 3 pi or end-stage disease were not influenced by a deficiency of viperin.

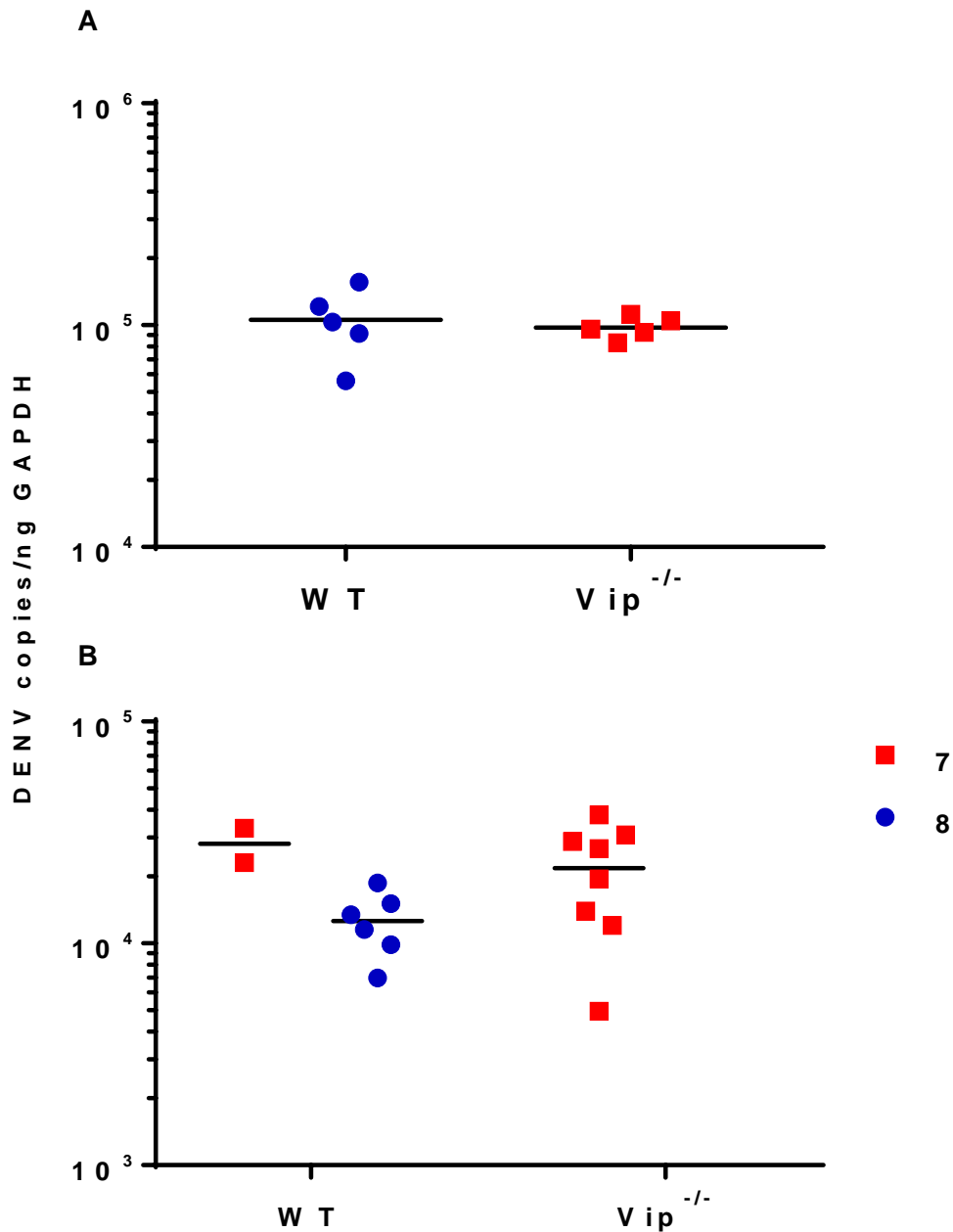


Figure 6. 4 DENV RNA levels in *Vip*^{-/-} mice

WT and *Vip*^{-/-} mice were ic infected with DENV as in Figure 6.3. RNA was extracted from infected brain tissue and subjected to a real-time RT-PCR for DENV. **(A)** at 3 dpi, n=5 for each mice strain, **(B)** at the time of humane euthanasia, representing 7 (n=2), and 8 (n=6) dpi for WT and 7 (n=8) dpi for *Vip*^{-/-} mice. Statistical significance was determined using unpaired student *t*-test for **(A)** and two-way ANOVA for **(B)**. Each symbol represents an individual mouse sample. Data represent average PCR values from individual mice.

6.2.2.3 A deficiency of viperin does not affect IFN- β and ISGs levels in mouse brain following DENV infection

We recently demonstrated the induction of IFN- β and ISGs in mouse brain in following DENV infection at both end stage disease and early time pi while DENV-infection of Vip^{-/-} 1^oMEFs (see section 6.2.1.2) demonstrate a significantly higher induction of IFN- β but comparable induction of IFIT1, Ifi2712a, and IRF7. Here, we sought to assess the effect of the loss of viperin protein on IFN- β and ISGs response in the mouse brain following DENV infection. In comparison to *in vitro* 1^oMEF, this model is not confounded by increased DENV replication (Figure 6.4). WT and Vip^{-/-} mice were ic DENV infected and total RNA extracted from harvested brain (as in Figure 6.3 and 6.4). The mRNA levels for IFN- β and ISGs IFIT, Ifi2712a, IRF7, and CXCL10 were analysed by qRT-PCR. At 3 dpi, IFN- β is not induced but IFIT, Ifi2712a, IRF7, and CXCL10 are induced following DENV infection in WT and Vip^{-/-} mice (Figure 6.5A). Further, at 3 dpi, the induction of IFN- β , IFIT, Ifi2712a, IRF7, and CXCL10 following DENV infection again was not affected by the lack of viperin in mouse brain (Figure 6.5A). At end stage disease (7-8 dpi), IFN- β and ISGs were induced in both DENV-infected WT and Vip^{-/-} mice (Figure 6.5B) as demonstrated previously. Of note, Ifi2712a level was significantly higher in DENV-infected Vip^{-/-} compared to WT mice. The mRNA levels of IFN- β and IFIT, IRF7, and CXCL10 however were not affected by the loss of viperin in the brain following DENV infection (Figure 6.5B). These data are indicative of a dispensable role of viperin for the production of IFN- β and induction of antiviral effectors in the brain but the potential link of Ifi2712a expression with viperin.

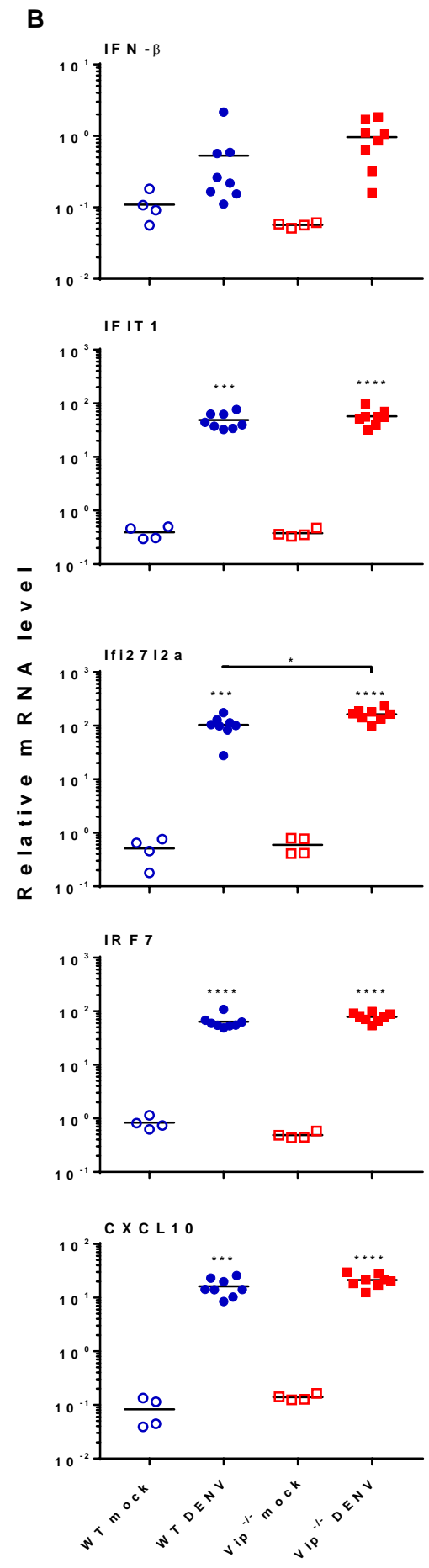
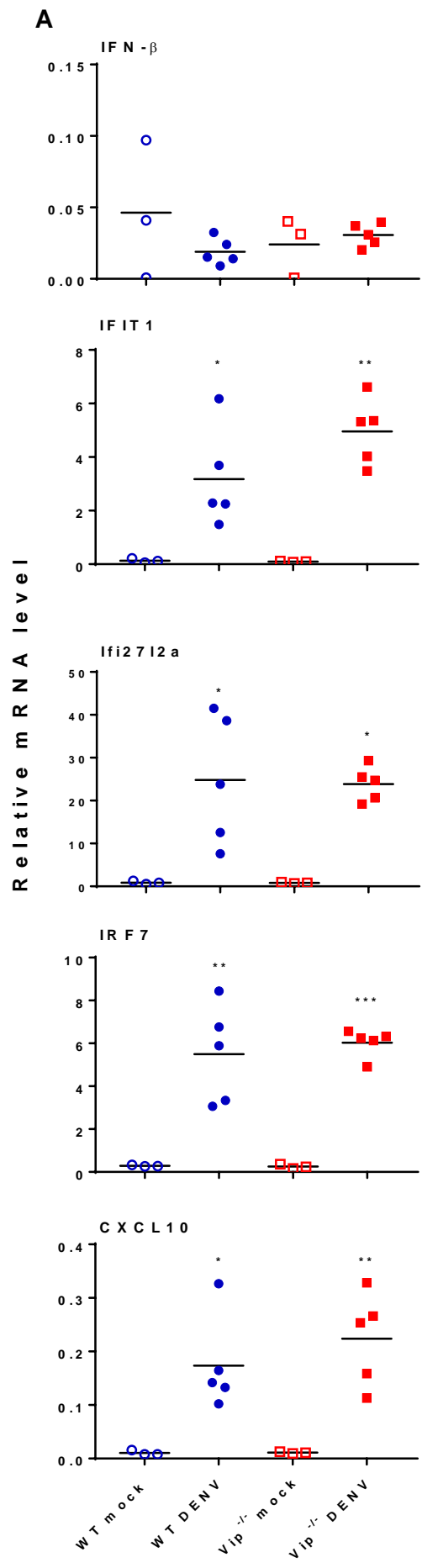


Figure 6. 5 Induction of IFN- β and ISGs in the brain of WT and Vip^{-/-} mice following ic DENV-2 injection

WT and Vip^{-/-} mice were ic infected with DENV, as in Figure 6.3. RNA was isolated and analysed by real time qRT-PCR for IFN- β , IFIT1, Ifi2712a, IRF7, and CXCL10. **A.** at 3 dpi, n=5 WT and Vip^{-/-} DENV-infected, n=3 WT and Vip^{-/-} mock-infected mice; **B.** at end stage disease for n=8 WT and Vip^{-/-} DENV-infected, n=4 WT and Vip^{-/-} mock-infected mice. Data represent average PCR values from individual mice and normalised against GAPDH by Δ Ct method. Statistical significance was assessed by one-way ANOVA. *= p < 0.05, **= p < 0.005, ***= p < 0.0005, ****= p < 0.00005.

6.2.2.4 A deficiency of viperin has no effect on T-cell infiltration at end stage infection

Our previous data using the ic DENV infection mouse model in chapter 4 showed that T-cells, particularly CD8⁺ but not CD4⁺ T-cells infiltrated the infected brain at later stage of DENV infection. Here, we defined the effect that the absence of viperin has on CD4⁺ and CD8⁺ T-cells recruitment into the mouse brain following DENV infection. WT and Vip^{-/-} mice were ic DENV challenged, as above, total RNA extracted, and mRNA levels of CD4⁺ and CD8⁺ quantitated by RT-PCR, as an index for T-cell infiltration. We did not analyse CD4⁺ and CD8⁺ mRNAs at day 3 pi since prior data (see chapter 4) suggested no cellular infiltrate at this time point. At end stage of DENV infection, CD4 mRNA levels were not significantly different in either WT and Vip^{-/-} DENV-infected mice strains compared to mock-infected controls (Figure 6.6A). In contrast, CD8 mRNA levels were significantly higher in WT and Vip^{-/-} mice following DENV infection compared to mock-infected controls (Figure 6.6B). CD8 mRNA levels, however were not significantly different between WT and Vip^{-/-} mice. This observation indicates that the lack of viperin does not alter CD4⁺ and CD8⁺ T-cells infiltration following DENV infection in mouse brain.

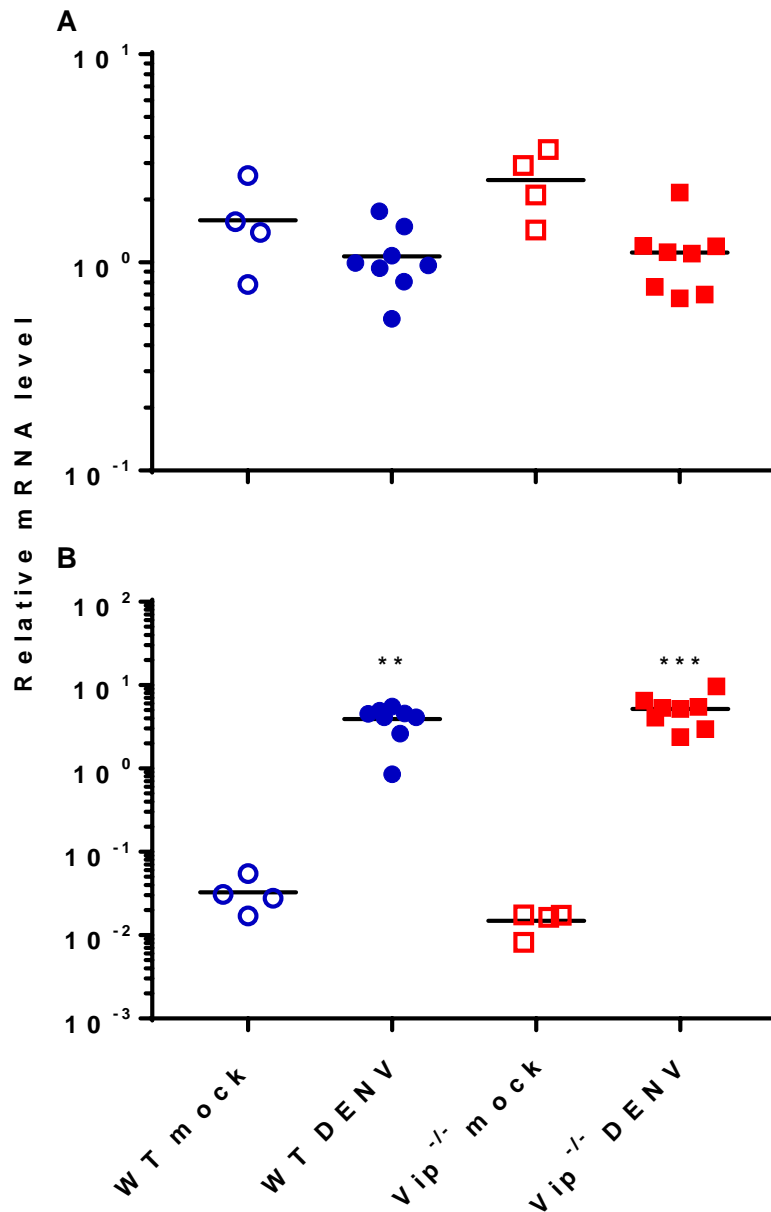


Figure 6.6 CD4 and CD8 levels in WT and Vip^{-/-} mice in the brain following ic DENV infection

WT and Vip^{-/-} mice were ic DENV infected as in Figure 6.3. At end stage disease, RNA was isolated from infected mice brain tissues and analysed by real time qRT-PCR for **A.** CD4 mRNA; **B.** CD8 mRNA. n=8 WT and Vip^{-/-} DENV-infected, n=4 WT and Vip^{-/-} mock-infected mice. Data represent average PCR values from individual mice and normalised against GAPDH by ΔCt method. Statistical significance was assessed by one-way ANOVA. **= $p < 0.005$, ***= $p < 0.0005$.

6.2.2.5 A deficiency of viperin significantly increases IL-6 but does not affect TNF- α mRNA levels following DENV infection

In addition to IFN responses, pro-inflammatory cytokines represent an important arm of innate defences for elimination of viral infections. We sought to define the induction of two pro-inflammatory cytokines TNF- α and IL-6 previously shown to be important in DENV infection [284], following DENV infection in mouse brain, and to assess whether the viperin deficiency affects their response. WT and Vip^{-/-} mice were ic DENV challenged, as above, and mRNA levels of TNF- α and IL-6 extracted from brain tissue were analysed by RT-PCR. At day 3 pi, no significant induction was observed for TNF- α and IL-6 mRNAs in DENV-infected compared to mock-infected WT mice (Figure 6.7A and B). In contrast, TNF- α mRNA levels tended to be increased in Vip^{-/-} compared to WT mice and approached significance (p=0.061) (Figure 6.7A). IL-6, however was significantly induced in DENV-infected Vip^{-/-} mice compared to mock mice and tend to be higher (p=0.084) in DENV-infected Vip^{-/-} compared to WT mice (Figure 6.7B). Further, at end stage disease, mRNA levels of TNF- α and IL-6 cytokines were significantly upregulated in both DENV-infected WT and Vip^{-/-} mice compared to mock-infected mice (Figure 6.7C and D). Notably, IL-6 induction was significantly higher in DENV-infected Vip^{-/-} compared to WT mice (Figure 6.7D). These results suggested that in the absence of viperin, other important pro-inflammatory cytokines, such as IL-6 are increased in response to DENV infection in mouse brain.

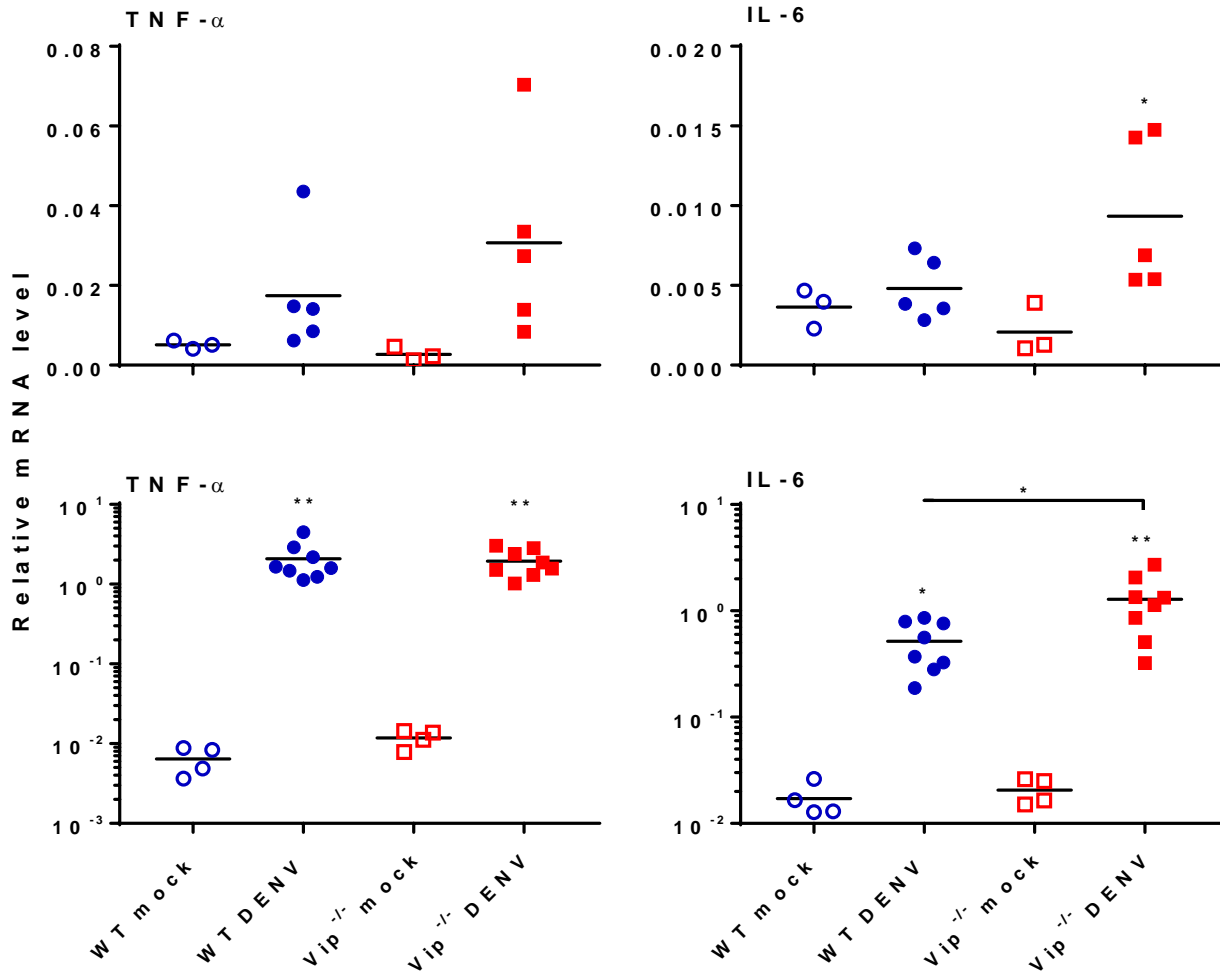


Figure 6. 7 TNF- α and IL-6 responses in WT and Vip^{-/-} mice in the brain following ic DENV infection

WT and Vip^{-/-} mice were ic DENV infected as in Figure 6.3. RNA was isolated from infected mice brain tissues and analysed by real time qRT-PCR. **A** and **B**. at 3 dpi for TNF- α and IL-6. n=5 WT and Vip^{-/-} DENV-infected mice, n=3 WT and Vip^{-/-} mock-infected mice; **C** and **D**. at end stage disease for TNF- α and IL-6. n=8 WT and Vip^{-/-} DENV-infected mice, n=4 WT and Vip^{-/-} mock-infected mice. Data represent average PCR values from individual mice and normalised against GAPDH by Δ Ct method. Statistical significance was assessed by one-way ANOVA. *= p < 0.05, **= p < 0.005.

6.2.2.6 DENV infection in the brain induces comparable morphological changes in both WT and Vip^{-/-} mice

DENV infection ic in mouse brain has been reported to induce neuroinflammatory damage in hippocampus region of the brain [284,285] and we have recently shown (see chapter 4) that DENV infection by direct ic injection induced T cell infiltration in the cortical area of the mouse brain [165]. We sought to assess the histological changes in the brain of WT and Vip^{-/-} following DENV-2 infection with a particular focus on the hippocampus. WT and Vip^{-/-} were ic DENV infected, brain harvested at end stage disease, fixed in 10% formalin and tissues subjected to H & E staining. Both DENV-infected WT and Vip^{-/-} mice showed pathological changes within the hippocampus characterised by intensive destruction of neurons, perivascular cuffing, and infiltration of inflammatory cells (Figure 6.8) compared to the hippocampus of mock-infected mice. A deficiency of viperin does not exacerbate hippocampal damage as both DENV-infected mice strains showed similar neuropathies in the brain (Figure 6.8), suggesting a negligible role of viperin to enhance the susceptibility of mouse brain to neurodamage after DENV inoculation.

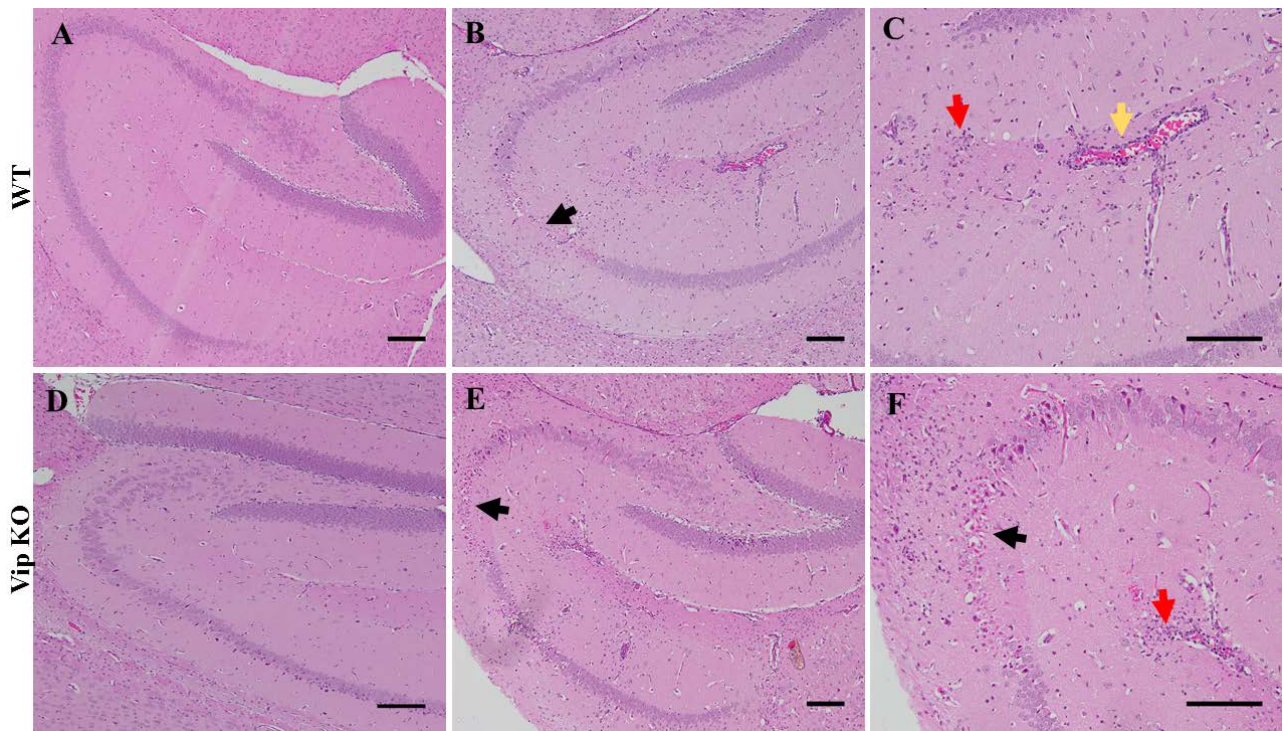


Figure 6. 8 Histopathological changes of the brain hippocampus in WT and $Vip^{-/-}$ mice following ic DENV infection

WT and $Vip^{-/-}$ mice were ic DENV injected as in Figure 6.3. At end stage disease, brains were harvested and fixed in 10% formalin for H & E staining. (A and D) Normal histology of mock brain hippocampus. (B, E and F) Destruction of neurons of hippocampus region (black arrow) from DENV-infected WT and $Vip^{-/-}$ mice brain. (C and F) Infiltration of immune cells (red arrow), and (C) perivascular cuffing (yellow arrow). Images were captured by a BX53 brightfield microscope and representative of n=2 DENV-infected WT and $Vip^{-/-}$ mice, and n=2 of mock-infected WT and $Vip^{-/-}$ mice. Bars indicate a 100- μ m scale.

6.2.2.7 Immunofluorescence staining of brain tissue from WT and Vip^{-/-} mice following ic DENV infection

We aimed to detect DENV protein in mouse brain tissue and to investigate the expression site of viperin using a fluorescent immunostaining approach. WT and Vip^{-/-} were ic DENV infected, brain harvested at end stage disease and fixed in 10% formalin for immunostaining. Brain tissue sections obtained from DENV-infected and mock-infected mice were immunostained with 4G2 to identify DENV E protein and anti-viperin antibody to identify viperin protein. No positive staining for DENV E protein was detected in the brain of either mock-infected WT or Vip^{-/-} mice (Figure 6.9A and B). Few cells stained positively for DENV E protein in either DENV infected WT or Vip^{-/-} mice. Additionally, the staining was not very intense. No cells were stained positive for viperin in either the brain of WT or Vip^{-/-} mice (Figure 6.9). Overall, however the trial to use immunofluorescence staining to investigate DENV protein and expression of viperin in the mouse brain was promising but the staining was not convincing. Due to time restrictions, this was not pursued further. Similarly, viperin staining was not detected in mock-infected sections (Figure 6.9A and B) or Vip^{-/-} sections following DENV infection (Figure 6.9B). Low-level viperin staining was detected in DENV-Ag + ve cells in WT mouse brain sections (Figure 6.9A). Additionally, viperin + ve cells correlated with DENV + ve cells (Figure 6.9A).

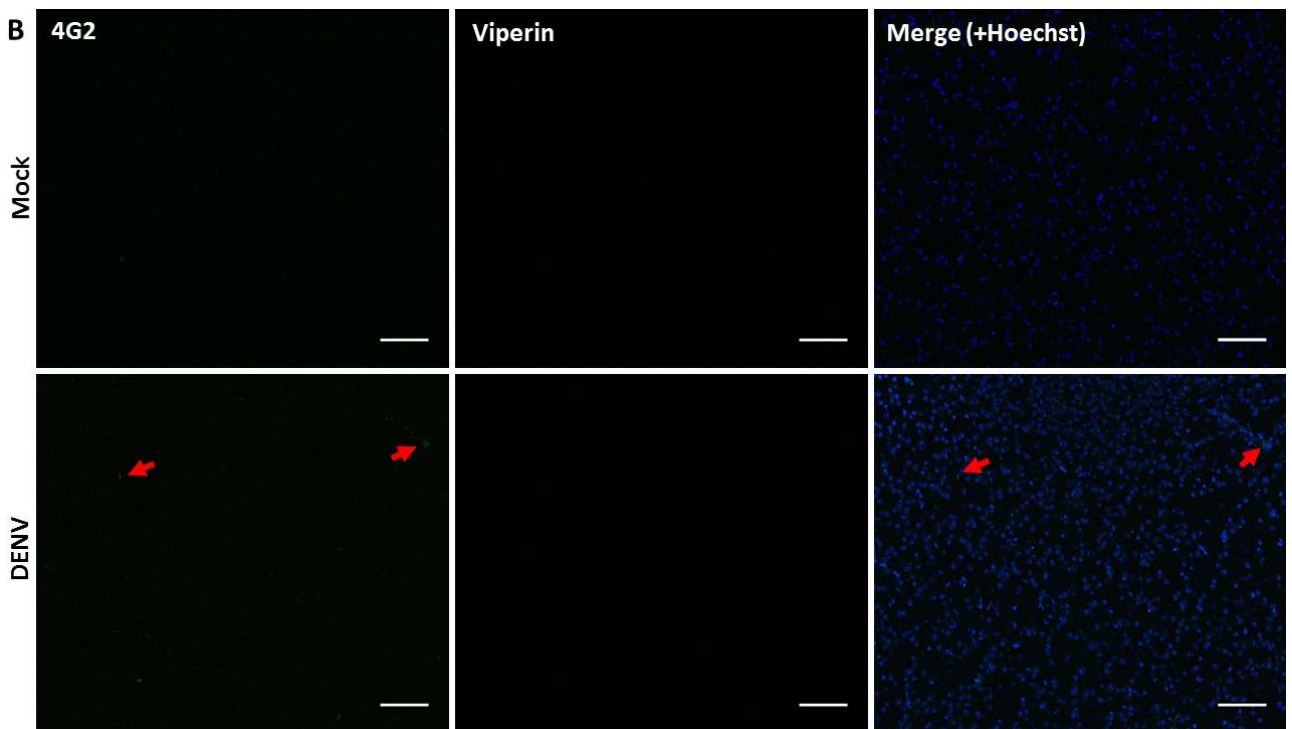
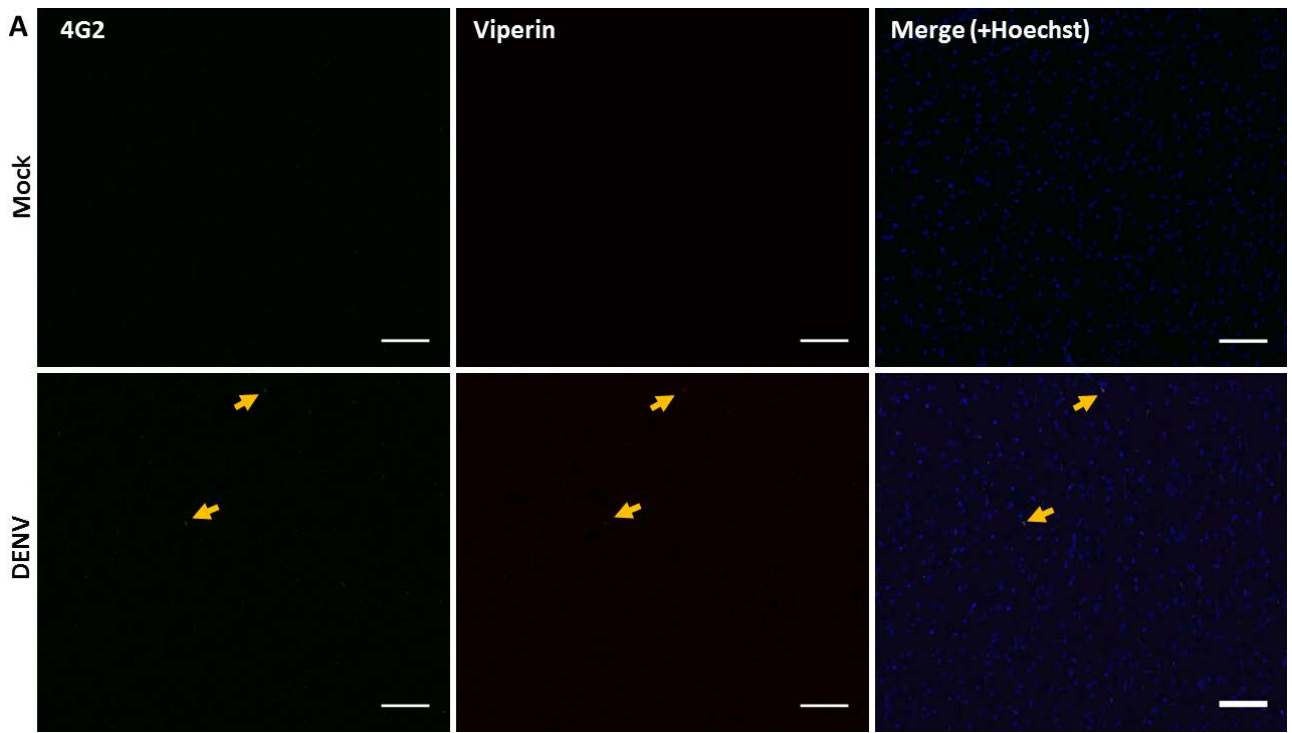


Figure 6. 9 Immunostaining of WT and Vip^{-/-} mice brain tissues following DENV infection

WT and Vip^{-/-} mice were ic injected as in Figure 6.3. At end stage disease, brain harvested and fixed in formalin for fluorescence staining. Tissue sections were immunostained for DENV E protein (green) and viperin (red) and Hoechst nuclear stain (blue). **(A)** Yellow Arrows represent cells stained for DENV and positive for viperin of WT mice. **(B)** Red Arrows represent cells stained positive for DENV but negative for viperin of Vip^{-/-} mice. Images were captured by AX50 fluorescence microscope representative n= 2 of DENV and mock-infected WT and Vip^{-/-} mice. Bars indicate a 100- μ m scale. Immunostaining was performed by Dr Ravinarayan Raghupathi.

6.3 Discussion

The ability of IFNs to eliminate viral infection is largely mediated by the transcription of a hundreds of ISGs such as viperin, which show diverse antiviral activities [280,286]. Viperin was initially recognised as an IFN-inducible gene stimulated by HCMV infection in human fibroblasts [149,150]. Viperin is a highly conserved gene between species, and is a part of the early immune response against wide range of microbial infections including bacterial and viral infections [147,287]. Data from our laboratory has suggested a role of viperin in restricting DENV infection *in vitro* using human primary cells [156], and that viperin is induced in MEFs [167] and in the brain of mice [165] in response to DENV-2 infection (see chapters 4 and 5). Here, we have investigated the role of viperin against DENV infection *in vitro* using *Vip*^{-/-} MEF and *in vivo* using immunocompetent C57BL/6 WT and *Vip*^{-/-} mice and direct ic DENV infection.

Our results have shown that the deficiency of viperin in 1°MEFs significantly increased DENV RNA levels and DENV infectious virus release at different times pi, suggesting an important role of murine viperin in reducing DENV infection *in vitro*. In contrast, *Vip*^{-/-} BMDMs and bone-marrow dendritic cells (BMDCs) were more susceptible to WNV infection *in vitro* but not *Vip*^{-/-} 1°MEFs [283], which the authors suggested implicated cell type specific roles for viperin in targeting WNV infection. Our data however is consistent with other studies that suggest a role of viperin in restricting viral infection in MEFs. A recent study by Van der Hoek *et al.*, 2017 using the same CRISPR/Cas viperin KO mouse line to that used here, has shown that a genetic deletion of viperin in MEFs increased ZIKV replication compared to WT MEFs [239]. Further, *Rsad2*^{-/-} MEFs showed increased susceptibility to CHIKV in comparison to WT MEFs [288]. Other investigations have targeted viperin transiently in other species including human cells and similarly observed increases in viral replication *in vitro*. Of note, siRNA-mediated knockdown of viperin enhanced HIV-1 infection in human MDMs [160] and increased production of equine infectious anaemia virus (EIAV) in MDMs [289]. Similarly, targeting of viperin mRNA using shRNA enhanced production

of Sindbis virus (SIN) in human A549 carcinoma cells but not JEV production [290] and increased DENV-2 release in Huh7 cells [156]. Further, viperin shRNA-mediated knockdown affected antiviral activity of IFN- α against HCV infection in Huh7 cells [155]. Thus, genetic knockout or knockdown of viperin impacts on the cells susceptibility to a wide spectrum of DNA and RNA human viruses, including flaviviruses ZIKV [239], WNV [283], DENV [156,162], JEV [290], TBEV [291], as well as HCMV [150], IAV [159] and HCV [161,292,293]. Further, viperin has antiviral activity against lentiviruses HIV-1 [160] and EIAV [289].

Viperin exerts antiviral functions through many biological pathways however the precise mechanism still unknown [148]. Structurally, viperin is a radical SAM enzyme [157], which comprises three domains implicated in the anti-microbial activity of viperin, an N-terminal amphipathic α helix, a radical SAM domain, and a C-terminal domain [148]. Viperin and HCV together localised to the lipid droplets on ER through their N-terminal amphipathic α -helical domain which allowed viperin to inhibit HCV [154]. The SAM domain is important for the enzymatic activity of viperin and mutation in this region inhibited the antiviral activity of viperin against DENV and WNV infection [162]. The C-terminal region is essential for viperin dimerisation and it has mediated the viperin antiviral activity against HCV [293] and DENV [156]. Additionally, viperin is reported to inhibit IAV release from infected cells by disrupting lipid rafts [159], preventing egress of HIV-1 [160], and diminishes the synthesis of viral proteins required for HCMV production [150].

Viperin expression can be induced following viral infection in a manner dependent on IFN production following infection with Sendai virus (SV) [294], pseudorabies virus [295], and lymphocytic choriomeningitis virus (LCMV) [296]. Further, viperin is also induced by IFN independent pathways during infection with HCMV [150], and VSV [295]. Notably, we found that the induction of IFN- β was significantly higher in *Vip*^{-/-} compared to WT 1^oMEFs following DENV infection, but this correlated with increased DENV RNA. Consistent with higher DENV replication driving higher IFN- β , CHIKV-infected *Rsad2*^{-/-} mouse fibroblasts showed higher production of

IFN- α and β compared to the infected WT fibroblasts [288]. Additionally, our results showed that the induction of ISGs IFIT1 and IRF7 was variable following DENV infection in MEF lines where it was significantly higher in *Vip*^{-/-} 1°MEFs at 24 hpi but comparable at 48 and 72 hpi compared to WT 1°MEFs. Further, the induction of *Ifi2712a*, an ISGs with reported antiviral action against WNV infection in mouse brain [297], was significantly higher in DENV-infected *Vip*^{-/-} compared to WT 1°MEFs also at 48 hpi. CXCL10 was higher at 24 and 72 hpi but not 48 hpi in *Vip*^{-/-} 1°MEF. Together, these results suggested that in the absence of viperin DENV replicates at higher levels, which induces higher levels of IFN- β . These higher levels of IFN- β in *Vip*^{-/-} cells initially drive higher ISGs (IFIT1, IRF7, *Ifi2712a*, and CXCL10) at 24 hpi but this is not sustained for IFIT1 and IRF7 suggesting viperin may have an IFN-independent role in maintaining expression of these ISGs. For CXCL10, an ISG but also NF- κ B driven factor, the influence of viperin is less apparent with levels at 24 ad 72 hpi correlating with increased DENV RNA. One IFN-independent pathway may be IRF1 driven since direct activation of IRF1 has previously been demonstrated to induce viperin transcription independently of IFNs [151]. Thus, our *in vitro* results supports an antiviral role of viperin against DENV, and suggest that this may, in part, be mediated by less effective induction of some other ISGs in the absence of viperin.

A previous *in vivo* study suggests a role of viperin in defending against lethal WNV infection in mouse brain since *viperin*^{-/-} adult mice were more susceptible to CNS disease caused by WNV [283]. Thus, we were interested to further analyse the role of viperin during DENV infection in the brain. Following ic infection with DENV, both WT and *Vip*^{-/-} mice developed body weight loss and induced signs of disease compared to mock-infected mice. No major difference in the body weight loss was observed between DENV-infected WT and *Vip*^{-/-} mice. Further, survival analysis showed there was a significant higher mortality rate of DENV-infected *Vip*^{-/-} mice compared to their counterpart WT mice with *Vip*^{-/-} mice succumbing to disease one day earlier than WT mice. This finding indicates that DENV-induced neurovirulence symptoms are worse in the viperin null mice. This is consistent with the higher susceptibility of *Vip*^{-/-} mice to lethal WNV infection following sc

infection compared to WT mice [283]. Additionally, viperin deficiency enhanced CHIKV-induced disease in viperin null mice following footpad CHIKV infection that was characterised by higher viremia and joint inflammation [288]. A slight increase in mortality of *Vip*^{-/-} mice following IAV infection in lungs has also been reported [298]. Although our finding of higher mortality rate in *Vip*^{-/-} mice ic infected with DENV aligns with the general literature of increased mortality with viral infections in the absence of viperin, the overall disease profile we observed in DENV-infected WT and *Vip*^{-/-} mice groups was not dramatically different.

Additionally, we have observed that DENV RNA level at both end stage-disease and before the onset of disease symptoms at day 3 pi was not significantly different in the brain of *Vip*^{-/-} mice compared to WT mice. These results suggest the absence of viperin does not influence DENV replication in mouse brain. Our data is in agreement with a study showing that the peak IAV titre was not significantly different in the lungs of *Vip*^{-/-} mice either at earlier or later stages of viral infection [298]. In contrast, WNV load was higher in the brain of *Vip*^{-/-} mice at day 8 pi compared to WT following ic infection [283]. Similarly, CHIKV showed higher viral load in the footpad of *Vip*^{-/-} mice at day 1 pi compared to WT mice [288]. Taken together these data suggest that viperin aids in controlling replication of many viruses *in vivo* including other flaviviruses in the brain. In the context of DENV in the brain, however viperin seemed to have a dispensable role in protecting against viral replication and disease. This *in vivo* data is inconsistent with our observation in 1°MEFs in which DENV RNA levels was higher in viperin deficient 1°MEFs compared to normal viperin 1°MEFs and our prior published anti-viral activity of viperin against DENV in Huh7 cells, MDM [156] and EC [166]. This highlights the potential for cell type specificity for the roles of viperin, as previously suggested [283] and/or the complexity and potential compensatory mechanisms that may occur following DENV-infection in the *in vivo* setting.

Further, the lack of viperin has no effect on the expression of IFN- β and ISGs IFIT1, IRF7, and CXCL10 in mouse brain at end stage-disease or at day 3 pi before the onset of DENV-induced disease. Consistent with our results, similar induction of IFN- β was observed in both IAV-infected

WT and *Vip*^{-/-} mice lungs [298]. Similarly, induction of IFN- β but not IFN- α , and other ISGs including IRF3, IRF7, and ISG15 following sc CHIKV injection in mouse footpad are comparable in WT and *Vip*^{-/-} mice [288]. Additionally, IFN- α/β levels in mice circulation was not affected by the absence of viperin after sc WNV infection in mice footpad [283]. Thus, in contrast to our *in vitro* findings and the previously suggested role for viperin in ISG induction in pDC's [168] these reports and our study all suggest a dispensable role for viperin in modulating host innate IFN responses to viral infections *in vivo*. Interesting, *Ifi2712a* mRNA was significantly increased in the brain of DENV-infected *Vip*^{-/-} mice at the terminal stages of disease compared to WT mice. This potential link between viperin and *Ifi2712a* remains to be investigated.

Previously we demonstrated a marked T-cell infiltration, particularly CD8⁺ but not CD4⁺ cells into DENV-infected mouse brain. Here we show that the absence of viperin has not altered the CD4⁺ and CD8⁺ mRNA levels in mouse brain following DENV infection suggesting no role for viperin in T-cell recruitment to the DENV-infected mouse brain. In agreement with our results, viperin null mice showed similar CD4⁺ and CD8⁺ T-cells accumulation in the brain tissue in response to WNV infection compared to the brain of WT mice [283]. A previous study showed that *Vip*^{-/-} CD4⁺ T-cells has a defect in Th2 cytokine production (IL-4, IL-5, and IL-13), suggested a role for viperin in activation and differentiation of CD4⁺ T-cells [299]. This role of viperin is likely of little consequence here, since CD4⁺ T-cells are not the predominant cell type recruited to the DENV-infected brain.

Our data demonstrated an increase in TNF- α and IL-6 mRNA following DENV infection in the brain. These results are consistent with previous studies that reported higher levels of TNF- α and IL-6 in mouse CNS in response to infection with DENV-2 and DENV-3 intracranially [193,194,284,300]. Further, it has showed that elevated concentrations of TNF- α is associated with severe dengue disease in human [99] and in a mouse model of DENV-2 infection [195]. There is growing evidence of the cross talk between innate IFN-driven and NF- κ B driven pro-inflammatory pathways. In support of this our data demonstrated a marked increase in the mRNA levels of IL-6 in

particular and a tendency towards increased TNF- α in Vip^{-/-} compared to WT mice strains following DENV infection in mouse brain. The interaction between viperin and IL-6 also is an area of future interest.

DENV infection by direct ic injection caused marked damage in the hippocampus region of the brain in both WT and Vip^{-/-} mice strains, which is characterised mainly by loss of neurons and infiltration of immune cells. Similarly, DENV-induced brain damage was also reported by other investigations demonstrating pathological changes in CNS, especially the hippocampus resulting from ic DENV injection [193,284,285]. Since a similar histopathological appearance of the hippocampus was observed in DENV infected WT and Vip^{-/-} brains, this suggests a negligible role for viperin in effecting DENV pathology. Similarly, the absence of viperin did not significantly alter IAV-induced pulmonary damage in a mouse model of infection [298]. In contrast, an increase in macrophage infiltration was observed in the footpads of viperin null mice following sc CHIKV infection [288]. Immunofluorescence staining of CNS tissues following ic WNV infection in mice has shown that viperin is expressed in the neurons of WNV-infected WT brain and adjacent uninfected cells including stimulated leukocytes at the site of WNV infection. In contrast, viperin is co-localised only with WNV-infected neural cells of the WT spinal cord [283]. Although our preliminary data suggests viperin expression in the cells of the brain infected with DENV, our results were inclusive and the staining problematic. Thus, unfortunately, we failed to successfully utilise immunofluorescent staining to define the cell types in the brain infected with DENV and also expressing viperin.

In conclusion, in this study we have reported conflicting roles for viperin during DENV infection, dependent on the model used for experimental analysis. The *in vitro* data suggested a protective role for viperin in controlling DENV infection since absence of viperin enhanced the susceptibility of cells to DENV infection. This model also demonstrated increased IFN production but a discord in the induction of some ISGs implying a role for viperin in promoting specific aspects of this process. However, the *in vivo* findings showed a dispensable anti-viral role for viperin during DENV

challenge in the mouse brain. The overall DENV-induced disease profile, induction of ISGs, infiltration of CD8⁺ T-cells, and activation of inflammatory cytokines were not impacted by the deficiency of viperin in the mouse brain, with the exception of a significant but small increase in mortality rate, induction of Ifi2712a and clear induction of IL-6. Thus, while viperin clearly has the ability to offer anti-viral protection against DENV-infection, the anti-viral role and functions of viperin in regulating other ISGs may be compensated for in the context of *in vivo* infection in the brain. The interesting exceptions of viperin's ability to influence Ifi2712a and IL-6, however warrants further investigation.

CHAPTER 7. GENERAL DISCUSSION

DENV infection is one of the most important mosquito-borne viral diseases of humans especially in tropical and subtropical regions of the world. Infection with DENV can result in mild febrile illness (DF) or may develop to produce severe symptoms of DHF and DSS illnesses. WHO has now classified DENV disease into dengue without/with warning signs and severe dengue [6]. Several factors have been reported to play a role in DENV pathogenesis in humans, but accumulating evidence suggests that the host immune responses against DENV infection contributes to the severe DHF [301]. The SK/S1P signalling pathway is an important regulator for numerous cellular functions including cell development and proliferation, and this pathway is also implicated in a wide variety of diseases including cancer and inflammatory illnesses [302,303]. Further, previous studies, including from our laboratory have demonstrated a role for the enzymes regulating the SK/S1P pathway during viral infections. This background led us to the hypothesis that SK1 and SK2 enzymes would be important during DENV infection. Following outcomes of the initial studies described in this thesis, we further hypothesised that the ISG viperin would have anti-viral roles against DENV *in vivo*, including in the brain, and would also influence other ISG induction.

7.1 The role of SK1 during DENV infection

In chapter 3 of this thesis, we assessed the effect of SK1 on DENV infection *in vitro* using selective SK1 chemical inhibitors. We showed that inhibition of SK activity prior to DENV infection reduced DENV infectious virus release and this reduction was mediated by SK1 since SKi treatment inhibits SK1 but not SK2 activity and similar findings were observed with the SK1 specific inhibitor, SK1-I. This finding is consistent with previous studies that have demonstrated that a reduction in SK1 activity inhibits viral infection *in vitro* [206]. We also showed that DENV infection stimulates IFN- β , ISGs and TNF- α responses but the ability to induce these factors is lower in cells pre-treated before DENV infection with a SK1 specific inhibitor.

Although there are no animal models that are ideal for investigating DENV pathogenesis [184], in this study we utilised a reliable animal model of direct ic injection in immunocompetent mice to study DENV infection and the effect of the lack of SK1 or SK2 on DENV infection *in vivo*. We demonstrated that DENV infection in the mouse brain induces neurovirulence symptoms that are positively correlated with higher DENV RNA levels similar to previous reports of DENV infection in the mouse brain [194,284,285]. Additionally, we show that DENV infection in mouse brain induces the transcription of IFN- β , ISGs and CD8⁺ T-cell infiltration. Unlike the effect of SK1 on DENV infection and ISGs *in vitro*, the genetic absence of SK1 does not affect DENV replication, IFN- β and ISGs levels or CD8⁺ T-cell infiltration in mouse brain. Additionally, DENV infection or the absence of SK1 in mouse brain did not change the SK1, SK2 and S1P levels indicating that SK1/S1P axis has no effect on DENV replication (chapter 4). These results are summarised in Figure 7.1A and D. Thus, our *in vitro* results did not correlate with *in vivo* results, which may be due to brain specific responses or compensatory functions *in vivo*. Since SK2 has been shown to have an important role for CHIKV infection, and SK2 is more prominent in mouse brain than SK1, this lead us to investigate the role of SK2 during DENV infection in both *in vitro* and *in vivo* systems.

7.2 The role of SK2 during DENV infection

Previous studies have suggested a significant role of SK2 for viral infections *in vitro* and our data above with SK1 in the brain did not correlate with *in vitro* outcomes and thus we sought to assess the role of SK2 *in vitro* and *in vivo* (chapter 5). Our results showed that the genetic absence of SK2 in iMEFs dramatically inhibited DENV infection similar to our laboratory results of a reduction of DENV infection in SK1^{-/-} MEFs [167], and most likely related to increased basal levels of antiviral ISGs that we believe are an artefact of the iMEF system. In contrast, while chemical inhibition of SK1 activity inhibited DENV infection, inhibition of SK2 activity had no effect on DENV infection *in vitro* (chapter 5, section 5.2.1) (Figure 7.1B). Even though our data did not demonstrate an

indispensable role for SK2 during DENV infection, since a pro-inflammatory role of SK2 has recently reported a potential function for SK2 against DENV induced inflammation may exist [275]. Targeting SK2 activity using ABC inhibitor has numerous potential therapeutic properties against a diverse range of illnesses *in vivo* including solid tumours and inflammatory diseases [211]. Our data however, suggest that treatment with this drug and potentially other SK2 inhibitors does not influence DENV replication and these compounds are not likely to be therapeutically useful. These findings are contrary to a previous report that demonstrated a significant role of SK2 against another mosquito-borne virus infection, CHIKV [236]. Using genetic SK2 null mice and DENV infection by ic route, our results showed that SK2 does not alter DENV replication in the mouse brain (chapter 5, section 5.2.2). Of note, the lack of SK2 in the mouse brain reduced the amounts of S1P without any compensatory change in SK1. Thus, in relation to DENV infection, both the lack of SK2 and subsequent reduction in S1P has no effect on DENV replication in the brain. Additionally, while S1P has been observed to modulate T-cell migration in some contexts [261], the low levels of S1P in SK2 null mice does not affect the infiltration of T-cells to the DENV infected mouse brain, as summarised in Figure 7.1E.

Throughout the studies in chapters 3-5, we consistently detected a significant induction of viperin, a factor we had previously shown to have anti-DENV effects [156] following DENV infection. Further, a publication arising during the course of this PhD study demonstrated the importance of viperin in particular regions of the brain in protecting against WNV infection [283]. Based on this, we utilised the techniques established in chapters 3-5 to investigate the role of viperin against DENV further.

7.3 The role of viperin against DENV infection

In response to an invading viral pathogen, PRRs rapidly stimulate the production of type I IFN and ISGs to control infection and prevent further infection spreading. In the context of DENV infection, we have shown in this thesis that viperin is one of such ISGs that is highly induced early following

DENV infection both *in vitro* and *in vivo*. Numerous studies have reported a crucial role for viperin in restricting viral infections *in vitro*. In the case of DENV infection, previous data from our laboratory has demonstrated that viperin shows antiviral activity against DENV infection *in vitro* [156]. These data support our hypothesis that viperin could inhibit DENV infection *in vivo*. In the chapter 6 of this thesis, we show that the lack of viperin in primary murine cells increased DENV infection, and that this correlated with a high-level induction of IFN- β but modest induction of other ISGs (Figure 7.1C). While DENV infection in the brain of viperin null mice enhanced the mortality rate of these mice compared to WT, viperin deficiency did not exacerbate weight loss and had no major overall effect on DENV infection following challenge by the ic route. Additionally, viperin had no role in the induction of IFN- β and ISGs following DENV infection in the brain. While DENV infection in the mouse brain induced the transcription of inflammatory mediators (TNF- α and IL-6), viperin deficiency did not affect induction of these factors in response to DENV infection. We also showed that the lack of viperin has no influence on T-cell infiltration and on morphological changes induced by DENV infection in mouse brain (Figure 7.1F). Thus, our data demonstrate that even though viperin has a significant effect on DENV infection in 1^oMEFs and in other *in vitro* systems [156], this factor has a dispensable role during DENV infection in the mouse brain.

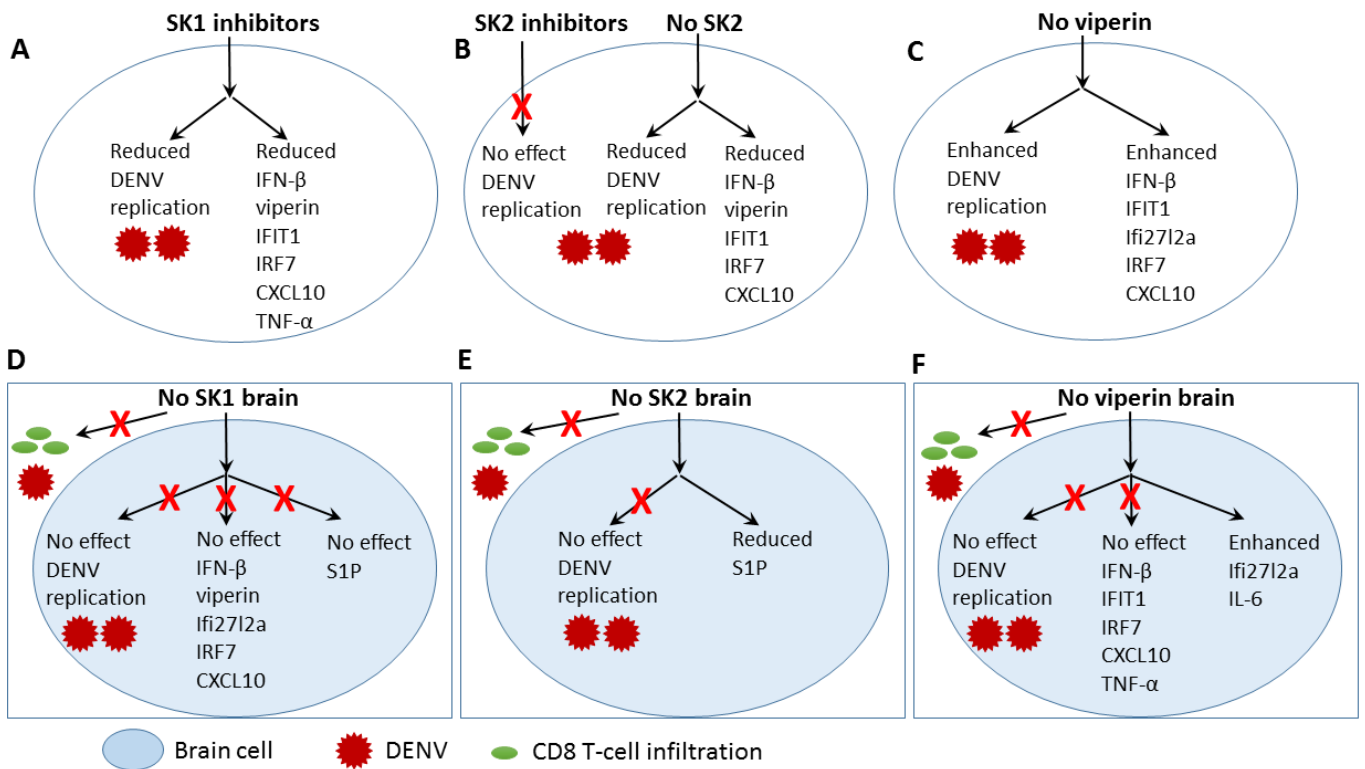


Figure 7. 1 Summary of the effect of SK1, SK2, and viperin during DENV infection

Inhibition of SK1 *in vitro* reduced both DENV infection and DENV-induced IFN- β , viperin, IFIT1, IRF7, CXCL10 and TNF- α responses (A). While *in vitro* SK2 inhibition had no effect on DENV replication, the lack of SK2 in iMEFs reduced DENV replication and induction of IFN- β , viperin, IFIT1, IRF7, CXCL10 following DENV infection (B). The lack of viperin in 1^oMEFs enhanced DENV infection and IFN- β , IFIT1, Ifi2712a, IRF7, and CXCL10 levels in response to DENV infection (C). Lack of SK1 (D) and SK2 (E) in mouse brain had no effect on DENV replication, and induction of IFN- β , viperin, Ifi2712a, IRF7, and CXCL10; and CD8⁺ T cell infiltration were not affected by the lack of SK1 in the mouse brain. While the lack of SK1 had no effect on S1P level (D), the absence of SK2 decreased S1P level (E). F. Lack of viperin did not affect DENV replication and induction of IFN- β , IFIT1, IRF7, CXCL10, and TNF- α but increased Ifi2712a and IL-6 induction following DENV infection. The red cross indicates no effect.

7.4 Future directions

Our data suggests that changes in SK1 can influence DENV infection and replication in some contexts. Additionally, IAV, measles virus and DENV itself have been shown to induce an activation of NF- κ B signalling pathways following viral replication [230,304,305]. Since SK1 and S1P have been reported to associate with the TNF- α receptor associated factor 2 (TRAF2) and enhance TNF- α -induced NF- κ B activation [306], and chemical inhibition of SK1 activity suppressed of NF- κ B signalling and subsequently reduced IAV and measles virus infections [229,230], the effect of SK1 on DENV-induced NF- κ B activation might be of interest. We have previously demonstrated an association of reduced SK1 activity late in DENV infection with inability to activate NF- κ B [232] but have not investigated the link between SK1 activity and NF- κ B early in DENV infection. Experiments could be performed to assess the effect of chemical inhibition of SK1 activity prior to DENV infection on activation of NF- κ B during the early time of DENV infection by analysis the effect of SK1 specific inhibitors on the phosphorylation of p65 NF- κ B subunits and an upstream NF- κ B signalling molecule, I κ B kinase complex (IKK α/β) by Western blot analysis. The effect of targeting SK1 and SK2 activity prior to DENV infection *in vitro* was detected by using specific SK1 and SK2 chemical inhibitors, and thus it would be of interest to use siRNA-specific mediated SK1 and SK2 knockdown during DENV infection to further confirm our *in vitro* results.

We observed here that the SK/S1P signalling pathway has no major role on DENV infection *in vivo* using immunocompetent WT mouse that lack either SK1 or SK2, with the latter also associated with low S1P levels in the brain. To further support this, DENV infection could be performed in the brain of mouse lacking of one of the S1P receptors (S1PRs). For instance, DENV infection in mice lacking S1PR1 [307] would be of interest to confirm the role of S1P signalling during DENV infection *in vivo*, since S1PR1 signalling has suggested to be important for IAV infection in BALB/c mice [308]. Additionally, administration of specific SK1 or 2 chemical inhibitors to mice

during DENV infection, instead of the use of SK genetic knockouts, may be utilised as an experimental tool to both confirm our results and test the potential therapeutic value of these compounds against DENV infection. The prior literature has shown that treatment of C57BL/6 mice with sphingosine analogue, AAL-R, reduced cytokines storm during IAV infection [309].

Treatment with another sphingosine analogue, FTY720, in BALB/c mice infected with HSV inhibited HSV-induced ocular lesions associated with diminished CD4⁺ T-cell infiltration [310].

Manipulating the SK/S1P pathway by administration with sphingosine analogues such as AAL-R and FTY720 that antagonise S1PRs to mice might thus be of particular interest to assess the effect of these agents against DENV infection *in vivo*. Furthermore, it could be possible to use the AG129 mouse that is deficient in IFN- α/β and γ receptors, as another ic DENV infection model to investigate whether the lack IFNs signalling can exacerbate DENV infection in mouse brain.

We analysed the infiltration of T-lymphocyte into DENV-infected mouse brain through detecting the mRNA levels of CD4⁺ and CD8⁺ T-cells. The possibility of using an alternative method to investigate the recruitment of T-cells into DENV infected brain tissues including flow cytometry that gives functional insights into numbers and phenotypes of infiltrating cells is warranted.

The lack of the ISGs viperin in BMDMs and BMDCs cells has been shown to increase WNV infection and viperin has been demonstrated to control WNV infection in subsets of primary cells, ie in myeloid cells but not in fibroblasts [283]. Here, we report that the lack of viperin in MEFs enhanced DENV replication. Throughout this PhD study, we attempted to generate BMDM from WT and viperin null mice and infect these with DENV. Unfortunately, this faced technical issues and in future studies the culture of these cells for *in vitro* infections could be pursued further. Thus, future work using other primary cells either BMDMs and/or BMDCs could be beneficial to confirm our findings since viperin has been demonstrated to control WNV infection in subsets of primary cells, ie in myeloid cells but not in fibroblasts. Further, WNV infection has shown to be prominent in mouse brain neurons that were positive for viperin and viperin has restricted WNV in a cell-specific manner in mouse brain tissue [283]. In chapter 6, we attempted to identify DENV infection

and viperin expression in mouse brain tissue using IF staining and fluorescent microscopy. While this yielded some preliminary data, it was not convincing and again hampered by technical issues. Further experiments could be undertaken to improve this including IF staining for DENV and viperin at the site of DENV injection (ipsilateral) and improving the IF staining procedure such as time of tissue fixation, antigen retrieval and blocking that could influence the outcomes of IF staining. The possibility to define this in the future may provide a better understanding the DENV infection and the role of viperin in mouse brain.

We have utilised the ic DENV mouse infection model here with mice with three different types of genetic deficiency. In none of these cases did we see any major difference in replication of DENV in the brain, which contrasted to our *in vitro* results. While we chose this infection model as it represents an *in vivo* situation with an intact IFN response, it is possible that this model is highly susceptible to DENV infection and not a sensitive model to assess changes in factors that may have smaller effects on replication or could be compensated by other factors in the complexity of the brain. Alternative immunocompetent *in vivo* models for DENV replication are not readily available. Although WT mice are not susceptible to systemic DENV challenge, in the future we could consider systemic challenge with DENV in viperin^{-/-} mice, where we expect replication may be increased.

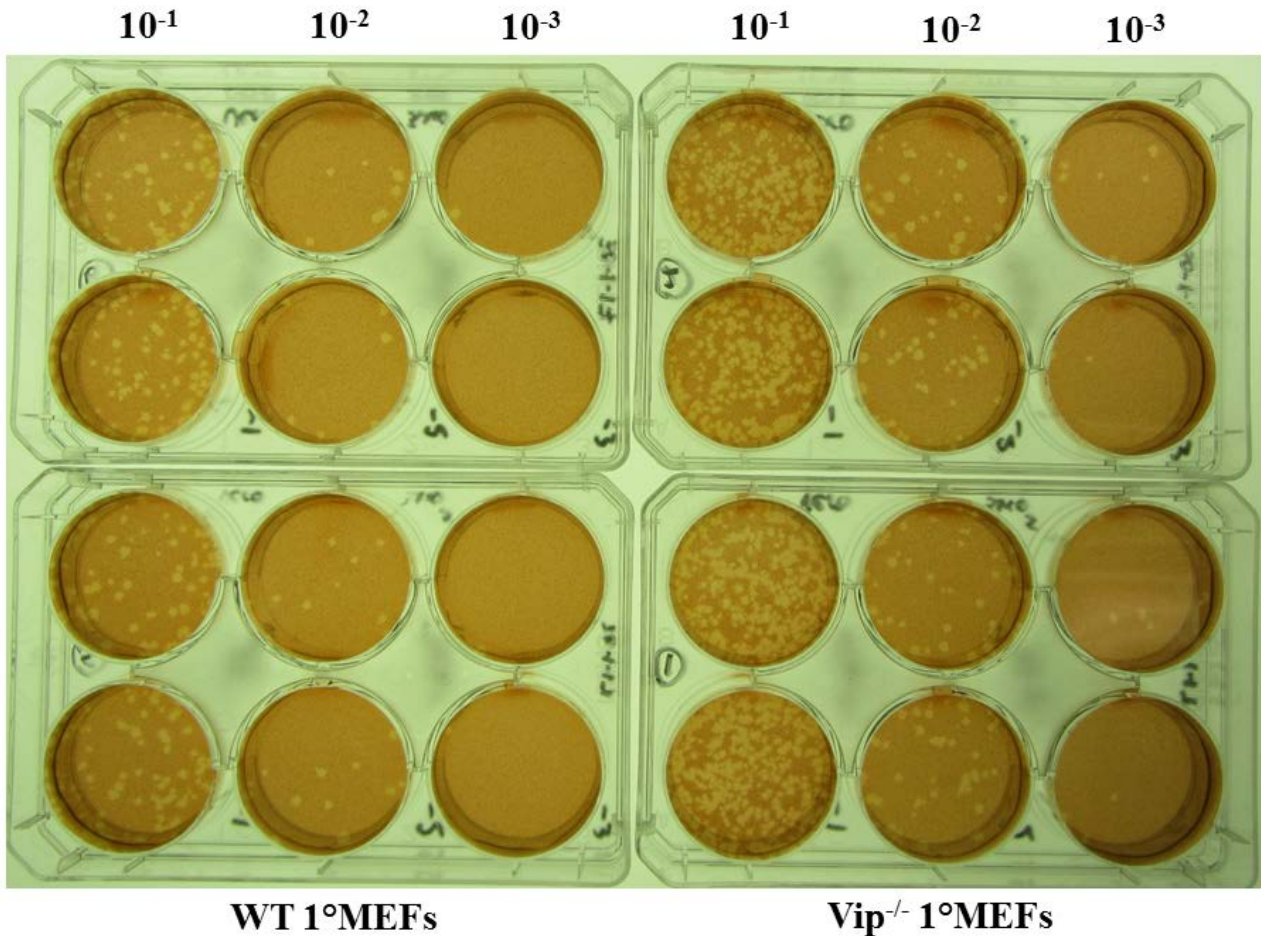
A novel finding from this thesis is the observation that the ISGs Ifi2712a is highly induced during DENV infection and induced significantly higher in the brain of viperin null mice. Ifi2712a is a relatively under-studied ISG and these results suggest that further and investigation of this factor might be a great value to define the role of ISGs against DENV infection and in particular, the interaction of Ifi2712a with viperin. Studies could include knockdown of Ifi2712a by treatment with specific siRNA molecule or blocking of Ifi2712a response by treatment with specific anti-Ifi2712a antibody to assess the effect of this ISG on DENV infection *in vitro*. Generation of mice with genetic deletion of Ifi2712a is another way to investigate the effect of the lack of Ifi2712a on DENV infection *in vivo* via ic route, as previously reported with WNV ic infection in the brain of this mice

strain [297]. The high levels of Ifi2712a and IL-6 following DENV infection in mice that lack viperin *in vivo* may require further investigations. This could include for example, knockdown of viperin *in vitro* using known cells expressing viperin shRNA (eg Huh7 cells as generated by Dr Nicholas Eyre [unpublished]) or using lentivirus mediated shRNA knockdown of viperin, as we have previously published [166], and measure the mRNA levels of IL-6 and Ifi2712a by RT-PCR to assess whether the viperin knockdown *in vitro* also would enhance induction of these factors following DENV infection *in vitro*.

7.5 Conclusion

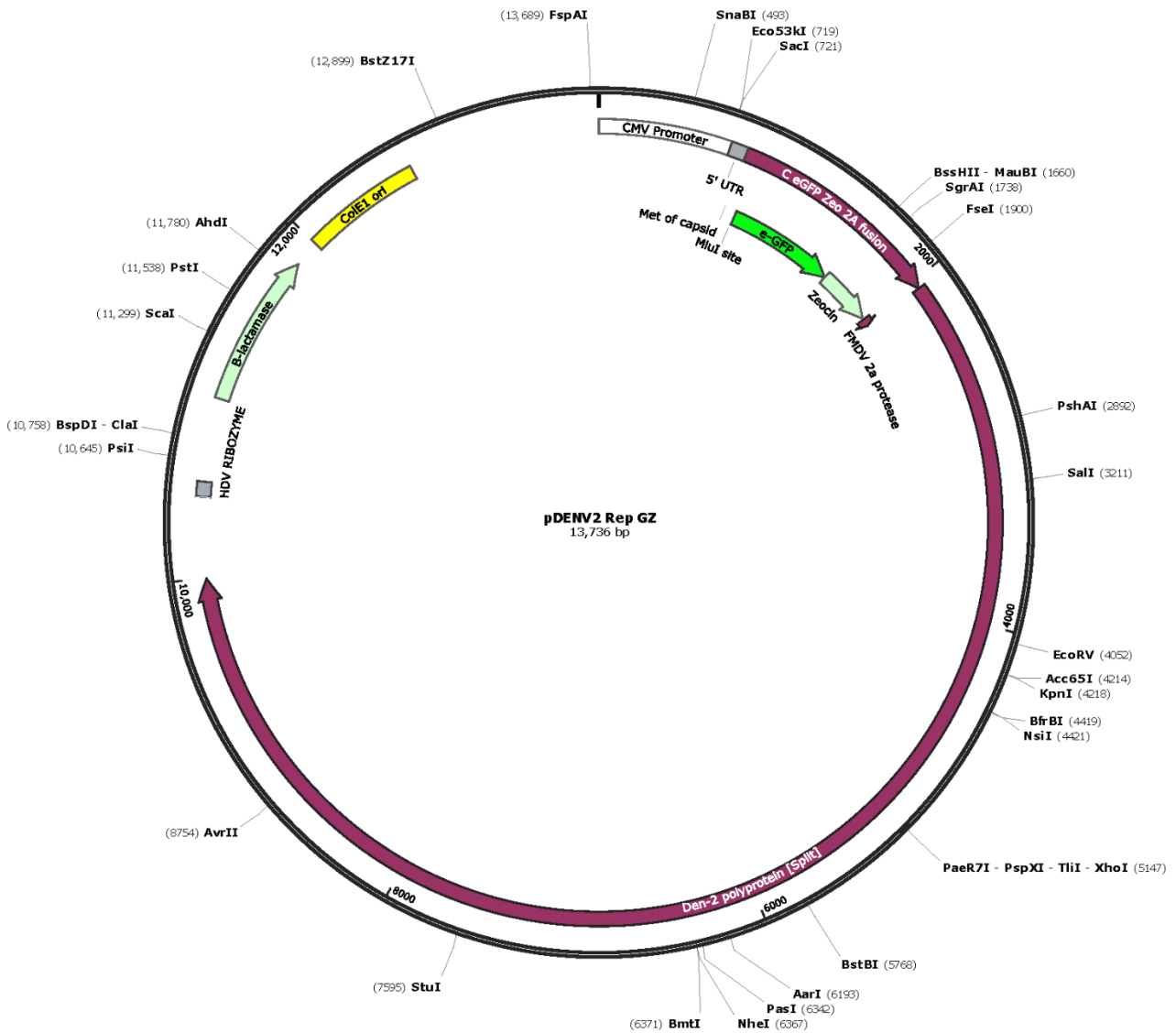
In this study, we have shown that the chemical inhibition of SK1 activity prior to DENV infection decreased DENV infection and downregulated the induction of innate responses against DENV *in vitro*. A genetic deletion of SK1 however had no major influence on DENV infection and DENV-induced immune responses in the *in vivo* setting. In contrast to the results with SK1, neither the inhibition of SK2 activity prior to DENV infection *in vitro* nor the genetic absence of SK2 *in vivo* had an effect on DENV infection or DENV-induced immune responses. Thus, the host factor SK1 but not SK2 is more likely to have a role either directly or indirectly for DENV infection. In terms of the role of viperin during DENV infection, viperin did confer protection against DENV infection *in vitro*. The viperin deficiency however did not enhance DENV replication or exacerbate DENV-induced disease in mouse brain. The lack of the effect of the viperin deficiency on DENV infection *in vivo* could be compensated by other ISGs such as Ifi2712a and/or cytokines such as IL-6 since both of these factors were highly induced in DENV-infected viperin null mice. Thus, outcomes from this thesis have advanced our understanding of host-cell responses to DENV infection and defined a foundation for further investigation of drugs or targets that may manipulate the SK/S1P axis and act as anti-viral or anti-inflammatory agents. Additionally, we have extended our knowledge of the antiviral roles of viperin and linked viperin to induction of other potential anti-viral and inflammatory responses such as IL6 and Ifi2712a during DENV-infection.

APPENDICES



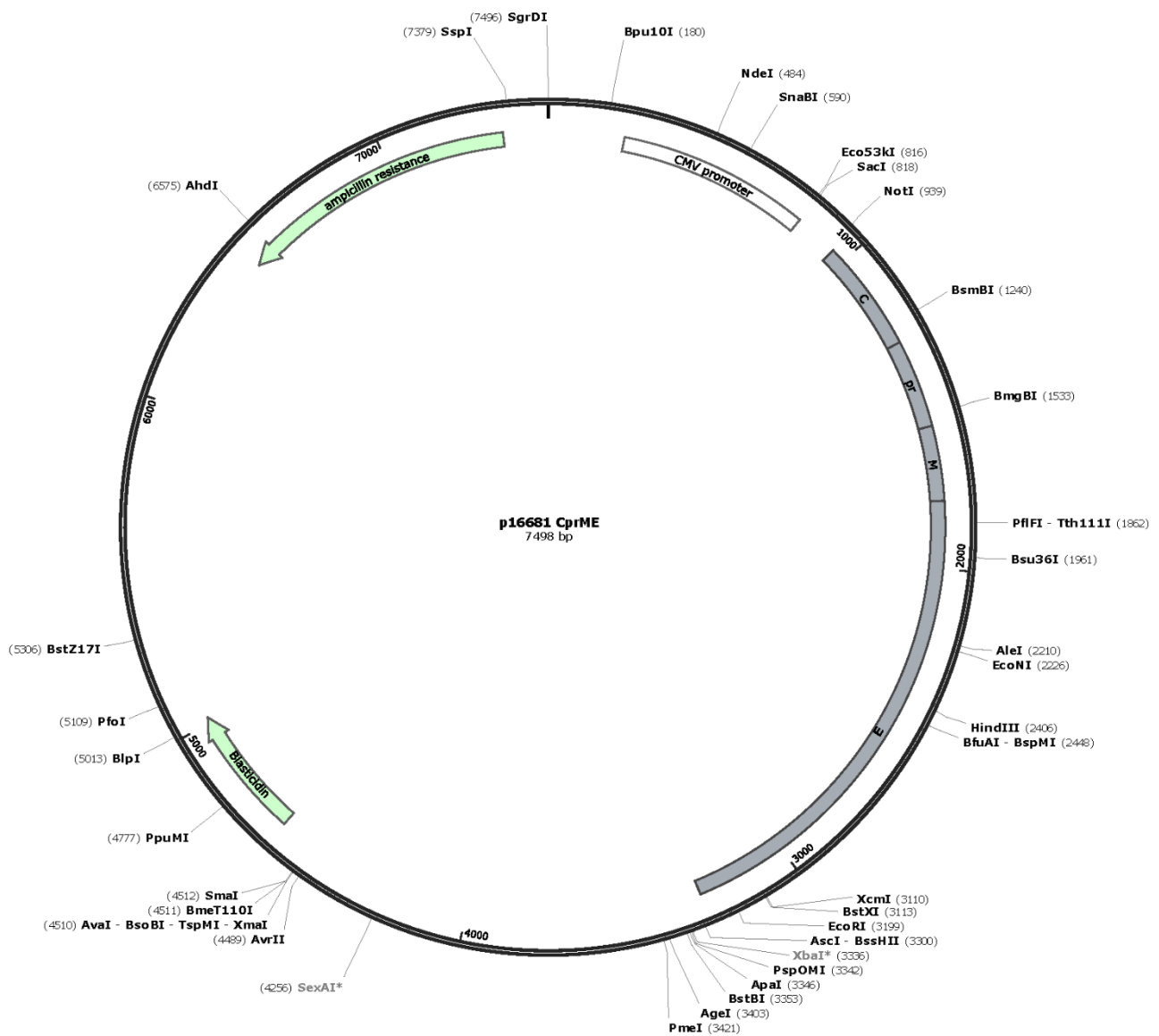
Appendix 1. A representative plaque assay result

Infectious S/Ns were serially diluted in a serum-free DMEM and cells infected in a volume of 300 μ l/well. Following infection, plates were overlaid with a SeaKem agarose, 2X DMEM and 10% FBS and then incubated until plaques become visible. Visible plaques were counted and used to calculate PFU/ml of virus from the original sample. The samples are in duplicate.



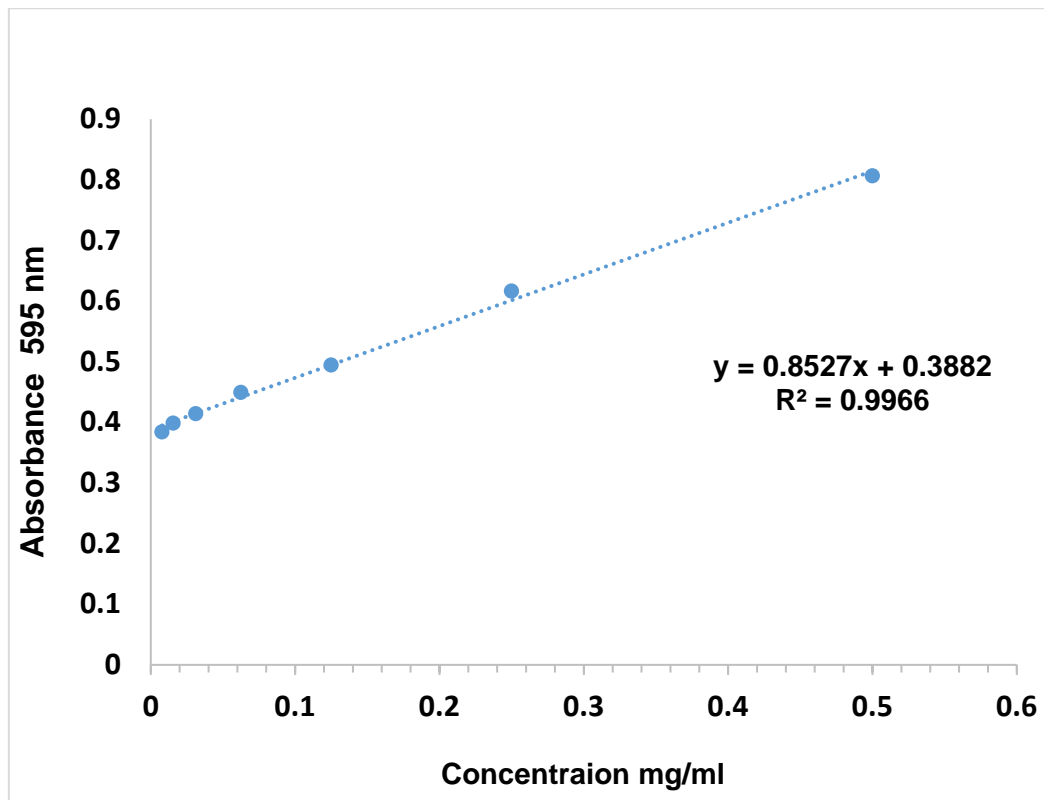
Appendix 2A. A map of pDENV-2 Rep GZ (pREP) vector

A DENV subgenomic replicon containing the DENV 5' and 3'UTR and NS1-5 coding sequence but with GFP and a zeocin selection marker in placed of the DENV C, prM, and E genes. This map was provided by Prof Theodore C Pierson (National Institutes of Health (NIH), Bethesda, Maryland, USA).



Appendix 2B. A map of p16681 DENV-2 strain vector

Vector expressing the C-prM-E genes from DENV-2 strain 16681 under control of the CMV promoter with blasticidin selection marker. This map was provided by Prof Theodore C Pierson (NIH, Bethesda, Maryland, USA).

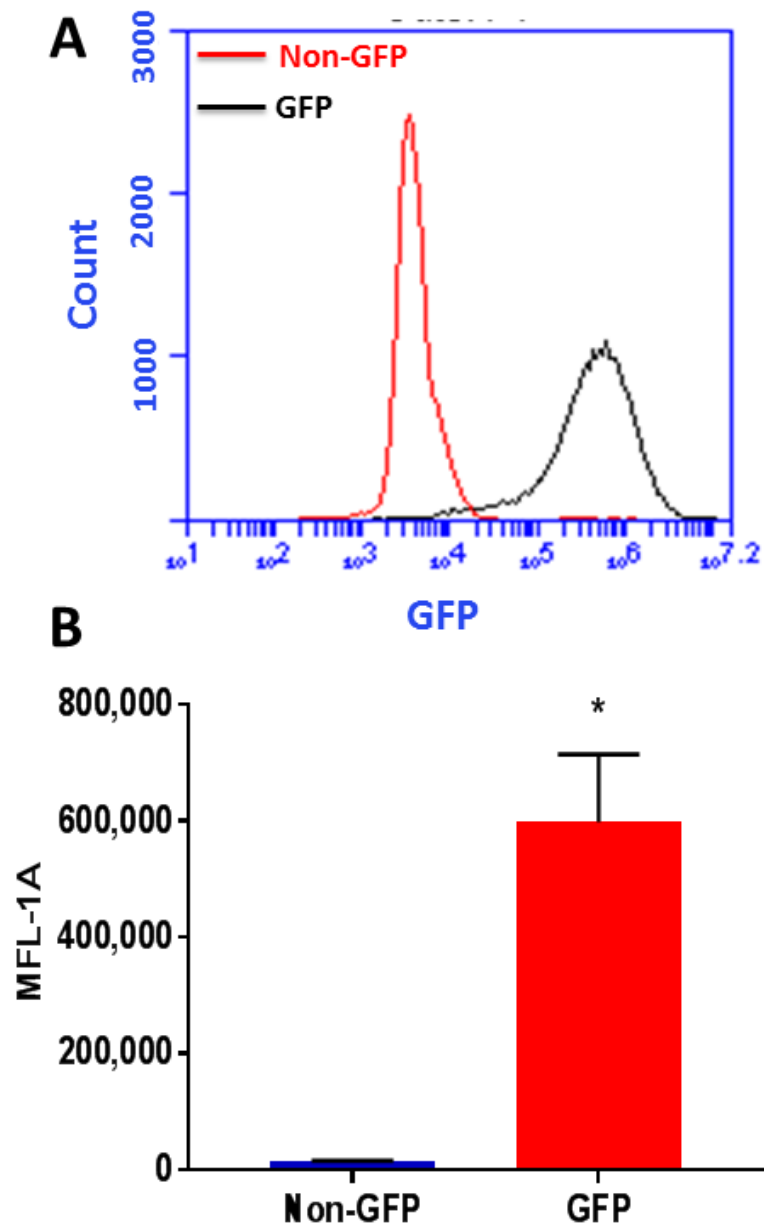


Appendix 3. A representative of BSA standard curve for protein quantification

A protein concentration was determined by protein assay as described in chapter 2 section 2.2.10. If the absorbance of a target mouse protein sample, for instance, is 0.7840, the equation:

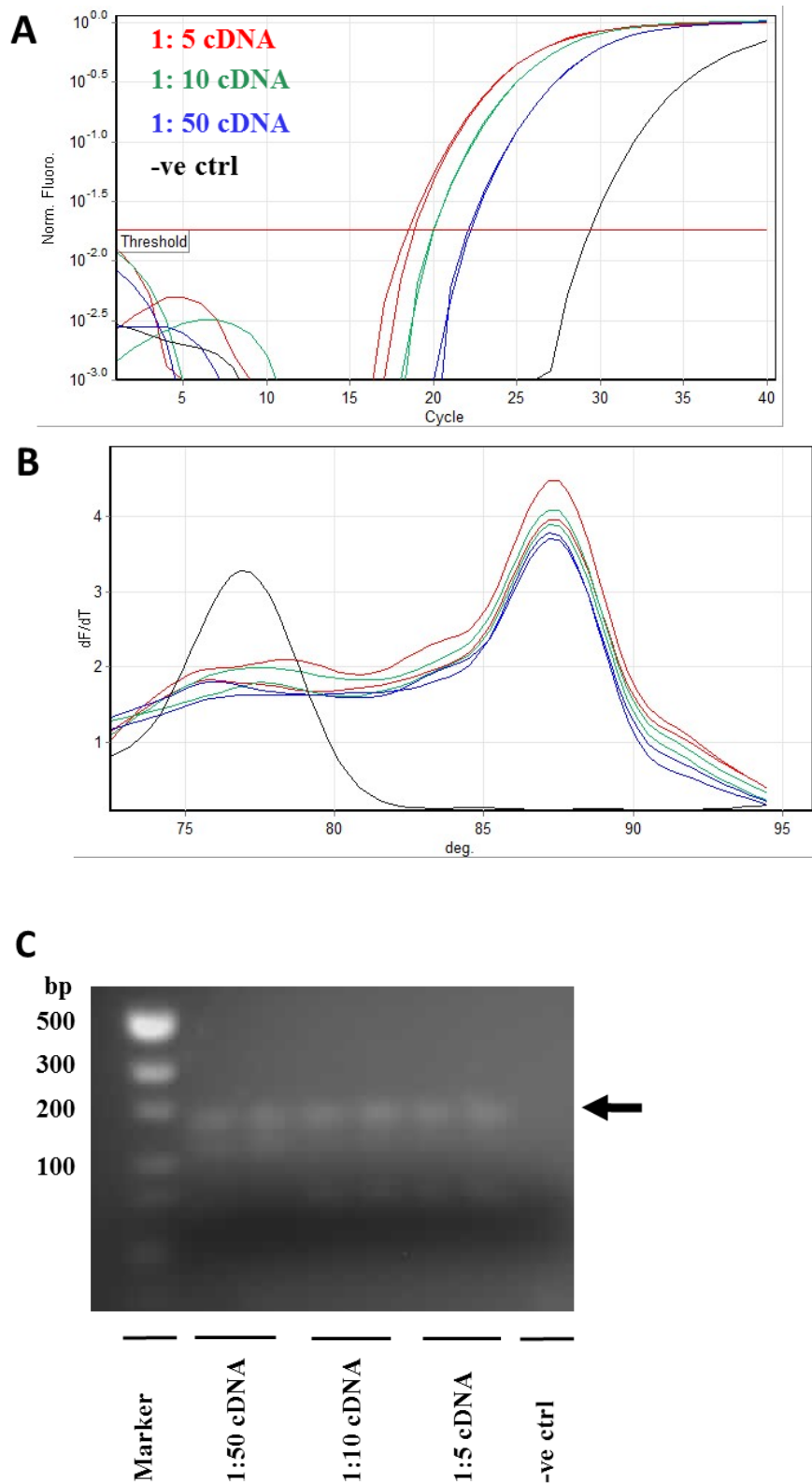
$$0.7840 = 0.8527x + 0.3882$$

X=0.4641 mg/ml, and times by 100 (the dilution factor) gives 46.41 mg/ml



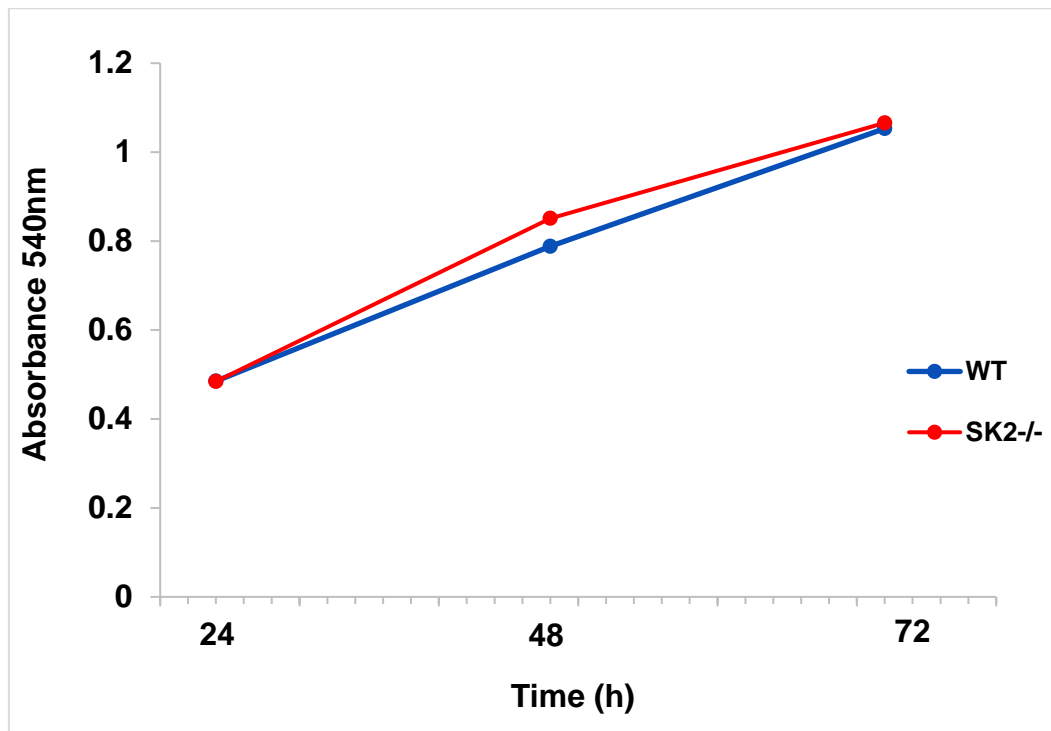
Appendix 4. Expression of a GFP in HEK293 cells

Non-GFP and GFP cells were fixed in 4% PFA O/N prior to flow cytometry. **(A)** Histograms showing profile difference in GFP intensity. **(B)** MFI of GFP as in A. Results represent mean \pm SD of n=2 assay replicates. Statistical significance was determined by un-paired student *t*-test. * $p < 0.05$.



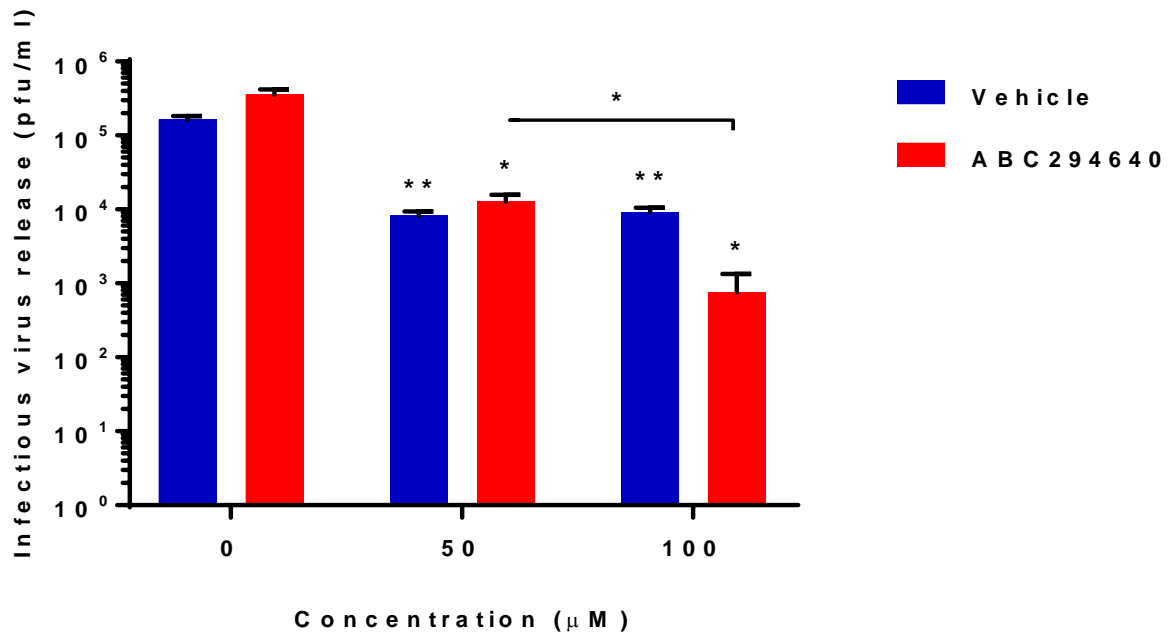
Appendix 5. Validation of a RT-PCR for human IRF7

A cDNA template was diluted 1:5, 1:10, 1:50 and subjected to RT-PCR. (A) Amplification curve. (B) Melt curve. (C) Agarose gel electrophoresis of RT-PCR products where the arrow represents the expected size of the human IRF7 of 158 bp.



Appendix 6. Growth rate analysis of WT and SK2^{-/-} iMEFs

WT and SK2^{-/-} iMEFs were seeded at a density of 5×10^3 , and growth rate was determined by cell viability assay as described in chapter 2 section 2.2.2.



Appendix 7. Pre-treatment with ABC O/N is toxic to HEK293 cells

HEK293 cells were pre-treated with 0, 50, and 100 µM ABC O/N before DENV infection. Cells were DENV infected at MOI of 1 and S/N harvested. Viral release was measured by plaque assay. Results represent mean ± SD of n=2 assay replicates. Statistical significance was determined by unpaired student *t*-test to 0-µM concentration. * $p < 0.05$, ** $p < 0.005$.

REFERENCES

1. Simmonds P, Becher P, Bukh J, Gould EA, Meyers G, Monath T, et al. (2017) ICTV Virus Taxonomy Profile: Flaviviridae. *J Gen Virol* 98: 2-3.
2. Guzman MG, Harris E (2015) Dengue. *Lancet* 385: 453-465.
3. Gibbons RV (2010) Dengue conundrums. *Int J Antimicrob Agents* 36 Suppl 1: S36-39.
4. Simmons CP, Farrar JJ, Nguyen v V, Wills B (2012) Dengue. *N Engl J Med* 366: 1423-1432.
5. Halstead SB (2007) Dengue. *Lancet* 370: 1644-1652.
6. WHO (2009) Dengue: Guidelines for Diagnosis, Treatment, Prevention and Control. Geneva: World Health Organization.
7. Noble CG, Chen YL, Dong H, Gu F, Lim SP, Schul W, et al. (2010) Strategies for development of Dengue virus inhibitors. *Antiviral Res* 85: 450-462.
8. Gubler DJ (1998) Dengue and dengue hemorrhagic fever. *Clin Microbiol Rev* 11: 480-496.
9. Guzman A, Isturiz RE (2010) Update on the global spread of dengue. *Int J Antimicrob Agents* 36 Suppl 1: S40-42.
10. Monath TP (1994) Dengue: the risk to developed and developing countries. *Proc Natl Acad Sci U S A* 91: 2395-2400.
11. Gubler DJ (2011) Dengue, Urbanization and Globalization: The Unholy Trinity of the 21(st) Century. *Trop Med Health* 39: 3-11.
12. Kumar SR, Patil JA, Cecilia D, Cherian SS, Barde PV, Walimbe AM, et al. (2010) Evolution, dispersal and replacement of American genotype dengue type 2 viruses in India (1956-2005): selection pressure and molecular clock analyses. *J Gen Virol* 91: 707-720.
13. Halstead SB (1980) Dengue haemorrhagic fever--a public health problem and a field for research. *Bull World Health Organ* 58: 1-21.
14. Gubler DJ (2002) The global emergence/resurgence of arboviral diseases as public health problems. *Arch Med Res* 33: 330-342.
15. Shepard DS, Coudeville L, Halasa YA, Zambrano B, Dayan GH (2011) Economic impact of dengue illness in the Americas. *Am J Trop Med Hyg* 84: 200-207.
16. Holmes EC, Twiddy SS (2003) The origin, emergence and evolutionary genetics of dengue virus. *Infect Genet Evol* 3: 19-28.
17. Shepard DS, Undurraga EA, Halasa YA (2013) Economic and disease burden of dengue in Southeast Asia. *PLoS Negl Trop Dis* 7: e2055.
18. WHO (2012) Global strategy for dengue prevention and control, 2012-2020. Geneva: World Health Organization.
19. Bhatt S, Gething PW, Brady OJ, Messina JP, Farlow AW, Moyes CL, et al. (2013) The global distribution and burden of dengue. *Nature* 496: 504-507.
20. Ferreira GL (2012) Global dengue epidemiology trends. *Rev Inst Med Trop Sao Paulo* 54 Suppl 18: S5-6.
21. Murray NE, Quam MB, Wilder-Smith A (2013) Epidemiology of dengue: past, present and future prospects. *Clin Epidemiol* 5: 299-309.
22. WHO (2011) Dengue, countries or areas at risk, 2011. Geneva, World Health Organization,
23. Gibbons RV, Vaughn DW (2002) Dengue: an escalating problem. *Bmj* 324: 1563-1566.
24. Back AT, Lundkvist A (2013) Dengue viruses - an overview. *Infect Ecol Epidemiol* 3.
25. Weaver SC, Vasilakis N (2009) Molecular evolution of dengue viruses: contributions of phylogenetics to understanding the history and epidemiology of the preeminent arboviral disease. *Infect Genet Evol* 9: 523-540.
26. Carrington LB, Simmons CP (2014) Human to mosquito transmission of dengue viruses. *Front Immunol* 5: 290.
27. Viennet E, Ritchie SA, Faddy HM, Williams CR, Harley D (2014) Epidemiology of dengue in a

- high-income country: a case study in Queensland, Australia. *Parasites and Vectors* 7: 379.
28. Knope KE, Kurucz N, Doggett SL, Muller M, Johansen CA, Feldman R, et al. (2016) Arboviral diseases and malaria in Australia, 2012-13: Annual report of the National Arbovirus and Malaria Advisory Committee. *Commun Dis Intell Q Rep* 40: E17-47.
 29. Viennet E, Ritchie SA, Williams CR, Faddy HM, Harley D (2016) Public Health Responses to and Challenges for the Control of Dengue Transmission in High-Income Countries: Four Case Studies. *PLoS Negl Trop Dis* 10: e0004943.
 30. Ritchie SA, Pyke AT, Hall-Mendelin S, Day A, Mores CN, Christofferson RC, et al. (2013) An explosive epidemic of DENV-3 in Cairns, Australia. *PLoS One* 8: e68137.
 31. Mukhopadhyay S, Kuhn RJ, Rossmann MG (2005) A structural perspective of the flavivirus life cycle. *Nat Rev Microbiol* 3: 13-22.
 32. Lindenbach B, Thiel H-J, Rice C (2007) Flaviviridae: the viruses and their replication In Knipe DM HP, Griffin DE, Lamb RA, Martin MA, Roizman B, Straus SE (ed), editor. Philadelphia, PA: Lippincott-Raven Publishers. 1101-1152 p.
 33. Acosta EG, Castilla V, Damonte EB (2009) Alternative infectious entry pathways for dengue virus serotypes into mammalian cells. *Cell Microbiol* 11: 1533-1549.
 34. Holbrook MR (2017) Historical Perspectives on Flavivirus Research. *Viruses* 9: e97.
 35. Guzman MG, Halstead SB, Artsob H, Buchy P, Farrar J, Gubler DJ, et al. (2010) Dengue: a continuing global threat. *Nat Rev Microbiol* 8: S7-16.
 36. Acosta EG, Kumar A, Bartenschlager R (2014) Revisiting dengue virus-host cell interaction: new insights into molecular and cellular virology. *Adv Virus Res* 88: 1-109.
 37. Clyde K, Kyle JL, Harris E (2006) Recent advances in deciphering viral and host determinants of dengue virus replication and pathogenesis. *J Virol* 80: 11418-11431.
 38. Kuhn RJ, Zhang W, Rossmann MG, Pletnev SV, Corver J, Lenches E, et al. (2002) Structure of dengue virus: implications for flavivirus organization, maturation, and fusion. *Cell* 108: 717-725.
 39. Zhang Y, Corver J, Chipman PR, Zhang W, Pletnev SV, Sedlak D, et al. (2003) Structures of immature flavivirus particles. *Embo j* 22: 2604-2613.
 40. Zhang X, Sheng J, Plevka P, Kuhn RJ, Diamond MS, Rossmann MG (2013) Dengue structure differs at the temperatures of its human and mosquito hosts. *Proc Natl Acad Sci U S A* 110: 6795-6799.
 41. Fibriansah G, Ng TS, Kostyuchenko VA, Lee J, Lee S, Wang J, et al. (2013) Structural changes in dengue virus when exposed to a temperature of 37 degrees C. *J Virol* 87: 7585-7592.
 42. Ma L, Jones CT, Groesch TD, Kuhn RJ, Post CB (2004) Solution structure of dengue virus capsid protein reveals another fold. *Proc Natl Acad Sci U S A* 101: 3414-3419.
 43. Jones CT, Ma L, Burgner JW, Groesch TD, Post CB, Kuhn RJ (2003) Flavivirus capsid is a dimeric alpha-helical protein. *J Virol* 77: 7143-7149.
 44. Morrison J, Garcia-Sastre A (2014) STAT2 signaling and dengue virus infection. *JAKSTAT* 3: e27715.
 45. Zhang W, Chipman PR, Corver J, Johnson PR, Zhang Y, Mukhopadhyay S, et al. (2003) Visualization of membrane protein domains by cryo-electron microscopy of dengue virus. *Nat Struct Biol* 10: 907-912.
 46. Hsieh SC, Zou G, Tsai WY, Qing M, Chang GJ, Shi PY, et al. (2011) The C-terminal helical domain of dengue virus precursor membrane protein is involved in virus assembly and entry. *Virology* 410: 170-180.
 47. Modis Y, Ogata S, Clements D, Harrison SC (2004) Structure of the dengue virus envelope protein after membrane fusion. *Nature* 427: 313-319.
 48. Lin SR, Zou G, Hsieh SC, Qing M, Tsai WY, Shi PY, et al. (2011) The helical domains of the stem region of dengue virus envelope protein are involved in both virus assembly and entry. *J Virol* 85: 5159-5171.
 49. Murphy BR, Whitehead SS (2011) Immune response to dengue virus and prospects for a vaccine. *Annu Rev Immunol* 29: 587-619.

50. Amorim JH, Alves RP, Boscardin SB, Ferreira LC (2014) The dengue virus non-structural 1 protein: Risks and benefits. *Virus Res* 181: 53-60.
51. Muller DA, Landsberg MJ, Bletchly C, Rothnagel R, Waddington L, Hankamer B, et al. (2012) Structure of the dengue virus glycoprotein non-structural protein 1 by electron microscopy and single-particle analysis. *J Gen Virol* 93: 771-779.
52. Muller DA, Young PR (2013) The flavivirus NS1 protein: molecular and structural biology, immunology, role in pathogenesis and application as a diagnostic biomarker. *Antiviral Res* 98: 192-208.
53. Welsch S, Miller S, Romero-Brey I, Merz A, Bleck CK, Walther P, et al. (2009) Composition and three-dimensional architecture of the dengue virus replication and assembly sites. *Cell Host Microbe* 5: 365-375.
54. Alcon S, Talarmin A, Debruyne M, Falconar A, Deubel V, Flamand M (2002) Enzyme-linked immunosorbent assay specific to Dengue virus type 1 nonstructural protein NS1 reveals circulation of the antigen in the blood during the acute phase of disease in patients experiencing primary or secondary infections. *J Clin Microbiol* 40: 376-381.
55. Fry SR, Meyer M, Semple MG, Simmons CP, Sekaran SD, Huang JX, et al. (2011) The diagnostic sensitivity of dengue rapid test assays is significantly enhanced by using a combined antigen and antibody testing approach. *PLoS Negl Trop Dis* 5: e1199.
56. Modhiran N, Watterson D, Muller DA, Panetta AK, Sester DP, Liu L, et al. (2015) Dengue virus NS1 protein activates cells via Toll-like receptor 4 and disrupts endothelial cell monolayer integrity. *Sci Transl Med* 7: 304ra142.
57. Modhiran N, Watterson D, Blumenthal A, Baxter AG, Young PR, Stacey KJ (2017) Dengue virus NS1 protein activates immune cells via TLR4 but not TLR2 or TLR6. *Immunol Cell Biol* 95: 491-495.
58. Xie X, Gayen S, Kang C, Yuan Z, Shi PY (2013) Membrane topology and function of dengue virus NS2A protein. *J Virol* 87: 4609-4622.
59. Xie X, Zou J, Puttikhunt C, Yuan Z, Shi PY (2015) Two distinct sets of NS2A molecules are responsible for dengue virus RNA synthesis and virion assembly. *J Virol* 89: 1298-1313.
60. Huang Q, Chen AS, Li Q, Kang C (2011) Expression, purification, and initial structural characterization of nonstructural protein 2B, an integral membrane protein of Dengue-2 virus, in detergent micelles. *Protein Expr Purif* 80: 169-175.
61. de la Cruz L, Chen WN, Graham B, Otting G (2014) Binding mode of the activity-modulating C-terminal segment of NS2B to NS3 in the dengue virus NS2B-NS3 protease. *Febs j* 281: 1517-1533.
62. Luo D, Xu T, Hunke C, Gruber G, Vasudevan SG, Lescar J (2008) Crystal structure of the NS3 protease-helicase from dengue virus. *J Virol* 82: 173-183.
63. Yin Z, Patel SJ, Wang WL, Chan WL, Ranga Rao KR, Wang G, et al. (2006) Peptide inhibitors of dengue virus NS3 protease. Part 2: SAR study of tetrapeptide aldehyde inhibitors. *Bioorg Med Chem Lett* 16: 40-43.
64. Li H, Clum S, You S, Ebner KE, Padmanabhan R (1999) The serine protease and RNA-stimulated nucleoside triphosphatase and RNA helicase functional domains of dengue virus type 2 NS3 converge within a region of 20 amino acids. *J Virol* 73: 3108-3116.
65. Lescar J, Luo D, Xu T, Sampath A, Lim SP, Canard B, et al. (2008) Towards the design of antiviral inhibitors against flaviviruses: the case for the multifunctional NS3 protein from Dengue virus as a target. *Antiviral Res* 80: 94-101.
66. Matusan AE, Pryor MJ, Davidson AD, Wright PJ (2001) Mutagenesis of the Dengue virus type 2 NS3 protein within and outside helicase motifs: effects on enzyme activity and virus replication. *J Virol* 75: 9633-9643.
67. Miller S, Kastner S, Krijnse-Locker J, Buhler S, Bartenschlager R (2007) The non-structural protein 4A of dengue virus is an integral membrane protein inducing membrane alterations in a 2K-regulated manner. *J Biol Chem* 282: 8873-8882.
68. Stern O, Hung YF, Valdau O, Yaffe Y, Harris E, Hoffmann S, et al. (2013) An N-terminal

- amphipathic helix in dengue virus nonstructural protein 4A mediates oligomerization and is essential for replication. *J Virol* 87: 4080-4085.
69. Miller S, Sparacio S, Bartenschlager R (2006) Subcellular localization and membrane topology of the Dengue virus type 2 Non-structural protein 4B. *J Biol Chem* 281: 8854-8863.
 70. Munoz-Jordan JL, Sanchez-Burgos GG, Laurent-Rolle M, Garcia-Sastre A (2003) Inhibition of interferon signaling by dengue virus. *Proc Natl Acad Sci U S A* 100: 14333-14338.
 71. Munoz-Jordan JL, Laurent-Rolle M, Ashour J, Martinez-Sobrido L, Ashok M, Lipkin WI, et al. (2005) Inhibition of alpha/beta interferon signaling by the NS4B protein of flaviviruses. *J Virol* 79: 8004-8013.
 72. McLean JE, Wudzinska A, Datan E, Quaglino D, Zakeri Z (2011) Flavivirus NS4A-induced autophagy protects cells against death and enhances virus replication. *J Biol Chem* 286: 22147-22159.
 73. Zhao Y, Soh TS, Lim SP, Chung KY, Swaminathan K, Vasudevan SG, et al. (2015) Molecular basis for specific viral RNA recognition and 2'-O-ribose methylation by the dengue virus nonstructural protein 5 (NS5). *Proc Natl Acad Sci U S A* 112: 14834-14839.
 74. Egloff MP, Benarroch D, Selisko B, Romette JL, Canard B (2002) An RNA cap (nucleoside-2'-O-)-methyltransferase in the flavivirus RNA polymerase NS5: crystal structure and functional characterization. *Embo j* 21: 2757-2768.
 75. Ackermann M, Padmanabhan R (2001) De novo synthesis of RNA by the dengue virus RNA-dependent RNA polymerase exhibits temperature dependence at the initiation but not elongation phase. *J Biol Chem* 276: 39926-39937.
 76. Best SM (2017) The Many Faces of the Flavivirus NS5 Protein in Antagonism of Type I Interferon Signaling. *J Virol* 91: e01970-01916.
 77. Medin CL, Fitzgerald KA, Rothman AL (2005) Dengue virus nonstructural protein NS5 induces interleukin-8 transcription and secretion. *J Virol* 79: 11053-11061.
 78. Pryor MJ, Rawlinson SM, Butcher RE, Barton CL, Waterhouse TA, Vasudevan SG, et al. (2007) Nuclear localization of dengue virus nonstructural protein 5 through its importin alpha/beta-recognized nuclear localization sequences is integral to viral infection. *Traffic* 8: 795-807.
 79. Smit JM, Moesker B, Rodenhuis-Zybert I, Wilschut J (2011) Flavivirus cell entry and membrane fusion. *Viruses* 3: 160-171.
 80. Hilgard P, Stockert R (2000) Heparan sulfate proteoglycans initiate dengue virus infection of hepatocytes. *Hepatology* 32: 1069-1077.
 81. Germi R, Crance JM, Garin D, Guimet J, Lortat-Jacob H, Ruigrok RW, et al. (2002) Heparan sulfate-mediated binding of infectious dengue virus type 2 and yellow fever virus. *Virology* 292: 162-168.
 82. Lozach PY, Burleigh L, Staropoli I, Navarro-Sanchez E, Harriague J, Virelizier JL, et al. (2005) Dendritic cell-specific intercellular adhesion molecule 3-grabbing non-integrin (DC-SIGN)-mediated enhancement of dengue virus infection is independent of DC-SIGN internalization signals. *J Biol Chem* 280: 23698-23708.
 83. Miller JL, de Wet BJ, Martinez-Pomares L, Radcliffe CM, Dwek RA, Rudd PM, et al. (2008) The mannose receptor mediates dengue virus infection of macrophages. *PLoS Pathog* 4: e17.
 84. Watson AA, Lebedev AA, Hall BA, Fenton-May AE, Vagin AA, Dejnirattisai W, et al. (2011) Structural flexibility of the macrophage dengue virus receptor CLEC5A: implications for ligand binding and signaling. *J Biol Chem* 286: 24208-24218.
 85. Reyes-Del Valle J, Chavez-Salinas S, Medina F, Del Angel RM (2005) Heat shock protein 90 and heat shock protein 70 are components of dengue virus receptor complex in human cells. *J Virol* 79: 4557-4567.
 86. Cruz-Oliveira C, Freire JM, Conceicao TM, Higa LM, Castanho MA, Da Poian AT (2015) Receptors and routes of dengue virus entry into the host cells. *FEMS Microbiol Rev* 39: 155-170.

87. Kuadkitkan A, Wikan N, Fongsaran C, Smith DR (2010) Identification and characterization of prohibitin as a receptor protein mediating DENV-2 entry into insect cells. *Virology* 406: 149-161.
88. Mercado-Curiel RF, Esquinca-Aviles HA, Tovar R, Diaz-Badillo A, Camacho-Nuez M, Munoz Mde L (2006) The four serotypes of dengue recognize the same putative receptors in *Aedes aegypti* midgut and *Ae. albopictus* cells. *BMC Microbiol* 6: 85.
89. Acosta EG, Castilla V, Damonte EB (2008) Functional entry of dengue virus into *Aedes albopictus* mosquito cells is dependent on clathrin-mediated endocytosis. *J Gen Virol* 89: 474-484.
90. Screaton G, Mongkolsapaya J, Yacoub S, Roberts C (2015) New insights into the immunopathology and control of dengue virus infection. *Nat Rev Immunol* 15: 745-759.
91. Murray CL, Jones CT, Rice CM (2008) Architects of assembly: roles of Flaviviridae non-structural proteins in virion morphogenesis. *Nat Rev Microbiol* 6: 699-708.
92. Perera R, Kuhn RJ (2008) Structural proteomics of dengue virus. *Curr Opin Microbiol* 11: 369-377.
93. Chatel-Chaix L, Bartenschlager R (2014) Dengue virus- and hepatitis C virus-induced replication and assembly compartments: the enemy inside--caught in the web. *J Virol* 88: 5907-5911.
94. Wu SJ, Grouard-Vogel G, Sun W, Mascola JR, Brachtel E, Putvatana R, et al. (2000) Human skin Langerhans cells are targets of dengue virus infection. *Nat Med* 6: 816-820.
95. Marovich M, Grouard-Vogel G, Louder M, Eller M, Sun W, Wu SJ, et al. (2001) Human dendritic cells as targets of dengue virus infection. *J Invest Dermatol Symp Proc* 6: 219-224.
96. Libraty DH, Pichyangkul S, Ajariyakhajorn C, Endy TP, Ennis FA (2001) Human dendritic cells are activated by dengue virus infection: enhancement by gamma interferon and implications for disease pathogenesis. *J Virol* 75: 3501-3508.
97. Kou Z, Quinn M, Chen H, Rodrigo WW, Rose RC, Schlesinger JJ, et al. (2008) Monocytes, but not T or B cells, are the principal target cells for dengue virus (DV) infection among human peripheral blood mononuclear cells. *J Med Virol* 80: 134-146.
98. Jessie K, Fong MY, Devi S, Lam SK, Wong KT (2004) Localization of dengue virus in naturally infected human tissues, by immunohistochemistry and in situ hybridization. *J Infect Dis* 189: 1411-1418.
99. Yacoub S, Wertheim H, Simmons CP, Screaton G, Wills B (2014) Cardiovascular manifestations of the emerging dengue pandemic. *Nat Rev Cardiol* 11: 335-345.
100. Hadinegoro SR (2012) The revised WHO dengue case classification: does the system need to be modified? *Paediatr Int Child Health* 32 Suppl 1: 33-38.
101. Guzman MG, Jaenisch T, Gaczkowski R, Ty Hang VT, Sekaran SD, Kroeger A, et al. (2010) Multi-country evaluation of the sensitivity and specificity of two commercially-available NS1 ELISA assays for dengue diagnosis. *PLoS Negl Trop Dis* 4: e811.
102. Srikiatkachorn A (2009) Plasma leakage in dengue haemorrhagic fever. *Thromb Haemost* 102: 1042-1049.
103. Guzman MG, Kouri G, Bravo J, Valdes L, Vazquez S, Halstead SB (2002) Effect of age on outcome of secondary dengue 2 infections. *Int J Infect Dis* 6: 118-124.
104. Gamble J, Bethell D, Day NP, Loc PP, Phu NH, Gartside IB, et al. (2000) Age-related changes in microvascular permeability: a significant factor in the susceptibility of children to shock? *Clin Sci (Lond)* 98: 211-216.
105. Sierra B, Alegre R, Perez AB, Garcia G, Sturn-Ramirez K, Obasanjo O, et al. (2007) HLA-A, -B, -C, and -DRB1 allele frequencies in Cuban individuals with antecedents of dengue 2 disease: advantages of the Cuban population for HLA studies of dengue virus infection. *Hum Immunol* 68: 531-540.
106. Stephens HA, Klaythong R, Sirikong M, Vaughn DW, Green S, Kalayanarooj S, et al. (2002) HLA-A and -B allele associations with secondary dengue virus infections correlate with

- disease severity and the infecting viral serotype in ethnic Thais. *Tissue Antigens* 60: 309-318.
107. Coffey LL, Mertens E, Brehin AC, Fernandez-Garcia MD, Amara A, Despres P, et al. (2009) Human genetic determinants of dengue virus susceptibility. *Microbes Infect* 11: 143-156.
 108. Kalayanarooj S, Gibbons RV, Vaughn D, Green S, Nisalak A, Jarman RG, et al. (2007) Blood group AB is associated with increased risk for severe dengue disease in secondary infections. *J Infect Dis* 195: 1014-1017.
 109. Fernandez-Mestre MT, Gendzekhadze K, Rivas-Vetencourt P, Layrisse Z (2004) TNF-alpha-308A allele, a possible severity risk factor of hemorrhagic manifestation in dengue fever patients. *Tissue Antigens* 64: 469-472.
 110. Simmons CP, Popper S, Dolocek C, Chau TN, Griffiths M, Dung NT, et al. (2007) Patterns of host genome-wide gene transcript abundance in the peripheral blood of patients with acute dengue hemorrhagic fever. *J Infect Dis* 195: 1097-1107.
 111. Vasilakis N, Weaver SC (2008) The history and evolution of human dengue emergence. *Adv Virus Res* 72: 1-76.
 112. Rico-Hesse R (2003) Microevolution and virulence of dengue viruses. *Adv Virus Res* 59: 315-341.
 113. Pryor MJ, Carr JM, Hocking H, Davidson AD, Li P, Wright PJ (2001) Replication of dengue virus type 2 in human monocyte-derived macrophages: comparisons of isolates and recombinant viruses with substitutions at amino acid 390 in the envelope glycoprotein. *Am J Trop Med Hyg* 65: 427-434.
 114. Cologna R, Rico-Hesse R (2003) American genotype structures decrease dengue virus output from human monocytes and dendritic cells. *J Virol* 77: 3929-3938.
 115. Leitmeyer KC, Vaughn DW, Watts DM, Salas R, Villalobos I, de C, et al. (1999) Dengue virus structural differences that correlate with pathogenesis. *J Virol* 73: 4738-4747.
 116. Twiddy SS, Woelk CH, Holmes EC (2002) Phylogenetic evidence for adaptive evolution of dengue viruses in nature. *J Gen Virol* 83: 1679-1689.
 117. Guzman MG, Alvarez M, Halstead SB (2013) Secondary infection as a risk factor for dengue hemorrhagic fever/dengue shock syndrome: an historical perspective and role of antibody-dependent enhancement of infection. *Arch Virol* 158: 1445-1459.
 118. Goncalvez AP, Engle RE, St Claire M, Purcell RH, Lai CJ (2007) Monoclonal antibody-mediated enhancement of dengue virus infection in vitro and in vivo and strategies for prevention. *Proc Natl Acad Sci U S A* 104: 9422-9427.
 119. Chau TN, Hieu NT, Anders KL, Wolbers M, Lien le B, Hieu LT, et al. (2009) Dengue virus infections and maternal antibody decay in a prospective birth cohort study of Vietnamese infants. *J Infect Dis* 200: 1893-1900.
 120. Mongkolsapaya J, Dejnirattisai W, Xu XN, Vasanawathana S, Tangthawornchaikul N, Chairunsri A, et al. (2003) Original antigenic sin and apoptosis in the pathogenesis of dengue hemorrhagic fever. *Nat Med* 9: 921-927.
 121. Rothman AL (2011) Immunity to dengue virus: a tale of original antigenic sin and tropical cytokine storms. *Nat Rev Immunol* 11: 532-543.
 122. Pang T, Cardoso MJ, Guzman MG (2007) Of cascades and perfect storms: the immunopathogenesis of dengue haemorrhagic fever-dengue shock syndrome (DHF/DSS). *Immunol Cell Biol* 85: 43-45.
 123. Nguyen TH, Nguyen TL, Lei HY, Lin YS, Le BL, Huang KJ, et al. (2005) Association between sex, nutritional status, severity of dengue hemorrhagic fever, and immune status in infants with dengue hemorrhagic fever. *Am J Trop Med Hyg* 72: 370-374.
 124. Chakravarti A, Kumaria R (2006) Circulating levels of tumour necrosis factor-alpha & interferon-gamma in patients with dengue & dengue haemorrhagic fever during an outbreak. *Indian J Med Res* 123: 25-30.
 125. Perez AB, Garcia G, Sierra B, Alvarez M, Vazquez S, Cabrera MV, et al. (2004) IL-10 levels in Dengue patients: some findings from the exceptional epidemiological conditions in Cuba.

- J Med Virol 73: 230-234.
126. Atrasheuskaya A, Petzelbauer P, Fredeking TM, Ignatyev G (2003) Anti-TNF antibody treatment reduces mortality in experimental dengue virus infection. *FEMS Immunol Med Microbiol* 35: 33-42.
 127. Carr JM, Hocking H, Bunting K, Wright PJ, Davidson A, Gamble J, et al. (2003) Supernatants from dengue virus type-2 infected macrophages induce permeability changes in endothelial cell monolayers. *J Med Virol* 69: 521-528.
 128. Anderson R, Wang S, Osiowy C, Issekutz AC (1997) Activation of endothelial cells via antibody-enhanced dengue virus infection of peripheral blood monocytes. *J Virol* 71: 4226-4232.
 129. Lin CF, Wan SW, Cheng HJ, Lei HY, Lin YS (2006) Autoimmune pathogenesis in dengue virus infection. *Viral Immunol* 19: 127-132.
 130. Wan SW, Lin CF, Yeh TM, Liu CC, Liu HS, Wang S, et al. (2013) Autoimmunity in dengue pathogenesis. *J Formos Med Assoc* 112: 3-11.
 131. Chen MC, Lin CF, Lei HY, Lin SC, Liu HS, Yeh TM, et al. (2009) Deletion of the C-terminal region of dengue virus nonstructural protein 1 (NS1) abolishes anti-NS1-mediated platelet dysfunction and bleeding tendency. *J Immunol* 183: 1797-1803.
 132. Avirutnan P, Fuchs A, Hauhart RE, Somnuk P, Youn S, Diamond MS, et al. (2010) Antagonism of the complement component C4 by flavivirus nonstructural protein NS1. *J Exp Med* 207: 793-806.
 133. Avirutnan P, Punyadee N, Noisakran S, Komoltri C, Thiemmecca S, Auethavornanan K, et al. (2006) Vascular leakage in severe dengue virus infections: a potential role for the nonstructural viral protein NS1 and complement. *J Infect Dis* 193: 1078-1088.
 134. Akira S, Uematsu S, Takeuchi O (2006) Pathogen recognition and innate immunity. *Cell* 124: 783-801.
 135. Alexopoulou L, Holt AC, Medzhitov R, Flavell RA (2001) Recognition of double-stranded RNA and activation of NF-kappaB by Toll-like receptor 3. *Nature* 413: 732-738.
 136. Heil F, Hemmi H, Hochrein H, Ampenberger F, Kirschning C, Akira S, et al. (2004) Species-specific recognition of single-stranded RNA via toll-like receptor 7 and 8. *Science* 303: 1526-1529.
 137. Tsai YT, Chang SY, Lee CN, Kao CL (2009) Human TLR3 recognizes dengue virus and modulates viral replication in vitro. *Cell Microbiol* 11: 604-615.
 138. Nasirudeen AM, Wong HH, Thien P, Xu S, Lam KP, Liu DX (2011) RIG-I, MDA5 and TLR3 synergistically play an important role in restriction of dengue virus infection. *PLoS Negl Trop Dis* 5: e926.
 139. Wang JP, Liu P, Latz E, Golenbock DT, Finberg RW, Libraty DH (2006) Flavivirus activation of plasmacytoid dendritic cells delineates key elements of TLR7 signaling beyond endosomal recognition. *J Immunol* 177: 7114-7121.
 140. Lee KG, Xu S, Kang ZH, Huo J, Huang M, Liu D, et al. (2012) Bruton's tyrosine kinase phosphorylates Toll-like receptor 3 to initiate antiviral response. *Proc Natl Acad Sci U S A* 109: 5791-5796.
 141. Green AM, Beatty PR, Hadjilaou A, Harris E (2014) Innate Immunity to Dengue Virus Infection and Subversion of Antiviral Responses. *J Mol Biol* 426: 1148-1160.
 142. Schoggins JW, Dorner M, Feulner M, Imanaka N, Murphy MY, Ploss A, et al. (2012) Dengue reporter viruses reveal viral dynamics in interferon receptor-deficient mice and sensitivity to interferon effectors in vitro. *Proc Natl Acad Sci U S A* 109: 14610-14615.
 143. Plataniias LC (2005) Mechanisms of type-I- and type-II-interferon-mediated signalling. *Nat Rev Immunol* 5: 375-386.
 144. Aguirre S, Maestre AM, Pagni S, Patel JR, Savage T, Gutman D, et al. (2012) DENV inhibits type I IFN production in infected cells by cleaving human STING. *PLoS Pathog* 8: e1002934.
 145. Ashour J, Morrison J, Laurent-Rolle M, Belicha-Villanueva A, Plumlee CR, Bernal-Rubio D,

- et al. (2010) Mouse STAT2 restricts early dengue virus replication. *Cell Host Microbe* 8: 410-421.
146. Lubick KJ, Robertson SJ, McNally KL, Freedman BA, Rasmussen AL, Taylor RT, et al. (2015) Flavivirus Antagonism of Type I Interferon Signaling Reveals Prolidase as a Regulator of IFNAR1 Surface Expression. *Cell Host Microbe* 18: 61-74.
 147. Mattijssen S, Pruijn GJ (2012) Viperin, a key player in the antiviral response. *Microbes Infect* 14: 419-426.
 148. Seo JY, Yaneva R, Cresswell P (2011) Viperin: a multifunctional, interferon-inducible protein that regulates virus replication. *Cell Host Microbe* 10: 534-539.
 149. Zhu H, Cong JP, Shenk T (1997) Use of differential display analysis to assess the effect of human cytomegalovirus infection on the accumulation of cellular RNAs: induction of interferon-responsive RNAs. *Proc Natl Acad Sci U S A* 94: 13985-13990.
 150. Chin KC, Cresswell P (2001) Viperin (cig5), an IFN-inducible antiviral protein directly induced by human cytomegalovirus. *Proc Natl Acad Sci U S A* 98: 15125-15130.
 151. Stirnweiss A, Ksienzyk A, Klages K, Rand U, Grashoff M, Hauser H, et al. (2010) IFN regulatory factor-1 bypasses IFN-mediated antiviral effects through viperin gene induction. *J Immunol* 184: 5179-5185.
 152. Andersen J, VanScoy S, Cheng TF, Gomez D, Reich NC (2008) IRF-3-dependent and augmented target genes during viral infection. *Genes Immun* 9: 168-175.
 153. Hinson ER, Cresswell P (2009) The N-terminal amphipathic alpha-helix of viperin mediates localization to the cytosolic face of the endoplasmic reticulum and inhibits protein secretion. *J Biol Chem* 284: 4705-4712.
 154. Hinson ER, Cresswell P (2009) The antiviral protein, viperin, localizes to lipid droplets via its N-terminal amphipathic alpha-helix. *Proc Natl Acad Sci U S A* 106: 20452-20457.
 155. Helbig KJ, Eyre NS, Yip E, Narayana S, Li K, Fiches G, et al. (2011) The antiviral protein viperin inhibits hepatitis C virus replication via interaction with nonstructural protein 5A. *Hepatology* 54: 1506-1517.
 156. Helbig KJ, Carr JM, Calvert JK, Wati S, Clarke JN, Eyre NS, et al. (2013) Viperin is induced following dengue virus type-2 (DENV-2) infection and has anti-viral actions requiring the C-terminal end of viperin. *PLoS Negl Trop Dis* 7: e2178.
 157. Duschene KS, Broderick JB (2010) The antiviral protein viperin is a radical SAM enzyme. *FEBS Lett* 584: 1263-1267.
 158. Fenwick MK, Li Y, Cresswell P, Modis Y, Ealick SE (2017) Structural studies of viperin, an antiviral radical SAM enzyme. *Proc Natl Acad Sci U S A* 114: 6806-6811.
 159. Wang X, Hinson ER, Cresswell P (2007) The interferon-inducible protein viperin inhibits influenza virus release by perturbing lipid rafts. *Cell Host Microbe* 2: 96-105.
 160. Nasr N, Maddocks S, Turville SG, Harman AN, Woolger N, Helbig KJ, et al. (2012) HIV-1 infection of human macrophages directly induces viperin which inhibits viral production. *Blood* 120: 778-788.
 161. Wang S, Wu X, Pan T, Song W, Wang Y, Zhang F, et al. (2012) Viperin inhibits hepatitis C virus replication by interfering with binding of NS5A to host protein hVAP-33. *J Gen Virol* 93: 83-92.
 162. Jiang D, Weidner JM, Qing M, Pan XB, Guo H, Xu C, et al. (2010) Identification of five interferon-induced cellular proteins that inhibit west nile virus and dengue virus infections. *J Virol* 84: 8332-8341.
 163. Fink J, Gu F, Ling L, Tolfvenstam T, Olfat F, Chin KC, et al. (2007) Host gene expression profiling of dengue virus infection in cell lines and patients. *PLoS Negl Trop Dis* 1: e86.
 164. Sariol CA, Munoz-Jordan JL, Abel K, Rosado LC, Pantoja P, Giavedoni L, et al. (2007) Transcriptional activation of interferon-stimulated genes but not of cytokine genes after primary infection of rhesus macaques with dengue virus type 1. *Clin Vaccine Immunol* 14: 756-766.
 165. Al-Shujairi WH, Clarke JN, Davies LT, Alsharifi M, Pitson SM, Carr JM (2017) Intracranial

- Injection of Dengue Virus Induces Interferon Stimulated Genes and CD8+ T Cell Infiltration by Sphingosine Kinase 1 Independent Pathways. *PLoS One* 12: e0169814.
166. Calvert JK, Helbig KJ, Dimasi D, Cockshell M, Beard MR, Pitson SM, et al. (2015) Dengue Virus Infection of Primary Endothelial Cells Induces Innate Immune Responses, Changes in Endothelial Cells Function and Is Restricted by Interferon-Stimulated Responses. *J Interferon Cytokine Res* 35: 654-665.
 167. Clarke JN, Davies LK, Calvert JK, Gliddon BL, Al Shujari WH, Aloia AL, et al. (2016) Reduction in sphingosine kinase 1 influences the susceptibility to dengue virus infection by altering antiviral responses. *J Gen Virol* 97: 95-109.
 168. Saitoh T, Satoh T, Yamamoto N, Uematsu S, Takeuchi O, Kawai T, et al. (2011) Antiviral protein Viperin promotes Toll-like receptor 7- and Toll-like receptor 9-mediated type I interferon production in plasmacytoid dendritic cells. *Immunity* 34: 352-363.
 169. Rothman AL (2003) Immunology and immunopathogenesis of dengue disease. *Adv Virus Res* 60: 397-419.
 170. Vaughan K, Greenbaum J, Blythe M, Peters B, Sette A (2010) Meta-analysis of all immune epitope data in the Flavivirus genus: inventory of current immune epitope data status in the context of virus immunity and immunopathology. *Viral Immunol* 23: 259-284.
 171. Bashyam HS, Green S, Rothman AL (2006) Dengue virus-reactive CD8+ T cells display quantitative and qualitative differences in their response to variant epitopes of heterologous viral serotypes. *J Immunol* 176: 2817-2824.
 172. Imrie A, Meeks J, Gurary A, Sukhbataar M, Kitsutani P, Effler P, et al. (2007) Differential functional avidity of dengue virus-specific T-cell clones for variant peptides representing heterologous and previously encountered serotypes. *J Virol* 81: 10081-10091.
 173. Mangada MM, Rothman AL (2005) Altered cytokine responses of dengue-specific CD4+ T cells to heterologous serotypes. *J Immunol* 175: 2676-2683.
 174. Liu Y, Liu J, Cheng G (2016) Vaccines and immunization strategies for dengue prevention. *Emerg Microbes Infect* 5: e77.
 175. Hadinegoro SR, Arredondo-Garcia JL, Capeding MR, Deseda C, Chotpitayasunondh T, Dietze R, et al. (2015) Efficacy and long-term safety of a dengue vaccine in regions of endemic disease. *N Engl J Med* 373: 1195-1206.
 176. Constenla D, Clark S (2016) Financing dengue vaccine introduction in the Americas: challenges and opportunities. *Expert Rev Vaccines* 15: 547-559.
 177. Pitisuttithum P, Bouckennooghe A (2016) The first licensed dengue vaccine: an important tool for integrated preventive strategies against dengue virus infection. *Expert Rev Vaccines* 15: 795-798.
 178. Moreira LA, Iturbe-Ormaetxe I, Jeffery JA, Lu G, Pyke AT, Hedges LM, et al. (2009) A *Wolbachia* symbiont in *Aedes aegypti* limits infection with dengue, Chikungunya, and *Plasmodium*. *Cell* 139: 1268-1278.
 179. Hoffmann AA, Iturbe-Ormaetxe I, Callahan AG, Phillips BL, Billington K, Axford JK, et al. (2014) Stability of the wMel *Wolbachia* Infection following invasion into *Aedes aegypti* populations. *PLoS Negl Trop Dis* 8: e3115.
 180. Hugo LE, Jeffery JA, Trewin BJ, Wockner LF, Nguyen TY, Nguyen HL, et al. (2014) Adult survivorship of the dengue mosquito *Aedes aegypti* varies seasonally in central Vietnam. *PLoS Negl Trop Dis* 8: e2669.
 181. Yacoub S, Mongkolsapaya J, Sreaton G (2016) Recent advances in understanding dengue. *F1000Res* 5.
 182. Zompi S, Harris E (2012) Animal models of dengue virus infection. *Viruses* 4: 62-82.
 183. Clark KB, Onlamoon N, Hsiao HM, Perng GC, Villinger F (2013) Can non-human primates serve as models for investigating dengue disease pathogenesis? *Front Microbiol* 4: 305.
 184. Chan KW, Watanabe S, Kavishna R, Alonso S, Vasudevan SG (2015) Animal models for studying dengue pathogenesis and therapy. *Antiviral Res* 123: 5-14.
 185. Zellweger RM, Shresta S (2014) Mouse models to study dengue virus immunology and

- pathogenesis. *Front Immunol* 5: 151.
186. Bente DA, Rico-Hesse R (2006) Models of dengue virus infection. *Drug Discov Today Dis Models* 3: 97-103.
 187. Plummer EM, Shresta S (2014) Mouse models for dengue vaccines and antivirals. *J Immunol Methods* 410: 34-38.
 188. Shresta S, Sharar KL, Prigozhin DM, Beatty PR, Harris E (2006) Murine model for dengue virus-induced lethal disease with increased vascular permeability. *J Virol* 80: 10208-10217.
 189. Tan GK, Ng JK, Trasti SL, Schul W, Yip G, Alonso S (2010) A non mouse-adapted dengue virus strain as a new model of severe dengue infection in AG129 mice. *PLoS Negl Trop Dis* 4: e672.
 190. Yauch LE, Shresta S (2008) Mouse models of dengue virus infection and disease. *Antiviral Res* 80: 87-93.
 191. An J, Kimura-Kuroda J, Hirabayashi Y, Yasui K (1999) Development of a novel mouse model for dengue virus infection. *Virology* 263: 70-77.
 192. Akkina R (2013) New generation humanized mice for virus research: comparative aspects and future prospects. *Virology* 435: 14-28.
 193. Amaral DC, Rachid MA, Vilela MC, Campos RD, Ferreira GP, Rodrigues DH, et al. (2011) Intracerebral infection with dengue-3 virus induces meningoencephalitis and behavioral changes that precede lethality in mice. *J Neuroinflammation* 8: 23.
 194. Oliveira ER, Amorim JF, Paes MV, Azevedo AS, Goncalves AJ, Costa SM, et al. (2015) Peripheral effects induced in BALB/c mice infected with DENV by the intracerebral route. *Virology* 489: 95-107.
 195. Chen HC, Hofman FM, Kung JT, Lin YD, Wu-Hsieh BA (2007) Both virus and tumor necrosis factor alpha are critical for endothelium damage in a mouse model of dengue virus-induced hemorrhage. *J Virol* 81: 5518-5526.
 196. Chen HC, Lai SY, Sung JM, Lee SH, Lin YC, Wang WK, et al. (2004) Lymphocyte activation and hepatic cellular infiltration in immunocompetent mice infected by dengue virus. *J Med Virol* 73: 419-431.
 197. Bartke N, Hannun YA (2009) Bioactive sphingolipids: metabolism and function. *J Lipid Res* 50 Suppl: S91-96.
 198. Strub GM, Maceyka M, Hait NC, Milstien S, Spiegel S (2010) Extracellular and intracellular actions of sphingosine-1-phosphate. *Adv Exp Med Biol* 688: 141-155.
 199. Hannun YA, Obeid LM (2008) Principles of bioactive lipid signalling: lessons from sphingolipids. *Nat Rev Mol Cell Biol* 9: 139-150.
 200. Woodcock J (2006) Sphingosine and ceramide signalling in apoptosis. *IUBMB Life* 58: 462-466.
 201. Pyne NJ, Pyne S (2010) Sphingosine 1-phosphate and cancer. *Nat Rev Cancer* 10: 489-503.
 202. Arish M, Husein A, Kashif M, Saleem M, Akhter Y, Rub A (2016) Sphingosine-1-phosphate signaling: unraveling its role as a drug target against infectious diseases. *Drug Discov Today* 21: 133-142.
 203. Leclercq TM, Pitson SM (2006) Cellular signalling by sphingosine kinase and sphingosine 1-phosphate. *IUBMB Life* 58: 467-472.
 204. Pyne NJ, Tonelli F, Lim KG, Long JS, Edwards J, Pyne S (2012) Sphingosine 1-phosphate signalling in cancer. *Biochem Soc Trans* 40: 94-100.
 205. Pitson SM (2011) Regulation of sphingosine kinase and sphingolipid signaling. *Trends Biochem Sci* 36: 97-107.
 206. Carr JM, Mahalingam S, Bonder CS, Pitson SM (2013) Sphingosine kinase 1 in viral infections. *Rev Med Virol* 23: 73-84.
 207. Taha TA, Hannun YA, Obeid LM (2006) Sphingosine kinase: biochemical and cellular regulation and role in disease. *J Biochem Mol Biol* 39: 113-131.
 208. Pitson SM, Moretti PA, Zebol JR, Zareie R, Derian CK, Darrow AL, et al. (2002) The nucleotide-binding site of human sphingosine kinase 1. *J Biol Chem* 277: 49545-49553.

209. Yokota S, Taniguchi Y, Kihara A, Mitsutake S, Igarashi Y (2004) Asp177 in C4 domain of mouse sphingosine kinase 1a is important for the sphingosine recognition. *FEBS Lett* 578: 106-110.
210. Sugiura M, Kono K, Liu H, Shimizugawa T, Minekura H, Spiegel S, et al. (2002) Ceramide kinase, a novel lipid kinase. Molecular cloning and functional characterization. *J Biol Chem* 277: 23294-23300.
211. Neubauer HA, Pitson SM (2013) Roles, regulation and inhibitors of sphingosine kinase 2. *FEBS J* 280: 5317-5336.
212. Siow DL, Anderson CD, Berdyshev EV, Skobeleva A, Natarajan V, Pitson SM, et al. (2011) Sphingosine kinase localization in the control of sphingolipid metabolism. *Adv Enzyme Regul* 51: 229-244.
213. Kohama T, Olivera A, Edsall L, Nagiec MM, Dickson R, Spiegel S (1998) Molecular cloning and functional characterization of murine sphingosine kinase. *J Biol Chem* 273: 23722-23728.
214. Liu H, Sugiura M, Nava VE, Edsall LC, Kono K, Poulton S, et al. (2000) Molecular cloning and functional characterization of a novel mammalian sphingosine kinase type 2 isoform. *J Biol Chem* 275: 19513-19520.
215. Mizugishi K, Yamashita T, Olivera A, Miller GF, Spiegel S, Proia RL (2005) Essential role for sphingosine kinases in neural and vascular development. *Mol Cell Biol* 25: 11113-11121.
216. Maceyka M, Sankala H, Hait NC, Le Stunff H, Liu H, Toman R, et al. (2005) SphK1 and SphK2, sphingosine kinase isoenzymes with opposing functions in sphingolipid metabolism. *J Biol Chem* 280: 37118-37129.
217. Neubauer HA, Pham DH, Zebol JR, Moretti PA, Peterson AL, Leclercq TM, et al. (2016) An oncogenic role for sphingosine kinase 2. *Oncotarget* 7: 64886-64899.
218. Pitman MR, Pitson SM (2010) Inhibitors of the sphingosine kinase pathway as potential therapeutics. *Curr Cancer Drug Targets* 10: 354-367.
219. Pitson SM, D'Andrea R J, Vandeleur L, Moretti PA, Xia P, Gamble JR, et al. (2000) Human sphingosine kinase: purification, molecular cloning and characterization of the native and recombinant enzymes. *Biochem J* 350 Pt 2: 429-441.
220. Pitson SM, Moretti PA, Zebol JR, Lynn HE, Xia P, Vadas MA, et al. (2003) Activation of sphingosine kinase 1 by ERK1/2-mediated phosphorylation. *EMBO J* 22: 5491-5500.
221. Jarman KE, Moretti PA, Zebol JR, Pitson SM (2010) Translocation of sphingosine kinase 1 to the plasma membrane is mediated by calcium- and integrin-binding protein 1. *J Biol Chem* 285: 483-492.
222. Barr RK, Lynn HE, Moretti PA, Khew-Goodall Y, Pitson SM (2008) Deactivation of sphingosine kinase 1 by protein phosphatase 2A. *J Biol Chem* 283: 34994-35002.
223. Hait NC, Bellamy A, Milstien S, Kordula T, Spiegel S (2007) Sphingosine kinase type 2 activation by ERK-mediated phosphorylation. *J Biol Chem* 282: 12058-12065.
224. Ding G, Sonoda H, Yu H, Kajimoto T, Goparaju SK, Jahangeer S, et al. (2007) Protein kinase D-mediated phosphorylation and nuclear export of sphingosine kinase 2. *J Biol Chem* 282: 27493-27502.
225. Machesky NJ, Zhang G, Raghavan B, Zimmerman P, Kelly SL, Merrill AH, Jr., et al. (2008) Human cytomegalovirus regulates bioactive sphingolipids. *J Biol Chem* 283: 26148-26160.
226. Monick MM, Cameron K, Powers LS, Butler NS, McCoy D, Mallampalli RK, et al. (2004) Sphingosine kinase mediates activation of extracellular signal-related kinase and Akt by respiratory syncytial virus. *Am J Respir Cell Mol Biol* 30: 844-852.
227. Seo YJ, Blake C, Alexander S, Hahm B (2010) Sphingosine 1-phosphate-metabolizing enzymes control influenza virus propagation and viral cytopathogenicity. *J Virol* 84: 8124-8131.
228. Seo YJ, Alexander S, Hahm B (2011) Does cytokine signaling link sphingolipid metabolism to host defense and immunity against virus infections? *Cytokine Growth Factor Rev* 22: 55-61.
229. Seo YJ, Pritzl CJ, Vijayan M, Bomb K, McClain ME, Alexander S, et al. (2013) Sphingosine

- kinase 1 serves as a pro-viral factor by regulating viral RNA synthesis and nuclear export of viral ribonucleoprotein complex upon influenza virus infection. *PLoS One* 8: e75005.
230. Vijayan M, Seo YJ, Pritzl CJ, Squires SA, Alexander S, Hahm B (2014) Sphingosine kinase 1 regulates measles virus replication. *Virology* 450-451: 55-63.
 231. Yamane D, Zahoor MA, Mohamed YM, Azab W, Kato K, Tohya Y, et al. (2009) Inhibition of sphingosine kinase by bovine viral diarrhea virus NS3 is crucial for efficient viral replication and cytopathogenesis. *J Biol Chem* 284: 13648-13659.
 232. Wati S, Rawlinson SM, Ivanov RA, Dorstyn L, Beard MR, Jans DA, et al. (2011) Tumour necrosis factor alpha (TNF-alpha) stimulation of cells with established dengue virus type 2 infection induces cell death that is accompanied by a reduced ability of TNF-alpha to activate nuclear factor kappaB and reduced sphingosine kinase-1 activity. *J Gen Virol* 92: 807-818.
 233. Carr JM, Kua T, Clarke JN, Calvert JK, Zebol JR, Beard MR, et al. (2013) Reduced sphingosine kinase 1 activity in dengue virus type-2 infected cells can be mediated by the 3' untranslated region of dengue virus type-2 RNA. *J Gen Virol* 94: 2437-2448.
 234. Dai L, Plaisance-Bonstaff K, Voelkel-Johnson C, Smith CD, Ogretmen B, Qin Z, et al. (2014) Sphingosine kinase-2 maintains viral latency and survival for KSHV-infected endothelial cells. *PLoS One* 9: e102314.
 235. Yamane D, McGivern DR, Wauthier E, Yi M, Madden VJ (2014) Regulation of the hepatitis C virus RNA replicase by endogenous lipid peroxidation. *PLoS One* 20: 927-935.
 236. Reid SP, Tritsch SR, Kota K, Chiang CY, Dong L, Kenny T, et al. (2015) Sphingosine kinase 2 is a chikungunya virus host factor co-localized with the viral replication complex. *Emerg Microbes Infect* 4: e61.
 237. Gualano RC, Pryor MJ, Cauchi MR, Wright PJ, Davidson AD (1998) Identification of a major determinant of mouse neurovirulence of dengue virus type 2 using stably cloned genomic-length cDNA. *J Gen Virol* 79 (Pt 3): 437-446.
 238. Cong L, Ran FA, Cox D, Lin S, Barretto R, Habib N, et al. (2013) Multiplex genome engineering using CRISPR/Cas systems. *Science* 339: 819-823.
 239. Van der Hoek KH, Eyre NS, Shue B, Khantisitthiporn O, Glab-Ampi K, Carr JM, et al. (2017) Viperin is an important host restriction factor in control of Zika virus infection. *Sci Rep* 7: 4475.
 240. Schmittgen TD, Livak KJ (2008) Analyzing real-time PCR data by the comparative C(T) method. *Nat Protoc* 3: 1101-1108.
 241. Ansarah-Sobrinho C, Nelson S, Jost CA, Whitehead SS, Pierson TC (2008) Temperature-dependent production of pseudoinfectious dengue reporter virus particles by complementation. *Virology* 381: 67-74.
 242. Pitman MR, Pham DH, Pitson SM (2012) Isoform-selective assays for sphingosine kinase activity. *Methods Mol Biol* 874: 21-31.
 243. Leclercq TM, Moretti PA, Vadas MA, Pitson SM (2008) Eukaryotic elongation factor 1A interacts with sphingosine kinase and directly enhances its catalytic activity. *J Biol Chem* 283: 9606-9614.
 244. Allende ML, Sasaki T, Kawai H, Olivera A, Mi Y, van Echten-Deckert G, et al. (2004) Mice deficient in sphingosine kinase 1 are rendered lymphopenic by FTY720. *J Biol Chem* 279: 52487-52492.
 245. Alvarez SE, Milstien S, Spiegel S (2007) Autocrine and paracrine roles of sphingosine-1-phosphate. *Trends Endocrinol Metab* 18: 300-307.
 246. Spiegel S, Milstien S (2011) The outs and the ins of sphingosine-1-phosphate in immunity. *Nat Rev Immunol* 11: 403-415.
 247. Alemany R, van Koppen CJ, Danneberg K, Ter Braak M, Meyer Zu Heringdorf D (2007) Regulation and functional roles of sphingosine kinases. *Naunyn Schmiedebergs Arch Pharmacol* 374: 413-428.
 248. French KJ, Schrecengost RS, Lee BD, Zhuang Y, Smith SN, Eberly JL, et al. (2003)

- Discovery and evaluation of inhibitors of human sphingosine kinase. *Cancer Res* 63: 5962-5969.
249. French KJ, Upson JJ, Keller SN, Zhuang Y, Yun JK, Smith CD (2006) Antitumor activity of sphingosine kinase inhibitors. *J Pharmacol Exp Ther* 318: 596-603.
250. Newton J, Lima S, Maceyka M, Spiegel S (2015) Revisiting the sphingolipid rheostat: Evolving concepts in cancer therapy. *Exp Cell Res* 333: 195-200.
251. Lai WQ, Irwan AW, Goh HH, Howe HS, Yu DT, Valle-Onate R, et al. (2008) Anti-inflammatory effects of sphingosine kinase modulation in inflammatory arthritis. *J Immunol* 181: 8010-8017.
252. Loveridge C, Tonelli F, Leclercq T, Lim KG, Long JS, Berdyshev E, et al. (2010) The sphingosine kinase 1 inhibitor 2-(p-hydroxyanilino)-4-(p-chlorophenyl)thiazole induces proteasomal degradation of sphingosine kinase 1 in mammalian cells. *J Biol Chem* 285: 38841-38852.
253. Aloia AL, Calvert JK, Clarke JN, Davies LT, Helbig KJ, Pitson SM, et al. (2017) Investigation of sphingosine kinase 1 in interferon responses during dengue virus infection. *Clin Trans Immunol* 6: e151.
254. Finnegan CM, Rawat SS, Puri A, Wang JM, Ruscetti FW, Blumenthal R (2004) Ceramide, a target for antiretroviral therapy. *Proc Natl Acad Sci U S A* 101: 15452-15457.
255. Voisset C, Lavie M, Helle F, Op De Beeck A, Bilheu A, Bertrand-Michel J, et al. (2008) Ceramide enrichment of the plasma membrane induces CD81 internalization and inhibits hepatitis C virus entry. *Cell Microbiol* 10: 606-617.
256. Medigeshi GR, Hirsch AJ, Streblow DN, Nikolich-Zugich J, Nelson JA (2008) West Nile virus entry requires cholesterol-rich membrane microdomains and is independent of alphavbeta3 integrin. *J Virol* 82: 5212-5219.
257. Harikumar KB, Yester JW, Surace MJ, Oyeniran C, Price MM, Huang WC, et al. (2014) K63-linked polyubiquitination of transcription factor IRF1 is essential for IL-1-induced production of chemokines CXCL10 and CCL5. *Nat Immunol* 15: 231-238.
258. Raut CG, Deolankar RP, Kolhapure RM, Goverdhan MK (1996) Susceptibility of laboratory-bred rodents to the experimental infection with dengue virus type 2. *Acta Virol* 40: 143-146.
259. French KJ, Zhuang Y, Maines LW, Gao P, Wang W, Beljanski V, et al. (2010) Pharmacology and antitumor activity of ABC294640, a selective inhibitor of sphingosine kinase-2. *J Pharmacol Exp Ther* 333: 129-139.
260. Liu K, Guo TL, Hait NC, Allegood J, Parikh HI, Xu W, et al. (2013) Biological characterization of 3-(2-amino-ethyl)-5-[3-(4-butoxyl-phenyl)-propylidene]-thiazolidine-2,4-dione (K145) as a selective sphingosine kinase-2 inhibitor and anticancer agent. *PLoS One* 8: e56471.
261. Baeyens A, Fang V, Chen C, Schwab SR (2015) Exit Strategies: S1P Signaling and T Cell Migration. *Trends Immunol* 36: 778-787.
262. Giacobbi NS, Gupta T, Coxon AT, Pipas JM (2015) Polyomavirus T antigens activate an antiviral state. *Virology* 476: 377-385.
263. Chen HW, King K, Tu J, Sanchez M, Luster AD, Shresta S (2013) The roles of IRF-3 and IRF-7 in innate antiviral immunity against dengue virus. *J Immunol* 191: 4194-4201.
264. Hsieh MF, Lai SL, Chen JP, Sung JM, Lin YL, Wu-Hsieh BA, et al. (2006) Both CXCR3 and CXCL10/IFN-inducible protein 10 are required for resistance to primary infection by dengue virus. *J Immunol* 177: 1855-1863.
265. Canlas J, Holt P, Carroll A, Rix S, Ryan P, Davies L, et al. (2015) Sphingosine kinase 2-deficiency mediated changes in spinal pain processing. *Front Mol Neurosci* 8: 29.
266. Kharel Y, Lee S, Snyder AH, Sheasley-O'Neill S L, Morris MA, Setiady Y, et al. (2005) Sphingosine kinase 2 is required for modulation of lymphocyte traffic by FTY720. *J Biol Chem* 280: 36865-36872.
267. Sensken SC, Bode C, Nagarajan M, Peest U, Pabst O, Graler MH (2010) Redistribution of sphingosine 1-phosphate by sphingosine kinase 2 contributes to lymphopenia. *J Immunol*

- 184: 4133-4142.
268. Schwab SR, Cyster JG (2007) Finding a way out: lymphocyte egress from lymphoid organs. *Nat Immunol* 8: 1295-1301.
269. Lai WQ, Irwan AW, Goh HH, Melendez AJ, McInnes IB, Leung BP (2009) Distinct roles of sphingosine kinase 1 and 2 in murine collagen-induced arthritis. *J Immunol* 183: 2097-2103.
270. Maines LW, French KJ, Wolpert EB, Antonetti DA, Smith CD (2006) Pharmacologic manipulation of sphingosine kinase in retinal endothelial cells: implications for angiogenic ocular diseases. *Invest Ophthalmol Vis Sci* 47: 5022-5031.
271. Fitzpatrick LR, Green C, Maines LW, Smith CD (2011) Experimental osteoarthritis in rats is attenuated by ABC294640, a selective inhibitor of sphingosine kinase-2. *Pharmacology* 87: 135-143.
272. Beljanski V, Lewis CS, Smith CD (2011) Antitumor activity of sphingosine kinase 2 inhibitor ABC294640 and sorafenib in hepatocellular carcinoma xenografts. *Cancer Biol Ther* 11: 524-534.
273. Ding X, Chaiteerakij R, Moser CD, Shaleh H, Boakye J, Chen G, et al. (2016) Antitumor effect of the novel sphingosine kinase 2 inhibitor ABC294640 is enhanced by inhibition of autophagy and by sorafenib in human cholangiocarcinoma cells. *Oncotarget* 7: 20080-20092.
274. Gao P, Smith CD (2011) Ablation of sphingosine kinase-2 inhibits tumor cell proliferation and migration. *Mol Cancer Res* 9: 1509-1519.
275. Pyne NJ, Adams DR, Pyne S (2017) Sphingosine Kinase 2 in Autoimmune/Inflammatory Disease and the Development of Sphingosine Kinase 2 Inhibitors. *Trends Pharmacol Sci* 38: 581-591.
276. Wilkins C, Gale M, Jr. (2010) Recognition of viruses by cytoplasmic sensors. *Curr Opin Immunol* 22: 41-47.
277. Thompson MR, Kaminski JJ, Kurt-Jones EA, Fitzgerald KA (2011) Pattern recognition receptors and the innate immune response to viral infection. *Viruses* 3: 920-940.
278. Torres S, Hernandez JC, Giraldo D, Arboleda M, Rojas M, Smit JM, et al. (2013) Differential expression of Toll-like receptors in dendritic cells of patients with dengue during early and late acute phases of the disease. *PLoS Negl Trop Dis* 7: e2060.
279. Wu J, Chen ZJ (2014) Innate immune sensing and signaling of cytosolic nucleic acids. *Annu Rev Immunol* 32: 461-488.
280. Schneider WM, Chevillotte MD, Rice CM (2014) Interferon-stimulated genes: a complex web of host defenses. *Annu Rev Immunol* 32: 513-545.
281. Schoggins JW (2014) Interferon-stimulated genes: roles in viral pathogenesis. *Curr Opin Virol* 6: 40-46.
282. Helbig KJ, Beard MR (2014) The role of viperin in the innate antiviral response. *J Mol Biol* 426: 1210-1219.
283. Szretter KJ, Brien JD, Thackray LB, Virgin HW, Cresswell P, Diamond MS (2011) The interferon-inducible gene viperin restricts West Nile virus pathogenesis. *J Virol* 85: 11557-11566.
284. de Miranda AS, Rodrigues DH, Amaral DC, de Lima Campos RD, Cisalpino D, Vilela MC, et al. (2012) Dengue-3 encephalitis promotes anxiety-like behavior in mice. *Behav Brain Res* 230: 237-242.
285. Tsai T-T, Chen C-L, Lin Y-S, Chang C-P, Tsai C-C, Cheng Y-L, et al. (2016) Microglia retard dengue virus-induced acute viral encephalitis. *Scientific Reports* 6: 27670.
286. Schoggins JW, Rice CM (2011) Interferon-stimulated genes and their antiviral effector functions. *Curr Opin Virol* 1: 519-525.
287. Dang W, Zhang M, Hu YH, Sun L (2010) Differential regulation of *Sciaenops ocellatus* viperin expression by intracellular and extracellular bacterial pathogens. *Fish Shellfish Immunol* 29: 264-270.
288. Teng TS, Foo SS, Simamarta D, Lum FM, Teo TH, Lulla A, et al. (2012) Viperin restricts

- chikungunya virus replication and pathology. *J Clin Invest* 122: 4447-4460.
289. Tang YD, Na L, Zhu CH, Shen N, Yang F, Fu XQ, et al. (2014) Equine viperin restricts equine infectious anemia virus replication by inhibiting the production and/or release of viral Gag, Env, and receptor via distortion of the endoplasmic reticulum. *J Virol* 88: 12296-12310.
 290. Chan YL, Chang TH, Liao CL, Lin YL (2008) The cellular antiviral protein viperin is attenuated by proteasome-mediated protein degradation in Japanese encephalitis virus-infected cells. *J Virol* 82: 10455-10464.
 291. Upadhyay AS, Vonderstein K, Pichlmair A, Stehling O, Bennett KL, Dobler G, et al. (2014) Viperin is an iron-sulfur protein that inhibits genome synthesis of tick-borne encephalitis virus via radical SAM domain activity. *Cell Microbiol* 16: 834-848.
 292. Helbig KJ, Lau DT, Semendric L, Harley HA, Beard MR (2005) Analysis of ISG expression in chronic hepatitis C identifies viperin as a potential antiviral effector. *Hepatology* 42: 702-710.
 293. Jiang D, Guo H, Xu C, Chang J, Gu B, Wang L, et al. (2008) Identification of three interferon-inducible cellular enzymes that inhibit the replication of hepatitis C virus. *J Virol* 82: 1665-1678.
 294. Severa M, Coccia EM, Fitzgerald KA (2006) Toll-like receptor-dependent and -independent viperin gene expression and counter-regulation by PRDI-binding factor-1/BLIMP1. *J Biol Chem* 281: 26188-26195.
 295. Boudinot P, Riffault S, Salhi S, Carrat C, Sedlik C, Mahmoudi N, et al. (2000) Vesicular stomatitis virus and pseudorabies virus induce a vig1/cig5 homologue in mouse dendritic cells via different pathways. *J Gen Virol* 81: 2675-2682.
 296. Hinson ER, Joshi NS, Chen JH, Rahner C, Jung YW, Wang X, et al. (2010) Viperin is highly induced in neutrophils and macrophages during acute and chronic lymphocytic choriomeningitis virus infection. *J Immunol* 184: 5723-5731.
 297. Lucas TM, Richner JM, Diamond MS (2015) The Interferon-Stimulated Gene Ifi2712a Restricts West Nile Virus Infection and Pathogenesis in a Cell-Type- and Region-Specific Manner. *J Virol* 90: 2600-2615.
 298. Tan KS, Olfat F, Phoon MC, Hsu JP, Howe JL, Seet JE, et al. (2012) In vivo and in vitro studies on the antiviral activities of viperin against influenza H1N1 virus infection. *J Gen Virol* 93: 1269-1277.
 299. Qiu LQ, Cresswell P, Chin KC (2009) Viperin is required for optimal Th2 responses and T-cell receptor-mediated activation of NF-kappaB and AP-1. *Blood* 113: 3520-3529.
 300. Ferreira GP, Figueiredo LB, Coelho LF, S PA, Jr., Cecilio AB, Ferreira PC, et al. (2010) Dengue virus 3 clinical isolates show different patterns of virulence in experimental mice infection. *Microbes Infect* 12: 546-554.
 301. Rothman AL, Medin CL, Friberg H, Currier JR (2014) Immunopathogenesis Versus Protection in Dengue Virus Infections. *Curr Trop Med Rep* 1: 13-20.
 302. Maceyka M, Spiegel S (2014) Sphingolipid metabolites in inflammatory disease. *Nature* 510: 58-67.
 303. Pyne NJ, McNaughton M, Boomkamp S, MacRitchie N, Evangelisti C, Martelli AM, et al. (2015) Role of sphingosine 1-phosphate receptors, sphingosine kinases and sphingosine in cancer and inflammation. *Adv Biol Regul* 60: 151-159.
 304. Kumar N, Xin ZT, Liang Y, Ly H, Liang Y (2008) NF-kappaB signaling differentially regulates influenza virus RNA synthesis. *J Virol* 82: 9880-9889.
 305. Cheng YL, Lin YS, Chen CL, Wan SW, Ou YD, Yu CY, et al. (2015) Dengue Virus Infection Causes the Activation of Distinct NF-kappaB Pathways for Inducible Nitric Oxide Synthase and TNF-alpha Expression in RAW264.7 Cells. *Mediators Inflamm* 2015: 274025.
 306. Alvarez SE, Harikumar KB, Hait NC, Allegood J, Strub GM, Kim EY, et al. (2010) Sphingosine-1-phosphate is a missing cofactor for the E3 ubiquitin ligase TRAF2. *Nature* 465: 1084-1088.
 307. Allende ML, Yamashita T, Proia RL (2003) G-protein-coupled receptor S1P1 acts within

- endothelial cells to regulate vascular maturation. *Blood* 102: 3665-3667.
308. Tong S, Tian J, Wang H, Huang Z, Yu M, Sun L, et al. (2013) H9N2 avian influenza infection altered expression pattern of Sphingosine-1-phosphate Receptor 1 in BALB/c mice. *Virology Journal* 10: 296.
309. Walsh KB, Teijaro JR, Wilker PR, Jatzek A, Fremgen DM, Das SC, et al. (2011) Suppression of cytokine storm with a sphingosine analog provides protection against pathogenic influenza virus. *Proc Natl Acad Sci U S A* 108: 12018-12023.
310. Sehrawat S, Rouse BT (2008) Anti-inflammatory effects of FTY720 against viral-induced immunopathology: role of drug-induced conversion of T cells to become Foxp3+ regulators. *J Immunol* 180: 7636-7647.